CANCER THERAPEUTICS: TARGETING DNA REPAIR PATHWAYS

EDITED BY: Amila Suraweera, James A. L. Brown, Martin Francis Lavin and Yi Chieh Lim

PUBLISHED IN: Frontiers in Molecular Biosciences and Frontiers in Cell and Developmental Biology

frontiers Research Topics

ISSN 1664-8714
ISBN 978-2-88974-650-7
DOI 10.3389/978-2-88974-650-7

About Frontiers

Frontiers is more than just an open-access publisher of scholarly articles: it is a pioneering approach to the world of academia, radically improving the way scholarly research is managed. The grand vision of Frontiers is a world where all people have an equal opportunity to seek, share and generate knowledge. Frontiers provides immediate and permanent online open access to all its publications, but this alone is not enough to realize our grand goals.

Frontiers Journal Series

The Frontiers Journal Series is a multi-tier and interdisciplinary set of open-access, online journals, promising a paradigm shift from the current review, selection and dissemination processes in academic publishing. All Frontiers journals are driven by researchers for researchers; therefore, they constitute a service to the scholarly community. At the same time, the Frontiers Journal Series operates on a revolutionary invention, the tiered publishing system, initially addressing specific communities of scholars, and gradually climbing up to broader public understanding, thus serving the interests of the lay society, too.

Dedication to Quality

Each Frontiers article is a landmark of the highest quality, thanks to genuinely collaborative interactions between authors and review editors, who include some of the world's best academicians. Research must be certified by peers before entering a stream of knowledge that may eventually reach the public - and shape society; therefore, Frontiers only applies the most rigorous and unbiased reviews.
Frontiers revolutionizes research publishing by freely delivering the most outstanding research, evaluated with no bias from both the academic and social point of view. By applying the most advanced information technologies, Frontiers is catapulting scholarly publishing into a new generation.

What are Frontiers Research Topics?

Frontiers Research Topics are very popular trademarks of the Frontiers Journals Series: they are collections of at least ten articles, all centered on a particular subject. With their unique mix of varied contributions from Original Research to Review Articles, Frontiers Research Topics unify the most influential researchers, the latest key findings and historical advances in a hot research area! Find out more on how to host your own Frontiers Research Topic or contribute to one as an author by contacting the Frontiers Editorial Office: frontiersin.org/about/contact

CANCER THERAPEUTICS: TARGETING DNA REPAIR PATHWAYS

Topic Editors:
Amila Suraweera, Queensland University of Technology, Australia
James A. L. Brown, University of Limerick, Ireland
Martin Francis Lavin, The University of Queensland, Australia
Yi Chieh Lim, Danish Cancer Society Research Center (DCRC), Denmark

Citation: Suraweera, A., Brown, J. A. L., Lavin, M. F., Lim, Y. C., eds. (2022). Cancer Therapeutics: Targeting DNA Repair Pathways. Lausanne: Frontiers Media SA.
doi: 10.3389/978-2-88974-650-7

Table of Contents

frontiers in Molecular Biosciences

EDITORIAL
published: 15 February 2022
doi: 10.3389/fmolb.2022.858514

Editorial: Cancer Therapeutics: Targeting DNA Repair Pathways

Amila Suraweera[1,2]*, *James A. L. Brown*[3], *Yi Chieh Lim*[4] and *Martin F. Lavin*[5]

[1]Centre for Genomics and Personalised Health, School of Biomedical Sciences and Translational Research Institute, Queensland University of Technology (QUT), Brisbane, QLD, Australia, [2]Princess Alexandra Hospital, Woolloongabba, QLD, Australia, [3]Department of Biological Sciences, University of Limerick, Limerick, Ireland, [4]Danish Cancer Society Research Centre, Copenhagen, Denmark, [5]UQ Centre for Clinical Research (UQCCR), The University of Queensland, Brisbane, QLD, Australia

Keywords: DNA repair, genomic, stability, double strand break, repair, cancer, therapeutics, novel chemotherapeutics

Editorial on the Research Topic

Cancer Therapeutics: Targeting DNA Repair Pathways

A cell's genome is constantly challenged by exogenous and endogenous DNA damaging agents and failure to repair this damage can lead to genomic instability and tumorigenesis (Lavin et al., 2005; Jackson and Bartek, 2009). Genomic instability is an established hallmark of cancer and as tumorigenesis progresses, genetic streamlining leads to dysregulation of DNA repair pathways, selecting for cancer cells that have enhanced genomic instability and fitness. Importantly, this tumor evolution commonly leads to dependency on a single DNA repair pathway for survival through inactivation of alternate pathways, highlighting a key molecular weakness of cancer cells (Jeggo et al., 2016). Exploiting this weakness by accurately targeting the remaining or dysregulated DNA repair pathways in cancer cells using the next generation of precision/personalized medicine drugs, provides a therapeutic approach tailored to an individual's specific tumor profile (Aziz et al., 2012; Kelley et al., 2014; Jekimovs et al., 2014; Biau et al., 2019; Lavin and Yeo, 2020).

This Research Topic explores *Cancer Therapeutics: Targeting DNA Repair Pathways* and features ten articles that reflect the breadth and complexity of DNA repair pathways used by tumors and offers key insights into their potential exploitation for the next generation of cancer therapies. This topic consists of reviews and original research articles on key DNA repair proteins and pathways that are critical for cancer development or survival, highlighting their future importance for targeted therapies.

This topic highlights significant reviews, with the manuscript by Ren et al. discussing the structure of the regulator of chromosome condensation 1 (RCC1), a protein involved in the regulation of the cell cycle, DNA damage and in the development of cancer. RCC1 is overexpressed in cancer cells and the role of RCC1 in spindle formation, nuclear envelope formation and in nuclear transport is discussed. The authors highlight the role of RCC1 in tumorigenesis and further discuss its potential as a tumor biomarker (Ren et al.). The review *Regulator of Chromosome Condensation 2 Modulates Cell Cycle Progression, Tumorigenesis, and Therapeutic Resistance*, highlights the function of RCC2 in tumor development in different cancers and its role in resistance to current therapeutics. Guo et al. demonstrate that RCC2 functions in the oncogenesis of many cancers including colorectal, lung, breast and ovarian. The authors discuss an emerging role for RCC2 in the DNA repair process. The authors suggest that interaction of RCC2 with numerous signalling pathways leads to therapeutic resistance and poor cancer outcomes in patients, highlighting its potential as a cancer biomarker and future therapeutic target. The review by Sobanski et al. *Cell Metabolism and DNA Repair Pathways: Implications for Cancer Therapy* focuses on the dependence of DNA repair on cellular metabolism. The authors highlight the interplay of DNA repair and cell metabolism in tumor development and progression, and discuss how the next generation of potential novel therapies will target both processes concurrently (Sobanski et al.). Fernandez et al. provide a comprehensive review on epigenetic therapies currently in clinical trials or FDA approved for clinical use in cancer therapy, in their review *Epigenetic*

OPEN ACCESS

Edited by:
William C Cho,
QEH, Hong Kong SAR, China

Reviewed by:
Alexandros G Georgakilas,
National Technical University of Athens, Greece

****Correspondence:***
Amila Suraweera
amila.suraweera@qut.edu.au

Specialty section:
This article was submitted to Molecular Diagnostics and Therapeutics, a section of the journal Frontiers in Molecular Biosciences

Received: *20 January 2022*
Accepted: *26 January 2022*
Published: *15 February 2022*

Citation:
Suraweera A, Brown JAL, Lim YC and Lavin MF (2022) Editorial: Cancer Therapeutics: Targeting DNA Repair Pathways. Front. Mol. Biosci. 9:858514. doi: 10.3389/fmolb.2022.858514

Mechanisms in DNA Double Strand Break Repair: A Clinical Review. The authors focus on the role of histone deacetylase and DNA methyltransferase inhibitors as targeted therapies and their clinical use alone or in combination with current therapies, to highlight the emerging role of these epigenetic therapies as the next wave of personalized cancer medicine (Fernandez et al.).

This topic highlights research articles investigating new biomarkers. In the article *PAXX, Not NHEJ is an Independent Prognosticator in Colon Cancer* Arora et al., performing a comprehensive analysis of several essential genes, the authors studied their association with molecular and pathological features in colon cancer. In this study, high *PAXX* expression was shown to be the only independent prognostic biomarker for disease specific and overall survival in colon cancer, amongst the non-homologous end-joining genes analysed. The authors further suggest that PAXX may represent a novel therapeutic target in colon cancer, in addition to its use as a biomarker in colon cancer. Bian et al. set out to identify the N6-methyladenosine (m^6A) RNA methylation regulator-based prognostic signature, using the TCGA datasets, for hepatocellular carcinoma. Using a combination of bioinformatics and experimental data, the authors showed that m^6A regulator, YTHDF1, is an oncogenic gene in hepatocellular carcinoma and functions as both a prognostic biomarker and therapeutic target in this type of cancer (Bian et al.). In order to diagnose prostate cancer (PCa) patients with a high risk of biochemical recurrence, Long et al., used a bioinformatics approach to profile DNA repair genes. The authors identified a DNA repair gene signature, developing a prognostic nomogram for PCa, accurately predicting biochemical recurrence in PCa patients. Their research highlights the importance of such predictive models for personalized treatment options and decision making in PCa.

Liu et al. demonstrated that mini-chromosome maintenance protein 4 (MCM4) is a potential biomarker in soft-tissue sarcoma which correlates with clinical staging and survival outcome in patients. Tumors with overexpression of MCM4 were therapeutically sensitive to PARP inhibitors. This highlights the potential of PARP inhibitors (alone or in combination with chemotherapy) to treat soft-tissue sarcoma patients with MCM4 overexpression. Buck et al. investigated whether veliparib, a PARP inhibitor, could enhance the radiosensitivity of medulloblastoma cells. The author's *in vitro* data corroborated *in vivo* data from an orthotopic implant model of medulloblastoma, demonstrating that combination therapy of veliparib and irradiation decreased tumor growth rates and increased intra-tumoral apoptosis of medulloblastoma (Buck et al.). Al-Asmari et al. described the pharmacological inhibition of the STING pathway in cancer cell lines. The authors showed that induction of DNA damage in cancer cells leads to a rapid IL-6 response via non-canonical and canonical STING signalling. Furthermore, the authors suggest that targeting ERK1/2 may lead to a better response in patients, by reducing IL-6 production, whilst maintaining the anti-tumor activity of STING interferon signalling.

Together, this collection of manuscripts highlights the growing understanding and use of DNA repair pathways as both cancer biomarkers and for new precision medicine-based targeted therapeutic approaches for cancer treatment. This is particularly exemplified here by the manuscripts exploring PARP inhibitors, which we anticipate will be of interest to researchers and clinician-scientists alike. Advances in exploiting personalised profiling of tumors, combined with new biomarkers and targeted therapeutics, have, and will continue to improve clinical outcomes in patients.

AUTHOR CONTRIBUTIONS

All authors listed have made a substantial, direct and intellectual contribution to the work, and have approved it for publication.

FUNDING

AS is supported by a grant from the QUT Centre for Genomics and Personalised Health and ML is supported by an NHMRC Medical Research Futures Fund grant for rare genetic disorders.

REFERENCES

Aziz, K., Nowsheen, S., Pantelias, G., Iliakis, G., Gorgoulis, V. G., and Georgakilas, A. G. (2012). Targeting DNA Damage and Repair: Embracing the Pharmacological Era for Successful Cancer Therapy. *Pharmacol. Ther.* 133, 334–350. doi:10.1016/j.pharmthera.2011.11.010

Biau, J., Chautard, E., Verrelle, P., and Dutreix, M. (2019). Altering DNA Repair to Improve Radiation Therapy: Specific and Multiple Pathway Targeting. *Front. Oncol.* 9, 1009. doi:10.3389/fonc.2019.01009

Jackson, S. P., and Bartek, J. (2009). The DNA-Damage Response in Human Biology and Disease. *Nature* 461, 1071–1078. doi:10.1038/nature08467

Jeggo, P. A., Pearl, L. H., and Carr, A. M. (2016). DNA Repair, Genome Stability and Cancer: a Historical Perspective. *Nat. Rev. Cancer* 16, 35–42. doi:10.1038/nrc.2015.4

Jekimovs, C., Bolderson, E., Suraweera, A., Adams, M., O'Byrne, K. J., and Richard, D. J. (2014). Chemotherapeutic Compounds Targeting the DNA Double-Strand Break Repair Pathways: The Good, the Bad, and the Promising. *Front. Oncol.* 4, 86. doi:10.3389/fonc.2014.00086

Kelley, M. R., Logsdon, D., and Fishel, M. L. (2014). Targeting DNA Repair Pathways for Cancer Treatment: What's New? *Future Oncol.* 10, 1215–1237. doi:10.2217/fon.14.60

Lavin, M. F., and Yeo, A. J. (2020). Clinical Potential of ATM Inhibitors. *Mutat. Res. Fundam. Mol. Mech. Mutagen.* 821, 111695. doi:10.1016/j.mrfmmm.2020.111695

Lavin, M. F., Birrell, G., Chen, P., Kozlov, S., Scott, S., and Gueven, N. (2005). ATM Signaling and Genomic Stability in Response to DNA Damage. *Mutat. Res. Fundam. Mol. Mech. Mutagen.* 569, 123–132. doi:10.1016/j.mrfmmm.2004.04.020

Conflict of Interest: The authors declare that the research was conducted in the absence of any commercial or financial relationships that could be construed as a potential conflict of interest.

frontiers in Molecular Biosciences

REVIEW
published: 15 September 2020
doi: 10.3389/fmolb.2020.00225

The Multifaceted Roles of RCC1 in Tumorigenesis

*Xuanqi Ren, Kai Jiang and Feng Zhang**

College of Life Sciences, Shanghai Normal University, Shanghai, China

RCC1 (regulator of chromosome condensation 1) is the only known guanine nucleotide exchange factor of Ran, a nuclear Ras-like G protein. RCC1 combines with chromatin and Ran to establish a concentration gradient of RanGTP, thereby participating in a series of cell physiological activities. In this review, we discuss the structure of RCC1 and describe how RCC1 affects the formation and function of the nuclear envelope, spindle formation, and nuclear transport. We mainly focus on the effect of RCC1 on the cell cycle during tumorigenesis and the recent research progress that has been made in relation to different tumor types.

Keywords: RCC1, Ran, chromatin, tumorigenesis, cell cycle

OPEN ACCESS

Edited by:
Amila Suraweera,
Queensland University of Technology, Australia

Reviewed by:
Yi Chieh Lim,
Danish Cancer Society Research Center (DCRC), Denmark
Huiming Lu,
The University of Texas Southwestern Medical Center, United States

***Correspondence:**
Feng Zhang
fengz@shnu.edu.cn

Specialty section:
This article was submitted to Cellular Biochemistry, a section of the journal Frontiers in Molecular Biosciences

Received: *02 June 2020*
Accepted: *11 August 2020*
Published: *15 September 2020*

Citation:
Ren X, Jiang K and Zhang F (2020) The Multifaceted Roles of RCC1 in Tumorigenesis. Front. Mol. Biosci. 7:225. doi: 10.3389/fmolb.2020.00225

RAN'S FUNCTION AFFECTS RAN-GTP GRADIENT

Decades of research have shown that regulator of chromosome condensation 1 (RCC1), the only known guanine nucleotide exchange factor in the nucleus for Ran (Bischoff and Ponstingl, 1995), a nuclear Ras-like G protein, directly participates in cellular processes such as nuclear envelope (NE) formation, nucleocytoplasmic transport, and spindle formation. RCC1 also regulates chromatin condensation in the late S and early M phases of the cell cycle (Dasso, 1993). The proper location of RCC1 in relation to chromatin is crucial for the functions of Ran throughout the cell division cycle (Bierbaum and Bastiaens, 2013). RanGTP gradients are generated at the nuclear pores, and this gradient across the nuclear envelop drives the nuclear cytoplasmic transport (NCT) of various cargo molecules (Bischoff and Ponstingl, 1991a,b). Ran GTPase also affects cell cycle and DNA damage response (DDR) kinetics (Thompson, 2010; Blackinton and Keene, 2014). Following disassembly of the nuclear envelope in mitotic cells, mitotic chromosomes are surrounded by diffusional RanGTP gradients, which support the assembly and function of mitotic spindles (Kalab et al., 2002, 2006; Forbes et al., 2015). RCC1 acts as a key cell cycle regulator (Ohtsubo et al., 1987) and can monitor the process of DNA synthesis RAN (Seino et al., 1991).

An increasing number of studies have found that RCC1 also plays an important role in tumors, where it mainly regulates the cell cycle process and affects tumorigenesis. RCC1 can also inhibit the occurrence of certain tumors. For example, the expression of RCC1 in gastric cancers and other tumors is significantly reduced, with different degrees of silencing occurring (Lin et al., 2015). However, in some tumors, high expression of RCC1 will also act as a pathogenic partner, promoting tumor development.

In this review, we highlight the newest findings about the RCC1's role in the cell cycle and tumorigenesis in the context of the published data.

STRUCTURE OF RCC1

The human amino acid sequence analysis has revealed that there are three isoforms, named RCC1α, RCC1β, and RCC1γ (Hood and Clarke, 2007; **Figure 1**). The N-terminus contains a lysine-rich region which includes the 20-residue bipartite nuclear localization signal sequence (NLS) located on the tail of the N-terminus. The NLS regulates intracellular transport of RCC1 through the importin α/β pathway. Phosphorylation of the NLS prevents importin α/β from binding to RCC1, so that RCC1 couples the production of RanGTP to chromosome binding. N-terminal binding to chromosomal DNA requires methylation of the second serine at the N-terminal by N-terminal RCC1 methyltransferase (NRMT).

The C-terminal 7-blade β propeller domain, constituting the RCC1-like domain (RLD), has strong structural similarity with the WD40 repeat protein (Renault et al., 1998). Each blade in the beta propeller structure consists of 51–68 residue repeats and forms four antiparallel chains with loops between them. Both sides of the β-propeller structure are decorated by equivalent rings and mediate protein–protein interactions (Ruthenburg et al., 2006; Schuetz et al., 2006; Patel et al., 2008; Song and Kingston, 2008). In fact, the crystal structure indicates that one side of the RCC1 β propeller interacts with Ran via a β-hairpin extension called a β-wedge that protrudes from blade-3. RCC1 produces a RanGTP gradient around the chromosome through this binding (England et al., 2010).

RCC1 COMBINES WITH CHROMATIN TO ESTABLISH A CONCENTRATION GRADIENT OF RANGTP

The cell cycle regulates RCC1 and chromatin affinity through the CDK/CyclinB1 complex. RCC1 relies on binding to chromatin, realizing the perception of chromatin state, and recruiting and converting RanGDP into RanGTP. This ability to maintain high levels of RanGTP in the nucleus, or a gradient of RanGTP concentration around the chromosome in the nuclear envelope breakdown (NEB) state, underlies the association of RCC1 with the cell cycle. Crucially, loss of RCC1 causes tsBN2 cells to condensate (Nishijima et al., 2000), indicating that the loss of RCC1 may lead to early cell cycle condensation, possibly due to the lack of RanGTP, and resulting in restricted nuclear protein output.

The structure of RCC1 bound to Ran shows that all seven blade rings on one side interact with Ran in the complex (Renault et al., 2001). Ran stabilizes the dynamic interaction of RCC1 and chromatin in living cells through the N-terminal tail of RCC1 (Hitakomate et al., 2010). Binding of RCC1 to chromatin in living cells has been studied by fluorescence redistribution (Beaudouin et al., 2006) and found to occur via the N-terminal region (NTR) of RCC1, via residues 21–25 (Seino et al., 1992), and one of the loop regions connecting the β-sheets (Bierbaum and Bastiaens, 2013). Bichromatic fluorescence correlation spectrometric measurements have shown that Ran interacts primarily with the stationary portion of RCC1, which points to catalytic sites on chromatin, and that chromatin interaction with RCC1 is more stable during metaphase than during interphase (Bierbaum and Bastiaens, 2013). It is possible that histones interact with RCC1 on the other side through the exposed spherical regions of the H2A/H2B surface (Nemergut et al., 2001; Hao and Macara, 2008; England et al., 2010). The localization of RCC1 to chromatin is critically dependent on the flexible NTR (Moore et al., 2002) which is likely to extend beyond the core structure. Chromatin interaction with RCC1 is transient (Beaudouin et al., 2006), with the residence time of RCC1 on chromatin an important kinetic parameter of the guanine nucleotide exchange reaction. The exchange response effectively binds to chromatin through the affinity of the RanGTP complex, allowing local Ran activation (Bierbaum and Bastiaens, 2013). Study of a D182A mutant found that reduced affinity between this mutant and chromatin disrupted the interaction with Ran (Azuma et al., 1999; Hutchins et al., 2004).

Because of this potential correlation between RCC1 binding to chromatin and RCC1's Ran guanosine exchange function, multiple epigenetic modifications to the N-terminal domain of RCC1 may also influence the distribution of the RanGTP gradient. The N-terminal α-methylation of RCC1 by NRMT is important for stabilizing chromatin association and normal mitosis of cells, and RCC1 is excluded from chromosome when N-terminal tail methylation is removed RCC1 (Chen et al., 2007; Tooley et al., 2010). However, it is controversial whether RCC1 phosphorylation also affects chromatin affinity. Affinity of RCC1 for the chromosome may rely on its phosphorylation status (Hood and Clarke, 2007). The N-terminal tail of RCC1 is phosphorylated during mitosis, which inhibits binding to importin α/β (Li and Zheng, 2004). According to Hutchins et al. (2004) the phosphorylation of RCC1 is also important in allowing dynamic binding to chromatin during mitosis. Li and Zheng (2004) came to the same conclusion through the loss of fluorescence in photobleaching experiments, finding that phosphorylation leads to more stable binding to chromatin. However, Bierbaum and Bastiaens (2013), studying the dynamics of diffusion and binding of RCC1 and chromatin, found no evidence of chromatin binding regulation by N-terminal serine residue phosphorylation during mitosis.

RCC1 REGULATES NUCLEAR ENVELOPE FORMATION, SPINDLE FORMATION AND NUCLEAR TRANSPORT

The binding of RCC1 to chromatin is critical for nuclear envelope formation, spindle formation, and nucleocytoplasmic transport. These functions require RCC1 to combine with the nucleosomes to establish RanGTP gradients. At the end of mitosis, a new nuclear envelope (NE) is formed around chromatin, nuclear pore complexes (NPCs) are assembled in the envelope, and nuclear barrier function and nucleocytoplasmic transport are reestablished. The docking of RCC1 with H2A/H2B

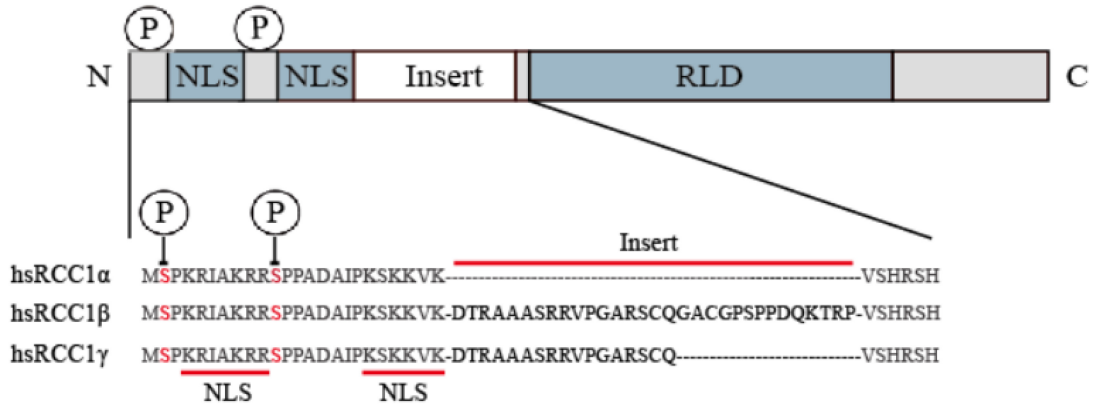

FIGURE 1 | RCC1 expression of three transcript variants in humans. The RCC1 protein domain is represented linearly (not to scale), showing the alignment of the NTR of the human RCC1 protein with the insert-containing RCC1 isoform (the inserted sequence is shown in bold). Serine 2 and 11 are phosphorylation sites of NTR and are indicated by circles labeled P.

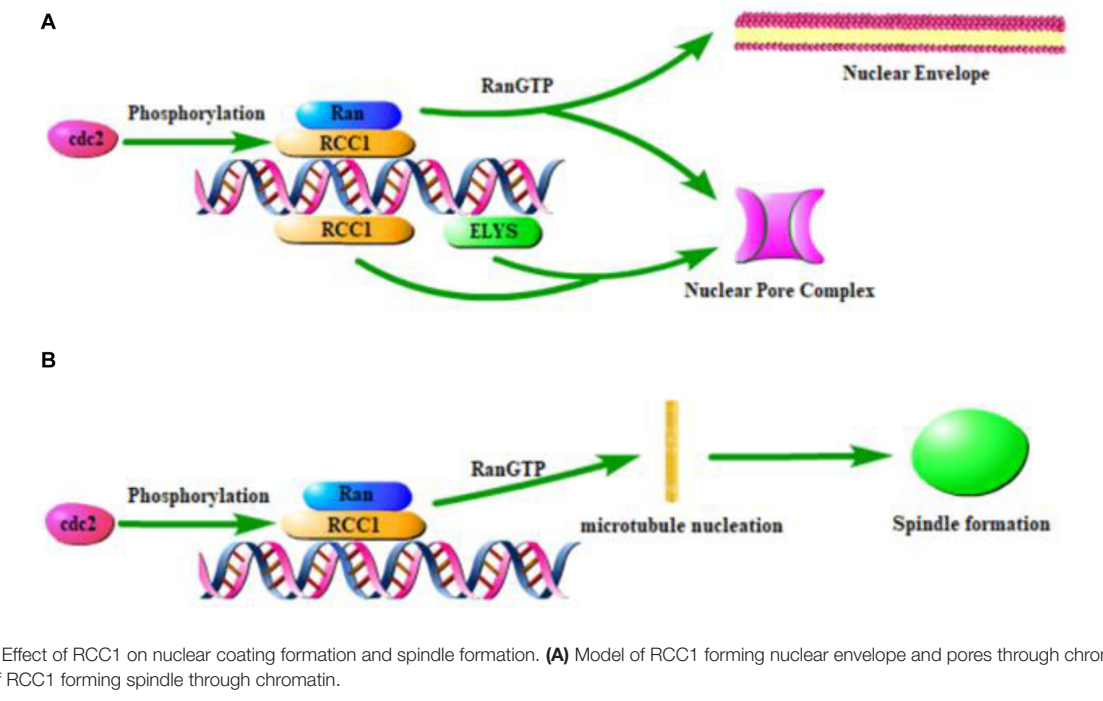

FIGURE 2 | Effect of RCC1 on nuclear coating formation and spindle formation. **(A)** Model of RCC1 forming nuclear envelope and pores through chromatin. **(B)** Model of RCC1 forming spindle through chromatin.

establishes the RanGTP gradient necessary for nuclear envelope assembly (Nemergut, 2001). Nucleosomes, but not DNA alone, mediate the chromosomal regulation of NE and NPC formation. This process first requires the generation of RanGTP by RCC1 recruited to nucleosomes (Zierhut and Funabiki, 2015). Then small GTPase Ran regulates NE/NPC assembly (Zhang et al., 2002; Horiike et al., 2009). Ran is activated by the chromatin-bound form of RCC1 (Redondo-Muñoz et al., 2015) and establishes a RanGTP gradient. NE/NPC assembly is therefore regulated by mechanisms that control RCC1 binding to chromatin (**Figure 2A**). This suggests that chromatin-associated RCC1 locally promotes NPC formation. Studies have shown that phosphoinositide 3-kinase β (PI3Kβ) regulates the localization of RCC1 on chromatin and subsequently the activation of Ran to exert regulation of the NE (Redondo-Muñoz et al., 2015). Localized chromatin-bound RCC1 promotes NPC formation inefficiently, which suggested that there may be a Ran independent mechanism that promotes NPC formation by nucleosomes. The nucleoporin ELYS (also known as MEL-28) can combine RCC1 with DNA and bypass the need for nucleosomes in the formation of NPC in a cooperative manner. Nucleosomes play a direct structural role in NPC recruitment by combining ELYS and RCC1 (Zierhut et al., 2014).

The location of RCC1 on the chromosome has been shown to be critical for the assembly of chromatin and RCC1-regulated spindles (**Figure 2B**), which requires the generation of a RanGTP

gradient (Clarke and Zhang, 2008; Halpin et al., 2011; Funabiki et al., 2018; Yau et al., 2020). During mitosis in mammalian cells, GTP-bound Ran is concentrated near mitotic chromatin, while GDP-bound Ran is more abundant distal to chromosomes. This pattern spatially controls spindle formation because RanGTP locally releases spindle assembly factors (Zierhut and Funabiki, 2015). Simultaneously, local enrichment of RCC1 can be used as a factor that triggers microtubule nucleation and subsequent spindle assembly (Moore et al., 2002). During mitosis, spindle assembly in cells without centrosomes is ensured by chromosome-induced microtubule aggregation.

Phosphorylation and methylation of RCC1 also play key roles in proper mitotic spindle assembly. Notably, methylation of the RCC1 N-terminal serine residue is necessary for proper mitotic spindle assembly, which increases the affinity for chromatin (Chen et al., 2007), while phosphorylation of serines, e.g., serine 11 in humans, located in or near the NLS of RCC1 by Cdc2 kinase is necessary for the generation of RanGTP on mitotic chromosomes in mammalian cells (Li and Zheng, 2004; Zierhut and Funabiki, 2015).

The biological function of RCC1 nuclear transport is to generate a RanGTP gradient through the nuclear pore, which is then used to drive various cargo molecules to overcome their concentration gradients for transportation (Kahana and Cleveland, 1999; Dworak et al., 2019). During the early stages of apoptosis, histone modification regulates RCC1 to inhibit nuclear transport. RCC1 is immobilized on the chromosome by Mst1 phosphorylation of histone H2B at Ser 14, leading to inactivation of the nuclear transport machinery (Wong et al., 2009).

THE ROLE OF RCC1 IN TUMORIGENESIS

Effect of RCC1 on the Cell Cycle

RCC1 has been shown to be a key cell cycle regulator which, in a Ran-dependent manner, monitors the process of DNA synthesis and links its completion to the occurrence of mitosis (Ohtsubo et al., 1987; Dasso, 1993). Many factors for re-entry of the cell cycle depend on nuclear cytoplasmic transport (NCT) activity regulated by RanGTP. The nuclear localization of interphase RCC1 ensures sufficient RanGTP concentration to form the driving force of NCT. For example, the realization of CyclinB1 and Gwl/Mastl kinase functions requires nuclear shuttling by importin 1 to achieve the S to G2/M phase transition (Dasso, 1993; Gavet and Pines, 2010). Twenty different NTRs interact with RanGTP such that RCC1 can run multiple NTRs simultaneously to speed up the cell cycle. In addition, there are several important large multidomain proteins that act as DNA repair regulators, and their transnuclear transport also depends on the level of RanGTP within the nucleus (Peng et al., 2013). Once spontaneous or drug-treated DNA damage occurs, the expression of RCC1 in normal cells is reduced, and the synergistic regulation of the Ran system amplifies this effect, leading to severe impairment of NCT function, which decelerates, or pauses, the cell cycle process. Alternatively, if RCC1/RanGTP is unable to respond immediately, cells carrying faulty genetic information go through the cell cycle smoothly, providing the potential for tumorigenesis.

Moreover, RCC1 is located on chromosomes in mitotic cells to maintain the gradient of RanGTP concentration around chromosomes during nuclear membrane disintegration and is involved in various genetic functions. Although RCC1 deficiency does not cause chromosome segregation defects in chicken TD40 cells, it does cause abnormalities in nuclear reconstitution, known as end-stage/G1 clover shaped abnormalities in nuclear morphology (Pemberton and Paschal, 2005). Thus, the correct location and expression of RCC1 at all stages of the cell cycle are crucial to its regulation. Of interest, Furuta et al. (2015) identified the presence of an NLS mediated nuclear localization of RCC1, through the introduction of RCC1 mutants into RCC1 deficient cells, i.e., by histone/DNA binding site of the catalytic domain, to bind chromatin and maintain binding state to the next intercellular phase by NEB state of fission (Pemberton and Paschal, 2005).

Since RCC1, ATM- and Rad3-related (ATR) kinases, and chromatin (chromosome or double-stranded DNA) all interact with each other, it is possible for RCC1 to regulate periodic monitoring points through ATR. Most likely, an ATR complex containing RCC1 is formed on chromatin after DNA damage or by inhibiting DNA replication (Abraham, 2001; Osborn et al., 2002; Furuta et al., 2015). Thus, RCC1 participates in the function of ATR cell cycle checkpoint, and this is supported by Nishitani et al.'s (2003) report of a correlation between RCC1-RAN cycles and ATR-dependent cell cycle checkpoints. If Ran is required to recruit ATR to damaged DNA or a closed DNA replication fork, RCC1 inactivation may inhibit ATR transport through the nucleoplasm. As an important functional target of ATR checkpoint, phosphorylation of Chk1 ensures DNA-induced cell cycle delay in response to unreplicated or UV-damaged DNA. Guo et al. (2000) found that the phosphorylation of Chk1 was eliminated in ATR-depleted xenopus egg extract indicating that defects in nuclear and cytoplasmic transport caused the checkpoint signal from ATR to Chk1 to be abolished (Cekan et al., 2016), which in turn weakened cell cycle arrest. Additionally, PIK-related protein kinase ATR restricts the NCT of CyclinB1-CDK1 signal by affecting CyclinB1 serine phosphorylation, ensuring the nuclear aggregation of CyclinB1 before NEB (Gavet and Pines, 2010). ATR functions as an S/G2 phase monitor during the cell cycle, responsible for preventing damaged DNA replication and inhibiting cell entry into mitosis before genome replication is complete. In this state, the reduction or inactivation of RCC1 destroys the ATR active complex composed of ATR, RCC1, and other proteins and its functions of DDR and cell cycle checkpoint. Excessive RCC1 will push the unrepaired or unreplicated cells into the division phase, also causing genomic instability and the possibility of tumorigenesis.

Effect of RCC1 on Tumorigenesis

The coordination of cell cycle progression with the repair of DNA damage supports the genomic integrity of dividing cells. Current research data indicate that differences in expression and function of RCC1 may depend on the type of tumor.

RCC1 Gene Mutations Have the Potential of Tumor Development

As an integral part of cell cycle regulation, the genetic and epigenetic stability of RCC1 is crucial for cell cycle progression and maintenance of genomic stability. Therefore, mutations of the RCC1 gene have the potential for tumor development. In gastric tumor tissues, the results of differential methylation hybridization microarray analysis reflected the hypermethylation level of the RCC1 gene at the lesion site, mainly at the ninth CpG site, which caused RCC1 silencing (Lin et al., 2015). There are three specific transcription factor binding sequences (HSF1, TFIIB, and NF-X3) in this region. Oxidated nitro domain containing protein 1 (NOR1) is a candidate tumor suppressor gene, and HSF1 is a functional promoter of NOR1. The transcription factor TFIIB acts as a bridge between TFIID and RNA polymerase and can recognize the interaction of TFIIB recognition elements that are destroyed by DNA methylation (Evans et al., 2001; Kalab and Heald, 2008; Li et al., 2011). Clinicopathologically, the loss of RCC1 expression in gastric cancer leads directly to the development of tumor differentiation and invasion depth (Lin et al., 2015). In addition, the RCC1* C. 1067_1086del19 mutation found in Tunisian familial breast cancer patients also indicates that RCC1 mutations have carcinogenic potential (Riahi et al., 2018).

RCC1 Promotes Tumor Progression as a Pathogenic Partner

For cancers not caused by RCC1 mutations, RCC1 appears to respond to tumor cycle progression through increased expression. For example, RCC1 expression is higher in clinical cancers, such as lung adenocarcinoma, than that of normal tissues (Hsu et al., 2016). In clinical and basic studies, RCC1 is more commonly involved in tumor development and progression in this manner than direct RCC1 mutations or RCC1 gene silencing. A typical example is in cervical cancer, as based on microarray gene expression profiles, where RCC1 overexpression has only been observed in the FIGO Stage III (Thomas et al., 2013). Similarly, in genome-wide transcriptional analysis of carboplatin sensitive/tolerant ovarian cancer cells, RCC1 expression was higher in resistant cells at 2 h after carboplatin exposure, rather than being sustained throughout the entire process (Peters et al., 2005). In a study of human papillomavirus-related cervical cancer, transcription factor c-Jun directly upregulated RCC1 transcription in HPV-E7 expressing cells (Qiao et al., 2018). Similarly, the absence of mutations in the tumor suppressor PTEN in many types of human cancers also leads to increased RCC1 expression (Qiao et al., 2018). Abundant evidence indicates that RCC1 is more consistent with the role of an intermediate effector protein in tumors, and its high expression is misled by upstream signals, thus promoting the cell cycle of cancer cells.

Therefore, in cancers that do not possess a mutated RCC1, it may be possible to induce cell cycle arrest, as well as senescence or apoptosis of cancer cells by lowering the expression of RCC1. This has been demonstrated in several studies including Zhang et al. (2011), who found that 6-bromine-5-hydroxy-4-methoxybenzaldehyde was associated with the down-regulation of RCC1 protein expression during inducing mitotic catastrophe in human hepatocellular carcinoma (HCC) cells, and Qiao et al. (2018), where RCC1 knockdown inhibited G1/S cell cycle progression and DNA synthesis of HPV-E7 expressing cells. A previous study on lung cancer showed that Latcripin-13 domain, which contains a regulator of the RCC1 domain, can induce apoptosis and cell cycle arrest in human lung cancer (Wang et al., 2016). In addition, although the knockdown of KPNB1 in advanced stage prostate cancer did not affect the expression of total RCC1, it did effectively reduce the expression of downstream cycle regulators and phosphorylation of RCC1, eventually leading to cycle arrest (Yang et al., 2019). Although there is no direct evidence, it is most likely that phosphorylation of RCC1γ is reduced. It is very interesting that, among the three isoforms of human RCC1, RCC1γ, while less abundant than RCC1α, when phosphorylated exhibits a strong chromatin binding capacity, resulting in persistently high RanGTP concentrations around chromatin (Hood and Clarke, 2007). Therefore, the inhibition of RCC1 phosphorylation can also be considered as a decrease of RCC1 activity to some extent.

RCC1 Has the Value of a Tumor Biomarker

The abnormal expression of RCC1 in a variety of malignant tumors suggests its potential as a cancer biomarker. Ideally, RCC1 is a Ran-dependent cell cycle regulator, and to some extent, its abnormal expression and epigenetic modification can effectively reflect the abnormal cell cycle of the patient's suspected cancerous tissue. RCC1 may be used as a lone indicator or in conjunction with other biomarkers for screening to assess cancer risk and cancer progression for prediction and prognosis, respectively (Dancey, 2014). Therefore, even though there have been relatively few published reports, the biological function of RCC1 and its overexpression in multiple types of cancer appears to be relatively consistent (Hsu et al., 2016; Wang et al., 2016). However, due to highly specific mutated forms of RCC1 in a small number of cancer types, RCC1 could be used as a marker for diagnosis of these specific cancers, examples being the two highly specific fusion genes formed by RCC1 in testicular germ cell tumor (Hoff et al., 2016) and the RCC1 truncated mutation specifically observed in some Tunisian breast cancers (Hsu et al., 2016). In addition, based on bioinformatics analysis and literature search, RCC1 is one of the potential biomarkers for identifying primary lung adenocarcinoma (Wong et al., 2009).

In conclusion, although RCC1 is still rarely used directly in the clinical diagnosis of cancer, it is valuable to determine the reference normal range of RCC1 in various tissues.

DISCUSSION

In recent years, an increasing number of studies have found that RCC1 is related to cell cycle, DNA damage, and cancer.

As an important cell cycle regulator, RCC1 affects the progress of the cell cycle. When DNA is damaged, the decrease in RCC1 expression in normal cells may lead to severe damage to NCT and affect re-entry of the cell cycle (Cekan et al., 2016). The continuous accumulation of DNA damage is also a major cause

of cancer. The loss of ATR-related cell cycle monitoring points increases the risk of DNA damage accumulation and increases the likelihood of tumors (Guo et al., 2000). The high expression of RCC1 in cancer cells accelerates the cell cycle and DNA repair, and, as such, tumor cells may regulate cell mitosis by increasing the expression of RCC1. RCC1 accelerates the formation of the nuclear membrane and the spindle to promote the mitotic process of cells. However, the mechanism by which RCC1 DNA damage responds to the cell cycle through the exact NCT or specific cell function requires further study.

Interestingly, RCC1 has different expression profiles and functions in different tumors. On the one hand, RCC1 expression is negatively correlated with the development of certain tumors. Targeting RCC1 can induce tumor cell apoptosis and cell cycle arrest (Hsu et al., 2016). RCC1 mutations or methylation can be key to tumor development, with this process showing the potential to inhibit tumors and regulate DNA replication (Lin et al., 2015). Already, there are nanoparticles treatments containing inhibitory peptides targeting RAN that have great potential in therapy of breast cancer (Haggag et al., 2019). On the other hand, RCC1 can also promote tumorigenesis. ERK1/2 can increase the expression of RCC1 through c-Jun, which affects the genome stability and promotes the development of tumors. ERK1/2 signaling could promote the development of osteosarcoma via regulating H2BK12ac (Xu et al., 2019). Histone interacts with RCC1 through the H2A/H2B surface area. Therefore, ERK1/2 may increase the expression of RCC1 through the c-Jun pathway to regulate H2BK12ac. Phosphorylation of RCC1 can affect its binding to chromosomes and also inhibit the proliferation of certain tumors. Its mechanism of action also has research value.

At the same time, RCC1 has different expression profiles in different tumors and shows promise as a potential biomarker. The reason for the different effects of RCC1 on different tumor types is not yet clear, but research on its role in the cell cycle, apoptosis, and genome stability has significant prospects.

AUTHOR CONTRIBUTIONS

XR: manuscript writing. FZ: review and modify. All authors contributed to the article and approved the submitted version.

FUNDING

This work was supported by grants from the National Natural Science Foundation of China (Grant Nos. 81572775 and 81773004 to FZ) and the Program for Professor of Special Appointment (Eastern Scholar) at Shanghai Institutions of Higher Learning (Grant No. TP2014055 to FZ).

REFERENCES

Abraham, R. T. (2001). Cell cycle checkpoint signaling through the ATM and ATR kinases. *Genes Dev.* 15, 2177–2196. doi: 10.1101/gad.914401

Azuma, Y., Renault, L., García-Ranea, J. A., Valencia, A., Nishimoto, T., and Wittinghofer, A. (1999). Model of the Ran-RCC1 interaction using biochemical and docking experiments. *J. Mol. Biol.* 289, 0–1130.

Beaudouin, J., Mora-Bermúdez, F., Klee, T., Daigle, N., and Ellenberg, J. (2006). Dissecting the Contribution of Diffusion and Interactions to the Mobility of Nuclear Proteins. *Biophys. J.* 90, 1878–1894. doi: 10.1529/biophysj.105.071241

Bierbaum, M., and Bastiaens, P. H. (2013). Cell Cycle-Dependent Binding Modes of the Ran Exchange Factor RCC1 to Chromatin. *Biophys. J.* 104, 1642–1651. doi: 10.1016/j.bpj.2013.03.024

Bischoff, F. R., and Ponstingl, H. (1991a). Catalysis of guanine nucleotide exchange on Ran by the mitotic regulator RCC1. *Nature* 354, 80–82. doi: 10.1038/354080a0

Bischoff, F. R., and Ponstingl, H. (1991b). Mitotic regulator protein RCC1 is complexed with a nuclear ras-related polypeptide. *Proc. Natl. Acad. Sci. U.S.A.* 88, 10830–10834. doi: 10.1073/pnas.88.23.10830

Bischoff, F. R., and Ponstingl, H. (1995). Catalysis of guanine nucleotide exchange of Ran by RCCI and stimulation of hydrolysis of Ran-bound GTP by Ran-GAP1. *Mebods Enzymol.* 257, 135–144. doi: 10.1016/s0076-6879(95)57019-5

Blackinton, J. G., and Keene, J. D. (2014). Post-transcriptional RNA regulons affecting cell cycle and proliferation. *Semin. Cell Dev. Biol.* 34, 44–54. doi: 10.1016/j.semcdb.2014.05.014

Cekan, P., Hasegawa, K., Pan, Y., Tubman, E., Odde, D., Chen, J. C., et al. (2016). RCC1-dependent activation of Ran accelerates cell cycle and DNA repair, inhibiting DNA damage-induced cell senescence. *Mol. Biol. Cell* 2016, 1346–1357. doi: 10.1091/mbc.e16-01-0025

Chen, T., Muratore, T. L., Schaner-Tooley, C. E., Shabanowitz, J., Hunt, D. F., Macara, I. G., et al. (2007). N-terminal α-methylation of RCC1 is necessary for stable chromatin association and normal mitosis. *Nat. Cell Biol.* 9, 596–603. doi: 10.1038/ncb1572

Clarke, P. R., and Zhang, C. (2008). Spatial and temporal coordination of mitosis by Ran GTPase. *Nat. Rev. Mol. Cell Biol.* 9, 464–477. doi: 10.1038/nrm2410

Dancey, J. E. (2014). Biomarker discovery and development through genomics. *Cancer Genomics* 2014, 93–107. doi: 10.1016/b978-0-12-396967-5.00007-4

Dasso, M. (1993). RCC1 in the cell cycle: the regulator of chromosome condensation takes on new roles. *Trends Biochem. Sci.* 18, 96–101. doi: 10.1016/0968-0004(93)90161-f

Dworak, N., Makosa, D., and Chatterjee, M. (2019). A nuclear lamina-chromatin-Ran GTPase axis modulates nuclear import and DNA damage signaling. *Aging Cell* 18:e12851. doi: 10.1111/acel.12851

England, J. R., Huang, J., Jennings, M. J., Makde, R. D., and Tan, S. (2010). RCC1 Uses a Conformationally Diverse Loop Region to Interact with the Nucleosome: a Model for the RCC1–Nucleosome Complex. *J. Mol. Biol.* 398, 0–529.

Evans, R., Fairley, J. A., and Roberts, S. G. (2001). Activator mediated disruption of sequence-specific DNA contacts by the general transcription factor TFIIB. *Genes Dev.* 15, 2945–2949. doi: 10.1101/gad.206901

Forbes, D. J., Travesa, A., Nord, M. S., and Bernis, C. (2015). Nuclear transport factors: global regulation of mitosis. *Curr. Opin. Cell Biol.* 35, 78–90. doi: 10.1016/j.ceb.2015.04.012

Funabiki, H., Jenness, C., and Zierhut, C. (2018). Nucleosome-Dependent Pathways That Control Mitotic Progression. *Cold. Spring Harb. Symp. Quant. Biol.* 2018:034512.

Furuta, M., Hori, T., and Fukagawa, T. (2015). Chromatin binding of RCC1 during mitosis is important for its nuclear localization in interphase. *Mol. Biol. Cell* 27, 371–381. doi: 10.1091/mbc.e15-07-0497

Gavet, O., and Pines, J. (2010). Activation of cyclin B1-Cdk1 synchronizes events in the nucleus and the cytoplasm at mitosis. *J. Cell Biol.* 189, 247–259. doi: 10.1083/jcb.200909144

Guo, Z., Kumagai, A., Wang, S. X., and Dunphy, W. G. (2000). Requirement for Atr in phosphorylation of Chk1 and cell cycle regulation in response to DNA replication blocks and UV-damaged DNA in Xenopus egg extracts. *Genes Dev.* 14, 2745–2756. doi: 10.1101/gad.842500

Haggag, Y., Matchett, K., Falconer, R., Isreb, M., Jones, J., Faheem, A., et al. (2019). Novel Ran-RCC1 inhibitory peptide-loaded nanoparticles have anti-cancer

efficacy in vitro and in vivo. *Cancers* 11:222. doi: 10.3390/cancers11020222

Halpin, D., Kalab, P., Wang, J., Weis, K., and Heald, R. (2011). Mitotic Spindle Assembly around RCC1-Coated Beads in Xenopus Egg Extracts. *PLoS Biol.* 9:e1001225. doi: 10.1371/journal.pbio.1001225

Hao, Y., and Macara, I. G. (2008). Regulation of chromatin binding by a conformational switch in the tail of the Ran exchange factor RCC1. *J. Cell Biol.* 182, 827–836. doi: 10.1083/jcb.200803110

Hitakomate, E., Hood, F. E., Sanderson, H. S., and Clarke, P. R. (2010). The methylated N-terminal tail of RCC1 is required for stabilisation of its interaction with chromatin by Ran in live cells. *BMC Cell Biol.* 11:43. doi: 10.1186/1471-2121-11-43

Hoff, A. M., Alagaratnam, S., Zhao, S., Bruun, J., Andrews, P. W., Lothe, R. A., et al. (2016). Identification of novel fusion genes in testicular germ cell tumors. *Cancer Res.* 76, 108–116. doi: 10.1158/0008-5472.can-15-1790

Hood, F. E., and Clarke, P. R. (2007). RCC1 isoforms differ in their affinity for chromatin, molecular interactions and regulation by phosphorylation. *J. Cell Sci.* 120, 3436–3445. doi: 10.1242/jcs.009092

Horiike, Y., Kobayashi, H., and Sekiguchi, T. (2009). Ran GTPase guanine nucleotide exchange factor RCC1 is phosphorylated on serine. *Mol. Biol. Rep.* 36, 717–723. doi: 10.1007/s11033-008-9234-3

Hsu, C. H., Hsu, C. W., Hsueh, C., and Wang, C. L. (2016). Identification and characterization of potential biomarkers by quantitative tissue proteomics of primary lung adenocarcinoma. *Mol. Cell. Proteomics* 15, 2396–2410. doi: 10.1074/mcp.m115.057026

Hutchins, J. R., Moore, W. J., Hood, F. E., Wilson, J. S., Andrews, P. D., Swedlow, J. R., et al. (2004). Phosphorylation regulates the dynamic interaction of RCC1 with chromosomes during mitosis. *Curr. Biol.* 14, 1099–1104. doi: 10.1016/j.cub.2004.05.021

Kahana, J. A., and Cleveland, D. W. (1999). Beyond nuclear transport. Ran-GTP as a determinant of spindle assembly. *J. Cell Biol.* 146, 1205–1209.

Kalab, P., and Heald, R. (2008). The RanGTP gradient—a GPS for the mitotic spindle. *J. Cell Sci.* 121, 1577–1586. doi: 10.1242/jcs.005959

Kalab, P., Pralle, A., Isacoff, E. Y., Heald, R., and Weis, K. (2006). Analysis of a RanGTP-regulated gradient in mitotic somatic cells. *Nature* 440, 697–701. doi: 10.1038/nature04589

Kalab, P., Weis, K., and Heald, R. (2002). Visualization of a Ran-GTP gradient in interphase and mitotic Xenopus egg extracts. *Science* 295, 2452–2456. doi: 10.1126/science.1068798

Li, H.-Y., and Zheng, Y. (2004). Phosphorylation of RCC1 in mitosis is essential for producing a high RanGTP concentration on chromosomes and for spindle assembly in mammalian cells. *Genes Dev.* 18, 512–527. doi: 10.1101/gad.1177304

Li, W., Li, X., Wang, W., Li, X., Tan, Y., Yi, M., et al. (2011). NOR1 is an HSF1- and NRF1-regulated putative tumor suppressor inactivated by promoter hypermethylation in nasopharyngeal carcinoma. *Carcinogenesis* 32, 1305–1314. doi: 10.1093/carcin/bgr174

Lin, Y. L., Chen, H. L., Cheng, S. B., Yeh, D. C., Huang, C. C., Peng, F. K., et al. (2015). Methylation-silencing RCC1 expression is associated with tumorigenesis and depth of invasion in gastric cancer. *Int. J. Clin. Exp. Pathol.* 8:14257.

Moore, W., Zhang, C., and Clarke, P. R. (2002). Targeting of RCC1 to chromosomes is required for proper mitotic spindle assembly in human cells. *Curr. Biol.* 12, 1442–1447. doi: 10.1016/s0960-9822(02)01076-x

Nemergut, M. E. (2001). Chromatin Docking and Exchange Activity Enhancement of RCC1 by Histones H2A and H2B. *Science* 292, 1540–1543. doi: 10.1126/science.292.5521.1540

Nemergut, M. E., Mizzen, C. A., Stukenberg, T., Allis, C. D., and Macara, I. G. (2001). Chromatin docking and exchange activity enhancement of RCC1 by histones H2And H2B. *Science* 292, 1540–1543. doi: 10.1126/science.292.5521.1540

Nishijima, H., Seki, T., Nishitani, H., and Nishimoto, T. (2000). *Premature Chromatin Condensation Caused by Loss of RCC1*. Berlin: Springer.

Nishitani, H., Saito, N., Nishitani, H., and Nishimoto, T. (2003). Caffeine mimics adenine and 2'-deoxyadenosine, both of which inhibit the guanine-nucleotide exchange activity of RCC1 and the kinase activity of ATR. *Genes Cells* 8, 423–435. doi: 10.1046/j.1365-2443.2003.00644.x

Ohtsubo, M., Kai, R., Furuno, N., Sekiguchi, T., Sekiguchi, M., Hayashida, H., et al. (1987). Isolation and characterization of the active cDNA of the human cell cycle gene (RCC1) involved in the regulation of onset of chromosome condensation. *Genes Dev.* 1, 585–593. doi: 10.1101/gad.1.6.585

Osborn, A. J., Elledge, S. J., and Zou, L. (2002). Checking on the fork: the DNA-replication stress-response pathway. *Trends Cell Biol.* 12, 509–516. doi: 10.1016/s0962-8924(02)02380-2

Patel, A., Dharmarajan, V., and Cosgrove, M. S. (2008). Structure of WDR5 bound to mixed lineage leukemia protein-1 peptide. *J. Biol. Chem.* 283, 32158–32161. doi: 10.1074/jbc.c800164200

Pemberton, L. F., and Paschal, B. M. (2005). Mechanisms of receptor-mediated nuclear import and nuclear export. *Traffic* 6, 187–198. doi: 10.1111/j.1600-0854.2005.00270.x

Peng, A., Wang, A., Jacob, A., Bonneil, E., Hickson, G. R. X., Roux, P. P., et al. (2013). Cell cycle regulation of Greatwall kinase nuclear localization facilitates mitotic progression. *J. Cell Biol.* 202:37535.

Peters, D., Freund, J., and Ochs, R. L. (2005). Genome-wide transcriptional analysis of carboplatin response in chemosensitive and chemoresistant ovarian cancer cells. *Mol. Cancer Ther.* 4, 1605–1616. doi: 10.1158/1535-7163.mct-04-0311

Qiao, L., Zheng, J., Tian, Y., Zhang, Q., Wang, X., Chen, J. J., et al. (2018). Regulator of chromatin condensation 1 abrogates the G1 cell cycle checkpoint via Cdk1 in human papillomavirus E7-expressing epithelium and cervical cancer cells. *Cell Death Dis.* 9, 583.

Redondo-Muñoz, J., Pérez-García, V., Rodríguez, M. J., Valpuesta, J. M., and Carrera, A. C. (2015). Phosphoinositide 3-Kinase beta protects nuclear envelope integrity by controlling RCC1 localization and ran activity. *Mol. Cell. Biol.* 35, 249–263. doi: 10.1128/mcb.01184-14

Renault, L., Kuhlmann, J., Henkel, A., and Wittinghofer, A. (2001). Structural basis for guanine nucleotide exchange on Ran by the regulator of chromosome condensation (RCC1). *Cell* 105, 245–255. doi: 10.1016/s0092-8674(01)00315-4

Renault, L., Nassar, N., Vetter, I., Becker, J., Klebe, C., Roth, M., et al. (1998). The 1.7 Å crystal structure of the regulator of chromosome condensation (RCC1) reveals a seven-bladed propeller. *Nature* 392, 97–101. doi: 10.1038/32204

Riahi, A., Radmanesh, H., Schürmann, P., Bogdanova, N., Geffers, R., Meddeb, R., et al. (2018). Exome sequencing and case-control analyses identify RCC1 as a candidate breast cancer susceptibility gene. *Int. J. Cancer* 142, 2512–2517. doi: 10.1002/ijc.31273

Ruthenburg, A. J., Wang, W., Graybosch, D. M., Li, H., Allis, C. D., Patel, D. J., et al. (2006). Histone H3 recognition and presentation by the WDR5 module of the MLL1 complex. *Nat. Struct. Mol. Biol.* 13, 704–712. doi: 10.1038/nsmb1119

Schuetz, A., Allali-Hassani, A., Martin, F., Loppnau, P., Vedadi, M., Bochkarev, A., et al. (2006). Structural basis for molecular recognition and presentation of histone H3 by WDR5. *EMBO J.* 25, 4245–4252. doi: 10.1038/sj.emboj.7601316

Seino, H., Hisamoto, N., Uzawa, S., Sekiguchi, T., and Nishimoto, T. (1992). DNA binding domain of RCC1 protein is not essential for coupling mitosis with DNA replication. *J. Cell Sci.* 102, 393–400.

Seino, H., Nishitani, H., Seki, T., Hisamoto, N., Tazunoki, T., Shiraki, N., et al. (1991). RCC1 Is a Nuclear Protein Required for Coupling Activation of cdc2 Kinase with DNA Synthesis and for Start of the Cell Cycle. *Cold. Spring Harb. Symp. Quant. Biol.* 1991, 367–375. doi: 10.1101/sqb.1991.056.01.044

Song, J. J., and Kingston, R. E. (2008). WDR5 interacts with mixed lineage leukemia (MLL) protein via the histone H3-binding pocket. *J. Biol. Chem.* 283, 35258–35264. doi: 10.1074/jbc.m806900200

Thomas, A., Mahantshetty, U., Kannan, S., Deodhar, K., Shrivastava, S. K., Kumar-Sinha, C., et al. (2013). Expression profiling of cervical cancers in Indian women at different stages to identify gene signatures during progression of the disease. *Cancer Med.* 2, 836–848. doi: 10.1002/cam4.152

Thompson, M. E. (2010). BRCA1 16 years later: nuclear import and export processes. *FEBS J.* 277, 3072–3078. doi: 10.1111/j.1742-4658.2010.07733.x

Tooley, C. E. S., Petkowski, J., Muratore-Schroeder, T. L., Balsbaugh, J. L., Shabanowitz, J., Sabat, M., et al. (2010). NRMT is an α-N-methyltransferase that methylates RCC1 and Retinoblastoma Protein. *Nature* 466, 1125–1128. doi: 10.1038/nature09343

Wang, J., Wan, X. Y., Gao, Y. F., Zhong, M. T., Sha, L., Liu, B., et al. (2016). Latcripin-13 domain induces apoptosis and cell cycle arrest at the G1 phase in human lung carcinoma A549 cells. *Oncol. Rep.* 36, 441–447. doi: 10.3892/or.2016.4830

Wong, C. H., Chan, H., Ho, C. Y., Lai, S. K., Koh, C. G., Li, H. Y., et al. (2009). Apoptotic histone modification inhibits nuclear transport by regulating RCC1. *Nat. Cell Biol.* 11, 226–226. doi: 10.1038/ncb0209-226

Xu, X., Yu, H., and Xu, Y. (2019). Ras-ERK1/2 Signaling Promotes The Development Of Osteosarcoma By Regulating H2BK12ac Through CBP. *Cancer Manag. Res.* 11, 9153–9163. doi: 10.2147/cmar.s219535

Yang, J., Guo, Y., Lu, C., Zhang, R., Wang, Y., Luo, L., et al. (2019). Inhibition of Karyopherin beta 1 suppresses prostate cancer growth. *Oncogene* 38:4700. doi: 10.1038/s41388-019-0745-2

Yau, K. C., Arnaoutov, A., Aksenova, V., Kaufhold, R., Chen, S., Dasso, M., et al. (2020). RanBP1 controls the Ran pathway in mammalian cells through regulation of mitotic RCC1 dynamics. *Cell Cycle* 2020, 1–18.

Zhang, B., Huang, B., Guan, H., Zhang, S. M., Xu, Q. Z., He, X. P., et al. (2011). Proteomic profiling revealed the functional networks associated with mitotic catastrophe of HepG2 hepatoma cells induced by 6bromine-5-hydroxy-4-methoxybenzaldehyde. *Toxicol. Appl. Pharmacol.* 252, 307–317. doi: 10.1016/j.taap.2011.03.003

Zhang, C., Goldberg, M. W., Moore, W. J., Allen, T. D., and Clarke, P. R. (2002). Concentration of Ran on chromatin induces decondensation nuclear envelope formation and nuclear pore complex assembly. *Eur. J. Cell Biol.* 81, 623–633. doi: 10.1078/0171-9335-00288

Zierhut, C., and Funabiki, H. (2015). Nucleosome functions in spindle assembly and nuclear envelope formation. *BioEssays* 37, 1074–1085. doi: 10.1002/bies.201500045

Zierhut, C., Jenness, C., Kimura, H., and Funabiki, H. (2014). Nucleosomal regulation of chromatin composition and nuclear assembly revealed by histone depletion. *Nat. Struct. Mol. Biol.* 21, 617–625. doi: 10.1038/nsmb.2845

Conflict of Interest: The authors declare that the research was conducted in the absence of any commercial or financial relationships that could be construed as a potential conflict of interest.

frontiers in Molecular Biosciences

ORIGINAL RESEARCH
published: 23 October 2020
doi: 10.3389/fmolb.2020.584053

PAXX, Not *NHEJ1* Is an Independent Prognosticator in Colon Cancer

Mohit Arora[1†], Sarita Kumari[2†], Jay Singh[2], Anita Chopra[2] and Shyam S. Chauhan[1*]*

[1] Department of Biochemistry, All India Institute of Medical Sciences, New Delhi, India, [2] Laboratory Oncology Unit, Dr. BRA-IRCH, All India Institute of Medical Sciences, New Delhi, India

Classical Non-homologous End Joining (NHEJ) pathway is the mainstay of cellular response to DNA double strand breaks. While aberrant expression of genes involved in this pathway has been linked with genomic instability and drug resistance in several cancers, limited information is available about its clinical significance in colon cancer. We performed a comprehensive analysis of seven essential genes, including *XRCC5*, *XRCC6*, *PRKDC*, *LIG4*, *XRCC4*, *NHEJ1,* and *PAXX* of this pathway, in colon cancer using multi-omics datasets, and studied their associations with molecular and clinicopathological features, including age, gender, stage, *KRAS* mutation, *BRAF* mutation, microsatellite instability status and promoter DNA methylation in TCGA colon cancer dataset. This analysis revealed upregulation of *XRCC5*, *PRKDC,* and *PAXX* in colon cancer compared to normal colon tissues, while *LIG4* and *NHEJ1 (*XLF) displayed downregulation. The expression of these genes was independent of age and *KRAS* status, while *XRCC5*, *PRKDC,* and *LIG4* exhibited reduced expression in *BRAF* mutant tumors. Interestingly, we observed a strong association between *XRCC6*, *XRCC5*, *PRKDC* and *LIG4* overexpression and microsatellite instability status of the tumors. In multivariate analysis, high *PAXX* expression emerged as an independent prognostic marker for poor overall and disease specific survival. We also observed hypomethylation of *PAXX* promoter in tumors, which exhibited a strong correlation with its overexpression. Furthermore, *PAXX* overexpression was also associated with several oncogenic pathways as well as a reduction in numbers of tumor-infiltrating lymphocytes.

Keywords: PAXX, NHEJ1 gene, colon cancer, The Cancer Genome Atlas, DNA methylation, DNA Repair

OPEN ACCESS

Edited by:
Amila Suraweera, Queensland University of Technology, Australia

Reviewed by:
Nikolay Mikhaylovich Borisov, Moscow Institute of Physics and Technology, Russia
Chinnadurai Mani, Texas Tech University Health Sciences Center, United States

****Correspondence:***
Shyam S. Chauhan
s_s_chauhan@hotmail.com
Anita Chopra
chopraanita2005@gmail.com

[†]These authors have contributed equally to this work

Specialty section:
This article was submitted to Molecular Diagnostics and Therapeutics, a section of the journal Frontiers in Molecular Biosciences

Received: *16 July 2020*
Accepted: *09 September 2020*
Published: *23 October 2020*

Citation:
Arora M, Kumari S, Singh J, Chopra A and Chauhan SS (2020) PAXX, Not NHEJ1 Is an Independent Prognosticator in Colon Cancer. Front. Mol. Biosci. 7:584053. doi: 10.3389/fmolb.2020.584053

INTRODUCTION

Colorectal cancer (CRC) is the fourth most commonly diagnosed cancer and the third most common cause of cancer related deaths worldwide (Bray et al., 2018; Rawla et al., 2019). It represents a group of heterogeneous diseases that are characterized by a range of genomic and epigenomic alterations (The Cancer Genome Atlas Network, 2012). The knowledge regarding the molecular landscapes of CRCs is rapidly increasing, which has led to advancements in early detection methodologies and hence reduction of mortality rates (Arnold et al., 2017).

DNA double strand breaks (DSBs) are inherently induced during several physiological conditions, including stem cell differentiation, cell division, autophagy, and senescence. Homologous recombination repair (HRR), classical non-homologous end joining (c-NHEJ

or NHEJ) and alternative end joining (Alt-EJ) are the three DNA damage repair systems, which efficiently repair DSBs, and thus maintain genomic stability during physiological stress (Chang et al., 2017). HRR functions by using a homologous DNA strand as a template to perform error free repair at DSB sites. Contrary to this, NHEJ is the primary DNA damage repair pathway and perform template independent repair of deleterious DSBs (Chang et al., 2017). Alt-EJ is a less characterized mechanism which works as a backup for both HRR and NHEJ in case of excessive DNA damage, and also utilizes micro-homologies between distant DNA sites for template dependent repair.

The core c-NHEJ system consists of Ku70/80 heterodimer (encoded by *XRCC6* and *XRCC5*, respectively), XRCC4, DNA-dependent protein kinase catalytic subunit (DNA-PKcs, encoded by *PRKDC*), DNA Ligase 4 (encoded by *LIG4*), and *XRCC4*-like factor (XLF, encoded by *NHEJ1*). DNA damage sites are quickly recognized by Ku70/Ku80 heterodimer or Ku70 homodimer, which after binding to DNA free ends undergo allosteric change, thereby providing a scaffold for recruitment of DNA-PKcs. The protein kinase activity of Ku/DNA-PKcs complex recruits accessory factors to modify free DNA ends, which cannot be ligated directly (Davis et al., 2014). Then, XRCC4 and XLF also assemble at DSB sites, aligns the chromatin in the vicinity, and mediates recruitment of Ligase IV which carry out the final (ligation) step of the repair. These core components are sufficient to recognize DSBs, align the broken DNA fragments, and anneal them, fixing the DSBs (Chang et al., 2017).

PAXX (Paralog of *XRCC4* and XLF; previously called C9orf142) is a recently characterized protein associated with the classical NHEJ pathway. It structurally resembles XRCC4 and XLF and facilitates the assembly of the core NHEJ complex at the DNA damage site (Ochi et al., 2015; Kumar et al., 2016). Although, PAXX and XLF perform overlapping functions and XLF can efficiently compensate for PAXX deficiency in colon cancer cells (Tadi et al., 2016), however, another study demonstrated that one protein between PAXX and XLF is essential for NHEJ repair, and PAXX also promotes Ku accumulation at DSBs (Liu et al., 2017). Interestingly, a recent study reported the synergistic role of PAXX, XRCC4, and XLF in the recruitment of DNA Pol λ as an accessory factor for DNA damage repair (Craxton et al., 2018). Although, these studies suggest that both PAXX and XLF perform overlapping but essential functions in NHEJ mediated DNA repair and influence drug resistance in solid tumors, the consequences and clinical implications of their altered expression in cancer patients have never been investigated. While XLF confers resistance to oxaliplatin and 5-fluorouracil in CRC cells (Liu et al., 2019), PAXX overexpression is associated with drug resistance in osteosarcoma cells (Ma et al., 2020).

Non-homologous end joining pathway genes in this CRC harbor both genetic and epigenetic alterations which promote cancer progression (Beggs et al., 2012; Mijnes et al., 2018). Variations at the 3′UTR of mRNA encoding DSB repair proteins have also been associated with a higher risk of CRC and poor outcome of the disease (Naccarati et al., 2015). Conventional cancer therapies including radiation and chemotherapy primarily exert their effect by inducing DSBs mediated cancer cell death. Therefore, the NHEJ pathway genes are considered as potential therapeutic targets to overcome drug resistance in CRC. Previous reports have analyzed the expression of NHEJ genes in different cancers, including some in colorectal cancer (Sishc and Davis, 2017). In the present study, we performed a comprehensive analysis of the core NHEJ pathway genes using well characterized multi-omics datasets to determine the deregulated expression pattern and clinical significance of NHEJ pathway genes in colon cancer.

MATERIALS AND METHODS

Data Acquisition and Analysis

Oncomine[1] a web online database was used to analyze the expression of mRNA encoded by NHEJ genes, in several colon cancer datasets. The parameters for comparing gene expression between normal and tumor tissues included mRNA data with a threshold of $p < 0.01$ with any fold change.

Gene expression and DNA methylation of colon cancer developed by The Cancer Genome Atlas (TCGA-COAD study) was extracted as fragment per kilobase million (FPKM) values from the UCSC Xena browser,[2] and used for subsequent analysis. Similarly, information about clinical features and tumor mutation status of colon cancer patients of TCGA study was

[1]https://www.oncomine.org/resource/login.html
[2]https://xena.ucsc.edu/

TABLE 1 | Expression of NHEJ pathway genes in colon cancer determined by Oncomine analysis.

	Upregulated		Downregulated	
Gene Name	**Analysis meet threshold of $p < 0.001$**	**Datasets covered in the analysis that meet the threshold**	**Analysis meet the threshold of $p < 0.001$**	**Datasets covered in the analysis that meet the threshold**
XRCC6	9/25	5/10	0/25	0/10
XRCC5	17/27	9/12	0/27	0/12
PRKDC	22/26	10/11	0/26	0/11
XRCC4	11/25	7/10	0/25	0/10
LIG4	0/25	0/10	8/25	5/10
NHEJ1	1/23	1/8	13/23	6/8
PAXX	10/24	5/9	0/24	0/9

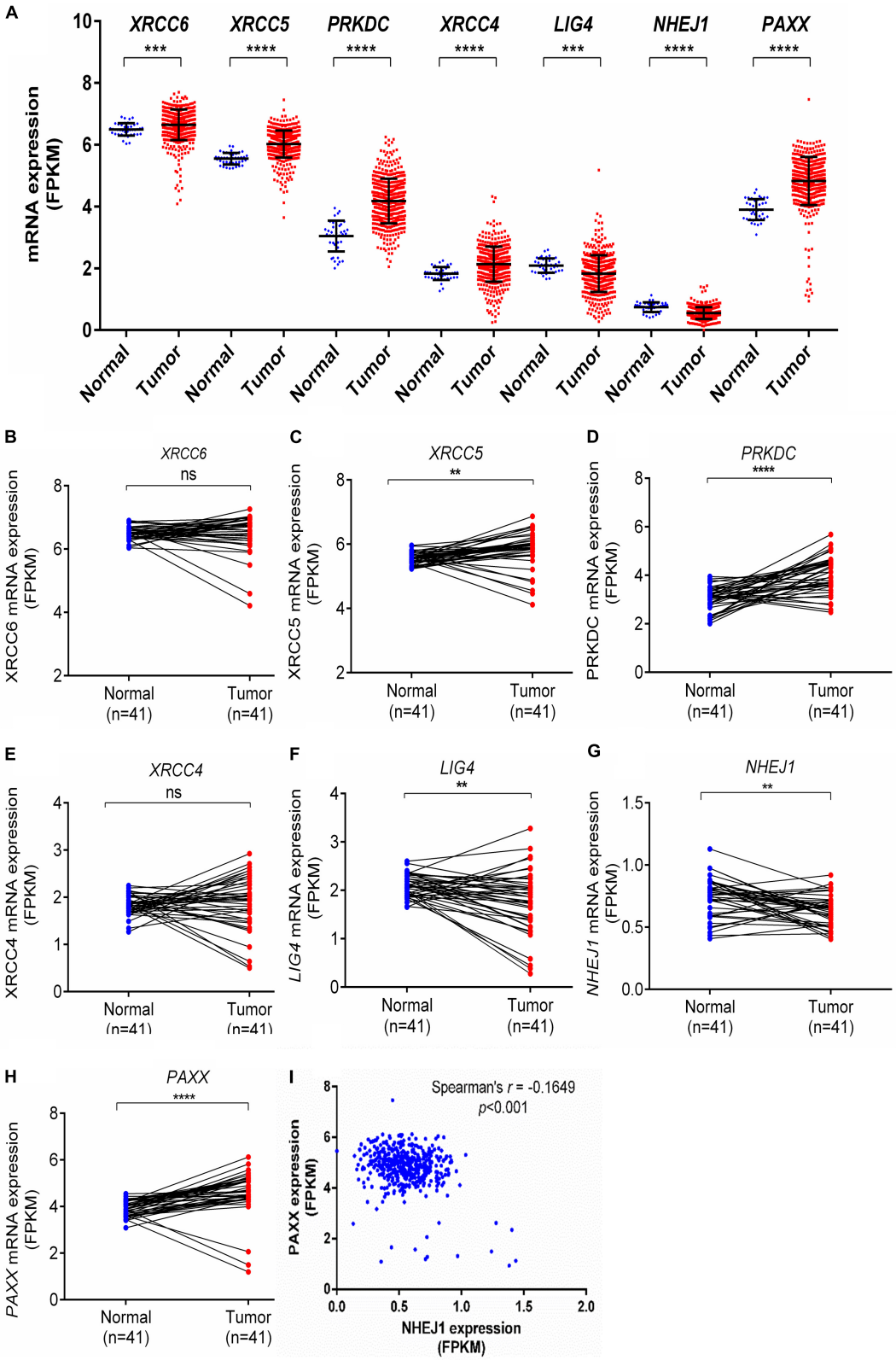

FIGURE 1 | Comparison of mRNA expression of NHEJ pathway genes in normal colon and colon cancer tissues from TCGA-COAD dataset including total samples for seven NHEJ genes **(A)**, and paired samples, including *XRCC6* **(B)**, *XRCC5* **(C)**, *PRKDC* **(D)**, *XRCC4* **(E)**, *LIG4* **(F)**, *NHEJ1* **(G)**, and PAXX **(H)**. $^{*}p < 0.05$, $^{**}p < 0.01$, $^{***}p < 0.001$, $^{****}p < 0.0001$. **(I)** Correlation between *NHEJ1* and *PAXX* expression in the same dataset. FPKM, Fragments per kilo million bases.

retrieved from cBioportal[3] by selecting the TCGA PanCancer Atlas - Colorectal Adenocarcinoma study and selecting patients with colon adenocarcinoma in cancer type (Cerami et al., 2012; Gao et al., 2013).

High throughput total protein and phosphoprotein estimation data for 100 normal colon and 97 colon cancer tissues, generated by mass spectrometry (MS) in Clinical Proteomic Tumor Analysis Consortium (CPTAC) study was analyzed using UALCAN web server[4] (Chen et al., 2019). The *z*-value, used to compare protein levels (depicted on the *y*-axis) represents the standard deviation from the median across samples. As described in UALCAN web server, log2 spectral count ratio values, downloaded from CPTAC colon cancer data were normalized within each sample profile and then normalized across samples to calculate *z*-values as relative protein levels. Available total protein and phosphoprotein levels of the NHEJ pathway were assessed using default parameters in the UALCAN web server.

MEXPRESS web server[5] hosts the DNA methylation data from TCGA studies developed on "Illumina Human Methylation 450 Bead Chip" platform and provides access to methylation levels of designated CpG sites of the queried gene and its association with gene expression (Koch et al., 2015). For DNA methylation analysis, correlation of PAXX expression with the methylation status of its gene was determined using the MEXPRESS web server using default parameters.

Survival Analysis

Kaplan Meier plot was constructed along with log-rank test *p*-values using the "survminer" package in R statistical software (version 4.0.1). Briefly, patients were categorized into high and low expression groups based on median gene expression values in FPKM (extracted from UCSC Xena browser). Univariate analysis was performed for overall survival (OS), disease-specific survival (DSS), disease-free interval (DFI), and progression-free interval (PFI) to establish the association of gene expression and clinicopathological parameters with patient outcome. Multivariate analysis was also performed for genes, which were significantly associated with prognosis in univariate analysis. Important clinical and molecular features, including age, gender, stage, histological subtype, KRAS status, and BRAF status were taken as covariates.

Pathway Analysis

Gene expression correlations of *PAXX* with whole gene expression profiles of colon cancer tissues from TCGA-COAD dataset were extracted from the cBioPortal web server (see text footnote 3). Briefly, *PAXX* expression was used as input in colon adenocarcinoma patient data from TCGA colon cancer (TCGA-COAD PanCancer study) dataset (Cerami et al., 2012; Gao et al., 2013) in cBioPortal. Then, by using the correlation module, the

[3]https://www.cbioportal.org/

[4]http://ualcan.path.uab.edu/

[5]https://mexpress.be/

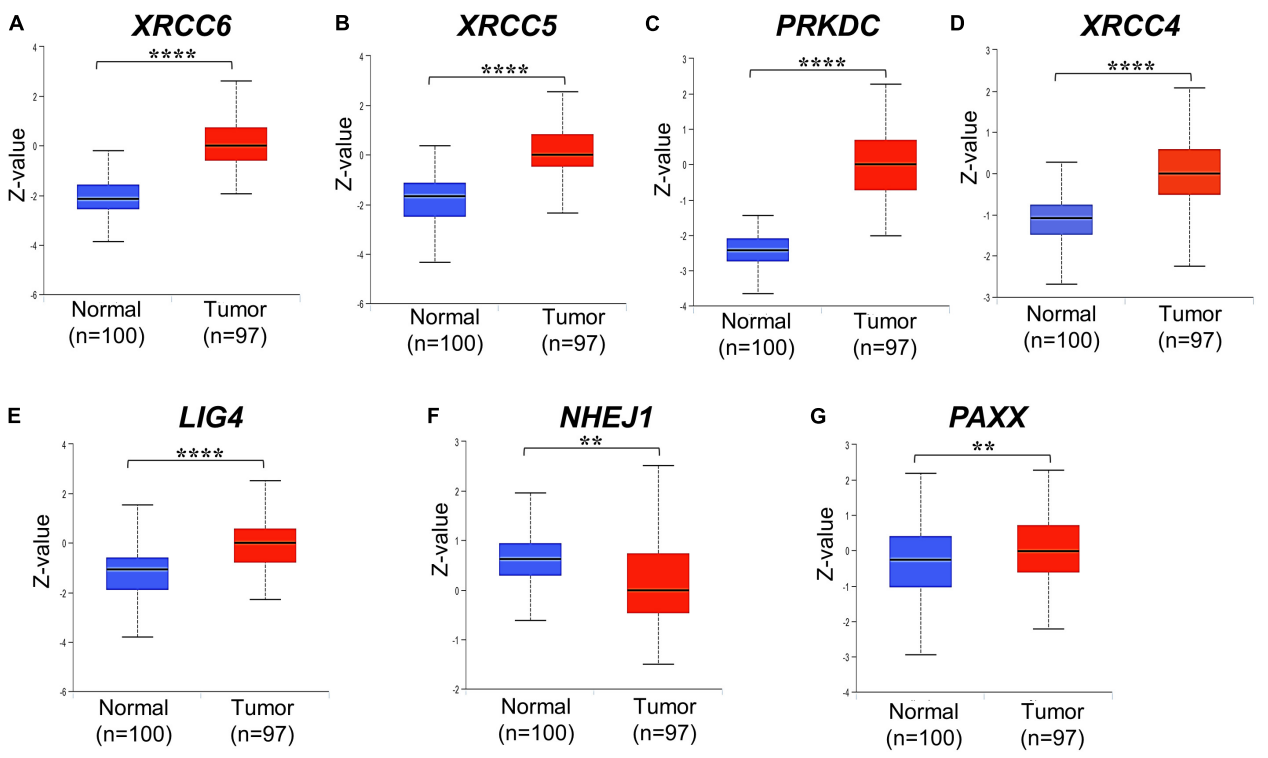

FIGURE 2 | Total protein levels of NHEJ pathway genes in normal tissues and colon cancer tissues from CPTAC study, including **(A)** XRCC6 **(B)** XRCC5 **(C)** PRKDC **(D)** XRCC4 **(E)** LIG4 **(F)** NHEJ1 and **(G)** PAXX. *$p < 0.05$, **$p < 0.01$, ***$p < 0.001$, ****$p < 0.0001$.

whole transcriptome correlations table of *PAXX* expression was retrieved. After filtering correlations with false detection rate normalized q-value < 0.05, genes were arranged by increasing value of Spearman's correlation constant, thus creating a ranked gene file. The ranked gene file was further used as input for the pre-ranked GSEA module in the gene set enrichment analysis tool from Broad Institute[6] with predefined molecular signature database hallmark gene set (version 7.1) as reference gene set for pathway enrichment (Liberzon et al., 2015). Genes enriched in the respective pathways were represented as direct image outputs along with calculated normalized enrichment score (NES), false discovery rate (FDR), and p-value.

Protein Interaction Analysis

Biophysical interactions of ORFeome-based complexes (BioPlex) network interactome tool,[7] a large-scale interactome database based on affinity purification mass spectrometry (AP-MS) data of baits from the human ORFeome (Huttlin et al., 2017) was utilized to identify PAXX interacting proteins in colon cancer cells HCT-116. Then an interaction network of PAXX associated proteins in these cells was constructed using default parameters.

TISIDB Analysis

The tumor-immune interactions database (TISIDB)[8] is an integral web portal for the interaction of tumor and immune system (Ru et al., 2019). This database enabled us to correlate *PAXX* gene expression and infiltration of different immune cells types including CD8 T cells (activated, central memory and effector memory), CD4 T cells (activated, central memory and effector memory), T helper cells (follicular, type 1 and 2), gamma delta T cells, B-cells (activated, immature and mature), dendritic cells (activated, plasmacytoid and immature), NK cells, macrophages, eosinophil, mast cell, neutrophils, and

[6]https://www.gsea-msigdb.org/

[7]https://bioplex.hms.harvard.edu

[8]http://cis.hku.hk/software.html

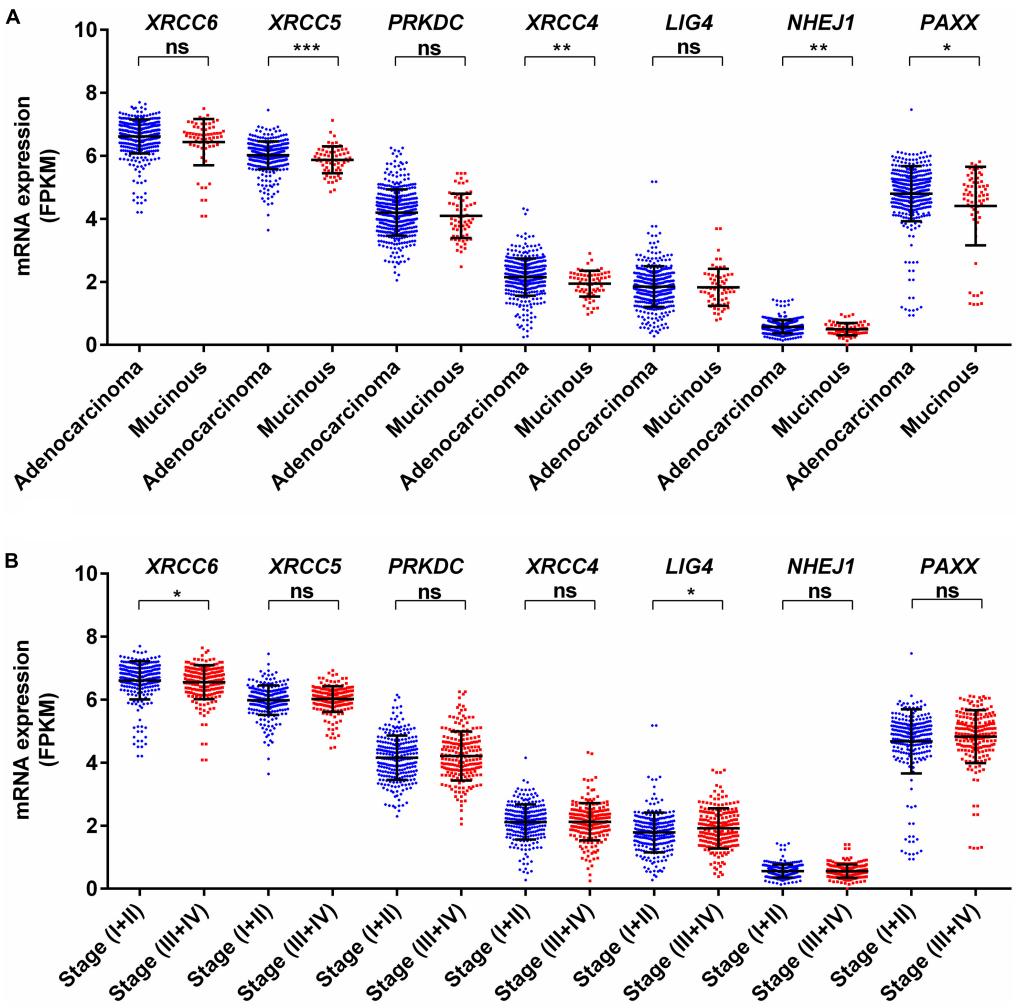

FIGURE 3 | Association of mRNA expression of NHEJ pathway genes with **(A)** tumor histology, and **(B)** stage. $^*p < 0.05$, $^{**}p < 0.01$, $^{***}p < 0.001$, $^{****}p < 0.0001$. FPKM, Fragments per kilo million bases.

monocytes. Immune cell fractions were determined using the computational "deconvolution" approach, which is based on determining mRNA contribution from immune cells from the bulk tumor RNA-sequencing profile.

Statistical Analysis

Gene expression analyses were performed on Graphpad Prism (version 6). Mann-Whitney *U*-test was used for comparing gene expression between normal and colon cancer tissues. *P*-value < 0.05 was considered statistically significant. Wilcoxon paired *t*-test was applied for paired expression analysis between normal and colon cancer tissues. Level of significance denoted on the expression graphs were represented as $^{*}p$-value < 0.05, $^{**}p$-value < 0.01, $^{***}p$-value < 0.001 and $^{****}p$-value < 0.0001. Patients were divided into two groups by median expression and a log-rank test was used to compare groups for Kaplan-Meier survival analysis. Univariate and multivariate survival data analysis were performed on Stata version 11.

RESULTS

mRNA Expression Pattern of NHEJ Pathway Genes in Colon Cancer

To determine the expression pattern of core NHEJ genes in colon cancer, we performed Oncomine analysis for *XRCC6* (Ku70), *XRCC5* (Ku80), *PRKDC* (DNA-PKcs), *XRCC4* (XRCC4), *LIG4* (DNA ligase 4), *NHEJ1* (XLF), and *PAXX* (PAXX/XLS). It provided the advantage of analyzing several datasets in parallel to assess the general expression pattern of these genes. This analysis revealed significant upregulation of five genes, (*XRCC6*, *XRCC4*, *PRKDC*, *XRCC4,* and *PAXX*) and downregulation of two (*LIG4* and *NHEJ1)* NHEJ pathway genes, in tumor tissues compared to the normal tissues (**Table 1**).

To corroborate our findings, we utilized a dataset of colon cancer from The Cancer Genome Atlas (TCGA) to compare the expression of NHEJ pathway genes between tumors and normal colon tissues. Consistent with the Oncomine

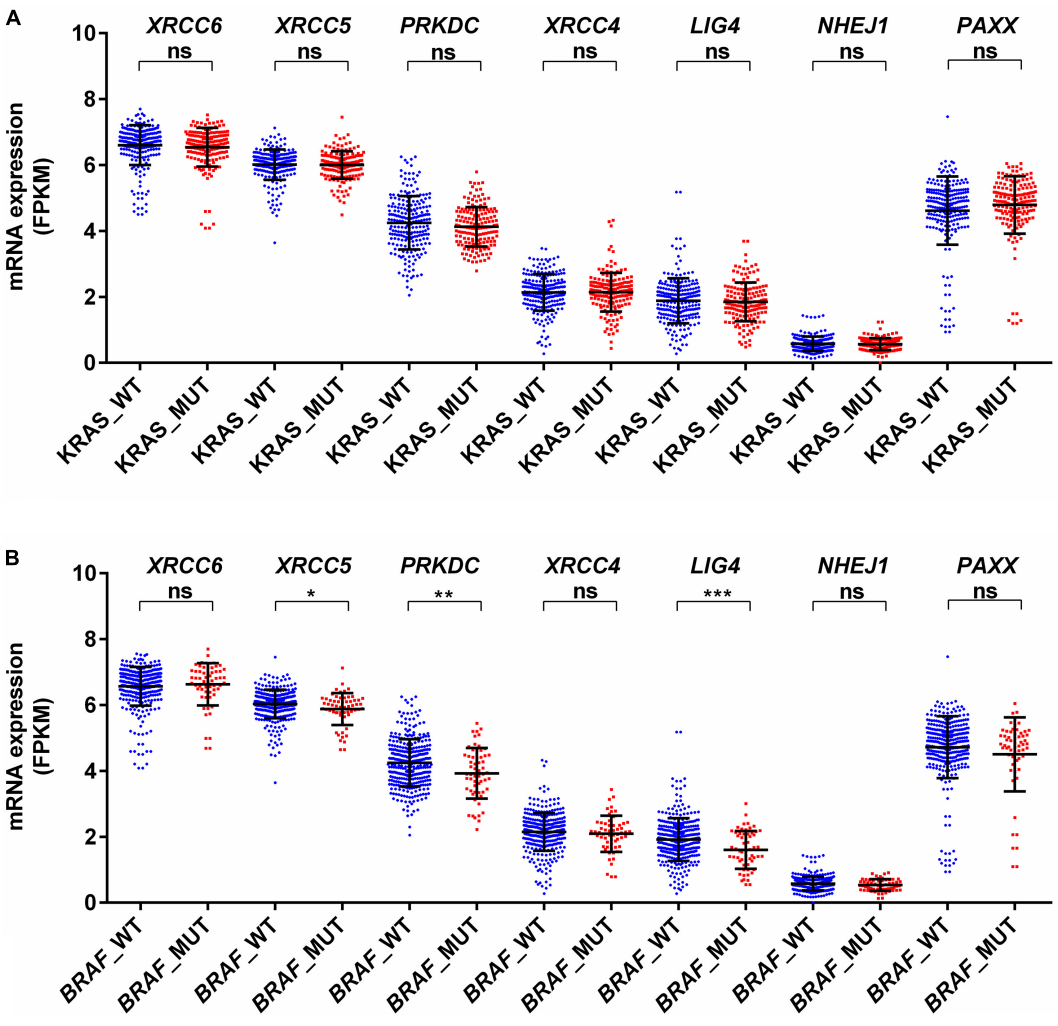

FIGURE 4 | Association of mRNA expression of NHEJ pathway genes with **(A)** *KRAS* mutation status, and **(B)** *BRAF* mutation status. $^{*}p < 0.05$, $^{**}p < 0.01$, $^{***}p < 0.001$, $^{****}p < 0.0001$. FPKM, Fragments per kilo million bases. WT, wild type; MUT, mutant.

analysis, comparison of all available normal (n = 41) and tumor tissues (n = 469) revealed overexpression of *XRCC6*, *XRCC5*, *PRKDC*, *XRCC4,* and *PAXX* in tumors compared to normal tissues, while *LIG4* and *NHEJ1* displayed lower expression in the tumor tissues (**Figure 1A**). However, analysis of 41 paired normal and tumor tissues revealed significant overexpression of only *XRCC5*, *PRKDC,* and *PAXX* genes in tumor tissues compared to the normal colon (**Figures 1C,D,H**, respectively), while *LIG4* and *NHEJ1* still displayed reduced expression (**Figures 1F,G**, respectively). Interestingly, in contrast to Oncomine analysis, *XRCC6* and *XRCC4* did not display differential expression between paired normal and tumor tissues (**Figures 1B,E**, respectively).

Co-expression analysis among all NHEJ pathway genes in TCGA-COAD dataset revealed a negative correlation between *PAXX* and *NHEJ1* expression (**Figure 1I**). While the expression of all other genes of this pathway exhibited positive correlations among them (**Supplementary Table S1**).

Expression of Proteins Encoded by NHEJ Pathway Genes in Colon Cancer

Further, the Clinical Proteomic Tumor Analysis Consortium (CPTAC) dataset, which consists of high throughput mass spectrometry based quantitative protein estimation data of colon cancer and respective normal colon tissues, was used to compare total and phosphorylated protein levels of NHEJ pathway in normal colon tissues (n = 100) and colon cancer (n = 97). Consistent with the Oncomine gene expression analysis, total protein levels of Ku70 (*XRCC6*), Ku80 (*XRCC5*), DNA-PKcs (*PRKDC*), XRCC4, and PAXX were found to be significantly higher in colon cancer tissue compared to normal colon tissues, while *LIG4*, which exhibited reduced mRNA expression in Oncomine analysis, also displayed higher total protein levels in tumors ($p < 0.01$ for all, **Figures 2A–G**). However, NHEJ1 protein levels in line with the Oncomine analysis were observed to be lower in tumor tissues compared to the controls ($p < 0.001$, **Figure 2F**).

DNA-PKcs has been shown to phosphorylate many of the core NHEJ factors *in vitro*, but most of these phosphorylations are non-essential for NHEJ function (Davis et al., 2014). We observed that some uncharacterized phosphorylated protein levels of Ku70 (*XRCC6*, position Ser520, and Thr455), DNA-PKcs (*PRKDC*, Ser893, Ser3995 and Ser3205), and PAXX (Ser148) were higher in colon cancer tissues compared to normal colon tissues (**Supplementary Figures S1A–K**), whereas phosphorylated XLF (*NHEJ1*, Ser287) was lesser in colon cancer tissues.

Interestingly, it has been previously demonstrated that PRKDC is phosphorylated at Ser3995 in response to IR radiation, by ATM serine/threonine kinase (ATM) protein, but this phosphorylation does not affect NHEJ repair (Neal et al., 2011). Further, Douglas et al. (2014) reported that DNA-PKcs is phosphorylated and dephosphorylated at Ser3205 by PLK1 (polo-like kinase 1) and PP6 (protein phosphatase 6), respectively during mitosis. Phospho-mimicry of PAXX phosphorylation at Ser134, Thr145, Ser148, and Ser152 has been reported to destabilize the PAXX-Ku-DNA ternary complex, but it does not

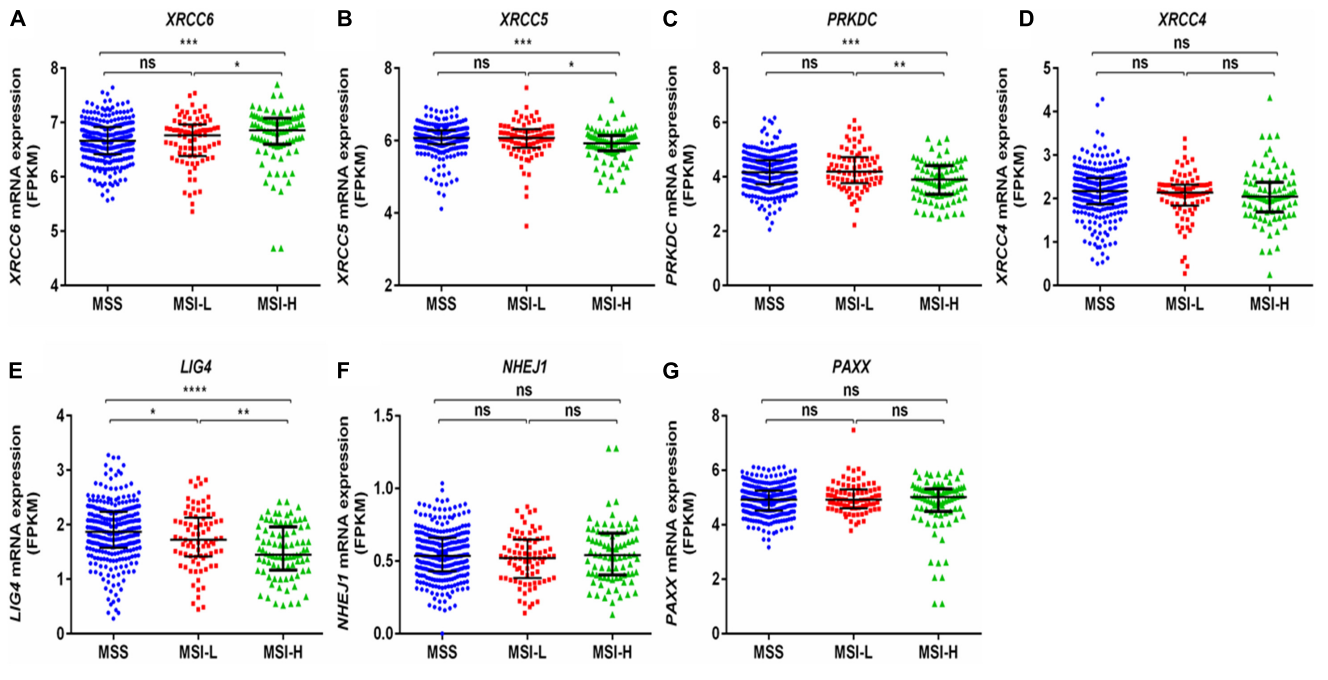

FIGURE 5 | Comparison of mRNA expression of NHEJ pathway genes based on microsatellite instability status from TCGA-COAD dataset. **(A)** XRCC6 **(B)** XRCC5 **(C)** PRKDC **(D)** XRCC4 **(E)** LIG4 **(F)** NHEJ1, and **(G)** PAXX. FPKM, Fragments per kilo million bases. MSI-H, MSI-high; MSI-L, MSI-low; MSS, microsatellite stable. $^{*}p < 0.05$, $^{**}p < 0.01$, $^{***}p < 0.001$, $^{****}p < 0.0001$.

affect the stimulation of LIG4/XRCC4 blunt-ended DNA-ligation activity by PAXX (Tadi et al., 2016). Therefore, the exact role of the modifications of DNA-PKcs and PAXX in NHEJ activity remains unclear and warrants further studies.

Associations of NHEJ Pathway Gene Expression With Clinicopathological Features in Colon Cancer

We analyzed associations of NHEJ pathway gene expression with other clinicopathological features, such as age, gender, histological type, stage, *KRAS* mutation status, *BRAF* mutation status, and microsatellite instability (MSI) status in colon cancer by performing a direct comparison between mRNA expressions of respective genes. None of the seven NHEJ pathway genes analyzed in the present study displayed any association with age (**Supplementary Figures S2A–G**). Only *LIG4* was associated with gender and exhibited higher expression in males compared to females (**Supplementary Figure S3E**). Between two histological subtypes, no difference was observed in the expression of *XRCC6*, *PRKDC*, *LIG4,* and *PAXX*, while expression of *XRCC5*, *XRCC4,* and *NHEJ1* was higher in adenocarcinoma compared to mucinous adenocarcinoma (**Figure 3A**). We further compared the mRNA expression of NHEJ genes between stage (I + II) group with stage (III + IV) group colon tumors. This analysis revealed reduced expression of *XRCC6* in advanced stage group while *LIG4* displayed elevated expression in the same group (**Figure 3B**). However, no difference in mRNA levels of *XRCC5*, *PRKDC*, *XRCC4*, *NHEJ1,* and *PAXX* between the two groups.

KRAS mutations have been reported to enhance homologous recombination repair in preference to NHEJ in colorectal cancer cells (Kalimutho et al., 2017). In agreement with this report, we observed no difference for mRNA expression in all analyzed genes between KRAS wild type and mutant tumors (**Figure 4A**). Therefore, *KRAS* mediated oncogenic reprogramming does not seem to be involved in the altered NHEJ pathway in colon cancer. Concerning *BRAF* mutation in thyroid cancer, two reports

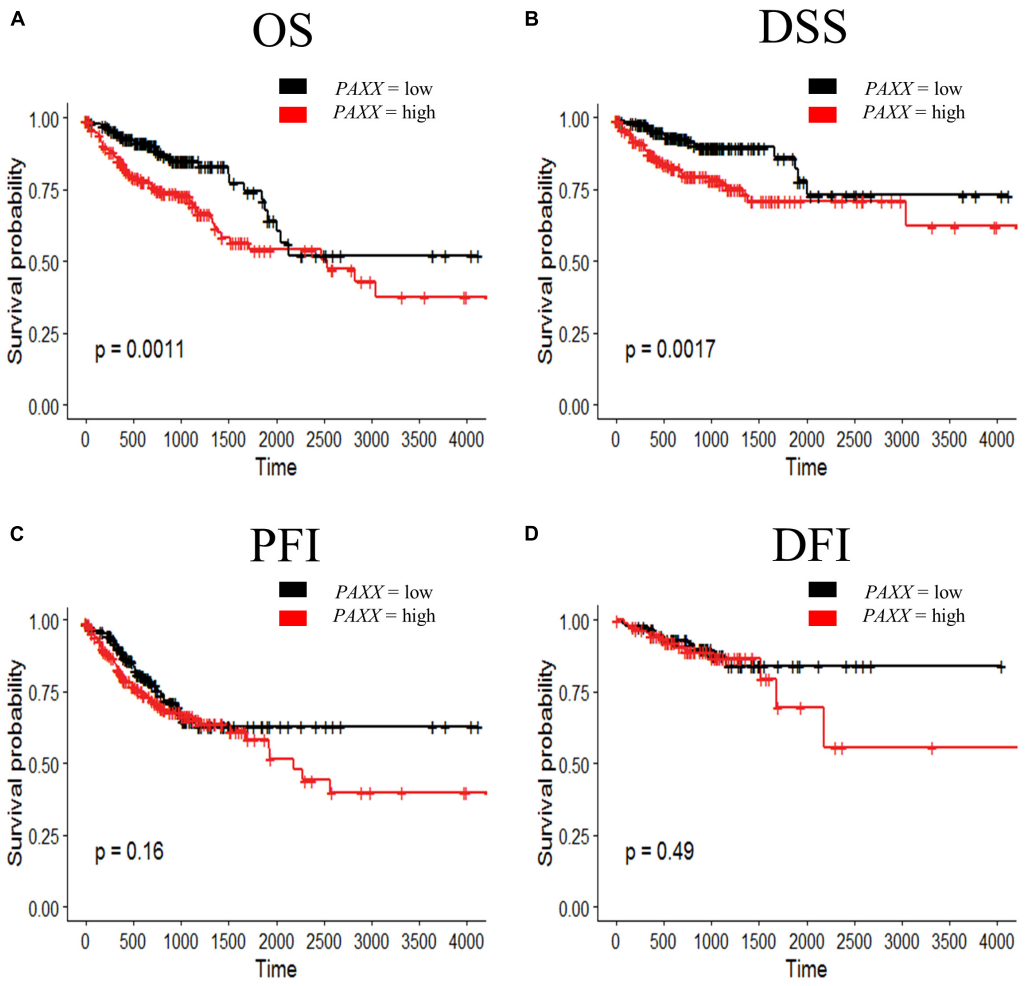

FIGURE 6 | Kaplan-Meier survival curve for prognostic significance of PAXX gene expression in TCGA-COAD dataset, including **(A)** overall survival (OS), **(B)** disease-specific survival (DSS), **(C)** progression-free interval (PFI), and **(D)** disease-free interval (DFI). Survival probabilities are presented on the *y*-axis and time in days on the *x*-axis in all graphs. The log-rank test *p*-value has been depicted in respective graphs.

have demonstrated that *BRAF* mutation promotes NHEJ activity through upregulation of *NHEJ1* and it is also associated with radioresistance (Robb et al., 2018, 2019). In a melanoma cell line model, it has been shown that mutant *BRAF* inhibition may increase DNA damage by downregulation of NHEJ pathway genes, including *XRCC6*, *XRCC5,* and *PRKDC* (Fatkhutdinov et al., 2016). Our analysis revealed that *BRAF* mutant colon cancer did not harbor higher *NHEJ1* expression compared to *BRAF* wild type tumors and three NHEJ pathway genes, *XRCC5*, *PRKDC,* and *LIG4* are indeed lowly expressed in *BRAF* mutant tumors (**Figure 4B**). These results suggest that a detailed study of the NHEJ pathway concerning *BRAF* mutation in colon cancer is further warranted.

Interestingly, a previous report suggests that the NHEJ pathway is impaired in several mismatch repair deficient colon cancer cell lines (Koh et al., 2005). We observed that expression of *XRCC6* was higher in MSI-high tumors compared to MSI-low and microsatellite stable (MSS) tumors, while *XRCC5*, *PRKDC,* and *LIG4* exhibited reduced expression in MSI-high tumors compared to both MSI-low and MSS tumors (**Figures 5A–G**).

Survival Analysis

To further determine the clinical significance of the expression of NHEJ pathway genes in colon cancer, we performed Kaplan-Meier survival analysis for overall survival (OS), disease-specific survival (DSS), progression-free interval (PFI), and disease-free interval (DFI) using TCGA colon cancer dataset. We observed that among all NHEJ pathway genes only elevated *PAXX* expression was associated with poor overall survival (p = 0.0011, **Figure 6A**), while other genes did not display significant association with OS (**Supplementary Figure S4**), DSS (**Supplementary Figure S5**), or PFI (**Supplementary**

TABLE 2 | Univariate analysis of the NHEJ pathway genes and clinicopathological parameters in TCGA-COAD dataset.

	OS			DSS			DFI			PFI		
Variable	**HR**	**95% CI**	***p*-value**	**HR**	**95% CI**	***p*-value**	**HR**	**95% CI**	***p*-value**	**HR**	**95% CI**	***p*-value**
Age	1.017	1.000–1.033	0.041	0.996	0.977–1.016	0.745	1.015	0.981–1.051	0.372	0.996	0.982–1.011	0.675
Gender	**Ref**			**Ref**			**Ref**			**Ref**		
Male										0.811	0.564–1.166	0.260
Female	0.898	0.603–1.335	0.596	0.901	0.540–1.500	0.689	0.592	0.251–1.396	0.231			
Stage I	**Ref**			**Ref**			**Ref**			**Ref**		
II	2.341	0.819–6.694	0.112	3.294	0.416–26 .040	0.258	2.020	0.567–7.195	0.278	2.327	0.979–5.530	0.056
III	4.648	1.650–13.094	0.004	10.45945	1.398–78.212	0.022	2.043	0.539–7.734	0.293	3.707	1.561–8.803	0.003
IV	11.573	4.080–32.827	0.000	.001	6.132–330.249	0.000				14.456	6.113–34.181	0.000
Histology: COAD	**Ref**			**Ref**			**Ref**			**Ref**		
Mucinous COAD	1.300	0.759–2.225	0.338	0.991	0.470–2.088	0.983	0.328	0.044–2.441	0.277	1.029	0.608–1.744	0.913
MSI status: MSS	**Ref**			**Ref**			**Ref**			**Ref**		
MSI-L	1.205	0.732–1.984	0.461	1.282	0.692–2.372	0.429	1.370	0.530–3.539	0.515	1.456	0.939–2.258	0.093
MSI-H	0.918	0.534–1.577	0.758	0.791	0.381–1.642	0.531	0.320	0.072–1.407	0.132	0.828	0.493–1.390	0.476
***KRAS*: WT**	**Ref**			**Ref**			**Ref**			**Ref**		
Mutation	0.982	0.642–1.501	0.933	1.519	0.874–2.641	0.138	2.240	0.927–5.408	0.073	1.770	1.203–2.604	0.004
***BRAF*: WT**	**Ref**			**Ref**			**Ref**			**Ref**		
Mutation	1.159	0.663–2.026	0.604	0.613	0.243–1.547	0.301	0.661	0.153–2.845	0.579	0.793	0.443–1.417	0.434
Gene expression												
PAXX expression	**1.560**	**1.164–1.164**	**0.003***	**1.908**	**1.280–2.844**	**0.002***	1.315	0.796–2.172	0.283	1.153	0.942–1.411	0.166
NHEJ1 expression	0.774	0.288–2.080	0.613	0.298	0.076–1.166	0.082	0.869	0.144–5.221	0.878	0.718	0.305–1.690	0.449
XRCC4 expression	1.051	0.723–1.527	0.794	1.164	0.723–1.872	0.531	1.816	0.880–3.749	0.106	1.042	0.747–1.454	0.806
XRCC5 expression	0.922	0.587–1.450	0.728	1.067	0.591–1.926	0.829	1.768	0.747–4.182	0.195	1.055	0.701–1.589	0.795
XRCC6 expression	1.075	0.762–1.517	0.679	1.127	0.724–1.754	0.594	1.433	0.641–3.204	0.380	1.000	0.749–1.335	0.998
PRKDC expression	0.860	0.652–1.135	0.289	0.837	0.588–1.192	0.325	0.864	0.491–1.520	0.614	0.954	0.744–1.225	0.717
LIG4 expression	1.010	0.745–1.368	0.947	0.978	0.663–1.445	0.915	1.242	0.742–2.080	0.408	1.060	0.813–1.381	0.665

*OS, overall survival; DSS, disease-specific survival; DFI, disease-free interval; PFI, progression-free interval; HR, hazard ratio; CI, confidence interval; * indicates $p < 0.05$. Bold values represent any significant association of analyzed gene with patient prognosis.*

Figure S6). Interestingly, *PAXX* overexpression was also associated with poor DSS (p = 0.0011, **Figure 6B**), but not with PFI or DFI (**Figures 6C,D**, respectively). Furthermore, higher *XRCC4* expression was associated with poor DFI (**Supplementary Figure S7D**).

To assess the robustness of these gene products as prognostic biomarkers, we performed univariate analysis followed by a multivariate analysis using a Cox proportional hazards model. Gene expression was taken as a continuous variable while important clinical features including age, gender, stage, *KRAS* mutation, *BRAF* mutation, and MSI status were taken as covariates. The results of univariate analysis have been presented in **Table 2**. Interestingly, we observed that only *PAXX* overexpression was associated with poor OS and DSS, while the levels of other gene products were not associated with OS, DSS, PFI, or DFI. Therefore, the expression of *PAXX* was considered for multivariate analysis. Interestingly, in multivariate analysis, *PAXX* overexpression emerged as an independent marker for poor OS and DSS (**Table 3**).

Methylation Analysis of the *PAXX* Gene

PAXX gene contains a CpG island spanning its transcription start site (TSS) and the first two exons (**Figure 7A**). Given this information, it was of interest to investigate the role of epigenetic modifications in the overexpression of *PAXX* in colon tumors. For this purpose, we assessed DNA methylation and paired RNA expression data of TCGA-COAD through the MEXPRESS web server. Pearson correlation analysis between methylation of five CpG sites of *PAXX* promoter and transcription of its gene revealed that DNA methylation of two distinct sites captured by probes, cg01126560 and cg25499748 exhibited significant negative correlation to *PAXX* gene expression in TCGA-COAD dataset ($r = -0.232$, $p < 0.001$ and $r = -0.338$, $p < 0.001$, respectively, **Figure 7A**). Further, the level of methylation of cg01126560 was lower in a group of all available colon cancer tissues compared to normal tissues ($p < 0.0001$, **Figure 7B**). Furthermore, a comparison of paired colon cancer tissues with respective normal tissues also revealed that colon cancer tissues exhibit lower methylation of cg01126560 ($p < 0.0001$, **Figure 7C**). These results suggested the involvement of methylation in transcriptional regulation of *PAXX* expression in colon carcinoma.

Cellular Pathways Associated With *PAXX* Expression in Colon Cancer

To assess the oncogenic pathways associated with *PAXX* expression in colon cancer, we performed gene set enrichment analysis (GSEA) for cancer hallmarks pathways using genes that exhibited significant correlations with *PAXX*. Among

TABLE 3 | Multivariate analysis of *PAXX* expression and clinicopathological parameters in TCGA-COAD dataset.

	OS			DSS			DFI			PFI		
Variable	**HR**	**95% CI**	***p*-value**	**HR**	**95% CI**	***p*-value**	**HR**	**95% CI**	***p*-value**	**HR**	**95% CI**	***p*-value**
Age	1.038	1.018–1.058	0.000	1.022	0.998–1.047	0.065	1.002	0.959–1.048	0.903	1.006	0.989–1.023	0.436
Gender	**Ref**			**Ref**			**Ref**			**Ref**		
Male												
Female	1.049	0.658–1.673	0.839	1.263	0.708–2.252	0.428	0.526	0.190–1.460	0.218	0.849	0.561–1.287	0.442
Stage I	**Ref**			**Ref**			**Ref**			**Ref**		
II	2.614	0.784–8.718	0.118	2.640	0.327–21.280	0.362	2.274	0.622–8.300	0.214	3.265	1.152–9.249	0.026
III	6.039	1.809–20.155	0.003	10.240	1.346–77.872	0.025	2.257	0.542–9.398	0.263	6.349	2.227–18.101	0.001
IV	20.672	6.042–70.719	0.000	52.407	6.937–395.919	0.000				21.135	7.284–61.319	0.000
Histology: COAD	**Ref**			**Ref**			**Ref**			**Ref**		
Mucinous COAD	1.495	0.820–2.725	0.189	0.931	0.387–2.238	0.874	0.00	0.000–0.000	1.000	0.870	0.460–1.646	0.670
MSI status: MSS	**Ref**			**Ref**			**Ref**			**Ref**		
MSI-L	1.305	0.750–2.269	0.346	1.417	0.726–2.766	0.306	1.457	0.536–3.958	0.460	1.799	1.127–2.873	0.014
MSI-H	0.967	0.403–2.318	0.941	1.376	0.430–4.404	0.590	0.268	0.033–2.144	0.215	1.462	0.709–3.017	0.303
***KRAS*: WT**	**Ref**			**Ref**			**Ref**			**Ref**		
Mutation	1.178	0.714–1.944	0.520	1.955	1.062–3.601	0.031	2.062	0.804–5.287	0.132	1.918	1.247–2.949	0.003
***BRAF*: WT**	**Ref**			**Ref**			**Ref**			**Ref**		
Mutation	1.694	0.691–4.153	0.249	1.337	0.362–4.940	0.663	2.842	0.356–22.656	0.324	1.251	0.539–2.903	0.601
***PAXX* expression**	**1.562**	**1.065–2.291**	**0.022***	**1.858**	**1.122–3.075**	**0.016***	1.036	0.495–2.167	0.924	1.049	0..764–1.442	0.764

*OS, overall survival; DSS, disease-specific survival; DFI, disease-free interval; PFI, progression-free interval; HR, hazard ratio; CI, confidence interval; * indicates $p < 0.05$. Bold values represent any significant association of analyzed gene with patient prognosis.*

positively correlated pathways, *PAXX* expression exhibited the most significant correlation with oxidative phosphorylation (**Figure 8A**), besides other metabolic pathways including glycolysis (**Figure 8F**), fatty acid metabolism (**Figure 8G**), and adipogenesis (**Figure 8H**). We also observed a positive correlation of PAXX with DNA repair (**Figure 8E**), MYC targets (**Figures 8B,C**), E2F targets (**Figure 8D**), G2M checkpoint (**Figure 8I**), and reactive oxygen species (**Figure 8J**), pathways. Further, protein interaction data of *PAXX* protein in HCT-116 colon cancer cell line from "Bioplex 2.0" database also revealed interaction of *PAXX* with Werner syndrome ATP-dependent helicase (*WRN*), an established mediator of NHEJ pathway, supporting the involvement of *PAXX* in NHEJ pathway in colon cancer (**Figure 8K**). Interestingly, PAXX was also observed to interact with genes involved in glutathione metabolism, including glutathione peroxidase 1 and 7 (GPX1 and GPX7, respectively), which are primarily involved in protecting cells from oxidative stress, suggesting additional pro-tumor roles of PAXX in conferring therapeutic resistance to colon cancer cells.

We observed a significant negative correlation between PAXX expression and epithelial to mesenchymal transition pathway (**Supplementary Figure S8A**). Other pathways that exhibited a negative correlation with PAXX included downregulated genes in UV response, KRAS signaling, Hedgehog signaling, and angiogenesis (**Supplementary Figures S8B–E**). Interestingly, we also observed a negative correlation of PAXX with immunity associated pathways including inflammatory response, TGF beta signaling, and complement pathway (**Supplementary Figures S8F–H**). We further correlated *PAXX* expression with the computationally determined abundance of different tumor-infiltrating immune cells in TCGA-COAD dataset. *PAXX* was observed to be negatively correlated with twenty different immune cells, thereby suggesting the association of *PAXX* expression with overall reduced tumor immune infiltration in colon cancer (**Supplementary Figure S9**).

DISCUSSION

Aberrations in the NHEJ pathway are common in cancers. Hosoi et al. reported elevated expression of Ku70 and Ku80 mRNA as well as proteins in colorectal carcinoma compared to the normal colon (Hosoi et al., 2004). In contrast, Beggs et al. reported reduced expression of Ku70 in colon cancer cells, which was associated with higher genomic instability (Beggs et al., 2012). In another study, it was observed that cytoplasmic Ku70 protein levels are higher in patients who do not respond to chemoradiotherapy, while Ku80 was lost in those patients (Pucci et al., 2017). Thus, previous studies have described both overexpression and downregulation of NHEJ pathway genes in colorectal cancer. Also, some of these studies have estimated mRNA levels while others have assessed protein expression. To resolve this paradox, we performed a comprehensive analysis of the core NHEJ pathway genes in colon cancer. Our analysis revealed elevated mRNA and protein expression of *XRCC6* (Ku70) and *XRCC5* (Ku80) in colon cancer compared to normal

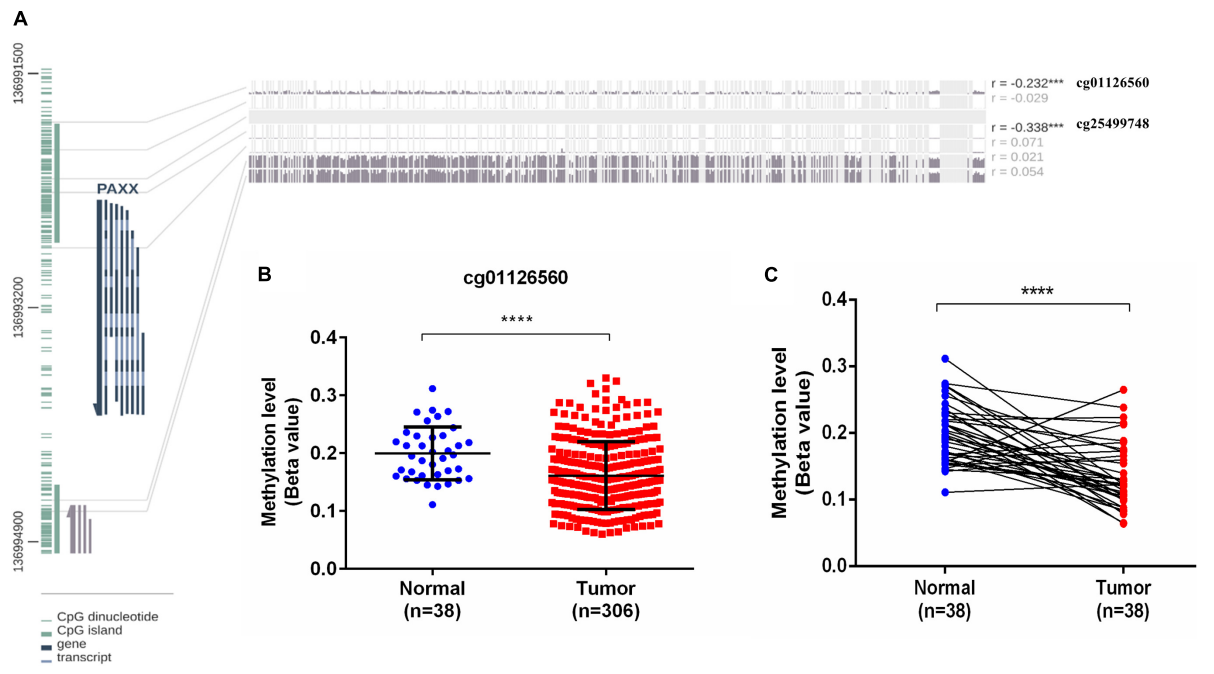

FIGURE 7 | DNA methylation analysis of the PAXX gene from TCGA-COAD dataset. **(A)** Graphical representation of CpG Island and sites around PAXX genomic locus with Pearson's correlation values of PAXX expression with methylation of different CpG sites. **(B)** Comparison of DNA methylation levels of cg01126560 between total normal and colon cancer tissues. **(C)** Comparison of DNA methylation levels of cg01126560 between paired normal colon and colon cancer tissues. $^{*}p < 0.05$, $^{**}p < 0.01$, $^{***}p < 0.001$, $^{****}p < 0.0001$.

colon tissue. Furthermore, the overexpression pattern is more robust for *XRCC5* as observed in paired normal and tumor tissue comparison, while *XRCC6* did not exhibit significant difference. Indeed, we observed reduced *XRCC6* expression in tumors at an advanced stage (stage III + IV) compared to the lower stage (stage I + II).

PRKDC exhibited overexpression in Oncomine analysis, TCGA dataset as well as CPTAC study suggesting consistent overexpression of this protein in colon cancer, both at the mRNA and protein levels. *PRKDC* expression was not associated with age, gender, stage, and histology. A previous study had also reported higher mRNA and protein levels of *PRKDC* in colorectal cancer tissues compared to normal tissues, which also exhibited a positive correlation with expression of *XRCC6* and *XRCC5* (Hosoi et al., 2004). In our analysis these three proteins exhibited a significant positive correlation with each other. Further, a recent report highlighted the dependency of colorectal cancer cells on *PRKDC* and also showed that *PRKDC* overexpression in colon cancer is associated with poor OS (Sun et al., 2016). While we observed a similar pattern of overexpression of *PRKDC* in colon cancer, its mRNA expression was not associated with any of the four types of survival parameters analyzed. Therefore, the collective data along with our results validate *PRKDC* overexpression as a potential therapeutic target in colon cancer.

Gene polymorphism in *XRCC4* has been associated with CRC risk (Bau et al., 2010; Zhang and Hu, 2011). Our analysis revealed elevated levels of *XRCC4* mRNA in Oncomine and protein data analysis, respectively, whereas the comparison of expression between paired normal and tumor tissues in TCGA dataset did not exhibit a significant difference in *XRCC4* expression. A previous detailed report suggests that LIG4 protein levels are upregulated in colon cancer tissues and mediate Wnt/beta-catenin signaling induced radioresistance (Jun et al., 2016). In another study, quantitative RT–PCR in 61 paired normal colon and 393 CRCs demonstrated *LIG4* downregulation in colon cancer tissues, which was further associated with its promoter hypermethylation (Kuhmann et al., 2014). While our results also suggest consistent downregulation of *LIG4* mRNA expression in tumor cells, proteomic analysis displayed higher *LIG4* levels in colon tumors. Furthermore, we observed higher expression of *LIG4* in advanced stage tumors and male patients. Association of *LIG4* mRNA expression with its protein levels and gender has not been reported and requires further exploration.

XLF (*NHEJ1*) was recently shown to enhance resistance to oxaliplatin and 5-fluorouracil in colorectal cancer cell lines (Liu

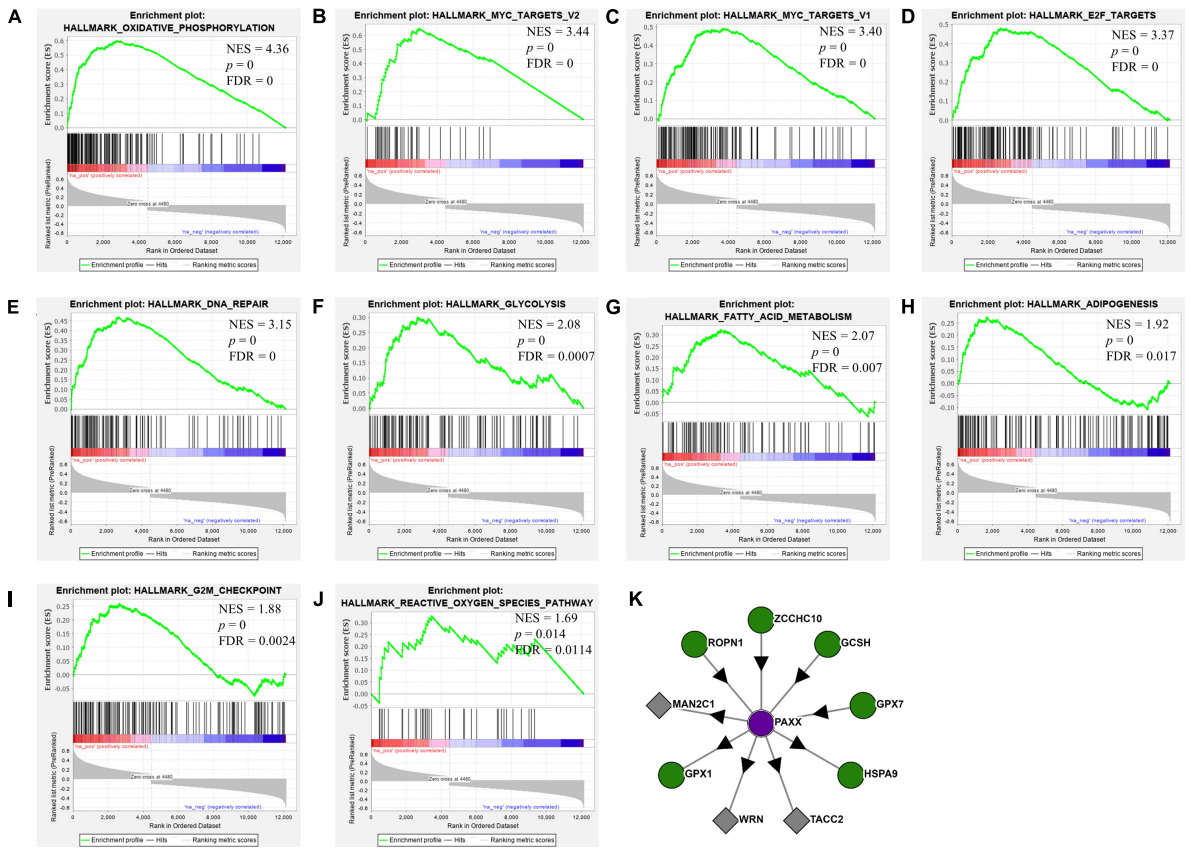

FIGURE 8 | Gene set enrichment analysis of PAXX correlated genes in the TCGA-COAD dataset. Each plot **(A–J)** depicts positively enriched pathways of PAXX correlated genes with normalized enrichment score (NES), false discovery rate (FDR), and *p*-value depicted inside the respective pathway. **(K)** Depict results from the Bioplex 2.0 web server, showing protein-protein interactions of PAXX in HCT-116 colon cancer cell line.

et al., 2019). Association of higher XLF expression with drug resistance in hepatocellular carcinoma has also been reported (Yang and Wang, 2017). Contrary to these observations, we found consistent downregulation of XLF in colon cancer in our analysis, both at mRNA and the protein levels. Furthermore, its reduced mRNA expression was associated with the mucinous subtype, while no association was observed with the tumor stage. These results signify that although XLF is capable to induce drug resistance in CRC cells, its expression is nevertheless, downregulated in colon cancer. Intriguingly, we observed that *NHEJ1* expression is negatively correlated with *PAXX* expression, and PAXX was observed to be consistently overexpressed in colon tumors compared to the normal tissues, both at the mRNA and protein levels. Interestingly, PAXX and XLF are functionally redundant (Kumar et al., 2016; Tadi et al., 2016), and also exhibit synthetic lethality (Liu et al., 2017). These results suggest that *PAXX* may preferentially function over XLF in DSB repair in colon cancer, which has been graphically represented in **Figure 9**.

Our survival analysis revealed that among the NHEJ pathway genes analyzed in the current study, only *PAXX* emerged as an independent prognostic biomarker, while other *NHEJ1* genes did not display any prognostic significance. In concordance to *PAXX* overexpression observed in colon tumors, higher expression of *PAXX* was associated with poor OS and DSS. Further, the expression and prognostic value of *PAXX* did not display any association with the stage and MSI status. DNA methylation analysis revealed a negative correlation of *PAXX* expression with its promoter methylation and the extent of methylation in this gene was found to be lower in tumors compared to the normal colon. We conclude from these results that *PAXX* expression in colon cancer is at least partly under epigenetic control.

As our results suggest the utility of *PAXX* as a potential therapeutic target in colon cancer, we performed gene set enrichment analysis to further determine the association of *PAXX* expression with underlying oncogenic pathways in colon cancer. In agreement with its established role in DNA repair, *PAXX* associated genes were highly enriched in DNA repair and cell cycle related processes. Recently, Yang et al., reported that *PAXX* also plays an important role in the base excision repair pathway and *PAXX* deficient cells display higher sensitivity to temozolomide in glioma cells (Yang et al., 2018). These results collectively suggest that *PAXX* may play important roles in different DNA repair pathways as well and *PAXX* may serve as a novel therapeutic target for DNA repair in cancer cells. Much before the detailed functions of PAXX were determined, Meyer et al. reported the association of *PAXX* overexpression with rapid leukemia establishment in a mouse model of human acute lymphocytic leukemia xenograft, and shorter time to relapse in the corresponding patients

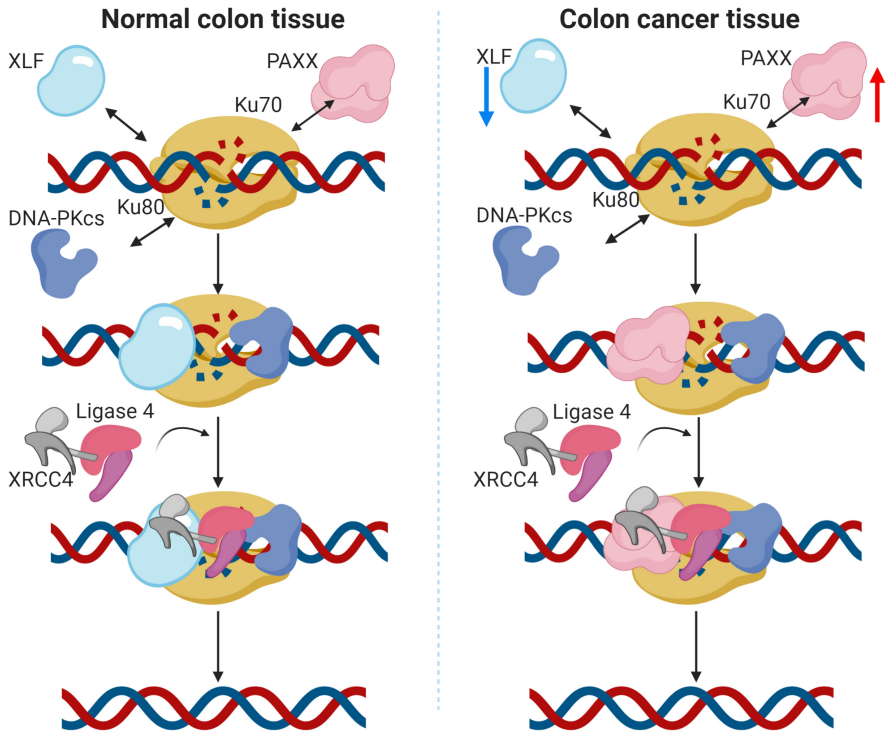

FIGURE 9 | Graphical representation of the proposed function of PAXX in the NHEJ pathway in colon cancer. In normal colon tissues (**left** panel), DNA double strand breaks (DSBs) are actively identified by Ku70 and Ku80, followed by the recruitment of DNA-PKcs. The Ku/DNA-PKcs complex phosphorylates and recruits other accessory factors for DNA end processing. XRCC4 and XLF also bind to the DSB site and recruit DNA Ligase IV, which eventually seals the DSBs. PAXX has been demonstrated to work in the absence of XLF, as a backup in c-NHEJ repair (Tadi et al., 2016). In the case of colon cancer (**right** panel), protein levels of these proteins are altered. Notably, XLF is downregulated and PAXX is upregulated, suggesting PAXX may preferentially take over the XLF functions in colon cancer cells.

(Meyer et al., 2011). Other pathways associated with higher *PAXX* expression, were related to cell metabolism, including higher oxidative phosphorylation and glycolytic pathway while UV response, *KRAS* signaling, and angiogenesis pathways were associated with lower *PAXX* expression. While pathway analysis in the present study revealed close associations of *PAXX* expression with several other oncogenic pathways as well, it requires further exploration to provide causal relationships between *PAXX* expression and alterations of these pathways. Nevertheless, we observed that several immune system associated pathways including inflammatory response, TGF beta signaling, and complement pathway were negatively associated with *PAXX* expression. Furthermore, *PAXX* expression exhibited a negative association with the abundance of immune cells in the colon tumor microenvironment, which suggests its association with reduced overall infiltration of immune cells in colon cancer. Interestingly, reduced tumor inflammatory infiltrate is generally associated with poor prognosis in colorectal cancers (Mei et al., 2014). Thus our study provides novel insights into NHEJ pathway status in colon cancer and suggests the potential utility of PAXX as a novel prognostic marker and a therapeutic target in colon cancer.

DATA AVAILABILITY STATEMENT

All datasets presented in this study are included in the article/**Supplementary Material**.

ETHICS STATEMENT

Ethical review and approval was not required for the study on human participants in accordance with the local legislation and institutional requirements.

AUTHOR CONTRIBUTIONS

MA conceptualized the study. SC supervised the study and provided infrastructure to carry out this work. MA, SK, JS, and AC performed the data curation, interpretation, and statistical analysis. MA and SK wrote the original manuscript. AC and SC reviewed and edited the manuscript. All the authors approved the final manuscript.

FUNDING

This work is supported by the DBT/Wellcome Trust India Alliance Fellowship (grant number: IA/CPHI/17/1/503333) awarded to AC. SC acknowledges financial support from Indian Council of Medical Research (ICMR, India), (grant number: 2019-2914).

ACKNOWLEDGMENTS

MA acknowledges financial support as a fellowship from Council of Scientific and Industrial Research, Government of India. SK acknowledges financial support as fellowship from Department of Health Research, Government of India. JS acknowledges financial support as fellowship from Department of Biotechnology, Government of India.

SUPPLEMENTARY MATERIAL

The Supplementary Material for this article can be found online at: https://www.frontiersin.org/articles/10.3389/fmolb.2020.584053/full#supplementary-material

REFERENCES

Arnold, M., Sierra, M. S., Laversanne, M., Soerjomataram, I., Jemal, A., and Bray, F. (2017). Global patterns and trends in colorectal cancer incidence and mortality. *Gut* 66, 683–691. doi: 10.1136/gutjnl-2015-310912

Bau, D.-T., Yang, M.-D., Tsou, Y.-A., Lin, S.-S., Wu, C.-N., Hsieh, H.-H., et al. (2010). Colorectal cancer and genetic polymorphism of dna double-strand break repair gene XRCC4 in Taiwan. *Anticancer. Res.* 30, 2727–2730.

Beggs, A. D., Domingo, E., McGregor, M., Presz, M., Johnstone, E., Midgley, R., et al. (2012). Loss of expression of the double strand break repair protein ATM is associated with worse prognosis in colorectal cancer and loss of Ku70 expression is associated with CIN. *Oncotarget* 3, 1348–1355. doi: 10.18632/oncotarget.694

Bray, F., Ferlay, J., Soerjomataram, I., Siegel, R. L., Torre, L. A., and Jemal, A. (2018). Global cancer statistics 2018: GLOBOCAN estimates of incidence and mortality worldwide for 36 cancers in 185 countries. *CA Cancer J. Clin.* 68, 394–424. doi: 10.3322/caac.21492

Cerami, E., Gao, J., Dogrusoz, U., Gross, B. E., Sumer, S. O., Aksoy, B. A., et al. (2012). The cBio cancer genomics portal: an open platform for exploring multidimensional cancer genomics data. *Cancer Discov.* 2, 401–404. doi: 10.1158/2159-8290.CD-12-0095

Chang, H. H. Y., Pannunzio, N. R., Adachi, N., and Lieber, M. R. (2017). Non-homologous DNA end joining and alternative pathways to double-strand break repair. *Nat. Rev. Mol. Cell Biol.* 18, 495–506. doi: 10.1038/nrm.2017.48

Chen, F., Chandrashekar, D. S., Varambally, S., and Creighton, C. J. (2019). Pan-cancer molecular subtypes revealed by mass-spectrometry-based proteomic characterization of more than 500 human cancers. *Nat. Commun.* 10, 1–15. doi: 10.1038/s41467-019-13528-0

Craxton, A., Munnur, D., Jukes-Jones, R., Skalka, G., Langlais, C., Cain, K., et al. (2018). PAXX and its paralogs synergistically direct DNA polymerase λ activity in DNA repair. *Nat. Commun.* 9:3877. doi: 10.1038/s41467-018-06127-y

Davis, A. J., Chen, B. P. C., and Chen, D. J. (2014). DNA-PK: a dynamic enzyme in a versatile DSB repair pathway. *DNA Repair.* 17, 21–29. doi: 10.1016/j.dnarep.2014.02.020

Douglas, P., Ye, R., Trinkle-Mulcahy, L., Neal, J. A., De Wever, V., Morrice, N. A., et al. (2014). Polo-like kinase 1 (PLK1) and protein phosphatase 6 (PP6) regulate DNA-dependent protein kinase catalytic subunit (DNA-PKcs) phosphorylation in mitosis. *Biosci. Rep.* 34:e00113. doi: 10.1042/BSR20140051

Fatkhutdinov, N., Sproesser, K., Krepler, C., Liu, Q., Brafford, P. A., Herlyn, M., et al. (2016). Targeting RRM2 and Mutant BRAF is a novel combinatorial strategy for melanoma. *Mol. Cancer Res.* 14, 767–775. doi: 10.1158/1541-7786.MCR-16-0099

Gao, J., Aksoy, B. A., Dogrusoz, U., Dresdner, G., Gross, B., Sumer, S. O., et al. (2013). Integrative analysis of complex cancer genomics and clinical profiles using the cBioPortal. *Sci. Signal.* 6:pl1. doi: 10.1126/scisignal.2004088

Hosoi, Y., Watanabe, T., Nakagawa, K., Matsumoto, Y., Enomoto, A., Morita, A., et al. (2004). Up-regulation of DNA-dependent protein kinase activity and Sp1 in colorectal cancer. *Int. J. Oncol.* 25, 461–468.

Huttlin, E. L., Bruckner, R. J., Paulo, J. A., Cannon, J. R., Ting, L., Baltier, K., et al. (2017). Architecture of the human interactome defines protein communities and disease networks. *Nature* 545, 505–509. doi: 10.1038/nature22366

Jun, S., Jung, Y.-S., Suh, H. N., Wang, W., Kim, M. J., Oh, Y. S., et al. (2016). LIG4 mediates Wnt signalling-induced radioresistance. *Nat. Commun.* 7, 1–13. doi: 10.1038/ncomms10994

Kalimutho, M., Bain, A. L., Mukherjee, B., Nag, P., Nanayakkara, D. M., Harten, S. K., et al. (2017). Enhanced dependency of KRAS-mutant colorectal cancer cells on RAD51-dependent homologous recombination repair identified from genetic interactions in *Saccharomyces cerevisiae*. *Mol. Oncol.* 11, 470–490. doi: 10.1002/1878-0261.12040

Koch, A., De Meyer, T., Jeschke, J., and Van Criekinge, W. (2015). MEXPRESS: visualizing expression, DNA methylation and clinical TCGA data. *BMC Genomics* 16:636. doi: 10.1186/s12864-015-1847-z

Koh, K. H., Kang, H. J., Li, L. S., Kim, N.-G., You, K. T., Yang, E., et al. (2005). Impaired nonhomologous end-joining in mismatch repair-deficient colon carcinomas. *Lab. Invest.* 85, 1130–1138. doi: 10.1038/labinvest.3700315

Kuhmann, C., Li, C., Kloor, M., Salou, M., Weigel, C., Schmidt, C. R., et al. (2014). Altered regulation of DNA ligase IV activity by aberrant promoter DNA methylation and gene amplification in colorectal cancer. *Hum. Mol. Genet.* 23, 2043–2054. doi: 10.1093/hmg/ddt599

Kumar, V., Alt, F. W., and Frock, R. L. (2016). PAXX and XLF DNA repair factors are functionally redundant in joining DNA breaks in a G1-arrested progenitor B-cell line. *PNAS* 113, 10619–10624. doi: 10.1073/pnas.1611882113

Liberzon, A., Birger, C., Thorvaldsdóttir, H., Ghandi, M., Mesirov, J. P., and Tamayo, P. (2015). The molecular signatures database (MSigDB) hallmark gene set collection. *Cell Syst.* 1, 417–425. doi: 10.1016/j.cels.2015.12.004

Liu, X., Shao, Z., Jiang, W., Lee, B. J., and Zha, S. (2017). PAXX promotes KU accumulation at DNA breaks and is essential for end-joining in XLF-deficient mice. *Nat. Commun.* 8:13816. doi: 10.1038/ncomms13816

Liu, Z., Yu, M., Fei, B., Sun, J., and Wang, D. (2019). Nonhomologous end joining key factor XLF enhances both 5-florouracil and oxaliplatin resistance in colorectal cancer. *Onco Targets Ther.* 12, 2095–2104. doi: 10.2147/OTT.S192923

Ma, W., Yang, L., Liu, H., Chen, P., Ren, H., and Ren, P. (2020). PAXX is a novel target to overcome resistance to doxorubicin and cisplatin in osteosarcoma. *Biochem. Biophys. Res. Commun.* 521, 204–211. doi: 10.1016/j.bbrc.2019.10.108

Mei, Z., Liu, Y., Liu, C., Cui, A., Liang, Z., Wang, G., et al. (2014). Tumour-infiltrating inflammation and prognosis in colorectal cancer: systematic review and meta-analysis. *Br. J. Cancer* 110, 1595–1605. doi: 10.1038/bjc.2014.46

Meyer, L. H., Eckhoff, S. M., Queudeville, M., Kraus, J. M., Giordan, M., Stursberg, J., et al. (2011). Early relapse in ALL is identified by time to leukemia in NOD/SCID mice and is characterized by a gene signature involving survival pathways. *Cancer Cell* 19, 206–217. doi: 10.1016/j.ccr.2010.11.014

Mijnes, J., Veeck, J., Gaisa, N. T., Burghardt, E., de Ruijter, T. C., Gostek, S., et al. (2018). Promoter methylation of DNA damage repair (DDR) genes in human tumor entities: RBBP8/CtIP is almost exclusively methylated in bladder cancer. *Clin. Epigenet.* 10:15. doi: 10.1186/s13148-018-0447-6

Naccarati, A., Rosa, F., Vymetalkova, V., Barone, E., Jiraskova, K., Di Gaetano, C., et al. (2015). Double-strand break repair and colorectal cancer: gene variants within 3′ UTRs and microRNAs binding as modulators of cancer risk and clinical outcome. *Oncotarget* 7, 23156–23169. doi: 10.18632/oncotarget.6804

Neal, J. A., Dang, V., Douglas, P., Wold, M. S., Lees-Miller, S. P., Meek, K., et al. (2011). Inhibition of homologous recombination by DNA-dependent protein kinase requires kinase activity, is titratable, and is modulated by autophosphorylation. *Mol. Cell. Biol.* 31, 1719–1733. doi: 10.1128/MCB.01298-10.

Ochi, T., Blackford, A. N., Coates, J., Jhujh, S., Mehmood, S., Tamura, N., et al. (2015). PAXX, a paralog of XRCC4 and XLF, interacts with Ku to promote DNA double-strand break repair. *Science* 347, 185–188. doi: 10.1126/science.1261971

Pucci, S., Polidoro, C., Joubert, A., Mastrangeli, F., Tolu, B., Benassi, M., et al. (2017). Ku70, Ku80, and sClusterin: a cluster of predicting factors for response to neoadjuvant chemoradiation therapy in patients with locally advanced rectal cancer. *Int. J. Radiat. Oncol. Biol. Phys.* 97, 381–388. doi: 10.1016/j.ijrobp.2016.10.018

Rawla, P., Sunkara, T., and Barsouk, A. (2019). Epidemiology of colorectal cancer: incidence, mortality, survival, and risk factors. *Prz. Gastroenterol.* 14, 89–103. doi: 10.5114/pg.2018.81072

Robb, R., Yang, L., Shen, C., Saji, M., Ringel, M., and Williams, T. M. (2018). BRAF oncogenic activation induces radioresistance through non-homologous end-joining repair which is abrogated by targeted inhibition of braf mutational activity. *Int. J. Radiat. Oncol. Biol. Phys.* 102:S117. doi: 10.1016/j.ijrobp.2018.06.293

Robb, R., Yang, L., Shen, C., Wolfe, A., Webb, A., Zhang, X., et al. (2019). Inhibiting BRAF oncogene-mediated radioresistance effectively radiosensitizes BRAFV600E mutant thyroid cancer cells by constraining DNA double-strand break repair. *Clin .Cancer Res.* 25:clincanres.3625.2018. doi: 10.1158/1078-0432.CCR-18-3625

Ru, B., Wong, C. N., Tong, Y., Zhong, J. Y., Zhong, S. S. W., Wu, W. C., et al. (2019). TISIDB: an integrated repository portal for tumor-immune system interactions. *Bioinformatics* 35, 4200–4202. doi: 10.1093/bioinformatics/btz210

Sishc, B. J., and Davis, A. J. (2017). The role of the core non-homologous end joining factors in carcinogenesis and cancer. *Cancers* 9:81. doi: 10.3390/cancers9070081

Sun, S., Cheng, S., Zhu, Y., Zhang, P., Liu, N., Xu, T., et al. (2016). Identification of PRKDC (Protein Kinase, DNA-Activated, Catalytic Polypeptide) as an essential gene for colorectal cancer (CRCs) cells. *Gene* 584, 90–96. doi: 10.1016/j.gene.2016.03.020

Tadi, S. K., Tellier-Lebègue, C., Nemoz, C., Drevet, P., Audebert, S., Roy, S., et al. (2016). PAXX Is an Accessory c-NHEJ Factor that Associates with Ku70 and Has Overlapping Functions with XLF. *Cell Rep.* 17, 541–555. doi: 10.1016/j.celrep.2016.09.026

The Cancer Genome Atlas Network (2012). Comprehensive molecular characterization of human colon and rectal cancer. *Nature* 487, 330–337. doi: 10.1038/nature11252

Yang, B., Fu, X., Hao, J., Sun, J., Li, Z., Li, H., et al. (2018). PAXX participates in base excision repair via interacting with Pol β and Contributes to TMZ resistance in glioma cells. *J. Mol. Neurosci.* 66, 214–221. doi: 10.1007/s12031-018-1157-4

Yang, S., and Wang, X. Q. (2017). XLF-mediated NHEJ activity in hepatocellular carcinoma therapy resistance. *BMC Cancer* 17:344. doi: 10.1186/s12885-017-3345-y

Zhang, Z., and Hu, W. (2011). A single nucleotide polymorphism in XRCC4 gene is associated with reduced colorectal cancer susceptibility in female. *J. Med Coll. PLA* 26, 85–93. doi: 10.1016/S1000-1948(11)60030-0

Conflict of Interest: The authors declare that the research was conducted in the absence of any commercial or financial relationships that could be construed as a potential conflict of interest.

frontiers in Molecular Biosciences

ORIGINAL RESEARCH
published: 10 December 2020
doi: 10.3389/fmolb.2020.604766

Identification and Validation of the N6-Methyladenosine RNA Methylation Regulator YTHDF1 as a Novel Prognostic Marker and Potential Target for Hepatocellular Carcinoma

Saiyan Bian[1,2†], Wenkai Ni[1,3†], Mengqi Zhu[2†], Qianqian Song[4], Jianping Zhang[2], Runzhou Ni[1] and Wenjie Zheng[2*]*

[1] Department of Gastroenterology, Affiliated Hospital of Nantong University, Nantong, China, [2] Research Center of Clinical Medicine, Affiliated Hospital of Nantong University, Nantong, China, [3] Endoscopy Center and Endoscopy Research Institute, Zhongshan Hospital, Fudan University, Shanghai, China, [4] Department of Radiology, Wake Forest School of Medicine, One Medical Center Boulevard, Winston-Salem, NC, United States

OPEN ACCESS

Edited by:
Amila Suraweera, Queensland University of Technology, Australia

Reviewed by:
Mark Nathaniel Adams, Queensland University of Technology, Australia
Larance Ronsard, Ragon Institute of MGH, MIT and Harvard, United States

***Correspondence:**
Wenjie Zheng
zwj007008009@163.com
Runzhou Ni
nirz@163.com

[†] These authors have contributed equally to this work

Specialty section:
This article was submitted to Molecular Diagnostics and Therapeutics, a section of the journal Frontiers in Molecular Biosciences

Received: *10 September 2020*
Accepted: *06 November 2020*
Published: *10 December 2020*

Citation:
Bian S, Ni W, Zhu M, Song Q, Zhang J, Ni R and Zheng W (2020) Identification and Validation of the N6-Methyladenosine RNA Methylation Regulator YTHDF1 as a Novel Prognostic Marker and Potential Target for Hepatocellular Carcinoma. Front. Mol. Biosci. 7:604766. doi: 10.3389/fmolb.2020.604766

Purpose: N6-methyladenosine (m^6A) RNA methylation has been implicated in various malignancies. This study aimed to identify the m^6A methylation regulator-based prognostic signature for hepatocellular carcinoma (HCC) as well as provide candidate targets for HCC treatment.

Methods: The least absolute shrinkage and selection operator (LASSO) analyses were performed to identify a risk signature in The Cancer Genome Atlas (TCGA) datasets. The risk signature was further validated in International Cancer Genome Consortium (ICGC) and Pan-Cancer Analysis of Whole Genomes (PCAWG) datasets. Following transfection of short hairpin RNA (shRNA) targeting YTHDF1, the biological activities of HCC cells were evaluated by Cell Counting Kit-8 (CCK-8), wound-healing, Transwell, flow cytometry, and xenograft tumor assays, respectively. The potential mechanisms mediated by YTHDF1 were predicted by overrepresentation enrichment analysis (ORA)/gene set enrichment analysis (GSEA) and validated by Western blotting.

Results: Overexpression of m^6A RNA methylation regulators was correlated with malignant clinicopathological characteristics of HCC patients. The Cox regression and LASSO analyses identified a risk signature with five m^6A methylation regulators (KIAA1429, ZC3H13, YTHDF1, YTHDF2, and METTL3). In accordance with HCC cases in TCGA, the prognostic value of risk signature was also determined in ICGC and PCAWG datasets. Following analyzing the expression and clinical implications in TCGA and Gene Expression Omnibus (GEO), YTHDF1 was chosen for further experimental validation. Knockdown of YTHDF1 significantly inhibited the proliferation, migration, and invasion of HCC cells, as well as enhanced the apoptosis *in vitro*. Moreover, silencing YTHDF1 repressed the growth of xenograft tumors *in vivo*. Mechanism investigation indicated that YTHDF1 might promote the aggressive phenotypes by facilitating epithelial–mesenchymal transition (EMT) and activating AKT/glycogen synthase kinase (GSK)-3β/β-catenin signaling.

Conclusion: The current study identified a robust risk signature consisting of m^{6}A RNA methylation regulators for HCC prognosis. In addition, YTHDF1 was a potential molecular target for HCC treatment.

Keywords: m^{6}A methylation, regulators, hepatocellular carcinoma, prognosis, YTHDF1, molecular target

INTRODUCTION

Hepatocellular carcinoma (HCC) is one of the most common malignancies and ranks the fourth leading cause of deaths worldwide (Bray et al., 2018). The major risk factors of HCC include hepatitis B virus (HBV) and hepatitis C virus (HCV) infection, non-alcoholic steatohepatitis (NASH), alcohol abuse, diabetes mellitus, and aflatoxin exposure (Makarova-Rusher et al., 2016). Exposure to these factors and genetic and epigenetic alterations progressively promote the initiation of HCC (Cancer Genome Atlas Research, 2017). Currently, surgery resection, liver transplantation, and systematic therapy are conventional therapies for HCC. Despite progression in therapeutic strategies for HCC, the overall survival (OS) remains unsatisfactory due to a high rate of postsurgical recurrence and metastasis (Finn et al., 2018). Therefore, it is of great need to elucidate the underlying molecular mechanisms and exploring more novel targets for HCC.

N6-methyladenosine (m^{6}A) is the most abundant posttranscriptional modification for eukaryotic mRNA. m^{6}A is enriched in the stop codon, 3′ untranslated region (UTR), and long internal exon with average 1–2 m^{6}A residues/1,000 nucleotides (Meyer et al., 2012). m^{6}A regulates the expression of target genes through the modification of RNA, such as splicing, degradation, exporting, and folding (Wang et al., 2014, 2015). m^{6}A can be catalyzed and removed by methyltransferase complexes (MTCs) and demethylases, respectively, which are vividly named as "writers" and "erasers." Writer proteins include KIAA1429, METTL3, METTL14, RBM15, ZC3H13, and WTAP, in which METTL3 methyltransferase is considered as the key catalytic subunit (Liu et al., 2014). Erasers consist of two demethylases FTO and ALKBH5. There is another type of m^{6}A regulators, called "readers," which consist of HNRNPC and YT521-B homology (YTH) family members (e.g., YTHDF1-3 and YTHDC1/2). These readers could recognize distinct subsets of m^{6}A-modified mRNAs specifically and facilitate the regulation of gene expression (Liao et al., 2018). In addition to these classical m^{6}A regulators, recent studies have identified some new regulators, such as METTL16 (Warda et al., 2017) and HNRNPA2B1(Alarcon et al., 2015). Interactions among these m^{6}A regulators have been implicated in diverse physiological functions and processes, including histogenesis, stem cell self-renewal capacity, and fate determination (Liu et al., 2017). More importantly, increasing studies demonstrate that aberrant m^{6}A methylation is correlated with tumorigenesis and progression in multiple cancer types, which functions as either a tumor promoter or a tumor suppressor in distinct states (He et al., 2019).

Some studies indicated that m^{6}A regulators were related to poor prognosis of HCC patients and promoted the malignant phenotypes of HCC cells. For example, KIAA1429 was shown to facilitate cell proliferation and invasion of HCC cells through m^{6}A modification of ID2 mRNA and GATA3 pre-mRNA (Cheng et al., 2019; Lan et al., 2019). WTAP-mediated m^{6}A modification contributed to the aggressiveness of HCC cells *via* posttranscriptional suppression of ETS proto-oncogene 1 (Chen Y. et al., 2019). Interestingly, YTHDF2 was described as an HCC suppressor by repressing cell proliferation *via* m^{6}A modification of epidermal growth factor receptor (EGFR). YTHDF2 also inhibited vascular reconstruction and metastasis *via* regulating interleukin 11 and serpin family E member 2 (Hou et al., 2019; Zhong et al., 2019). Moreover, METTL3-mediated m^{6}A modification could decrease the expression of suppressor of cytokine signaling 2 in HCC cells, thereby contributing to aggressive phenotype *in vitro* and *in vivo* (Chen et al., 2018). Despite these studies, the clinical significance of these m^{6}A regulators in HCC remains unclear and poorly explored. In this study, we aimed to investigate the expression characteristics and clinicopathological value of the m^{6}A RNA regulators comprehensively in order to identify robust risk signatures for HCC prognosis and potential targets for HCC treatment.

MATERIALS AND METHODS

Data Acquisition

The RNA-seq transcriptome data of liver hepatocellular carcinoma (LIHC) cohort and corresponding clinical or prognostic information were obtained from TCGA (https://cancergenome.nih.gov/) through the R package "TCGA-Assembler" (**Table 1**). The genomic alterations of YTHDF1 were identified by cBioPortal (www.cbioportal.org). The YTHDF1 mRNA profiles were also obtained from the International Cancer Genome Consortium (ICGC) and Pan-Cancer Analysis of Whole Genomes (PCAWG) datasets (www.icgc.org) with Gene Expression Omnibus (GEO) datasets including GSE22058, GSE25097, GSE36376, GSE46444, GSE54236, GSE63698, GSE64041, and GSE76427.

Selection of N6-Methyladenosine RNA Methylation Regulators

Currently, 13 genes (*KIAA1429, METTL3, METTL14, RBM15, ZC3H13, FTO, ALKBH5, YTHDF1, YTHDF2, YTHDC1, YTHDC2, HNRNPC*, and *WTAP*) are considered as classical m^{6}A RNA methylation regulators. To ensure comprehensiveness, we also incorporated three newly acknowledged m^{6}A RNA methylation regulator genes

TABLE 1 | The clinical characteristic information of the HCC patients in TCGA.

Characteristics	Number of cases	Percentages (%)
Age		
<65	223	59.63
≥65	150	40.11
Not available	1	0.26
Gender		
Male	253	67.65
Female	121	32.35
Survival status		
Alive	238	63.64
Dead	130	34.76
Not available	6	1.60
Stage		
I	173	46.26
II	87	23.26
III	85	22.73
IV	5	1.34
Not available	24	6.42
Histological grade		
G1	55	14.71
G2	178	47.59
G3	124	33.16
G4	12	3.21
Not available	5	1.34
T classification		
T1	183	48.93
T2	95	25.40
T3	80	21.39
T4	13	3.48
Not available	3	0.8
N classification		
N0	254	67.91
N1	4	1.07
NX	115	30.75
Not available	1	0.27
M classification		
M0	268	71.66
M1	4	1.07
MX	102	27.27

HCC, hepatocellular carcinoma; TCGA, The Cancer Genome Atlas.

(*YTHDF3*, *METTL16*, and *HNRNPA2B1*). The expression profiles of the above genes were extracted from TCGA LIHC cohort with corresponding clinical information. Heatmap and Vioplot were conducted to visualize the differential expressions of these genes in HCC. The protein–protein interactions (PPIs) among m^{6}A RNA methylation regulators were analyzed by STRING database (http://string-db.org). In addition, we performed the Pearson correlation analysis to identify the association among these m^{6}A RNA methylation regulators.

Consensus Clustering Analysis

To further explore m^{6}A RNA methylation regulators in the LIHC cohort, we applied consensus clustering analysis to the LIHC cohort based on m^{6}A RNA methylation regulators. Two subgroups were identified in the LIHC cohort. In addition, to identify the potential function and involved pathways, we conducted Gene Ontology (GO) and Kyoto Encyclopedia of Genes and Genomes (KEGG) analyses based on the different gene profiles of the two subgroups.

Prognostic Signature Generation

The correlation of m^{6}A RNA methylation regulator genes with OS of HCC patients was evaluated by univariate Cox regression model. A risky gene was characterized by hazard ratios (HRs) > 1, while HRs < 1 were considered a protective one. A five-gene risk signature (KIAA1429, ZC3H13, YTHDF1, YTHDF2, and METTL3) was identified based on the minimum criteria. In addition, risk score was calculated according to the coefficients in the least absolute shrinkage and selection operator (LASSO) algorithm. TCGA LIHC cohort was classified into high- or low-risk group based on the median value of the risk scores.

Genomic Alteration and Co-expression Gene Identification

The mutation, copy number variation (CNV), and mRNA alterations of YTHDF1 in HCC were analyzed by using the cBioPortal tool (http://cbioportal.org) (Gao et al., 2013). The OncoPrint presented an overview of genetic alterations of YTHDF1 in LIHC samples. Co-expression analysis was determined by using LinkedOmics platform (Vasaikar et al., 2018). The potential function was predicted by overrepresentation enrichment analysis (ORA) with GO_BP/CC/MF, KEGG pathways, Wiki pathway, and Reactome pathway.

Evaluating the Prognostic Value of the Gene Signature

The distribution of clinicopathological features (age, gender, grade stage, and survival state) was further evaluated in high- and low-risk groups calculated by chi-square test and visualized with heatmaps. Kaplan–Meier analysis with log-rank test was conducted to calculate the difference of OS between patients at high-risk score group and low-risk score group. Receiver operating characteristic (ROC) curve was constructed to evaluate the prognosis value of the signature in predicting the survival of patients. Univariate and multivariate Cox regression analyses were used to evaluate the risk score as an independent prognostic factor of HCC patients.

Cell Culture and Transfection

Hep3B, HepG2, MHCC97H, MHCC97L, and HCCLM3 were purchased from the Cell Bank of the Chinese Academy of Sciences (Shanghai, China). SMMC7721 and BEL7404 were obtained from American Type Culture Collection (Rockville, MD, USA). Cells were maintained in Dulbecco′s modified Eagle′s medium (GIBCO, USA) supplemented with 10% fetal bovine serum (FBS; GIBCO, USA) and 1% penicillin/streptomycin

solution. Plasmids for YTHDF1 knockdown were constructed by Dharmacon (CA, USA). The transfection was performed by Lipo3000 according to the manufacturer's instruction. The sequences of the short hairpin RNAs (shRNAs) were listed as follows: Kd-YTHDF1-1, GAACAUGCCAGUUUCAAAG; Kd-YTHDF1-2, GGACAGUCAAAUCAGAGUA; Kd-YTHDF1-3, CGACAUCCACCGCUCCAUU; Kd-YTHDF1-4, AAGGAACG GCAGAGUCGAA; NC, UAAGGCUAUGAAGAGAUAC.

Cell Proliferation Assay

Cell proliferation was evaluated by a Cell Counting Kit-8 (CCK-8; Dojindo Laboratories, Kumamoto, Japan) according to the manufacturer's introduction. Briefly, HCC cell lines (1,000 cells/well) transfected with control vector or Kd-YTHDF1 plasmids were incubated in 96-well plates for 24 to 96 h. Then, a working solution was administered into the culture medium at 37°C for 2 h. Subsequently, the plates were detected at 450-nm absorbance. Each assay was repeated three times.

Migration and Invasion Assays

The migration of the HCC cells was evaluated by the wound-healing assay. The HepG2 cells of each group were seeded in the six-well plates. Upon the confluency of 80%, 10-μl tips were used to construct wounds on the surface of each well. Then, the pre-marked places were compared at the indicated time point 0 and 24 h. The distances of migration in three random fields were calculated by ImageJ. The invasion assay was conducted by using the 8-μm Transwell chambers (Corning, Acton, MA, USA) placed in 24-well plates. Here, 200 μl of HepG2 cells were plated in the upper chambers pre-coated with Matrigel (BD, CA, USA), while the complete medium was plated in the lower chamber. Following incubation for 24 h, the chambers were fixed in 4% paraformaldehyde and stained in 0.1% crystal violet solution. Then, the samples of each group were counted under the microscope. Each assay was independently repeated at least three times.

Flow Cytometry

HCC cells at each group were collected and pre-fixed in 75% cold ethanol and stored at 4°C overnight. After rinsing in phosphate-buffered saline (PBS) three times, the samples were stained in propidium iodide (PI) for 30 min. Subsequently, cell cycle distribution was detected by a flow cytometer (Calibur, Becton Dickinson, CA, USA) and further analyzed by using ModFit Software. The apoptosis detection was conducted by Annexin V-Alexa Fluor 647/PI Apoptosis Detection kit (Fcmacs Biotech Co., Ltd., China) according to the manufacturer's instruction. The samples were stained in PI and 647 Annexin V for 30 min. Then, the samples were detected by a flow cytometer. Each experiment was independently performed at least three times.

Xenograft Tumor Assay

Four-week-old BALB/c nude mice were provided by the Animal Center of Nantong University (Nantong, China). HepG2 cells stably transfected with shRNA-YTHDF1 vector or control vector were subcutaneously injected into flanks of nude mice at the density of 5×10^6 cells/100 μl. Post-injection, tumor growth was monitored every 3 days by using calipers. The volume of the xenograft tumor was calculated as 0.5 × length × width^2. The protocols of this study were approved by the Animal Care and Use Committee of Nantong University.

Western Blotting

Cells of each group were collected for the extraction of total protein by using radioimmunoprecipitation assay (RIPA) buffer. Then, the samples were separated on a sodium dodecyl sulfate (SDS) gel and transferred onto polyvinylidene difluoride (PVDF) membranes (Bio-Rad, CA, USA). Following blocking in 5% bovine serum albumin (BSA) for 2 h, the membranes were incubated in primary antibodies at 4°C overnight. After rinsing in Tris-buffered saline and Tween 20 (TBST) three times, the samples were further exposed to horseradish peroxidase (HRP)-conjugated secondary antibodies for 2 h at room temperature. The membranes were visualized by using the enhanced chemiluminescence (ECL) kit (Millipore, MA, USA).

Statistical Analyses

All statistical analyses were calculated by using R software (Version 3.5) and GraphPad Prism 7 (CA, USA). Data are presented as means ± standard deviations. The Student's *t*-test and chi-square (χ^2) test were performed to evaluate differences between two groups. A one-way analysis of variance (ANOVA) test was used for multiple group comparisons. The risk score was obtained according to the coefficients in the LASSO algorithm. Kaplan–Meier analysis with a log-rank test was used to analyze the survival difference between the high- and low-risk groups. *P*-value threshold of 0.05 was considered as statistical significance.

RESULTS

The Expression Features of N6-Methyladenosine RNA Methylation Regulators

The expression features of 16 m^{6}A RNA methylation regulators in HCC tissues and normal liver tissues from TCGA are shown in **Figure 1**. Compared with normal tissues, 14 m^{6}A RNA methylation regulators (YTHDC1, KIAA1429, HNRNPA2B1, METTL16, RBM15, YTHDF3, ALKBH5, YTHDF2, HNRNPC, YTHDF1, METTL3, WTAP, YTHDC2, and FTO) were found overexpressed in HCC (**Figures 1A,B**). In addition, the interaction network among the 16 m^{6}A RNA methylation regulators were predicted by STRING, in which KIAA1429, WTAP, YTHDF2, and METTL3 were considered as hub genes (**Figure 1C**). Furthermore, the expression of m^{6}A RNA methylation regulators were positively correlated based on Pearson correlation. Remarkably, the most relevant among all the m^{6}A RNA methylation regulators was observed between the METTL3/HNRNPC ($r = 0.72$) and HNRNPA2B1/HNRNPC ($r = 0.78$) (**Figure 1D**).

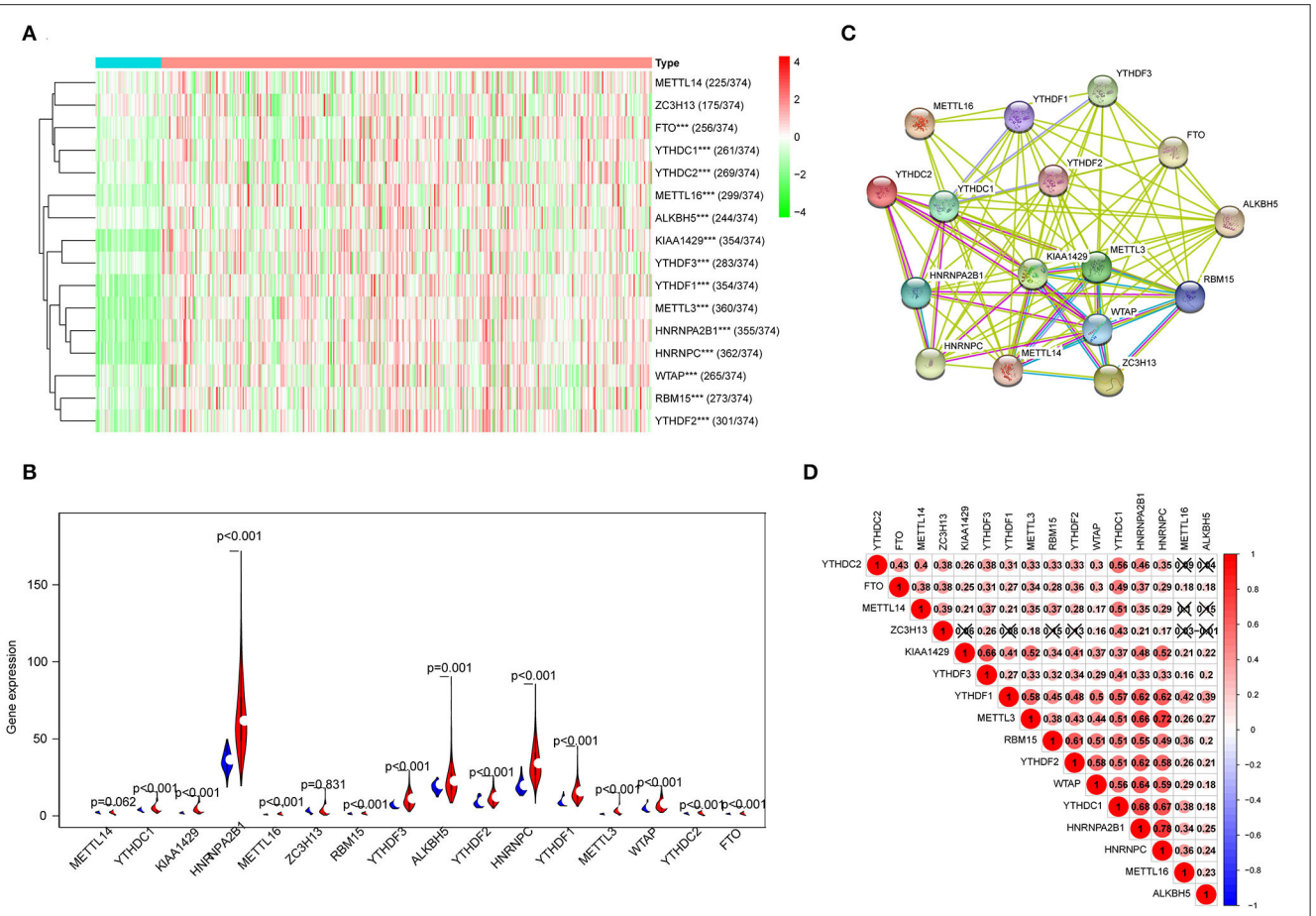

FIGURE 1 | The expression characteristics and correlations of N6-methyladenosine (m^6A) RNA methylation regulators in hepatocellular carcinoma (HCC). **(A)** Heatmaps presented the overall expression of 16 m^6A RNA methylation regulators in HCC tissues and normal liver tissues from The Cancer Genome Atlas (TCGA) datasets. **(B)** The differential expression of the m^6A RNA methylation regulators was visualized by Vioplot (blue means normal liver tissues; red means HCC samples). **(C)** The interaction of the m^6A RNA methylation regulators was analyzed by STRING. **(D)** Spearman correlation analysis of the 16 regulating genes in the liver hepatocellular carcinoma (LIHC) cohort. ***$P < 0.001$.

Correlation of N6-Methyladenosine RNA Methylation Regulators With Clinicopathological Features of Hepatocellular Carcinoma Patients

To develop a prognostic signature based upon m6A RNA methylation regulators, we sought to stratify 374 HCC patient samples by consensus clustering analysis (**Figures 2A,B**). Based on the cumulative distribution function (CDF) value, $k = 2$ was the optimal cluster number to divide the HCC cohort, namely, cluster 1 and cluster 2 (**Figure 2C**). Furthermore, principal component analysis (PCA) of total RNA expression profile was performed to evaluate the classification, which showed that cluster 1 and cluster 2 could be well-distinguished (**Figure 2D**). Next, we evaluated the associations between clusters and clinicopathological features in TCGA. As shown in **Figure 2E**, the general expression of m^6A RNA methylation regulators was higher in cluster 2, especially for YTHDC1/2, HNRNPA2B1, METTL16, RBM15, ALKBH5, HNRNPC, YTHDF1-3, METTL3, WTAP, and FTO. In addition, cluster 2 was significantly correlated with gender, advanced stage, and survival state. Moreover, the OS of patients in cluster 2 was significantly lower than that of cluster 1 (**Figure 2F**). Furthermore, we conducted GO and KEGG analyses based on differentially expressed genes to identify enriched functions and pathways in cluster 2. GO analysis indicated that differentially expressed genes were enriched in various processes, including extracellular matrix (ECM) organization, extracellular structure organization, plasma membrane protein complex, and cation transmembrane transporter activity (**Figure 2G**). In addition, KEGG analysis indicated that m^6A RNA methylation regulator-overexpressed cluster 2 was correlated with ECM–receptor interaction, cAMP signaling pathway, Hippo signaling pathway, and cell cycle, which were frequently implicated in the progression of HCC (Massimi et al., 2019; Huang et al., 2020; Wu et al., 2020) (**Figure 2H**).

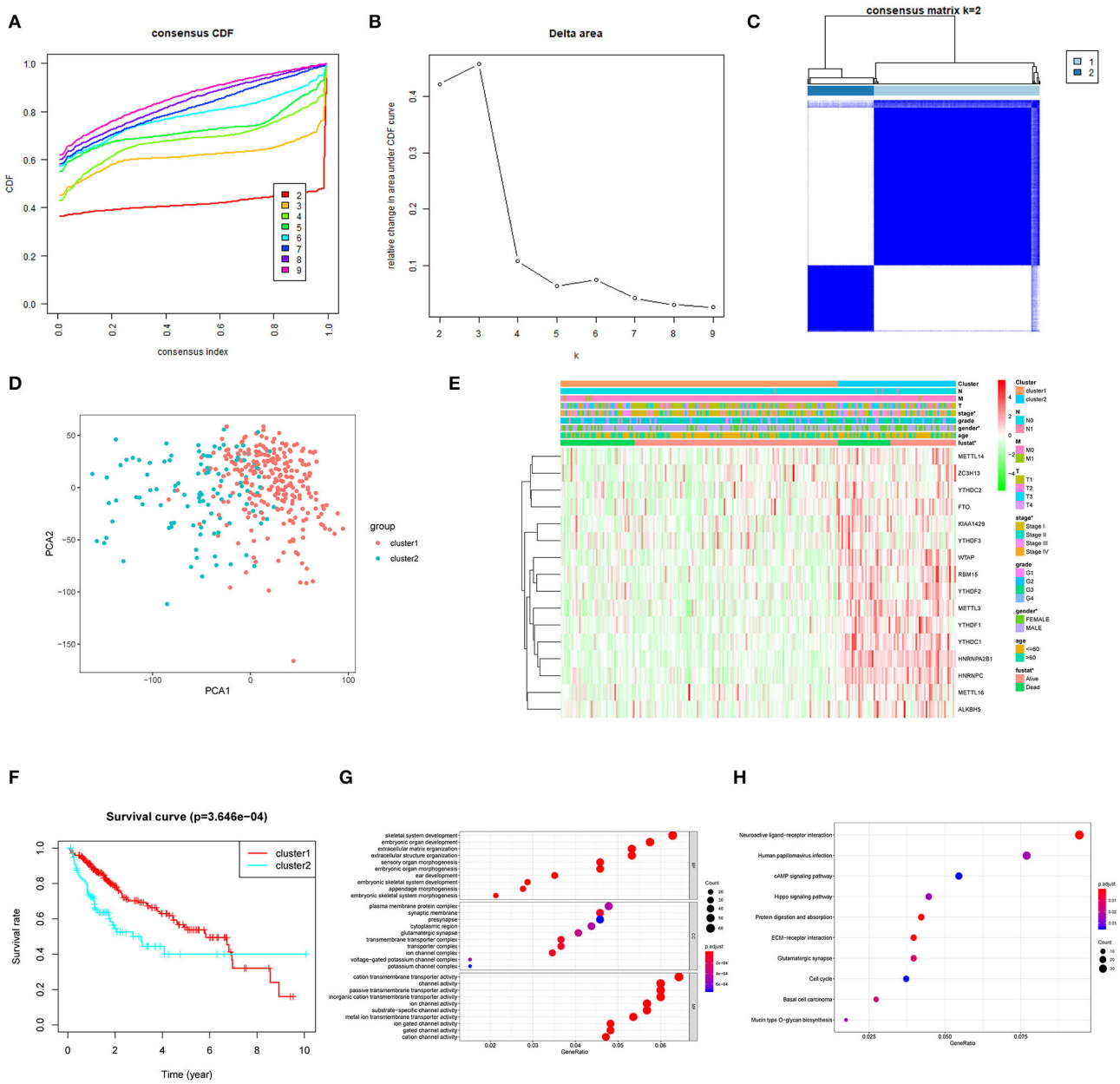

FIGURE 2 | Association between the N6-methyladenosine (m^6A) RNA methylation regulators and clinicopathological and prognostic features of hepatocellular carcinoma (HCC) patients. **(A)** Consensus clustering model with cumulative distribution function (CDF) for $k = 2$–9. **(B)** Relative change in area under the CDF curve for $k = 2$–9. **(C)** The Cancer Genome Atlas (TCGA) liver hepatocellular carcinoma (LIHC) cohort was classified into two clusters with $k = 2$. **(D)** Principal component analysis of the total RNA expression profile of cluster 1 (red) and the cluster 2 (blue). **(E)** The correlation of the two clusters with clinicopathologic features was visualized by heatmap. **(F)** The overall survival of HCC patients in the two clusters was calculated by Kaplan–Meier curves. **(G)** Gene Ontology (GO) analyses were conducted to predict the potential function of the differentially expressing genes between the two clusters. **(H)** Kyoto Encyclopedia of Genes and Genomes (KEGG) analyses were performed to predict the underlying potential pathways regarding the differentially expressing genes. *$P < 0.05$.

Prognostic Significance of the N6-Methyladenosine RNA Methylation Regulator-Based Signature

Then, the prognostic significance of m^6A RNA methylation regulators was evaluated for HCC patients. The univariate Cox regression and Kaplan–Meier analyses indicated that nine of the regulators were associated with poor survival of the HCC cases (**Figure 3A**; **Supplementary Figure 1**), including YTHDC1, KIAA1429, HNRNPA2B1, RBM15, YTHDF2, YTHDF1, HNRNPC, METTL3, and WTAP. In contrast, ZC3H13 was considered as a protective factor for HCC patients. Next, the LASSO algorithm, a generalized linear model, was

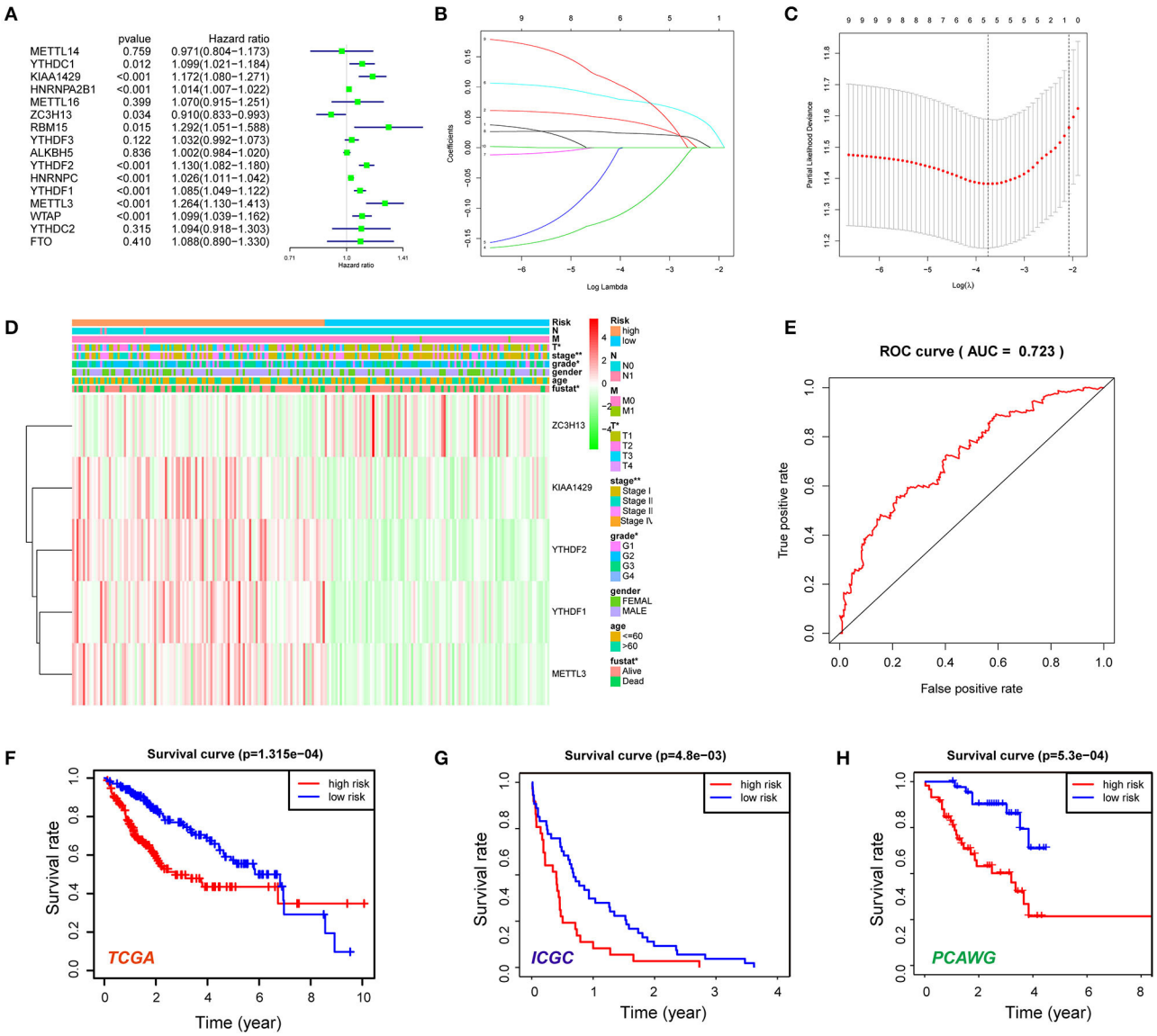

FIGURE 3 | Construction of the five N6-methyladenosine (m^6A) RNA methylation regulator-based risk signature. **(A)** Univariate Cox regression was performed to screen the signature in 16 m^6A RNA methylation regulators. **(B,C)** The coefficients of the five-gene signature (KIAA1429, ZC3H13, YTHDF1, YTHDF2, and METTL3) calculated by multivariate Cox regression with least absolute shrinkage and selection operator (LASSO). **(D)** The expression features of the five m^6A RNA methylation regulators and the distribution of clinicopathological features were compared between the low- and high-risk groups of The Cancer Genome Atlas (TCGA) liver hepatocellular carcinoma (LIHC) datasets. **(E)** Receiver operating characteristic (ROC) curves were calculated to evaluate the predictive efficiency of the five-gene risk signature. **(F)** The Kaplan–Meier curves of HCC patients at the high-risk group and low-risk group in TCGA cohort. **(G)** The Kaplan–Meier curves of HCC patients at the high-risk group and low-risk group in the International Cancer Genome Consortium (ICGC) cohort. **(H)** The Kaplan–Meier curves of HCC patients at the high-risk group and low-risk group in the Pan-Cancer Analysis of Whole Genomes (PCAWG) cohort. $^*P < 0.05$, $^{**}P < 0.01$.

performed to establish the prognostic signature. A coefficient profile plot was generated after the log2 transformation of the lambda (λ) value, which was determined by the smallest likelihood deviance (**Figure 3B**). Five m^6A RNA methylation regulators (KIAA1429, ZC3H13, YTHDF1, YTHDF2, and METTL3) and corresponding coefficients were identified with minimum 10-fold cross-validated mean square error in TCGA cohort (**Figure 3C**). The risk score for each patient = ∑gene expression * coefficient (glmnet R package). Based on the median of the risk score, we stratified the HCC cohort into high-risk group and low-risk group. High-risk score group was positively correlated with aggressive pathological features like T status, tumor stage, and histological grade (**Figure 3D**). As shown in **Figure 3E**, the signature's risk score could robustly predict survival rates for HCC patients [area under the curve (AUC) = 0.723]. Next, Kaplan–Meier

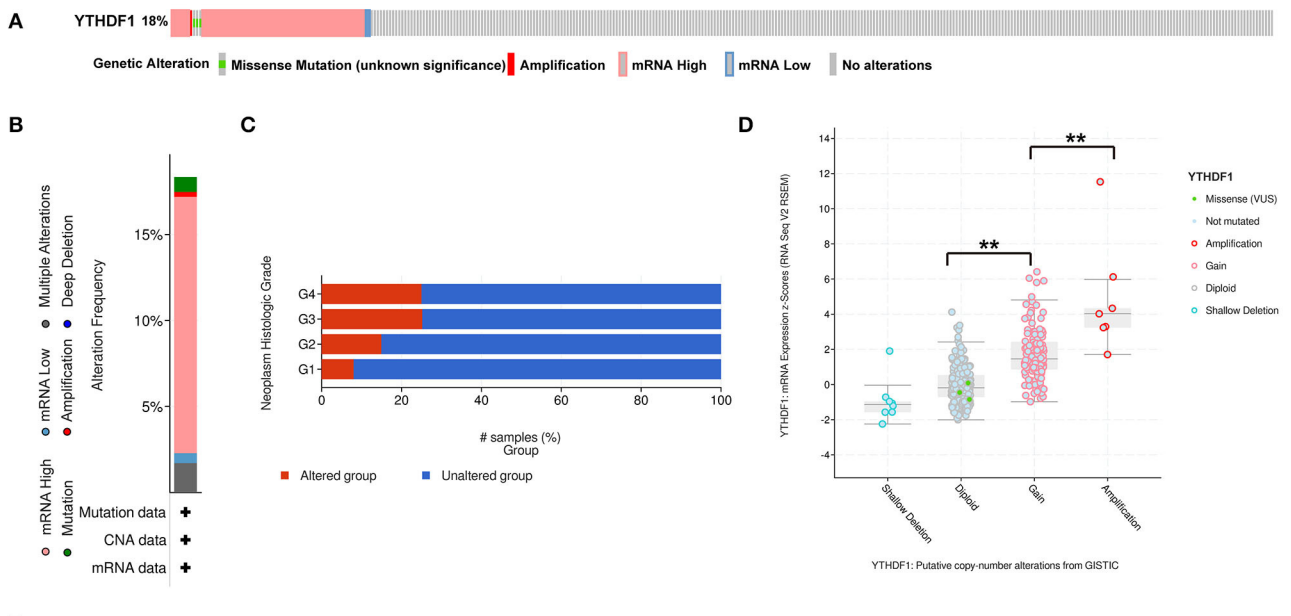

E

Dataset	P-value	Type	Nums	Mean	STD	IQR
GSE22058	0.01141	HCC	100	10.42	0.2766	0.3442
		Adjacent	97	10.32	0.2864	0.3618
GSE25097	6.900e-21	HCC	268	7.532	1.110	1.256
		Adjacent	243	6.694	0.8063	1.133
		Cirrhotic	40	7.261	0.6546	1.069
		Healthy	6	7.945	1.142	0.7882
GSE36376	3.920e-100	HCC	240	8.948	0.3681	0.5192
		Adjacent	193	8.089	0.2605	0.3415
GSE46444	0.6392	HCC	88	6.870	0.9828	1.280
		Adjacent	48	6.781	1.092	1.886
GSE54236	2.410e-7	HCC	81	10.35	0.3021	0.3740
		Adjacent	80	10.12	0.2254	0.3024
GSE63698	3.010e-10	HCC	228	5.836	0.3023	0.4268
		Adjacent	168	5.657	0.2459	0.2906
TCGA-LIHC	0.0001423	HCC	351	10.43	0.3236	0.4250
		Adjacent	49	10.28	0.2328	0.2200
GSE64041	0.00008780	HCC	60	9.380	0.2404	0.2909
		Adjacent	60	9.219	0.1894	0.1623
GSE76427	5.550e-11	HCC	115	10.04	0.3823	0.5100
		Adjacent	52	9.693	0.2477	0.3625
ICGC-LIRI-JP	1.760e-26	HCC	212	3.884	0.3942	0.5200
		Adjacent	177	3.447	0.3555	0.4500

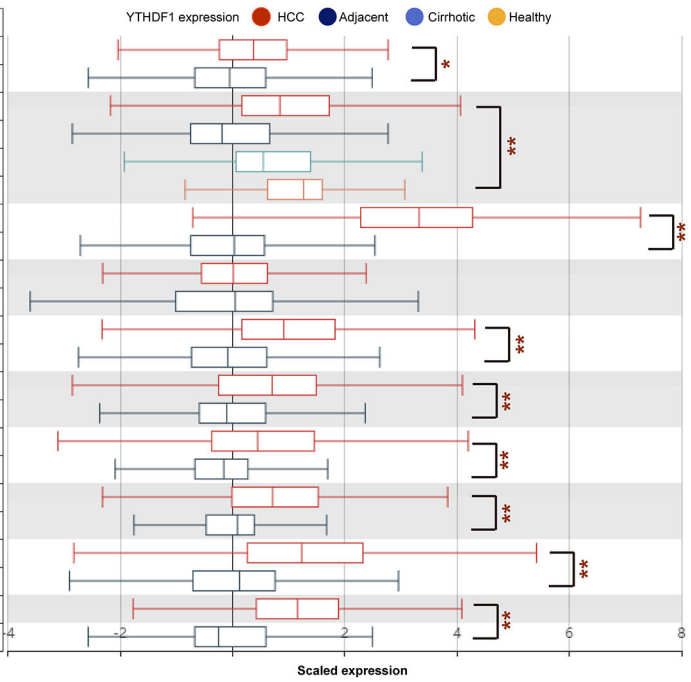

FIGURE 4 | YTHDF1 genomic alterations in hepatocellular carcinoma (HCC). **(A,B)** OncoPrint of YTHDF1 alterations in liver hepatocellular carcinoma (LIHC) cohort identified by cBioPortal. **(C)** YTHDF1 mRNA expression in different YTHDF1 copy number variation (CNV) groups. **(D)** Distribution of YTHDF1 CNV frequency in LIHC cases at different grades. **(E)** YTHDF1 expression in 10 Gene Expression Omnibus (GEO) datasets. *$P < 0.05$, **$P < 0.01$.

analysis demonstrated that patients in the high-risk group had significantly shorter OS than low-risk cases ($P < 0.001$; **Figure 3F**). Furthermore, we evaluated the five-gene signature in stratification analyses (**Supplementary Figures 2A,B**). The high-risk score could predict poor prognosis for HCC patients at early tumor stages ($P = 0.0018$) and histological grades ($P < 0.001$). Although the difference was not statistically significant, the OS of high-risk cases at advanced tumor stages or histological grades was obviously lower than that of the low-risk group. We further conducted the multivariate Cox regression analysis and identified the risk signature as an independent prognostic factor. Consistently, the univariate and multivariate Cox regression analyses demonstrated that the signature-based risk score was an independent factor ($P < 0.001$, HR = 1.166,

TABLE 2 | Correlation of YTHDF1 expression with clinical features of HCC patients in TCGA.

Clinical characteristics	Total (N)	Odds ratio in YTHDF1	*P*-value
Age (≥65 vs.<65)	370	1.07 (0.71,1.62)	0.75
Gender (female vs. male)	371	0.76 (0.49,1.17)	0.209
Stage (I/II vs. III/IV)	347	3.27 (1.96,5.47)	**<0.0001**
Histological grade (G1/G2 vs. G3/G4)	366	2.49 (1.61,3.87)	**<0.0001**
T (T1/T2 vs. T3/T4)	368	3.2 (1.93,5.32)	**<0.0001**
N (N0 vs. N1)	256	2.68 (0.28,26.15)	0.364
M (M0 vs. M1)	270	68825722.07 (0, Inf)	**0.021**

Bold, P < 0.05. HCC, hepatocellular carcinoma; TCGA, The Cancer Genome Atlas.

TABLE 3 | Univariate analysis and multivariate analysis of overall survival in HCC patients from TCGA.

Parameters	Univariate analysis				Multivariate analysis			
	HR	CI lower	CI upper	*P*	HR	CI lower	CI upper	*P*
Age	1	1	1	0.079	1.01	0.993	1.02	0.325
Gender	0.82	0.57	1.2	0.262	0.958	0.666	1.38	0.819
Histological grade	1.1	0.85	1.3	0.651	1.15	0.911	1.46	0.238
M	1.3	1.1	1.5	**0.0092**	1.29	1.01	1.66	**0.0416**
N	1.2	1	1.5	**0.0378**	1.1	0.851	1.43	0.455
T	1.2	1.2	1.3	**<0.0001**	1.21	1.1	1.33	**<0.0001**
Pathologic stage	1.2	1.1	1.3	**0.00012**	1.04	0.919	1.17	0.559
YTHDF1	2.7	1.5	4.6	**0.000462**	2.2	1.2	4.03	**0.011**

Bold, P < 0.05. CI, confidence interval; HCC, hepatocellular carcinoma; HR, hazard ratio; TCGA, The Cancer Genome Atlas.

95% CI = 1.099–1.236) for predicting the OS of HCC patients (**Supplementary Figures 3A,B**). In addition, we also evaluated the risk signature in ICGC and PCAWG datasets. In accordance, high-risk score indicated the poor survival of HCC patients in both of the two datasets (**Figures 3G,H**). The results above indicated that the m^{6}A RNA methylation regulators were involved in HCC progression and serve as a potential biomarker for prognosis.

The Genomic Alteration and Clinical Implication of YTHDF1 in Hepatocellular Carcinoma

Given that the m^{6}A regulator-based signature was correlated with tumor stage and histological grade, we further evaluated the expression of five regulators in different stages or grades of HCC (**Supplementary Figures 4A,B**). From early stages (grades) to advanced stages (grades), the expression level of YTHDF1 was remarkably elevated. Thus, we subsequently focused on the m^{6}A reader YTHDF1. Initially, the types and frequency of YTHDF1 alterations of YTHDF1 were determined by cBioPortal. According to the OncoPrint (**Figures 4A,B**), YTHDF1 was altered in 65 of 360 (18.06%) LIHC patients, including mRNA upregulation in 53 cases (14.72%), amplification in one case (0.28%), mutation in three cases (0.83%), and multiple alterations in six cases (1.67%). In addition, the YTHDF1 alteration was enhanced in advanced grades of HCC patients (**Figure 4C**). Compared with the diploid cases, gain or amplification cases had higher YTHDF1 expression levels ($P < 0.01$; **Figure 4D**). Next, we conducted a meta-analysis of YTHDF1 mRNA expression in ICGC and GEO datasets (**Figure 4E**). In most datasets (9/10), HCC tissues presented significantly higher expression of YTHDF1 than that of normal liver tissues. Then, we further evaluated the diagnostic value based on the expression features of YTHDF1 by using ROC curves. As shown in **Supplementary Figures 5A–E**, YTHDF1, with distinct expression level in contrast to normal tissues, showed a potential diagnostic value in the whole cohort or cases at all different stages. Then, the clinical implications of YTHDF1 was subsequently analyzed in TCGA datasets. Overexpression of YTHDF1 was correlated with tumor volume, distant metastasis, histological grade, and neoplasm stage (**Table 2**). Furthermore, the univariate analysis and multivariate analysis suggested YTHDF1 as an independent prognostic marker for OS and recurrence-free survival of HCC patients in TCGA (**Tables 3**, **4**).

TABLE 4 | Univariate analysis and multivariate analysis of recurrence-free survival in HCC patients from TCGA.

Parameters	Univariate analysis				Multivariate analysis			
	HR	CI lower	CI upper	*P*	HR	CI lower	CI upper	*P*
Age	1	0.99	1	0.849	0.996	0.983	1.01	0.608
Gender	0.98	0.69	1.4	0.919	1.17	0.811	1.7	0.395
Histological grade	0.98	0.8	1.2	0.873	0.982	0.791	1.22	0.87
M	0.96	0.79	1.2	0.694	0.92	0.704	1.2	0.543
N	1	0.87	1.3	0.656	1.17	0.913	1.51	0.212
T	1.3	1.2	1.4	**<0.0001**	1.23	1.1	1.38	**0.000308**
Pathologic stage	1.3	1.2	1.5	**<0.0001**	1.05	0.888	1.24	0.565
YTHDF1	2.5	1.5	4.3	**0.000581**	2.07	1.18	3.62	**0.0111**

Bold, P < 0.05. CI, confidence interval; HCC, hepatocellular carcinoma; HR, hazard ratio; TCGA, The Cancer Genome Atlas.

The Contribution of YTHDF1 to the Aggressive Behavior of Hepatocellular Carcinoma Cells

To further discover the roles of YTHDF1 in HCC, the current study conducted the functional assays *in vitro* and *in vivo*. First, we detected the protein and mRNA expressions of YTHDF1 in seven HCC cell lines, in which HepG2 had the highest expression level (**Figures 5A,B**). Then, four shRNAs were transfected into HepG2 cells to knock down YTHDF1, and Kd-YTHDF1-3 presented the best inhibitory efficiency (**Figures 5C,D**). Following knockdown of YTHDF1, the migration ($P < 0.001$) and invasion ($P < 0.001$) were

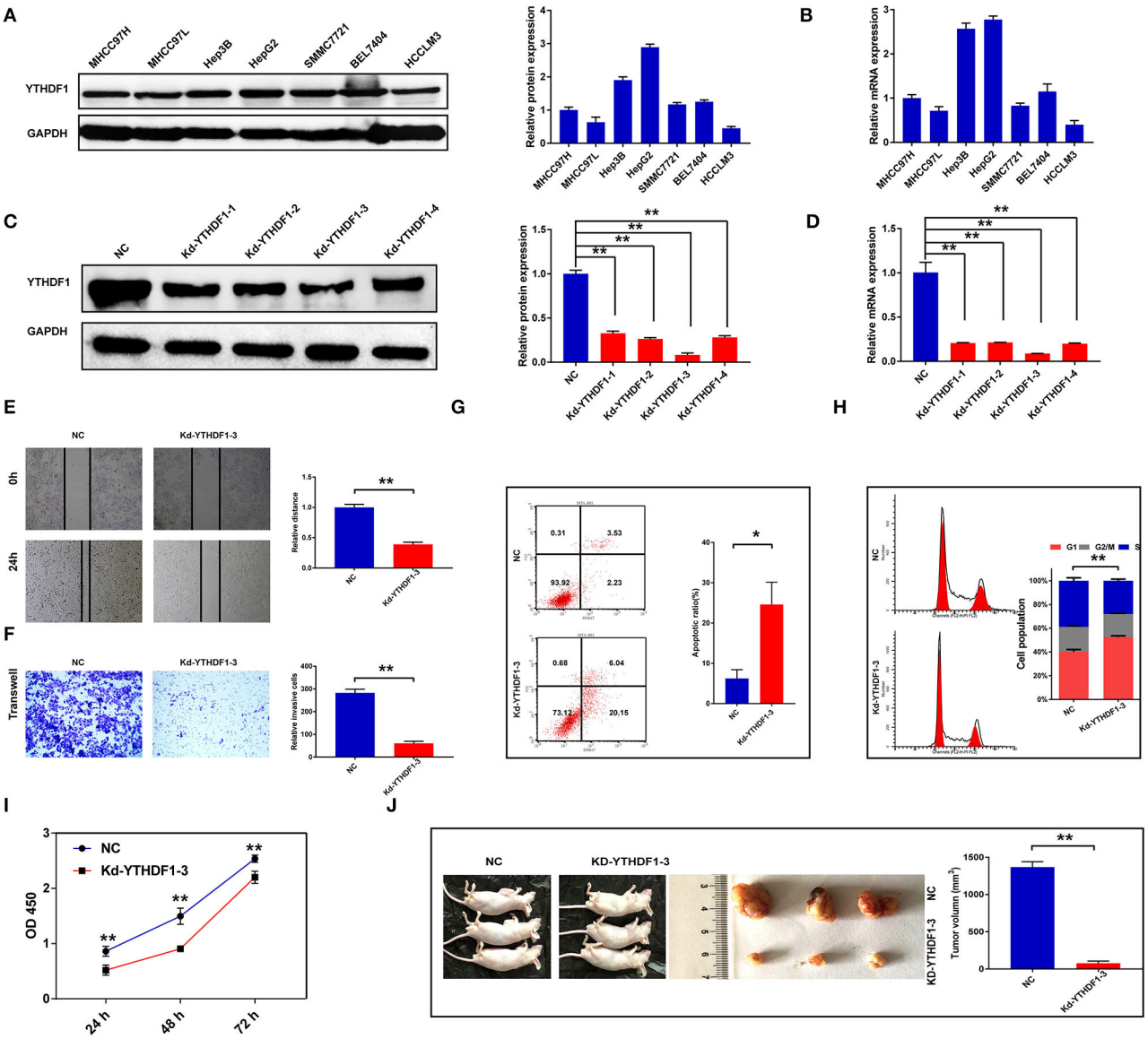

FIGURE 5 | Silencing YTHDF1 inhibited the aggressive behaviors of hepatocellular carcinoma (HCC) cells. **(A)** The expression of YTHDF1 in HCC cell lines was detected by Western blotting. **(B)** The mRNA level of YTHDF1 in HCC cell lines was detected by qRT-PCR. **(C)** Short hairpin RNAs (shRNAs) were transfected into HepG2 cells to block the YTHDF1 expression. The expression of YTHDF1 in each group was detected by Western blotting. **(D)** The mRNA expression of YTHDF1 in each group was detected by qRT-PCR. **(E,F)** Migration and invasion of HepG2 cells were detected by wound-healing assay and Transwell assay. **(G)** The apoptosis of HepG2 cells with YTHDF1 silencing. **(H)** Cell cycle of HepG2 cells was evaluated by flow cytometry. **(I)** The proliferation of cells was detected by Cell Counting Kit-8 (CCK-8). **(J)** The effects of YTHDF1 on tumor growth were evaluated by xenograft tumor in nude mice. $^{*}P < 0.05$, $^{**}P < 0.01$.

significantly inhibited (**Figures 5E,F**), while the apoptosis ratio of HepG2 cells was dramatically increased ($P = 0.0132$; **Figure 5G**). As presented in **Figure 5H**, the flow cytometry showed that depletion of YTHDF1 increased the proportion of cells in G0/G1. Consistently, the proliferation of HCC cells was significantly repressed in the Kd-YTHDF1-3 group (**Figure 5I**). Furthermore, knockdown of YTHDF1 obviously decreased the volume of xenograft tumors ($P < 0.001$; **Figure 5J**). These pieces of evidence suggested the correlation of YTHDF1 with aggressive phenotypes of HCC cells.

YTHDF1 Regulated Epithelial–Mesenchymal Transition and AKT/Glycogen Synthase Kinase-3β/β-Catenin Signaling of Hepatocellular Carcinoma Cells

Based on the observations above, we further discovered the underlying mechanisms regulated by YTHDF1. In general, co-occurrence genes shared similar functions and mechanisms. Thus, we examined the co-occurrence profiles with YTHDF1

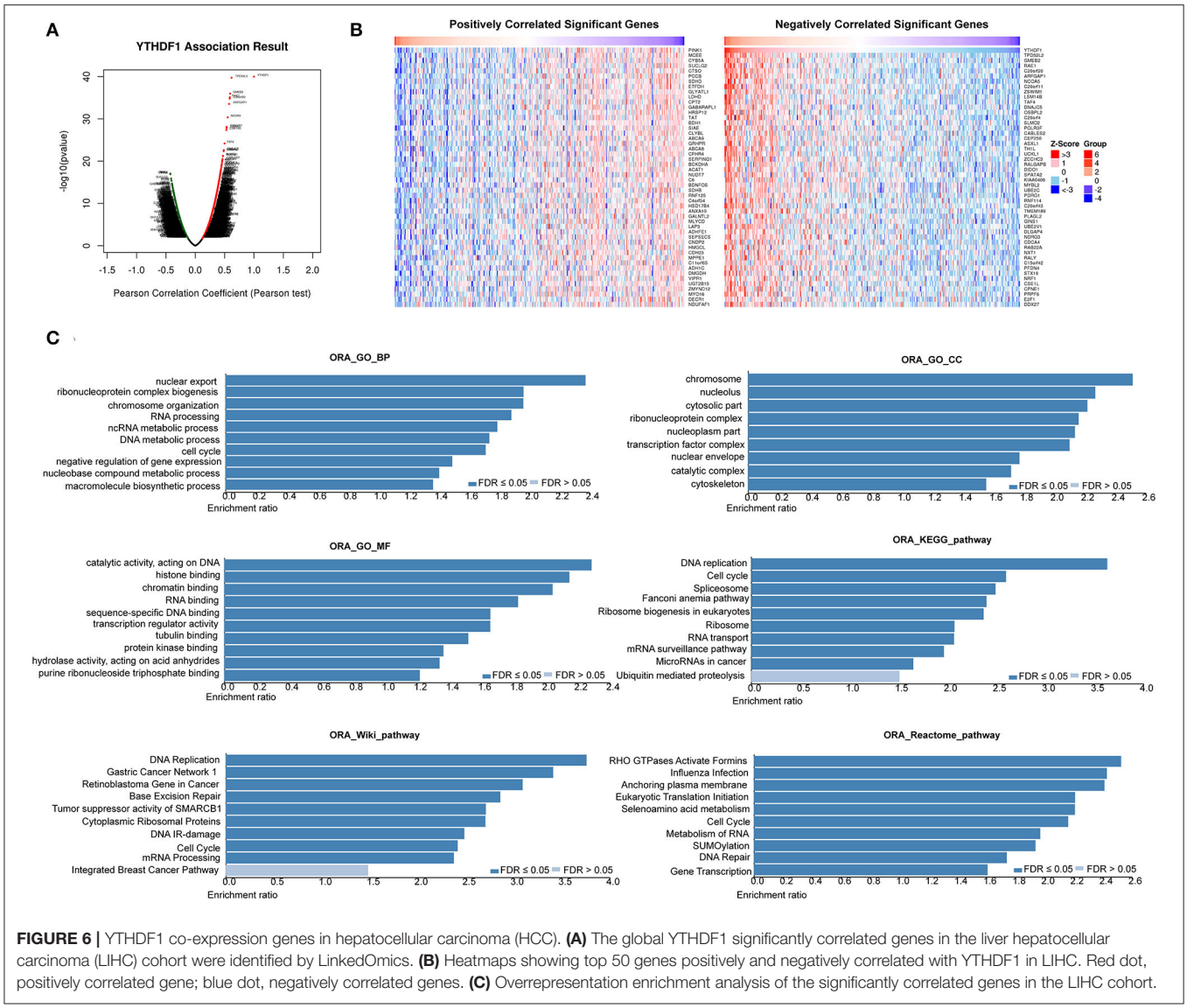

FIGURE 6 | YTHDF1 co-expression genes in hepatocellular carcinoma (HCC). **(A)** The global YTHDF1 significantly correlated genes in the liver hepatocellular carcinoma (LIHC) cohort were identified by LinkedOmics. **(B)** Heatmaps showing top 50 genes positively and negatively correlated with YTHDF1 in LIHC. Red dot, positively correlated gene; blue dot, negatively correlated genes. **(C)** Overrepresentation enrichment analysis of the significantly correlated genes in the LIHC cohort.

in HCC by LinkFinder. A total of 5,150 in 19,922 genes were defined as positively or negatively correlated significant genes with YTHDF1 (**Figures 6A,B**). ORA indicated that the co-occurrence genes were implicated in the RNA process, cell cycle, RNA binding, transcription regulator activity, DNA replication, and SUMOylation (**Figure 6C**). Next, GSEA was conducted to predict the potential functions and pathways induced by YTHDF1. The GO analysis suggested the association between YTHDF1 and G0/G1 transition, G1 damage checkpoint, mRNA splicing *via* spliceosome, and RNA splicing (**Figure 7A**). In addition, the KEGG analysis indicated that YTHDF1 was correlated with cell cycle, adherens junction, Wnt signaling, and phosphate metabolism (**Figure 7B**). As shown in **Figure 7C**, Hallmark analysis showed that YTHDF1 might be implicated in phosphoinositide 3-kinase (PI3K)/AKT signaling, MYC targets, Wnt/β-catenin signaling, and P53 pathway. Then, Western blotting was performed to verify the prediction above. Given the effects on invasion features and bioinformatic prediction, we initially detected epithelial–mesenchymal transition (EMT) markers. As shown in **Figure 7D**, knockdown of YTHDF1 significantly decreased the expression of N-cadherin and vimentin with the upregulation of E-cadherin, suggesting the positive effects of YTHDF1 on EMT process of HepG2 cells. Subsequently, we detected the pathways predicted by GSEA (**Figure 7E**). Following silencing YTHDF1, the expression of P-AKT(S308), P-AKT(S473), P-GSK-3β, β-catenin, c-MYC, TCF-1, cyclin D1, and CD44 was significantly downregulated, while the expression of total AKT and GSK-3β had no obvious changes. It suggested that YTHDF1 might enhance the aggressive behaviors of HCC

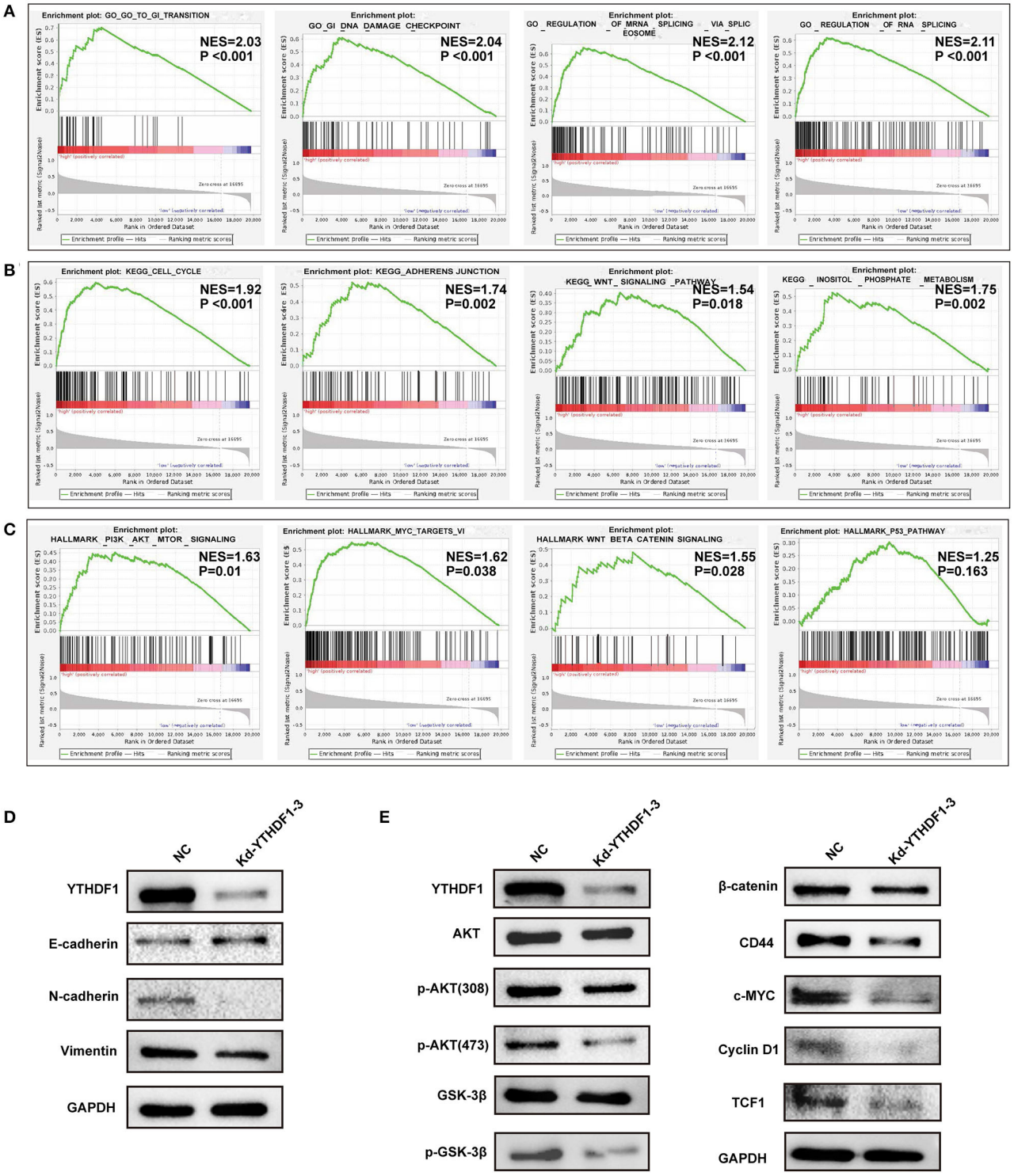

FIGURE 7 | YTHDF1 promoted epithelial–mesenchymal transition (EMT) and AKT/glycogen synthase kinase (GSK)-3β/β-catenin signaling of hepatocellular carcinoma (HCC) cells. **(A–C)** Gene set enrichment analysis (GSEA) was conducted to predict the potential functions and pathways regulated by YTHDF1 based on The Cancer Genome Atlas (TCGA) datasets. **(D)** The EMT markers were detected by Western blotting. **(E)** The markers of AKT/GSK-3β and Wnt/ β-catenin were detected by Western blotting.

cells through promoting the EMT process and activating AKT/GSK-3β/β-catenin signaling.

DISCUSSION

It is well-elucidated that the genetic and epigenetic alterations induced by the m^{6}A RNA methylation regulators modulate the related phenotypes. Aberrantly expressed m^{6}A RNA methylation regulators have been correlated with various malignant behaviors in multiple cancer types. For HCC, previous studies indicated that some m^{6}A RNA methylation regulators like KIAA1429, WTAP, and FTO were overexpressed in tissues and cell lines. In this study, we examined 16 widely reported m^{6}A RNA methylation regulators in TCGA LIHC datasets. Consistently, most m^{6}A regulators were overexpressed in HCC tissues compared with normal liver tissues. Based on the expression of m^{6}A regulators, we further divided the HCC cohort into two clusters by consensus clustering. Cluster 2, with high expression levels of m^{6}A RNA methylation regulators, showed significantly lower survival and higher tumor grades in contrast to those of cluster 1. It indicated that the expression of m^{6}A RNA methylation regulators might be associated with poor prognosis of HCC. According to the univariate Cox regression analysis, 10 of the 16 m^{6}A regulator genes were considered potential prognostic factors of HCC. Furthermore, differentially expressed genes between the two clusters were found enriched in well-known tumor-related pathways, including cAMP signaling pathway, Hippo signaling pathway, cell cycle, AMP-activated protein kinase (AMPK) signaling pathway, and PI3K–AKT signaling pathway. It further suggested the underlying correlations of m^{6}A methylation regulators with initiation and progression of HCC.

Furthermore, by using LASSO algorithm, we constructed a risk signature with five m^{6}A RNA methylation regulators, including KIAA1429, ZC3H13, YTHDF1, YTHDF2, and METTL3. The risk score of this signature was correlated with aggressive clinicopathological features, which could also act as an independent prognosis factor for the survival of patients. In addition, the risk score derived from five m^{6}A RNA methylation regulators showed potential prognostic value in patients at different tumor stages. One recent study reported a signature consisting of METTL14 and METTL3 as an independent prognosis factor in clear cell renal cell carcinoma (Wang et al., 2020). Similar results about the clinical value of m^{6}A regulators have also been found in bladder cancer, head and neck squamous cell carcinoma, and gastric cancer (Chen M. et al., 2019; Su et al., 2019; Zhao and Cui, 2019). However, different from previous studies, this study, for the first time, validated the prognostic value of the risk signature in two additional datasets, the ICGC and PCAWG datasets. As expected, the m^{6}A regulator-based risk signature could predict poor survival of HCC cases in both of the two datasets. Given the current data, further efforts should be put to evaluate m^{6}A methylation regulators as robust predictors in more HCC cohorts at multicenter level.

In addition to the prognostic value of the risk signature, the m^{6}A RNA methylation regulators might also be associated with tumor progression. Of them, the expressions of YTHDF1 and YTHDF2 are shown to be dramatically elevated in HCC cases from early to advanced stages. As is known, the YTH domain family members can recognize and directly bind m^{6}A methylation on RNA. Though YTHDF1 and YTHDF2 share the same m^{6}A site-related YTH domain, other domains may bring them distinct functions. In the cytoplasm, YTHDF1 facilitates ribosome loading and promotes target translation, while YTHDF2 localizes its targets to process bodies and induce further degradation. YTHDF2 was recently recognized as a tumor suppressor, in which proliferation and angiogenesis were impaired by YTHDF2 overexpression (Hou et al., 2019; Zhong et al., 2019). In contrast, YTHDF1 promoted malignant behaviors by regulating the translation of tumor-related genes (Liu et al., 2020). A recent study indicated that the aberrant expression of YTHDF1 was associated with poor survival of HCC patients (Zhao et al., 2018). According to the bioinformatic analysis, overexpression of YTHDF1 was observed in the ICGC and multiple GEO datasets. Thus, we further investigated the expression features, potential roles, and mechanisms of YTHDF1 in HCC. As shown in functional assays, silencing YTHDF1 significantly inhibited the malignant behaviors of HCC cells, including proliferation, migration, invasion, and growth of xenograft tumors. Then, the current study tried to investigate potential mechanisms in combination of the bioinformatic prediction and molecular validation. In consistence with the phenotype changes induced by YTHDF1 silencing, GSEA indicated that YTHDF1 might be implicated in cell cycle, G0/G1 transition, and adherens junction. Further molecular assays demonstrated that YTHDF1 could promote EMT of HCC cells. In addition, knockdown of YTHDF1 significantly downregulated the phosphorylation level of AKT and GSK-3β and expression of β-catenin and its downstream markers like CD44, c-MYC, and TCF-1, suggesting that YTHDF1 might enhance aggressive phenotypes by activating AKT/GSK-3β/β-catenin signaling. Interestingly, YTHDF1 was recently reported to facilitate cancer stem cell properties (Bai et al., 2019). β-Catenin and its downstream CD44 were known as canonical markers of liver cancer stem cells. It was speculated that YTHDF1 might be involved in the regulation of cancer stem cell properties, thereby facilitating HCC progression. Though existing pieces of evidence have shed light on the carcinogenic effects of m^{6}A RNA methylation regulator YTHDF1, more investigations should be conducted to further reveal its underlying mechanisms as well as the clinical significance in HCC.

CONCLUSION

In conclusion, this study established a risk signature formed by five m^{6}A RNA methylation regulators for HCC prognosis based on TCGA datasets, which was further validated in ICGC and PCAWG datasets. Furthermore, YTHDF1 was further identified

as an oncogenic gene for HCC by facilitating AKT/GSK-3β/β-catenin signaling. Our study provided evidence for future exploration of the prognostic and targeted value of m^6A methylation in HCC.

DATA AVAILABILITY STATEMENT

The datasets presented in this study can be found in online repositories. The names of the repository/repositories and accession number(s) can be found in the article/**Supplementary Material**.

ETHICS STATEMENT

The animal study was reviewed and approved by The Animal Care and Use Committee of Nantong University. Written informed consent was obtained from the owners for the participation of their animals in this study.

AUTHOR CONTRIBUTIONS

WZ and RN conceived and designed the study. QS, WN, and JZ analyzed the data. SB and MZ drafted the paper. WZ revised the manuscript. All authors read and approved the final manuscript.

FUNDING

This study was supported by grants from the National Natural Science Foundation (82070622 and 81702419), the Key Research and Development Plan of Jiangsu Province (BE2020668), and the Nantong Science and Technology Project (MS12019013).

SUPPLEMENTARY MATERIAL

The Supplementary Material for this article can be found online at: https://www.frontiersin.org/articles/10.3389/fmolb.2020.604766/full#supplementary-material

REFERENCES

Alarcon, C. R., Goodarzi, H., Lee, H., Liu, X., Tavazoie, S., and Tavazoie, S. F. (2015). HNRNPA2B1 is a mediator of m(6)A-dependent nuclear RNA processing events. *Cell* 162, 1299–1308. doi: 10.1016/j.cell.2015.08.011

Bai, Y., Yang, C., Wu, R., Huang, L., Song, S., Li, W., et al. (2019). YTHDF1 regulates Tumorigenicity and cancer stem cell-like activity in human colorectal carcinoma. *Front. Oncol.* 9:332. doi: 10.3389/fonc.2019.00332

Bray, F., Ferlay, J., Soerjomataram, I., Siegel, R. L., Torre, L. A., and Jemal, A. (2018). Global cancer statistics 2018: GLOBOCAN estimates of incidence and mortality worldwide for 36 cancers in 185 countries. *CA Cancer J. Clin.* 68, 394–424. doi: 10.3322/caac.21492

Cancer Genome Atlas Research (2017). Comprehensive and integrative genomic characterization of hepatocellular carcinoma. *Cell* 169, 1327–1341.e1323. doi: 10.1016/j.cell.2017.05.046

Chen, M., Nie, Z. Y., Wen, X. H., Gao, Y. H., Cao, H., and Zhang, S. F. (2019). m6A RNA methylation regulators can contribute to malignant progression and impact the prognosis of bladder cancer. *Biosci. Rep.* 39:BSR20192892. doi: 10.1042/BSR20192892

Chen, M., Wei, L., Law, C. T., Tsang, F. H., Shen, J., Cheng, C. L., et al. (2018). RNA N6-methyladenosine methyltransferase-like 3 promotes liver cancer progression through YTHDF2-dependent posttranscriptional silencing of SOCS2. *Hepatology* 67, 2254–2270. doi: 10.1002/hep.29683

Chen, Y., Peng, C., Chen, J., Chen, D., Yang, B., He, B., et al. (2019). WTAP facilitates progression of hepatocellular carcinoma via m6A-HuR-dependent epigenetic silencing of ETS1. *Mol. Cancer* 18:127. doi: 10.1186/s12943-019-1053-8

Cheng, X., Li, M., Rao, X., Zhang, W., Li, X., Wang, L., et al. (2019). KIAA1429 regulates the migration and invasion of hepatocellular carcinoma by altering m6A modification of ID2 mRNA. *Onco Targets Ther* 12, 3421–3428. doi: 10.2147/OTT.S180954

Finn, R. S., Zhu, A. X., Farah, W., Almasri, J., Zaiem, F., Prokop, L. J., et al. (2018). Therapies for advanced stage hepatocellular carcinoma with macrovascular invasion or metastatic disease: a systematic review and meta-analysis. *Hepatology* 67, 422–435. doi: 10.1002/hep.29486

Gao, J., Aksoy, B. A., Dogrusoz, U., Dresdner, G., Gross, B., Sumer, S. O., et al. (2013). Integrative analysis of complex cancer genomics and clinical profiles using the cBioPortal. *Sci Signal* 6:pl1. doi: 10.1126/scisignal.2004088

He, L., Li, H., Wu, A., Peng, Y., Shu, G., and Yin, G. (2019). Functions of N6-methyladenosine and its role in cancer. *Mol. Cancer* 18:176. doi: 10.1186/s12943-019-1109-9

Hou, J., Zhang, H., Liu, J., Zhao, Z., Wang, J., Lu, Z., et al. (2019). YTHDF2 reduction fuels inflammation and vascular abnormalization in hepatocellular carcinoma. *Mol. Cancer* 18:163. doi: 10.1186/s12943-019-1082-3

Huang, Z., Zhou, J. K., Wang, K., Chen, H., Qin, S., Liu, J., et al. (2020). PDLIM1 inhibits tumor metastasis through activating hippo signaling in hepatocellular carcinoma. *Hepatology* 71, 1643–1659. doi: 10.1002/hep.30930

Lan, T., Li, H., Zhang, D., Xu, L., Liu, H., Hao, X., et al. (2019). KIAA1429 contributes to liver cancer progression through N6-methyladenosine-dependent post-transcriptional modification of GATA3. *Mol. Cancer* 18:186. doi: 10.1186/s12943-019-1106-z

Liao, S., Sun, H., and Xu, C. (2018). YTH domain: a family of N(6)-methyladenosine (m(6)A) Readers. *Genom. Proteomics Bioinformatics* 16, 99–107. doi: 10.1016/j.gpb.2018.04.002

Liu, J., Yue, Y., Han, D., Wang, X., Fu, Y., Zhang, L., et al. (2014). A METTL3-METTL14 complex mediates mammalian nuclear RNA N6-adenosine methylation. *Nat. Chem. Biol.* 10, 93–95. doi: 10.1038/nchembio.1432

Liu, N., Zhou, K. I., Parisien, M., Dai, Q., Diatchenko, L., and Pan, T. (2017). N6-methyladenosine alters RNA structure to regulate binding of a low-complexity protein. *Nucleic Acids Res.* 45, 6051–6063. doi: 10.1093/nar/gkx141

Liu, T., Wei, Q., Jin, J., Luo, Q., Liu, Y., Yang, Y., et al. (2020). The m6A reader YTHDF1 promotes ovarian cancer progression via augmenting EIF3C translation. *Nucleic Acids Res.* 48, 3816–3831. doi: 10.1093/nar/gkaa048

Makarova-Rusher, O. V., Altekruse, S. F., Mcneel, T. S., Ulahannan, S., Duffy, A. G., Graubard, B. I., et al. (2016). Population attributable fractions of risk factors for hepatocellular carcinoma in the United States. *Cancer* 122, 1757–1765. doi: 10.1002/cncr.29971

Massimi, M., Ragusa, F., Cardarelli, S., and Giorgi, M. (2019). Targeting cyclic AMP signalling in hepatocellular carcinoma. *Cells* 8:1511. doi: 10.3390/cells8121511

Meyer, K. D., Saletore, Y., Zumbo, P., Elemento, O., Mason, C. E., and Jaffrey, S. R. (2012). Comprehensive analysis of mRNA methylation reveals enrichment in 3' UTRs and near stop codons. *Cell* 149, 1635–1646. doi: 10.1016/j.cell.2012.05.003

Su, Y., Huang, J., and Hu, J. (2019). m(6)A RNA methylation regulators contribute to malignant progression and have clinical prognostic impact in gastric cancer. *Front. Oncol.* 9:1038. doi: 10.3389/fonc.2019.01038

Vasaikar, S. V., Straub, P., Wang, J., and Zhang, B. (2018). LinkedOmics: analyzing multi-omics data within and across 32 cancer types. *Nucleic Acids Res.* 46, D956–D963. doi: 10.1093/nar/gkx1090

Wang, J., Zhang, C., He, W., and Gou, X. (2020). Effect of m(6)A RNA methylation regulators on malignant progression and prognosis in renal clear cell carcinoma. *Front. Oncol.* 10:3. doi: 10.3389/fonc.2020.00003

Wang, X., Lu, Z., Gomez, A., Hon, G. C., Yue, Y., Han, D., et al. (2014). N6-methyladenosine-dependent regulation of messenger RNA stability. *Nature* 505, 117–120. doi: 10.1038/nature12730

Wang, X., Zhao, B. S., Roundtree, I. A., Lu, Z., Han, D., Ma, H., et al. (2015). N(6)-methyladenosine modulates messenger RNA translation efficiency. *Cell* 161, 1388–1399. doi: 10.1016/j.cell.2015.05.014

Warda, A. S., Kretschmer, J., Hackert, P., Lenz, C., Urlaub, H., Hobartner, C., et al. (2017). Human METTL16 is a N(6)-methyladenosine (m(6)A) methyltransferase that targets pre-mRNAs and various non-coding RNAs. *EMBO Rep.* 18, 2004–2014. doi: 10.15252/embr.201744940

Wu, M., Miao, H., Fu, R., Zhang, J., and Zheng, W. (2020). Hepatic stellate cell: a potential target for hepatocellular carcinoma. *Curr Mol Pharmacol.* 13, 261–272. doi: 10.2174/1874467213666200224102820

Zhao, X., Chen, Y., Mao, Q., Jiang, X., Jiang, W., Chen, J., et al. (2018). Overexpression of YTHDF1 is associated with poor prognosis in patients with hepatocellular carcinoma. *Cancer Biomark.* 21, 859–868. doi: 10.3233/CBM-170791

Zhao, X., and Cui, L. (2019). Development and validation of a m(6)A RNA methylation regulators-based signature for predicting the prognosis of head and neck squamous cell carcinoma. *Am. J. Cancer Res.* 9, 2156–2169.

Zhong, L., Liao, D., Zhang, M., Zeng, C., Li, X., Zhang, R., et al. (2019). YTHDF2 suppresses cell proliferation and growth via destabilizing the EGFR mRNA in hepatocellular carcinoma. *Cancer Lett.* 442, 252–261. doi: 10.1016/j.canlet.2018.11.006

Conflict of Interest: The authors declare that the research was conducted in the absence of any commercial or financial relationships that could be construed as a potential conflict of interest.

frontiers in Molecular Biosciences

REVIEW
published: 13 January 2021
doi: 10.3389/fmolb.2020.620973

Regulator of Chromosome Condensation 2 Modulates Cell Cycle Progression, Tumorigenesis, and Therapeutic Resistance

*Kun Guo, Cheng Zhao, Bin Lang, Huiqin Wang, Hang Zheng and Feng Zhang**

College of Life Sciences, Shanghai Normal University, Shanghai, China

Accurate regulation of cell cycle is important for normal tissue development and homeostasis. RCC2 (Regulator of Chromosome Condensation 2) play a role as chromosomal passenger complex (CPC) implicated in all cell cycle phases. RCC2 was initially identified as Ran guanine exchange factor (GEF) for small G proteins. Therefore, RCC2 plays a key role in oncogenesis of most cancers. RCC2 is implicated in Colorectal Cancer (CRC), Lung Adenocarcinoma (LUAD), breast cancer, and ovarian cancer. Expression level of RCC2 protein determines regulation of tumor cell proliferation, invasion, metastasis, and radio-chemotherapeutic resistance. In this review, we explored proteins that interact with RCC2 to modulate tumor development and cancer therapeutic resistance by regulation of cell cycle process through various signaling pathways.

Keywords: regulator of chromosome condensation 2, chromosomal passenger complex, tumorgenesis, cancer therapeutic resistance, DNA damage

OPEN ACCESS

Edited by:
Yi Chieh Lim,
Danish Cancer Society Research Center (DCRC), Denmark

Reviewed by:
Hazel Quek,
The University of Queensland, Australia
Diana Aguilar-Morante,
Danish Cancer Society, Denmark

****Correspondence:***
Feng Zhang
fengz@shnu.edu.cn

Specialty section:
This article was submitted to Cellular Biochemistry, a section of the journal Frontiers in Molecular Biosciences

Received: *24 October 2020*
Accepted: *08 December 2020*
Published: *13 January 2021*

Citation:
Guo K, Zhao C, Lang B, Wang H, Zheng H and Zhang F (2021) Regulator of Chromosome Condensation 2 Modulates Cell Cycle Progression, Tumorigenesis, and Therapeutic Resistance. Front. Mol. Biosci. 7:620973. doi: 10.3389/fmolb.2020.620973

INTRODUCTION

Regulator of Chromosome Condensation 2 (RCC2) is a member of Regulator of Chromatin Condensation 1 (RCC1) superfamily. Genes of this family comprise one or more RCC1-like domains (RLDs) involved in protein-protein interactions (Hadjebi et al., 2008). Proteins in this superfamily play significant roles in nucleocytoplasmic transport (Riddick and Macara, 2005), ubiquitinoylation (Scheffner and Staub, 2007), cell cycle, and response to DNA damage (Tan and Lee, 2004; Choi et al., 2013; Smith et al., 2014). RCC2, also known as Telophase Disc-60 (TD-60), was initially identified as a telophase disk-binding protein during mitosis, as it mediates progression of prometaphase to metaphase (Andreassen et al., 1991; Mollinari et al., 2003). RCC2 gene has a mitotic phosphorylation motif implicated in regulation of protein localization during mitosis (Yang et al., 2007). Furthermore, previous studies report that RCC2 gene plays an essential role in regulating cell cycle progression during interphase (Yenjerla et al., 2013). In addition, RCC2 acts as a specific Guanine Exchange Factor (GEF) for both Rac1 and RalA proteins (Mollinari et al., 2003). Notably, RCC2/RalA are implicated in regulation of kinetochore-microtubule interactions during prometaphase stage of mitosis (Papini et al., 2015). Moreover, Hu et al. report that RCC2 plays a pivotal role in G2-M transition (Hu et al., 2018).

The function of RCC2 in tumor development has been studied extensively in recent years due to its involvement in tumor cell migration. For example, RCC2 interacts with Fibronectin-dependent (FN-dependent) adhesion signaling pathways, by inhibiting activation of Rac1 and Arf6, which regulate adhesion complexes, thereby facilitating continuous cell migration (Danen, 2009; Humphries et al., 2009). A previous study shows that RCC2 overexpression promotes metastasis of

Lung Adenocarcinoma (LUAD) by inducing Epithelial-Mesenchymal Transition (EMT) through modulation of mitogen-activated protein kinase-c-Jun N-terminal kinase (MAPK -JNK) signaling pathway (Pang et al., 2017). MAPK-JNK is a potential autophagy regulation pathway positively correlated with lung cancer tumorigenesis (Shih et al., 2012; Wang et al., 2014; Zhou et al., 2015). Additionally, RCC2 interacts with and deactivates Rac1, which is controlled by p53 (a short-lived tumor suppressor protein) signaling axis. These interactions regulate cell migration and suppression of metastasis in colorectal cancer (Song et al., 2018). Moreover, RCC2 plays an oncogenic role in breast cancer, by activating Wnt-signaling pathway, thus promoting cell proliferation and migration through Epithelial-mesenchymal transition (EMT) (Chen et al., 2019). Further, RCC2 is implicated in tumor cell proliferation (Matsuo et al., 2013; Chen et al., 2019; Yu et al., 2019), apoptosis and sensitivity (Wu et al., 2018; Gong et al., 2019; Yu et al., 2019), and poor prognosis of microsatellite stable (MSS) tumors (Bruun et al., 2015). Although several studies on RCC2 have been conducted, no review has previously reported its functions. Therefore, this review explores the functions of RCC2 in cell cycle and roles of RCC2 in cancer progression.

In this review, we present important aspects of RCC2 biology. The review summarizes the role of RCC2 in cell cycle, effects of overexpression of RCC2 gene in development of various cancers, such as promotion of tumor cell metastasis, RCC2 molecular features and proteins that interact with RCC2 as a tumor-promoting gene.

GENE AND PROTEIN STRUCTURES

Regulator of Chromosome Condensation 2 (RCC2) (OMIM accession # 609587) is encoded by a 4040 bp gene composed of 13 exons and located on the short arm of chromosome 1 (1p36.13) (**Figure 1**). RCC2 expression occurs during the late G2 phase of the cell cycle (Mollinari et al., 2003). Despite its location in the nucleus, RCC2 plays different roles in the cytoskeleton, plasma membrane, centromere, chromosome, and midbody (Andreassen et al., 1991; Martineau-Thuillier et al., 1998; Mollinari et al., 2003; Yenjerla et al., 2013; Williamson et al., 2014). A previous study reports that p53 binds to a palindromic motif in the promoter region of RCC2 to regulate its transcription (Song et al., 2018). Notably, RCC2 gene encodes a 522-amino acid protein which contains a conserved nuclear localization signal (NLS) in its amino-terminal region (**Figure 1**). A nuclear localization signal is an amino acid sequence that "tags" a protein for translocation into the nucleus by nuclear transport. RCC2 protein accumulates in the inner centromere region of chromosomes during prophase and redistributes to the midzone of the mitotic spindle during anaphase (Andreassen et al., 1991; Martineau-Thuillier et al., 1998; Mollinari et al., 2003). RCC2 protein structure consists of a RCC1-like domain (RLD) near the carboxyl-terminal region (**Figure 1**) (Ohtsubo et al., 1987). The structure of RLD comprises a seven-bladed propeller, which plays a role in protein-protein interaction, and in binding DNA (Ohtsubo et al., 1987; Aebi et al., 1990; Seki et al., 1996; Renault et al., 1998). RLD in RCC2 comprises five repetitive elements formed by 51–75 amino acid residues (**Figure 1**). Interestingly, Song et al. reported that the RLD domain of RCC2 binds to Rac1 through a β-hairpin comprising seven-bladed propeller structure thus inactivating it (Song et al., 2018).

RCC2 AND CELL CYCLE

Cell cycle is a complex process, comprising a series of events that strictly control cellular growth and division. Several proteins directly or indirectly interact with the continuously changing chromatin during cell cycle to ensure that chromosomes are accurately segregated into two daughter cells. Therefore, cell cycle is essential for normal growth and development of organisms.

In 1991, Paul et al. reported a new mammalian mitotic organelle, which they named "Telophase Disc-60xl0^{3}Mr" (TD-60) which was later confirmed as RCC2 by HUGO Gene Nomenclature Committee (HGNC) (Andreassen et al., 1991). The protein was identified in human autoimmune serum that revealed its role in cytokinesis (Andreassen et al., 1991). During prophase, RCC2 is located at the primary constriction of the chromosome. RCC2 dissociates from chromosomes until mid-anaphase, thus aligning with microtubules in the region between the sister chromatids (Andreassen et al., 1991). Thereafter, RCC2 migrates to the equator and becomes part of the microtubule-independent organelle (Andreassen et al., 1991). Subsequently, RCC2 is incorporated into a complex together with motor protein. The complex migrates to the plus end of the interpolar microtubules in anaphase and is finally incorporated into the telophase disc organelle. The complex then fully partitions the cell at the spindle equator in late anaphase and through telophase (**Figure 2**) (Andreassen et al., 1991).

Previous studies report that RCC2 is a member of passenger protein family, also known as chromosomal passenger complex (CPC). With the complex comprises Aurora B kinase (Adams et al., 2000), INCENP (Cooke et al., 1987), and Survivin (Gassmann et al., 2004). CPC regulates chromosomal alignment, spindle assembly, and cell cleavage during mitosis (**Figure 2**) (Mollinari et al., 2003). However, Diana et al. reported that RCC2 is a component of the complex but only associates with and functions as a CPC (Mollinari et al., 2003; Papini et al., 2015). Notably, RCC2 functions are vital for accurate completion of cytokinesis. Moreover, binding of RCC2 to microtubules and nucleotide-free form of the small G protein Rac1 is essential for interaction of kinetochores with spindle microtubules and passenger proteins at inner centromeres

Abbreviations: RCC2, Regulator of Chromosome Condensation 2; CPC, Chromosomal passenger complex; GEF, Ran guanine exchange factor; LUAD, Lung adenocarcinoma; RLDs, RCC1-like domains; EMT, Epithelial-mesenchymal transition; MSS, Microsatellite stable; NLS, Nuclear localization signal; TD-60, Telophase Disc-60xl0^{3}Mr; CRC, Colorectal cancer; MSI, Microsatellite instable; MMR, DNA mismatch repair; lncRNAs, Long non-coding RNAs; NSCLC, Non-small cell lung cancer; TCGA, The Cancer Genome Atlas; DNMT1, DNA methyltransferase 1; HCC, Hepatocellular carcinoma; XPO1, Exportin-1; DDP, Cisplatin; GBM, Glioblastoma; ECM, Extracellular matrix; MMPs, Matrix metalloproteinases; EOC, Epithelial ovarian carcinoma; DDR, DNA damage response; CSE, Cigarette smoke extract.

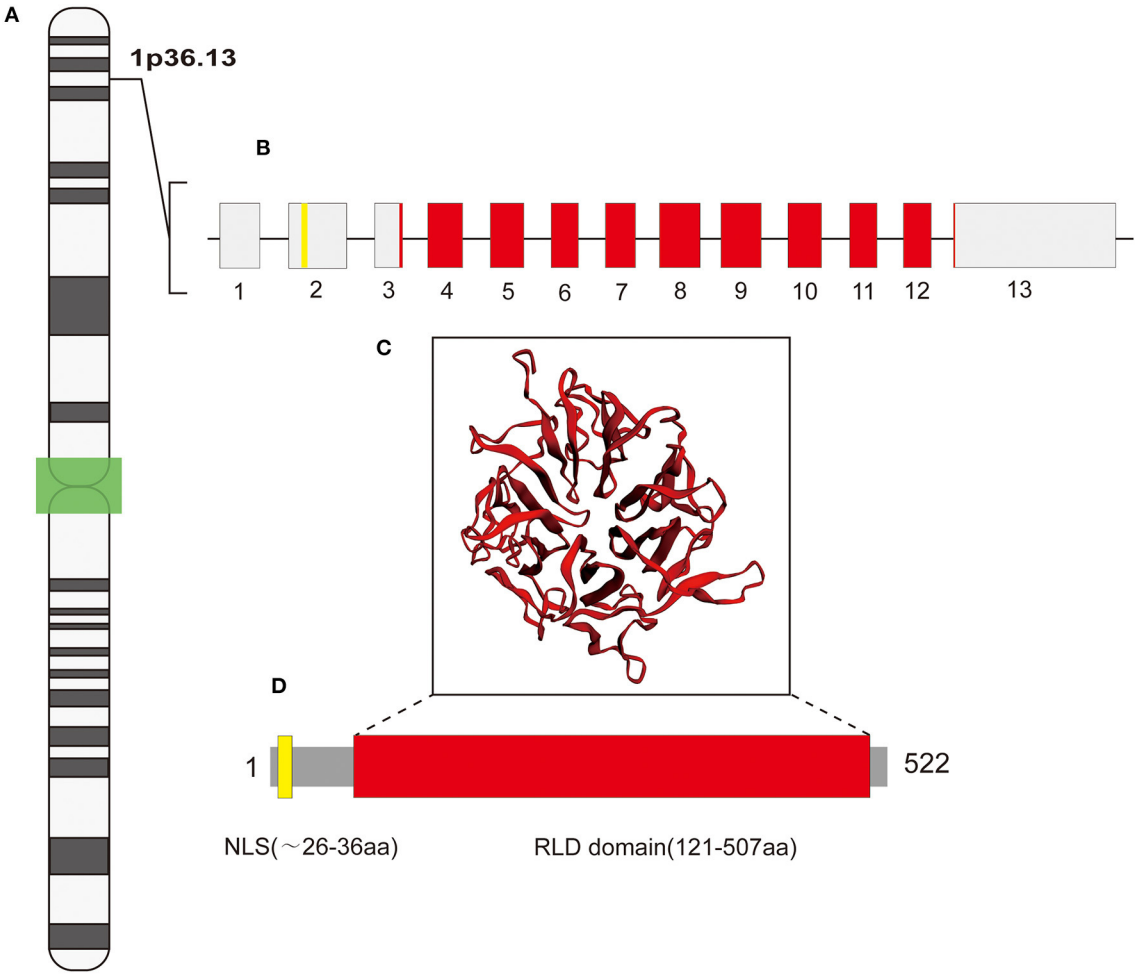

FIGURE 1 | A representation of RCC2 gene and its products. **(A)** The gene is located on chromosome 1p36.13; the structure on the left shows the chromosome cytobands, with the centromere (shown in green). **(B)** The gene is composed of 13 exons, whereby exon 2 encodes the NLS motif (depicted in yellow); RLD domain is encoded by the 3′ end of exon 3 to the 5′ start of exon 13 (in red). **(C)** RLD domain (in red) stretching from the middle to the carboxyl-terminal region. The inset represents β -propeller secondary structure of RLD domain [predicted by Phyre2 (Kelley et al., 2015)]. **(D)** The protein structure comprises 522 amino acid residues that includes an NLS motif at its amino-terminal region, starting approximately at the 26th residue and ending at the 36th residue (yellow box).

(Mollinari et al., 2003). Studies using G2/M arrested in Rac1 mutants showed that binding of RCC2 to microtubules regulates transition from prometaphase to metaphase and G2/M progression (**Figure 2**) (Mollinari et al., 2003; Bruun et al., 2015). In addition, RCC2 converts GTP-Rac1 to GDP-Rac1 (**Figure 2**) (Song et al., 2018). A new mitotic phosphorylation motif reported in RCC2 regulates protein localization during mitotic progression, thus regulating cell cycle process (Yang et al., 2007). Furthermore, RCC2 modulates activation of Rac1 and acts as a GEF for RalA. Therefore, RCC2/RalA modulates kinetochore-microtubule interactions by regulating CPC in prometaphase during mitosis (**Figure 2**) (Papini et al., 2015). Therefore, RCC2 plays an essential role during transition from prometaphase to metaphase and G2/M, whereas RCC1 is only implicated in G1 phase (Dasso et al., 1992; Moore, 2001).

Previous studies report that RCC2 interacts with Rac1 and Arf6 cell signaling, the interphase cell cycle progression related component (α5β1) integrins, and cortactin, implying that RCC2 plays a role in interphase (Humphries et al., 2009; Grigera et al., 2012). Mythili et al. report that loss of RCC2 affects normal cell cycle progression of G2 and suppresses G1/S (Yenjerla et al., 2013). These findings imply that RCC2 plays an essential role in regulating cell cycle progression during interphase.

In summary, low expression levels of RCC2 inhibits the cell cycle, through G1 and G2 arrest and blocking of prometaphase, thus inhibiting cell proliferation. Therefore, RCC2 plays a significant role in the cell cycle process, especially during mitosis and cell division.

ROLE OF RCC2 IN CANCERS

As mentioned earlier, RCC2 protein plays an important role in mitosis (Mollinari et al., 2003). Proteins involved in mitosis are highly expressed in various tumor cells implying that they play

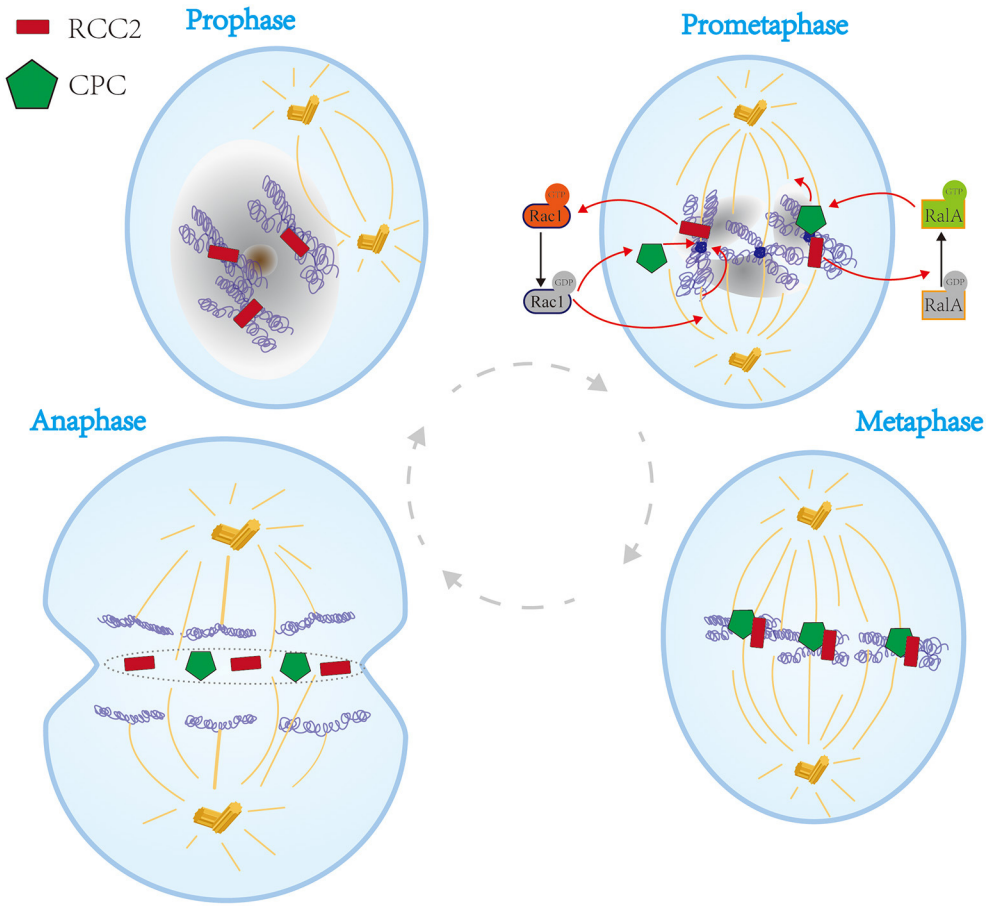

FIGURE 2 | Schematic representation of the functions of RCC2 in the cell cycle process. **In prophase**, RCC2 is located at the chromosome primary constriction. **In prometaphase**, RCC2 binds to microtubules and converts GTP-Rac1 to GDP-Rac1, which plays a vital role in association of kinetochores with spindle microtubules and association of passenger proteins with inner centromeres. Moreover, RCC2 acts as a GEF for RalA, which converts GDP-RalA to GTP-RalA thus modulating kinetochore-microtubule interactions by regulating CPC. **In metaphase**, RCC2 migrates to the equator together with CPC. **In anaphase**, RCC2 is incorporated into the telophase disc organelle, thus fully partitioning the cell at the spindle equator in late anaphase and telophase.

a role in cancer progression. Notably, RCC2 is highly expressed in several cancer types, including breast, ovarian, lymphoma, cervical, breast, gastric, colorectal, lung, and liver cancer (Chen et al., 2019).

RCC2 and Colorectal Cancer

Colorectal Cancer (CRC) is the fourth highest cause of cancer-related deaths worldwide (Brody, 2015). High incidence rate of CRC can be attributed to adoption of western diets and lifestyles in most parts of the world (Brody, 2015). Several genomic analyses show that RCC2 is one of the commonly mutated genes in CRC (Cancer Genome Atlas Network, 2012; Giannakis et al., 2014). RCC2 is a highly conserved protein implicated in prognosis of colorectal cancers, including microsatellite instable (MSI) tumors and microsatellite stable (MSS) tumors (Kim et al., 2002). However, studies report that RCC2 is implicated in colorectal carcinomas through MSI induced by DNA mismatch repair (MMR) deficiency (Kim et al., 2002).

Furthermore, protein expression levels of RCC2 are positively correlated with development of CRC. The (A)10 mononucleotide repeat located in the 5′UTR of RCC2 and 5′UTR region also implictaed in translational regulation (Pickering and Willis, 2005). Deletion of a single base in the (A) 10 repeat decreases RCC2 expression, whereas RCC2 knockdown causes MSI tumor arrest at the G2-M phase and increased levels of apoptosis (Bruun et al., 2015). Consequently, RCC2 has plays an oncogenic role in MSI tumors. However, low protein expression level of RCC2 is associated with poor prognosis of MSS, which is attributed to its functional inhibition of tumor cell metastasis by regulating integrin α5β1-fibronectin (FN) signaling pathway (Humphries et al., 2009; Bruun et al., 2015). A study by Gautam and colleagues showed that RCC2 is a novel p53 transcriptional target that interacts with small GTPase Rac1 to inhibit its activation.

Interestingly, depletion of RCC2 in human colon cancer cell line (HCT116) showed elongated cellular morphology and increased cell migration; however, cell proliferation differences were not observed (Song et al., 2018). Activation of Rac1 in cell

migration has been reported in previous studies (Pankov et al., 2005; Frank et al., 2006). In colorectal cancer, RCC2 interacts and deactivates Rac1, which is controlled by p53 signaling axis. Deactivation of Rac1 regulates cell migration and suppresses metastasis in colorectal cancer. In conclusion, mechanism of RCC2 in CRC is complex, therefore, further studies should be carried out to explore the molecular mechanism of RCC2 in development of CRC.

RCC2 and Lung Adenocarcinoma (LUAD)

Lung cancer is among the leading cause of cancer deaths, contributing about one-quarter of global cancer-related mortalities (Siegel et al., 2020). Adenocarcinoma is the most common histologic type of lung cancer worldwide (Cancer Genome Atlas Research Network, 2014). RCC2 is a poor independent prognostic factor for LUAD patients. RNA-seq analysis of data retrieved from The Cancer Genome Atlas (TCGA) database data showed overexpression of RCC2 in LUADs (Pang et al., 2017). High expression level of RCC2 is positively correlated with T status of the tumor, lymph node metastasis, advanced clinical stage, and poor overall survival in LUAD patients (Pang et al., 2017).

In LUAD, RCC2 is associated with EMT and extracellular matrix remodeling, which contributes to tumor metastasis (Pang et al., 2017). RCC2-transfected cells show high expression levels of JNK1/2 (Pang et al., 2017). In addition, LUAD samples show high RCC2 expression, which is positively correlated with high JNK1/2 activation (Pang et al., 2017). These findings show that RCC2 plays a role in JNK pathway which is implicated in progression and maintenance of phenotypic and cellular changes associated with EMT (Sahu et al., 2015). Furthermore, JNK inhibitor inhibits RCC2-induced EMT and expression of matrix metalloproteinases (MMPs) (MMP-2 and MMP-9). The-Jun N-terminal kinases (JNKs) which are members of mitogen-activated protein kinase (MAPK) family mediate important physiological processes (Zeke et al., 2016). JNK pathway, one of the major signaling cassettes of MAPK signaling pathway, plays an important role in apoptosis, inflammation, cytokine production, and metabolism (Zeke et al., 2016). EMT is a key event during metastasis and plays a critical role in tumor invasion and metastasis during tumor progression by regulating epithelial markers, mesenchymal markers, and transcription factors (Thiery et al., 2009; Valastyan and Weinberg, 2011). In this case, activation of phosphorylated JNK is mediated by expression level of RCC2 in human LUAD cell. Moreover, activation of JNK inhibits RCC2 activity in LUAD cell, including enhanced cell motility and invasiveness, RCC2-induced EMT and expression of MMP-2 and MMP-9. On the other hand, RCC2 overexpression promotes LUAD cell proliferation and promotes metastasis by inducing epithelial-mesenchymal transition (EMT) by modulating MAPK-JNK signaling pathway (Pang et al., 2017).

In addition, previous studies report that long non-coding RNAs (lncRNAs), ENST00000439577, are associated with expression of RCC2 and promotion of proliferation, invasion, and migration of non-small cell lung cancer (NSCLC) (Feng et al., 2016).

RCC2 and Breast Cancer

Breast cancer is the most common type of cancer in women worldwide (DeSantis et al., 2017; Siegel et al., 2020). A recent study reports that RCC2 is significantly highly expressed in breast cancer and is associated with poor overall survival in breast cancer patients (Chen et al., 2019). Previous studies report that RCC2 is highly expressed in basal-like subtype of breast cancer which is associated with higher propensity for metastasis and worse prognosis compared to other types of breast cancers (Carey et al., 2010; Chen et al., 2019). A recent study shows that RCC2 expression promotes estrogen receptor-positive (ER+) breast tumorigenesis by increasing expression of IGF1 and TWIST1, tumor-enhancing genes, and IL-6 (Wang W. et al., 2020).

Additionally, overexpression of RCC2 promotes cell proliferation and migratory capability in MCF7, and MDA-MB-468 human breast cancer cells. Therefore, RCC2 knockdown inhibits tumor progression and metastatic potential *in vivo* and *in vitro* (Chen et al., 2019). Subsequently, increased RCC2 expression promotes mesenchymal morphology and acquired migratory capability. Furthermore, overexpression of RCC2 promotes EMT progression, whereas RCC2 knockdown inhibits EMT (Chen et al., 2019). In addition, high expression levels of RCC2 regulates Wnt signaling genes, such as β-catenin, Cyclin D1 and c-Myc (Chen et al., 2019). Wnt signaling pathways are a group of signal transduction pathways implicated in physiological initiation and progression of breast cancer (Chu et al., 2004). A previous study reports that repression of Wnt/β-catenin signaling can prevent EMT, which further inhibits metastasis of basal-like breast cancer (DiMeo et al., 2009). Expression and nuclear translocation of β-catenin increases with increase in RCC2 expression levels (Chen et al., 2019). Moreover, RCC2 expression increases activation of β-catenin transcriptional targets including c-Myc and CyclinD1, further promoting progression of EMT, and resulting in breast cancer metastasis. In summary, RCC2 promotes development of breast cancer by inducing EMT and regulating Wnt-signaling pathway.

In conclusion, RCC2 functions as an oncogene in breast cancer.

RCC2 and Ovarian Cancer

Ovarian cancer is a common gynecologic malignancy in women that leads to gynecological-cancer-associated death (Holmes, 2015). Shipeng et al. report that RCC2 is implicated in the progression of ovarian cancer (Gong et al., 2019). Expression level of RCC2 is significantly higher in DDP-resistant ovarian cancer cells compared with DDP-sensitive ones. These finding implies that RCC2 plays a vital role in drug resistance (Gong et al., 2019). RCC2-RalA signaling pathway promotes ovarian cancer cell proliferation, migration, and inhibits apoptosis (Gong et al., 2019). In addition, RCC2 interacts with RalA and regulates RalA signaling pathway, resulting in cisplatin-resistance in ovarian cancer (Gong et al., 2019). RCC2 gene is a novel target for miR-331-3p that negatively regulates it (Buranjiang et al., 2019). Decreased expression of miR-331-3p promotes growth of ovarian cancer cells by reducing expression levels of RCC2 (Buranjiang et al., 2019). However, increased RCC2 expression levels in ovarian cancer restores capacity of cell proliferation,

migration, and invasion inhibited by miR-331-3p (Buranjiang et al., 2019). Therefore, RCC2 and associated proteins are potential therapeutic targets for treatment of ovarian cancer.

RCC2 and Other Cancers

MiR-29c tumor-suppressor in gastric carcinoma targets the 3′ untranslated region (3′UTR) of RCC2, reducing its expression, thus regulating tumor cell proliferation (Matsuo et al., 2013). A previous study reports that RCC2 promotes cell growth and motility by regulating the level of RalA-GTP and modulating MAPK/JNK pathway (Wang P. et al., 2020). Furthermore, RCC2 plays a role in stabilization and transcriptional activation of Sox2, an important transcription factor that promotes malignancy of esophageal cancer (Calderon-Aparicio et al., 2020). In glioblastoma, RCC2 is implicated in tumor proliferation, tumorigenicity, and promoting radio-resistance by activating DNA methyltransferase 1 (DNMT1) transcription in a p-STAT3 dependent manner (Yu et al., 2019). Two independent genome-wide SNP association analyses showed that RCC2 plays a role in tumorigenesis (Stacey et al., 2008). In addition, RCC2 is among the candidate genes which are associated with single nucleotide polymorphism (SNP) rs7538876, which is associated with cutaneous basal cell carcinoma (BCC) (Stacey et al., 2008). Therefore, RCC2 plays a role in early recurrence of melanoma (Rendleman et al., 2013), and hepatocellular carcinoma (Xiong et al., 2019). Moreover, a recent study reported that RCC2 promotes development of hepatocellular carcinoma (HCC), especially during tumor invasion, and is implicated in cisplatin resistance (Chen et al., 2020).

RCC2 AND THERAPEUTIC RESISTANCE

Extensive studies provide in-depth understanding of the functions of RCC2 in development of various cancers, and its association with therapeutic resistance. High expression level of RCC2 is reported in lung and ovarian cancers, where it functions as a GEF for Rac1, which is subsequently involved in superoxide-induced cell death (Williamson et al., 2014; Wu et al., 2018). Rac1 functions as a proapoptotic regulator that responds to various types of apoptotic stimuli and modulates anti-proapoptotic events (Wu et al., 2018). Forced RCC2 expression in tumor cells attenuates sensitivity of tumor cells to spontaneous or Staurosporine (STS)-induced apoptosis (Wu et al., 2018). However, activation of Rac1 inhibits RCC2-induced apoptosis. Therefore, overexpression of RCC2 in tumor cells prevents cellular apoptosis and promotes chemotherapeutic resistance by blocking Rac1 signaling (**Figure 3**) (Wu et al., 2018). Bioinformatic studies show that RCC2 is associated with Exportin-1 (XPO1), which is a crucial factor in a complex mechanism of bortezomib resistance in multiple myeloma (**Figure 3**) (Chanukuppa et al., 2019). This chemoresistance results in high mortality and incurable hematological malignancy.

Cisplatin (DDP) is the first-line drug for treatment of ovarian cancer. However, drug resistance lowers therapeutic outcomes in ovarian cancer patients (Gong et al., 2019). A previous study reports that expression level of RCC2, RalA, and RalBP1 is significantly higher in DDP-resistant ovarian cancer cell lines compared to the DDP-sensitive tissues (Gong et al., 2019). These finding implies that RalA and RalBP1 are involved in oncogenesis and chemoresistance of lung cancer (Drake et al., 2007; Kashatus, 2013; Gong et al., 2019). RCC2 play an oncogenic role by promoting proliferation and migration of DDP-resistant ovarian cancer cell lines and inhibiting cell apoptosis by regulating RalA signaling pathway (Gong et al., 2019). The interaction between RCC2 and RalA is implicated in chemoresistance of ovarian cancer. Furthermore, RalA knockdown activates DDP-resistant ovarian cancer apoptosis, which is inhibited by overexpression of RCC2 (**Figure 3**) (Gong et al., 2019). These findings imply that RCC2 regulates RalA signaling pathway by interacting with RalA, thus promoting cisplatin resistance in ovarian cancer.

In another study on glioblastoma (GBM), expression of RCC2, the activity of the cell cycle, mismatch repair, and JAK-STAT pathways were significantly increased, implying that RCC2 plays a role in radioresistance (Yu et al., 2019). Previous studies report that RCC2 silencing decreases radioresistance of GBM cells, demonstrating the fundamental role of RCC2 gene in therapeutic resistance (Yu et al., 2019). Moreover, -STAT3 regulates transcription of DNA methyltransferase 1 (DNMT1) (Yu et al., 2019). DNMT1 and p-STAT3 (downstream factors of RCC2) are implicated in therapeutic resistance in GBM tumor cells by functioning in an epistatic manner with RCC2 (Yu et al., 2019). Therefore, RCC2 plays a vital role in tumor proliferation, tumorigenicity, and promotes radioresistance by activating transcription of DNA methyltransferase 1 (DNMT1) through a p-STAT3 dependent pathway (**Figure 3**).

Taken together, RCC2 promotes therapeutic resistance in most cases via interacting with various signaling pathways, which resulted in poor effects in cancer treatment. Therefore, RCC2 could be considered to be a potential biomarker. Considering the expression level of RCC2 in the development of a cancer treatment plan may be a useful method. Likewise, taking measures to inhibit the high expression of RCC2 in some cancers also may bring a good therapeutic effect.

RCC2 AND TUMOR CELL METASTASIS

Metastasis is a major cause of most cancer-related deaths and is a major clinical challenge in cancer treatment (Santiago-Medina and Yang, 2016). Previous studies report two forms of cell migration in tumors (Santiago-Medina and Yang, 2016). Chemotaxis is an extensively studied migration process where random cell migration, invasion, and metastasis are driven by a series of signals generated through soluble cues (Santiago-Medina and Yang, 2016). On the other hand, haptotaxis, a rarely studied mode of migration, is a substrate-bound cue-mediated mode of cell migration where the gradient of the extracellular matrix (ECM) is sensed as a guidance cue for directional migration of tumor cells (Santiago-Medina and Yang, 2016).

In addition to RCC2 being involved in multiple steps of pro-tumorigenic phenomena, it is associated with tumor metastases. As mentioned earlier, RCC2 and Rac1 signaling pathways play a

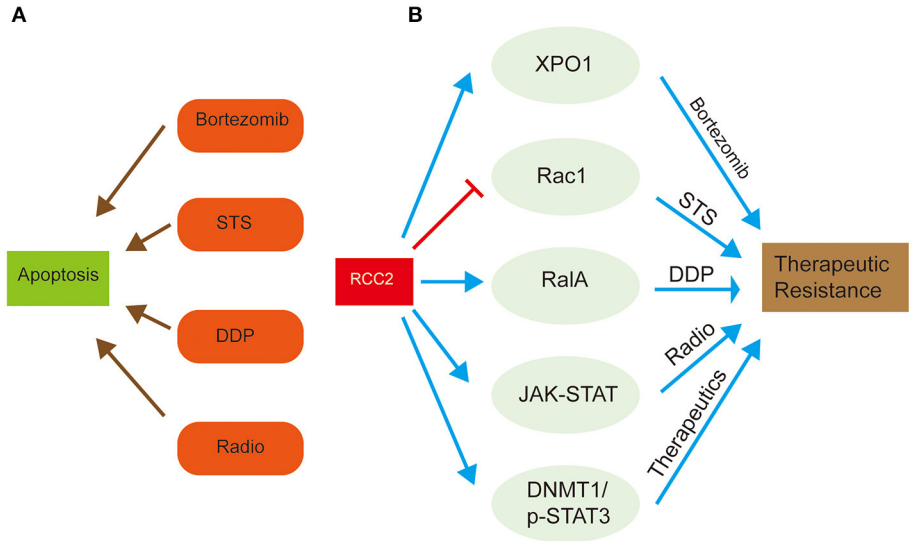

FIGURE 3 | Schematic representation of the role of RCC2 in therapeutic resistance of cancer treatment through regulation of related proteins. **(A)** The left side shows the common chemotherapy drugs, bortezomib, STS, and DDP, and radiotherapy, which are used for cancer treatment by inducing tumor cell apoptosis. **(B)** The right side shows how RCC2 regulates some special proteins, (Xpo1, Rac1, RalA), and signaling pathways (JAK-STAT, DNMT1/p-STAT3), which result in attenuated anti-cancer effect of therapeutics, leading to therapeutic resistance.

vital role in therapeutic resistance (Wu et al., 2018). In colorectal cancer, RCC2 plays a vital role in the regulation of tumor migration and metastasis through p53 (a tumor-suppressor gene)-RCC2 signaling (Muller et al., 2011). p53 plays numerous roles in tumor development, it binds to a palindromic motif in the promoter region of RCC2, thus activating its transcription (Song et al., 2018). Moreover, a previous study reports that RCC2 plays a vital role in regulating directional cell movement through fibronectin-activated signaling pathways (Byron et al., 2011). RCC2 promotes directional cell migration by binding to coronin-1C, which is crucial for RAC1 activation (Byron et al., 2011; Williamson et al., 2014).

RCC2 plays a role in α5β1-FN-signaling network and physically interacts and deactivates Rac1 (Yenjerla et al., 2013; Wu et al., 2018). Rac1, a small GTPase, interacts with RCC2's RCC1 like domain through its unique β-hairpin and participates in membrane protrusion (Wu et al., 2018). Moreover, RCC2 interacts with and deactivates Arf6, which is involved in integrin-dependent membrane trafficking (Pankov et al., 2005; Humphries et al., 2009; Song et al., 2018). Interaction between MENA (an actin regulator with roles in cell migration) and α5β1 integrin promotes cancer cell haptotaxis on fibronectin, leading to metastasis (Santiago-Medina and Yang, 2016). Therefore, α5β1 promotes progression of invasion of cancer cells. On the other hand, RCC2 plays a vital role in cellular response to changes in FN-concentrations (Song et al., 2018).

Expression of RCC2 is decreased by low levels of p53, which enhances activation of Rac1 and Arf6, and inhibition of cellular recognition of FN-concentrations (Pankov et al., 2005). This substrate surface ECM content concentrations leads to deterioration of haptotaxis. Activated Rac1 mediates random migration by promoting formation of peripheral lamellae, thus facilitating invasion of cancer cells (Pankov et al., 2005). Besides, haptotaxis functions as a sensor of varying concentration of underlying ECM, and inhibitory matrix cues cannot be sensed by deteriorated haptotaxis, resulting in random cell migration and tumor cell metastasis (Chan et al., 2014). Therefore, RCC2 inhibits tumor cell metastasis by inhibiting activation of small GTPases, Rac1, and Arf6, and by promoting α5β1-FN-signaling network and cellular recognition to FN concentrations (**Figure 4**).

Overexpression of RCC2 plays a functional role in LUAD metastasis. Overexpression of RCC2 increases expression of epithelial-mesenchymal transition (EMT) markers (N-cadherin and α-SMA), EMT-related transcription factors (Snail and Slug), and MMPs in LUAD (Pang et al., 2017). In addition, it decreases expression of β-catenin and E-cadherin, implying that RCC2 regulates EMT and ECM remodeling (Pang et al., 2017). Moreover, EMT and ECM remodeling are critical in promotion of tumor invasion and metastasis. RCC2-transfected cells increases expression of activated JNK, thus promoting migratory and invasive abilities of A549-RCC2 cells and RCC2-induced EMT and MMPs (Pang et al., 2017). These findings imply that MAPK-JNK signaling contributes to LUAD metastasis through induction by RCC2 (**Figure 4**). Therefore, overexpression of RCC2 promotes LUAD metastasis by inducing EMT and ECM remodeling through activation of MAPK-JNK signaling. Notably, mechanism of RCC2-induced metastasis in LUAD is similar to the mechanism in breast cancer. Although RCC2 promotes cell migration, by inducing EMT through activation of the Wnt-signaling pathway (**Figure 4**), it has been reported to promotes metastasis of ovarian cancer (Chen et al., 2019). Gulimire et al. report that direct targeting of RCC2 microRNA-331-3p (miR-331-3p) may function as a tumor suppressor in ovarian

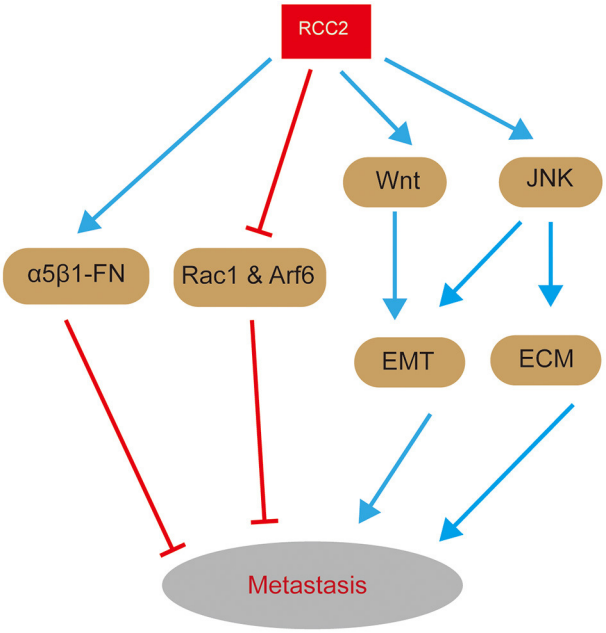

FIGURE 4 | A graphical representation of the role of RCC2 in signaling pathways related with metastasis. On one hand, RCC2 inhibits activation of Rac1 and Arf6 and ensures proper function of α5β1-FN-signaling network, thus inhibiting metastasis. On the other hand, RCC2 promotes metastasis by regulating EMT and ECM remodeling through MAPK-JNK and Wnt-signaling pathways.

epithelial carcinoma (EOC) (Buranjiang et al., 2019). Therefore, RCC2 regulating tumor cell metastasis by activating a series of signaling pathways.

RCC2 AND DNA DAMAGE

Few studies report on the relationship between RCC2 and DNA damage response (DDR). However, a previous study reports that RCC2 interacts with Ku86, which combines with Ku70 thus playing a core role in Non-homologous end joining (NHEJ), as detected by RP-RP MS, a precise mass spectrometric measurement (Zhou et al., 2010). Besides, another study reports that lncRNA LCPAT1 targets RCC2 during cigarette smoke extract (CSE) induced DNA damage (Gao et al., 2019). Interestingly, the study reported that a decrease in RCC2 expression decreases expression and foci numbers of γ-H2AX, a DNA damage marker, in CSE-treated Beas-2B cells, implying that loss of RCC2 exacerbates DNA damage (Gao et al., 2019). Association between RCC2 and γ-H2AX suggests that RCC2 is potentially associated with DDR. In summary, RCC2 may plays a role in DDR process, however further studies on the exact role of RCC2 in DDR should be carried out.

CONCLUDING REMARKS

RCC2 plays key roles in regulation of cell cycle. Previous studies report that RCC2 is involved in all phases of the cell cycle. RCC2 plays a major role in the M phase compared with the interphase. In M phase, RCC2 associates with the chromosome and microtubule and functions as CPC or its member. Therefore, RCC2 promotes transition from prometaphase to metaphase by regulating the switch of inactive and active states of small G protein Rac1 and RalA. After transition, it becomes part of the telophase disc organelle for cell cleavage. Although studies report that low levels of RCC2 affect normal progression of interphase, the mechanism should be explored further.

RCC2 functions as an oncogene in numerous kinds of cancers by promoting progression of tumor cells, facilitates metastatic behaviors and induces therapeutic resistance in tumor cells. Expression level of RCC2 is significantly high in most common cancer types. The mechanism of RCC2 in CRC is complex. RCC2 knockdown in MSI group promotes tumor cell apoptosis. On the other hand, low expression level of RCC2 aggravates tumor cell metastasis through α5β1-FN-signaling pathway. In LUAD, RCC2 plays a significant role in MAPK-JNK signaling pathway, thus promoting LUAD cell proliferation and metastasis. RCC2 is a poor independent prognostic factor for LUAD patients. Expression level of RCC2 is associated with progression of EMT and regulation of activation of Wnt-signaling pathway, which promote development of breast cancer. In addition, RCC2 promotes cisplatin-resistance in ovarian cancer by regulating RalA signaling pathway. These findings show that RCC2 is an oncogene in tumorigenesis. Therefore, RCC2 is a potential therapeutic target for cancer treatment.

Furthermore, RCC2 has a potential role in modulating DNA damage process as it interacts with Ku86 and is associated withγ-H2AX. DDR is closely related to genome stability and tumorigenesis. However, the exact relationship between RCC2 and DNA damage should be explored further.

In summary, RCC2 plays an important role in cell cycle, cancer development, and therapeutic resistance of anticancer drugs. The role of RCC2 in the cell cycle is positively correlated with tumor formation and tumor cell sensitivity to therapies. Therefore, RCC2 is a potential biomarker for development of new and specific anti-cancer therapeutic strategies.

AUTHOR CONTRIBUTIONS

KG and CZ contributed to concept generation and drafting of the article. BL contributed to drafting of the article: HW and HZ contributed to drafting and approval of the article. FZ contributed to concept generation, drafting, and approval of the article. All authors read and approved the final manuscript.

FUNDING

This work was supported by grants from the National Natural Science Foundation of China (Grant Nos. 81572775 and 81773004 to FZ) and the Program for Professor of Special Appointment (Eastern Scholar) at Shanghai Institutions of Higher Learning (Grant No. TP2014055 to FZ).

REFERENCES

Adams, R. R., Wheatley, S. P., Gouldsworthy, A. M., Kandels-Lewis, S. E., Carmena, M., Smythe, C., et al. (2000). INCENP binds the Aurora-related kinase AIRK2 and is required to target it to chromosomes, the central spindle, and cleavage furrow. *Curr. Biol.* 10, 1075–1078. doi: 10.1016/S0960-9822(00)00673-4

Aebi, M., Clark, M. W., Vijayraghavan, U., and Abelson, J. (1990). A yeast mutant, PRP20, altered in mRNA metabolism and maintenance of the nuclear structure, is defective in a gene homologous to the human gene RCC1 which is involved in the control of chromosome condensation. *Mol. Gen. Genet.* 224, 72–80. doi: 10.1007/BF00259453

Andreassen, P. R., Palmer, D. K., Wener, M. H., and Margolis, R. L. (1991). Telophase disc: a new mammalian mitotic organelle that bisects telophase cells with a possible function in cytokinesis. *J. Cell Sci.* 99(Pt 3), 523–534.

Brody, H. (2015). Colorectal cancer. *Nature* 521:S1. doi: 10.1038/521S1a

Bruun, J., Kolberg, M., Ahlquist, T. C., Røyrvik, E. C., Nome, T., Leithe, E., et al. (2015). Regulator of chromosome condensation 2 identifies high-risk patients within both major phenotypes of colorectal cancer. *Clin. Cancer Res.* 21, 3759–3770. doi: 10.1158/1078-0432.CCR-14-3294

Buranjiang, G., Kuerban, R., Abuduwanke, A., Li, X., and Kuerban, G. (2019). MicroRNA-331-3p inhibits proliferation and metastasis of ovarian cancer by targeting RCC2. *Arch. Med. Sci.* 15, 1520–1529. doi: 10.5114/aoms.2018.77858

Byron, A., Humphries, J. D., Bass, M. D., Knight, D., and Humphries, M. J. (2011). Proteomic analysis of integrin adhesion complexes. *Sci. Signal.* 4:pt2. doi: 10.1126/scisignal.2001827

Calderon-Aparicio, A., Yamamoto, H., De Vitto, H., Zhang, T., Wang, Q., Bode, A. M., et al. (2020). RCC2 promotes esophageal cancer growth by regulating activity and expression of the Sox2 transcription factor. *Mol. Cancer Res.* 18, 1660–1674. doi: 10.1158/1541-7786.MCR-19-1152

Cancer Genome Atlas Network (2012). Comprehensive molecular characterization of human colon and rectal cancer. *Nature* 487, 330–337. doi: 10.1038/nature11252

Cancer Genome Atlas Research Network (2014). Comprehensive molecular profiling of lung adenocarcinoma. *Nature* 511, 543–550. doi: 10.1038/nature13385

Carey, L., Winer, E., Viale, G., Cameron, D., and Gianni, L. (2010). Triple-negative breast cancer: disease entity or title of convenience? *Nat. Rev. Clin. Oncol.* 7, 683–692. doi: 10.1038/nrclinonc.2010.154

Chan, K. T., Asokan, S. B., King, S. J., Bo, T., Dubose, E. S., Liu, W., et al. (2014). LKB1 loss in melanoma disrupts directional migration toward extracellular matrix cues. *J. Cell Biol.* 207, 299–315. doi: 10.1083/jcb.201404067

Chanukuppa, V., Paul, D., Taunk, K., Chatterjee, T., Sharma, S., Kumar, S., et al. (2019). XPO1 is a critical player for bortezomib resistance in multiple myeloma: a quantitative proteomic approach. *J. Proteomics* 209:103504. doi: 10.1016/j.jprot.2019.103504

Chen, Q., Jiang, P., Jia, B., Liu, Y., and Zhang, Z. (2020). RCC2 contributes to tumor invasion and chemoresistance to cisplatin in hepatocellular carcinoma. *Hum. Cell* 33, 709–720. doi: 10.1007/s13577-020-00353-7

Chen, Z., Wu, W., Huang, Y., Xie, L., Li, Y., Chen, H., et al. (2019). RCC2 promotes breast cancer progression through regulation of Wnt signaling and inducing EMT. *J. Cancer* 10, 6837–6847. doi: 10.7150/jca.36430

Choi, H. J. C., Lin, J.-R., Vannier, J.-B., Slaats, G. G., Kile, A. C., Paulsen, R. D., et al. (2013). NEK8 links the ATR-regulated replication stress response and S phase CDK activity to renal ciliopathies. *Mol. Cell* 51, 423–439. doi: 10.1016/j.molcel.2013.08.006

Chu, E. Y., Hens, J., Andl, T., Kairo, A., Yamaguchi, T. P., Brisken, C., et al. (2004). Canonical WNT signaling promotes mammary placode development and is essential for initiation of mammary gland morphogenesis. *Development* 131, 4819–4829. doi: 10.1242/dev.01347

Cooke, C. A., Heck, M. M., and Earnshaw, W. C. (1987). The inner centromere protein (INCENP) antigens: movement from inner centromere to midbody during mitosis. *J. Cell Biol.* 105, 2053–2067. doi: 10.1083/jcb.105.5.2053

Danen, E. H. J. (2009). Integrin proteomes reveal a new guide for cell motility. *Sci. Signal.* 2:pe58. doi: 10.1126/scisignal.289pe58

Dasso, M., Nishitani, H., Kornbluth, S., Nishimoto, T., and Newport, J. W. (1992). RCC1, a regulator of mitosis, is essential for DNA replication. *Mol. Cell Biol.* 12, 3337–3345. doi: 10.1128/MCB.12.8.3337

DeSantis, C. E., Ma, J., Goding Sauer, A., Newman, L. A., and Jemal, A. (2017). Breast cancer statistics, racial disparity in mortality by state. *CA Cancer J. Clin.* 67, 439–448. doi: 10.3322/caac.21412

DiMeo, T. A., Anderson, K., Phadke, P., Fan, C., Feng, C., Perou, C. M., et al. (2009). A novel lung metastasis signature links Wnt signaling with cancer cell self-renewal and epithelial-mesenchymal transition in basal-like breast cancer. *Cancer Res.* 69, 5364–5373. doi: 10.1158/0008-5472.CAN-08-4135

Drake, K. J., Singhal, J., Yadav, S., Nadkar, A., Pungaliya, C., Singhal, S. S., et al. (2007). RALBP1/RLIP76 mediates multidrug resistance. *Int. J. Oncol.* 30, 139–144. doi: 10.3892/ijo.30.1.139

Feng, N., Ching, T., Wang, Y., Liu, B., Lin, H., Shi, O., et al. (2016). Analysis of Microarray data on gene expression and methylation to identify long non-coding RNAs in non-small cell lung cancer. *Sci. Rep.* 6:37233. doi: 10.1038/srep37233

Frank, S. R., Adelstein, M. R., and Hansen, S. H. (2006). GIT2 represses Crk- and Rac1-regulated cell spreading and Cdc42-mediated focal adhesion turnover. *EMBO J.* 25, 1848–1859. doi: 10.1038/sj.emboj.7601092

Gao, S., Lin, H., Yu, W., Zhang, F., Wang, R., Yu, H., et al. (2019). LncRNA LCPAT1 is involved in DNA damage induced by CSE. *Biochem. Biophys. Res. Commun.* 508, 512–515. doi: 10.1016/j.bbrc.2018.11.171

Gassmann, R., Carvalho, A., Henzing, A. J., Ruchaud, S., Hudson, D. F., Honda, R., et al. (2004). Borealin: a novel chromosomal passenger required for stability of the bipolar mitotic spindle. *J. Cell Biol.* 166, 179–191. doi: 10.1083/jcb.200404001

Giannakis, M., Hodis, E., Jasmine Mu, X., Yamauchi, M., Rosenbluh, J., Cibulskis, K., et al. (2014). RNF43 is frequently mutated in colorectal and endometrial cancers. *Nat. Genet.* 46, 1264–1266. doi: 10.1038/ng.3127

Gong, S., Chen, Y., Meng, F., Zhang, Y., Wu, H., Li, C., et al. (2019). RCC2, a regulator of the RalA signaling pathway, is identified as a novel therapeutic target in cisplatin-resistant ovarian cancer. *FASEB J.* 33, 5350–5365. doi: 10.1096/fj.201801529RR

Grigera, P. R., Ma, L., Borgman, C. A., Pinto, A. F., Sherman, N. E., Parsons, J. T., et al. (2012). Mass spectrometric analysis identifies a cortactin-RCC2/TD60 interaction in mitotic cells. *J. Proteomics* 75, 2153–2159. doi: 10.1016/j.jprot.2012.01.012

Hadjebi, O., Casas-Terradellas, E., Garcia-Gonzalo, F. R., and Rosa, J. L. (2008). The RCC1 superfamily: from genes, to function, to disease. *Biochim. Biophys. Acta* 1783, 1467–1479. doi: 10.1016/j.bbamcr.2008.03.015

Holmes, D. (2015). Ovarian cancer: beyond resistance. *Nature* 527:S217. doi: 10.1038/527S217a

Hu, K., Li, Y., Wu, W., Chen, H., Chen, Z., Zhang, Y., et al. (2018). High-performance gene expression and knockout tools using sleeping beauty transposon system. *Mob. DNA* 9:33. doi: 10.1186/s13100-018-0139-y

Humphries, J. D., Byron, A., Bass, M. D., Craig, S. E., Pinney, J. W., Knight, D., et al. (2009). Proteomic analysis of integrin-associated complexes identifies RCC2 as a dual regulator of Rac1 and Arf6. *Sci. Signal.* 2:ra51. doi: 10.1126/scisignal.2000396

Kashatus, D. F. (2013). Ral GTPases in tumorigenesis: emerging from the shadows. *Exp. Cell Res.* 319, 2337–2342. doi: 10.1016/j.yexcr.2013.06.020

Kelley, L. A., Mezulis, S., Yates, C. M., Wass, M. N., and Sternberg, M. J. E. (2015). The Phyre2 web portal for protein modeling, prediction, and analysis. *Nat. Protoc.* 10, 845–858. doi: 10.1038/nprot.2015.053

Kim, N.-G., Rhee, H., Li, L. S., Kim, H., Lee, J.-S., Kim, J.-H., et al. (2002). Identification of MARCKS, FLJ11383, and TAF1B as putative novel target genes in colorectal carcinomas with microsatellite instability. *Oncogene* 21, 5081–5087. doi: 10.1038/sj.onc.1205703

Martineau-Thuillier, S., Andreassen, P. R., and Margolis, R. L. (1998). Colocalization of TD-60 and INCENP throughout G2 and mitosis: evidence for their possible interaction in signalling cytokinesis. *Chromosoma* 107, 461–470. doi: 10.1007/s004120050330

Matsuo, M., Nakada, C., Tsukamoto, Y., Noguchi, T., Uchida, T., Hijiya, N., et al. (2013). MiR-29c is downregulated in gastric carcinomas and regulates cell proliferation by targeting RCC2. *Mol. Cancer* 12:15. doi: 10.1186/1476-4598-12-15

Mollinari, C., Reynaud, C., Martineau-Thuillier, S., Monier, S., Kieffer, S., Garin, J., et al. (2003). The mammalian passenger protein TD-60 is an RCC1 family member with an essential role in prometaphase to metaphase progression. *Dev. Cell* 5, 295–307. doi: 10.1016/S1534-5807(03)00205-3

Moore, J. D. (2001). The Ran-GTPase and cell-cycle control. *Bioessays* 23, 77–85. doi: 10.1002/1521-1878(200101)23:1<77::AID-BIES1010>3.0.CO;2-E

Muller, P. A. J., Vousden, K. H., and Norman, J. C. (2011). p53 and its mutants in tumor cell migration and invasion. *J. Cell Biol.* 192, 209–218. doi: 10.1083/jcb.201009059

Ohtsubo, M., Kai, R., Furuno, N., Sekiguchi, T., Sekiguchi, M., Hayashida, H., et al. (1987). Isolation and characterization of the active cDNA of the human cell cycle gene (RCC1) involved in the regulation of onset of chromosome condensation. *Genes Dev.* 1, 585–593. doi: 10.1101/gad.1.6.585

Pang, B., Wu, N., Guan, R., Pang, L., Li, X., Li, S., et al. (2017). Overexpression of RCC2 enhances cell motility and promotes tumor metastasis in lung adenocarcinoma by inducing epithelial-mesenchymal transition. *Clin. Cancer Res.* 23, 5598–5610. doi: 10.1158/1078-0432.CCR-16-2909

Pankov, R., Endo, Y., Even-Ram, S., Araki, M., Clark, K., Cukierman, E., et al. (2005). A Rac switch regulates random versus directionally persistent cell migration. *J. Cell Biol.* 170, 793–802. doi: 10.1083/jcb.200503152

Papini, D., Langemeyer, L., Abad, M. A., Kerr, A., Samejima, I., Eyers, P. A., et al. (2015). TD-60 links RalA GTPase function to the CPC in mitosis. *Nat. Commun.* 6:7678. doi: 10.1038/ncomms8678

Pickering, B. M., and Willis, A. E. (2005). The implications of structured 5' untranslated regions on translation and disease. *Semin. Cell Dev. Biol.* 16, 39–47. doi: 10.1016/j.semcdb.2004.11.006

Renault, L., Nassar, N., Vetter, I., Becker, J., Klebe, C., Roth, M., et al. (1998). The 1.7 A crystal structure of the regulator of chromosome condensation (RCC1) reveals a seven-bladed propeller. *Nature* 392, 97–101. doi: 10.1038/32204

Rendleman, J., Shang, S., Dominianni, C., Shields, J. F., Scanlon, P., Adaniel, C., et al. (2013). Melanoma risk loci as determinants of melanoma recurrence and survival. *J. Transl. Med.* 11:279. doi: 10.1186/1479-5876-11-279

Riddick, G., and Macara, I. G. (2005). A systems analysis of importin-{alpha}-{beta} mediated nuclear protein import. *J. Cell Biol.* 168, 1027–1038. doi: 10.1083/jcb.200409024

Sahu, S. K., Garding, A., Tiwari, N., Thakurela, S., Toedling, J., Gebhard, S., et al. (2015). JNK-dependent gene regulatory circuitry governs mesenchymal fate. *EMBO J.* 34, 2162–2181. doi: 10.15252/embj.201490693

Santiago-Medina, M., and Yang, J. (2016). MENA promotes tumor-intrinsic metastasis through ECM remodeling and haptotaxis. *Cancer Discov.* 6, 474–476. doi: 10.1158/2159-8290.CD-16-0231

Scheffner, M., and Staub, O. (2007). HECT E3s and human disease. *BMC Biochem.* 8(Suppl. 1):S6. doi: 10.1186/1471-2091-8-S1-S6

Seki, T., Hayashi, N., and Nishimoto, T. (1996). RCC1 in the ran pathway. *J. Biochem.* 120, 207–214. doi: 10.1093/oxfordjournals.jbchem.a021400

Shih, M. C., Chen, J. Y., Wu, Y. C., Jan, Y. H., Yang, B. M., Lu, P. J., et al. (2012). TOPK/PBK promotes cell migration via modulation of the PI3K/PTEN/AKT pathway and is associated with poor prognosis in lung cancer. *Oncogene* 31, 2389–2400. doi: 10.1038/onc.2011.419

Siegel, R. L., Miller, K. D., and Jemal, A. (2020). Cancer statistics, 2020. *CA Cancer J. Clin.* 70, 7–30. doi: 10.3322/caac.21590

Smith, S. C., Petrova, A. V., Madden, M. Z., Wang, H., Pan, Y., Warren, M. D., et al. (2014). A gemcitabine sensitivity screen identifies a role for NEK9 in the replication stress response. *Nucleic Acids Res.* 42, 11517–11527. doi: 10.1093/nar/gku840

Song, C., Liang, L., Jin, Y., Li, Y., Liu, Y., Guo, L., et al. (2018). RCC2 is a novel p53 target in suppressing metastasis. *Oncogene* 37, 8–17. doi: 10.1038/onc.2017.306

Stacey, S. N., Gudbjartsson, D. F., Sulem, P., Bergthorsson, J. T., Kumar, R., Thorleifsson, G., et al. (2008). Common variants on 1p36 and 1q42 are associated with cutaneous basal cell carcinoma but not with melanoma or pigmentation traits. *Nat. Genet.* 40, 1313–1318. doi: 10.1038/ng.234

Tan, B. C.-M., and Lee, S.-C. (2004). Nek9, a novel FACT-associated protein, modulates interphase progression. *J. Biol. Chem.* 279, 9321–9330. doi: 10.1074/jbc.M311477200

Thiery, J. P., Acloque, H., Huang, R. Y. J., and Nieto, M. A. (2009). Epithelial-mesenchymal transitions in development and disease. *Cell* 139, 871–890. doi: 10.1016/j.cell.2009.11.007

Valastyan, S., and Weinberg, R. A. (2011). Tumor metastasis: molecular insights and evolving paradigms. *Cell* 147, 275–292. doi: 10.1016/j.cell.2011.09.024

Wang, I. C., Ustiyan, V., Zhang, Y., Cai, Y., Kalin, T. V., and Kalinichenko, V. V. (2014). Foxm1 transcription factor is required for the initiation of lung tumorigenesis by oncogenic Kras(G12D.). *Oncogene* 33, 5391–5396. doi: 10.1038/onc.2013.475

Wang, P., Zhang, W., Wang, L., Liang, W., Cai, A., Gao, Y., et al. (2020). RCC2 interacts with small GTPase RalA and regulates cell proliferation and motility in gastric cancer. *Onco Targets Ther.* 13, 3093–3103. doi: 10.2147/OTT.S228914

Wang, W., Xu, B., Zhang, Z., Fang, K., and Chang, X. (2020). RCC2 expression stimulates ER-positive breast tumorigenesis. *J. Oncol.* 2020:5619462. doi: 10.1155/2020/5619462

Williamson, R. C., Cowell, C. A. M., Hammond, C. L., Bergen, D. J. M., Roper, J. A., Feng, Y., et al. (2014). Coronin-1C and RCC2 guide mesenchymal migration by trafficking Rac1 and controlling GEF exposure. *J. Cell Sci.* 127(Pt 19), 4292–4307. doi: 10.1242/jcs.154864

Wu, N., Ren, D., Li, S., Ma, W., Hu, S., Jin, Y., et al. (2018). RCC2 over-expression in tumor cells alters apoptosis and drug sensitivity by regulating Rac1 activation. *BMC Cancer* 18:67. doi: 10.1186/s12885-017-3908-y

Xiong, D.-D., Feng, Z.-B., Lai, Z.-F., Qin, Y., Liu, L.-M., Fu, H.-X., et al. (2019). High throughput circRNA sequencing analysis reveals novel insights into the mechanism of nitidine chloride against hepatocellular carcinoma. *Cell Death Dis.* 10:658. doi: 10.1038/s41419-019-1890-9

Yang, F., Camp, D. G., Gritsenko, M. A., Luo, Q., Kelly, R. T., Clauss, T. R. W., et al. (2007). Identification of a novel mitotic phosphorylation motif associated with protein localization to the mitotic apparatus. *J. Cell Sci.* 120(Pt 22), 4060–4070. doi: 10.1242/jcs.014795

Yenjerla, M., Panopoulos, A., Reynaud, C., Fotedar, R., and Margolis, R. L. (2013). TD-60 is required for interphase cell cycle progression. *Cell Cycle* 12, 837–841. doi: 10.4161/cc.23821

Yu, H., Zhang, S., Ibrahim, A. N., Wang, J., Deng, Z., and Wang, M. (2019). RCC2 promotes proliferation and radio-resistance in glioblastoma via activating transcription of DNMT1. *Biochem. Biophys. Res. Commun.* 516, 999–1006. doi: 10.1016/j.bbrc.2019.06.097

Zeke, A., Misheva, M., Reményi, A., and Bogoyevitch, M. A. (2016). JNK signaling: regulation and functions based on complex protein-protein partnerships. *Microbiol. Mol. Biol. Rev.* 80, 793–835. doi: 10.1128/MMBR.00043-14

Zhou, F., Cardoza, J. D., Ficarro, S. B., Adelmant, G. O., Lazaro, J.-B., and Marto, J. A. (2010). Online nanoflow RP-RP-MS reveals dynamics of multicomponent Ku complex in response to DNA damage. *J. Proteome Res.* 9, 6242–6255. doi: 10.1021/pr1004696

Zhou, Y.-Y., Li, Y., Jiang, W.-Q., and Zhou, L.-F. (2015). MAPK/JNK signalling: a potential autophagy regulation pathway. *Biosci. Rep.* 35:e00199. doi: 10.1042/BSR20140141

Conflict of Interest: The authors declare that the research was conducted in the absence of any commercial or financial relationships that could be construed as a potential conflict of interest.

frontiers in Molecular Biosciences

ORIGINAL RESEARCH
published: 11 March 2021
doi: 10.3389/fmolb.2021.608369

Identification of a DNA Repair Gene Signature and Establishment of a Prognostic Nomogram Predicting Biochemical-Recurrence-Free Survival of Prostate Cancer

Gongwei Long[1,2†], *Wei Ouyang*[1,2†], *Yucong Zhang*[1,2,3], *Guoliang Sun*[1,2], *Jiahua Gan*[1,2], *Zhiquan Hu*[1,2] *and Heng Li*[1,2*]

[1]Department of Urology, Tongji Hospital, Tongji Medical College, Huazhong University of Science and Technology, Wuhan, China, [2]Hubei Institute of Urology, Tongji Hospital, Tongji Medical College, Huazhong University of Science and Technology, Wuhan, China, [3]Department of Geriatrics, Tongji Hospital, Tongji Medical College, Huazhong University of Science and Technology, Wuhan, China

OPEN ACCESS

Edited by:
Martin Francis Lavin,
The University of Queensland,
Brisbane, QLD, Australia

Reviewed by:
Matthew Roberts,
The University of Queensland,
Brisbane, QLD, Australia
Luke Gaughan,
Newcastle University, United Kingdom

***Correspondence:**
Heng Li
lihengtjmu@163.com

[†]These authors have contributed equally to this work and share co-first authorship

Specialty section:
This article was submitted to Molecular Diagnostics and Therapeutics, a section of the journal Frontiers in Molecular Biosciences

Received: 25 September 2020
Accepted: 27 January 2021
Published: 11 March 2021

Citation:
Long G, Ouyang W, Zhang Y, Sun G, Gan J, Hu Z and Li H (2021) Identification of a DNA Repair Gene Signature and Establishment of a Prognostic Nomogram Predicting Biochemical-Recurrence-Free Survival of Prostate Cancer. Front. Mol. Biosci. 8:608369. doi: 10.3389/fmolb.2021.608369

Background: The incidence of prostate cancer (PCa) is high and increasing worldwide. The prognosis of PCa is relatively good, but it is important to identify the patients with a high risk of biochemical recurrence (BCR) so that additional treatment could be applied.

Method: Level 3 mRNA expression and clinicopathological data were obtained from The Cancer Genome Atlas (TCGA) to serve as training data. The GSE84042 dataset was used as a validation set. Univariate Cox, lasso Cox, and stepwise multivariate Cox regression were applied to identify a DNA repair gene (DRG) signature. The performance of the DRG signature was assessed based on Kaplan–Meier curve, receiver operating characteristic (ROC), and Harrell's concordance index (C-index). Furtherly, a prognostic nomogram was established and evaluated likewise.

Results: A novel four DRG signature was established to predict BCR of PCa, which included POLM, NUDT15, AEN, and HELQ. The ROC and C index presented good performance in both training dataset and validation dataset. The patients were stratified by the signature into high- and low-risk groups with distinct BCR survival. Multivariate Cox analysis revealed that the DRG signature is an independent prognostic factor for PCa. Also, the DRG signature high-risk was related to a higher homologous recombination deficiency (HRD) score. The nomogram, incorporating the DRG signature and clinicopathological parameters, was able to predict the BCR with high efficiency and showed superior performance compared to models that consisted of only clinicopathological parameters.

Conclusion: Our study identified a DRG signature and established a prognostic nomogram, which were reliable in predicting the BCR of PCa. This model could help with individualized treatment and medical decision making.

Keywords: DNA repair, prostate cancer, biochemical recurrence, nomogram, homologous recombination deficiency

INTRODUCTION

Prostate cancer (PCa) is one of the most frequently diagnosed neoplasm all over the world, with an estimated 191,930 new cases and 33,330 death in 2020 in the United States (Siegel et al., 2020). The curative therapies including radical prostatectomy (RP) and radical radiation are the standard treatment for localized PCa (Mottet et al., 2017; Sanda et al., 2018), but biochemical recurrence (BCR) still occurs for approximately 20–40% of patients (Van den Broeck et al., 2019). Without secondary treatment, patients with BCR would experience clinical progression within 5–8 years, and among these, 32–45% will succumb to PCa within 15 years (Brockman et al., 2015). Thus, a marker signature that can identify patients with a high risk of BCR has great clinical value.

Genomic instability is one of the hallmarks of cancer (Hanahan and Weinberg, 2011). To maintain genome integrity, a complex DNA damage response (DDR) was developed to repair the DNA damage. Defects in DDR are associated with increased mutational load and genome instability, leading to a neoplastic transformation and proliferation (Minchom et al., 2018). The DNA repair gene (DRG) alterations were common in cancers, including ovarian cancer, breast cancer, and prostate cancer (Ali et al., 2017; Mateo et al., 2017; Mirza-Aghazadeh-Attari et al., 2019). Due to the DDR defects, cancer cells are more reliant on other repair pathways for survival, which makes DDR targeting an attractive therapeutic strategy. An important example is homologous recombination deficiency (HRD). The BRCA 1/2 are the important homologous recombination-related genes, and the germline BRCA 1/2 mutation has been confirmed as independent predictive factor for prognosis of PCa (Castro et al., 2013). The HRD is also a predictive marker for therapy with PARP inhibition (PARPi) such as Olaparib in PCa and other kinds of cancers (Kaufman et al., 2015; Mateo et al., 2015; Robson et al., 2017; Mateo et al., 2020). These issues indicated that DDR defects could be powerful prognostic factors in PCa.

In this work, we used The Cancer Genome Atlas (TCGA) and Gene Expression Omnibus (GEO) to explore the DRGs related to the prognosis of PCa and potentially to explore biomarkers of DNA repair deficiency to improve the survival of PCa patients.

METHOD

Publicly Available mRNA Data and DNA Repair Gene Sets

Data from two publicly available datasets were incorporated into our study. The level three mRNA sequencing and clinical data of TCGA-PRAD were acquired from TCGA (https://portal.gdc.cancer.gov/). The HTSeq-Counts data were downloaded and normalized with the edgeR package (Robinson et al., 2010). The GSE84042 dataset with seventy three prostate cancer samples was used as a validation dataset. The normalized mRNA expression file of GSE84042 was downloaded from GEO (http://www.ncbi.nlm.nih.gov/geo) and the relevant clinical information was retrieved from the Supplementary Material of the original literature (Fraser et al., 2017). The list of DRG was retrieved from Knijnenburg's publication (Knijnenburg et al., 2018).

Signature Generation and Statistical Analysis

We matched the DRG list with the TCGA-PRAD mRNA expression profile of the TCGA dataset. A univariate Cox proportional regression model was used to calculate the association between the expression of each DRG and BCR survival. Next, we used the least absolute shrinkage and selection operator (LASSO) method for variable selection in a Cox regression model to determine significant prognostic genes, and one standard error (SE) above the minimum criteria was selected. To make our model more optimized and practical, a stepwise Cox proportional hazards regression model was used. Finally, a risk score formula was calculated by taking into account the expression of optimized genes and correlation estimated Cox regression coefficients: Risk score = (exp Gene1 × coef Gene1) + (exp Gene2 × coef Gene2) + . . . + (exp GeneN × coef GeneN).

Patients with PCa were classified into the high- or low-risk group by ranking the given risk score. The "surv_cutpoint" function in the survminer package was used to determine the optimal cut-off value of the risk score. Kaplan-Meier analysis, the area under the (AUC) of the receiver operating characteristic (ROC) curve (using the timeROC package), and Harrell's concordance index (C index, using the survcomp package) were used to evaluate the performance of the prognostic gene signature. The GSE84042 dataset was used for validation. The risk scores of each patient were calculated using the same formula and the optimal cut-off value was determined using the "surv_cutpoint" function.

To assess the DRG signature risk score distribution, we compared the risk scores according to different clinical status. The Mann–Whitney U test was used for comparison. Besides, the HRD scores, which was generated as a sum of genomic scar scores including the telomeric allelic imbalance (TAI) (Birkbak et al., 2012), loss of heterozygosity (LOH) (Abkevich et al., 2012), and large-scale transition (LST) (Popova et al., 2012), of TCGA dataset was retrieved from Knijnenburg's publication (Knijnenburg et al., 2018) to assess the association between HRD score and the DRG signature status.

Gene ontology (GO) and Kyoto Encyclopedia of Genes and Genomes (KEGG) pathway analyses were performed for these with prognostic significance in univariate Cox regression using DAVID 6.8 (Huang da et al., 2009).

Identification of Independent Prognostic Parameters for PCa

To identify independent prognostic parameters for PCa associated with the BCR-free survival and to validate the independent prognostic value of the gene signature, univariate and multivariate

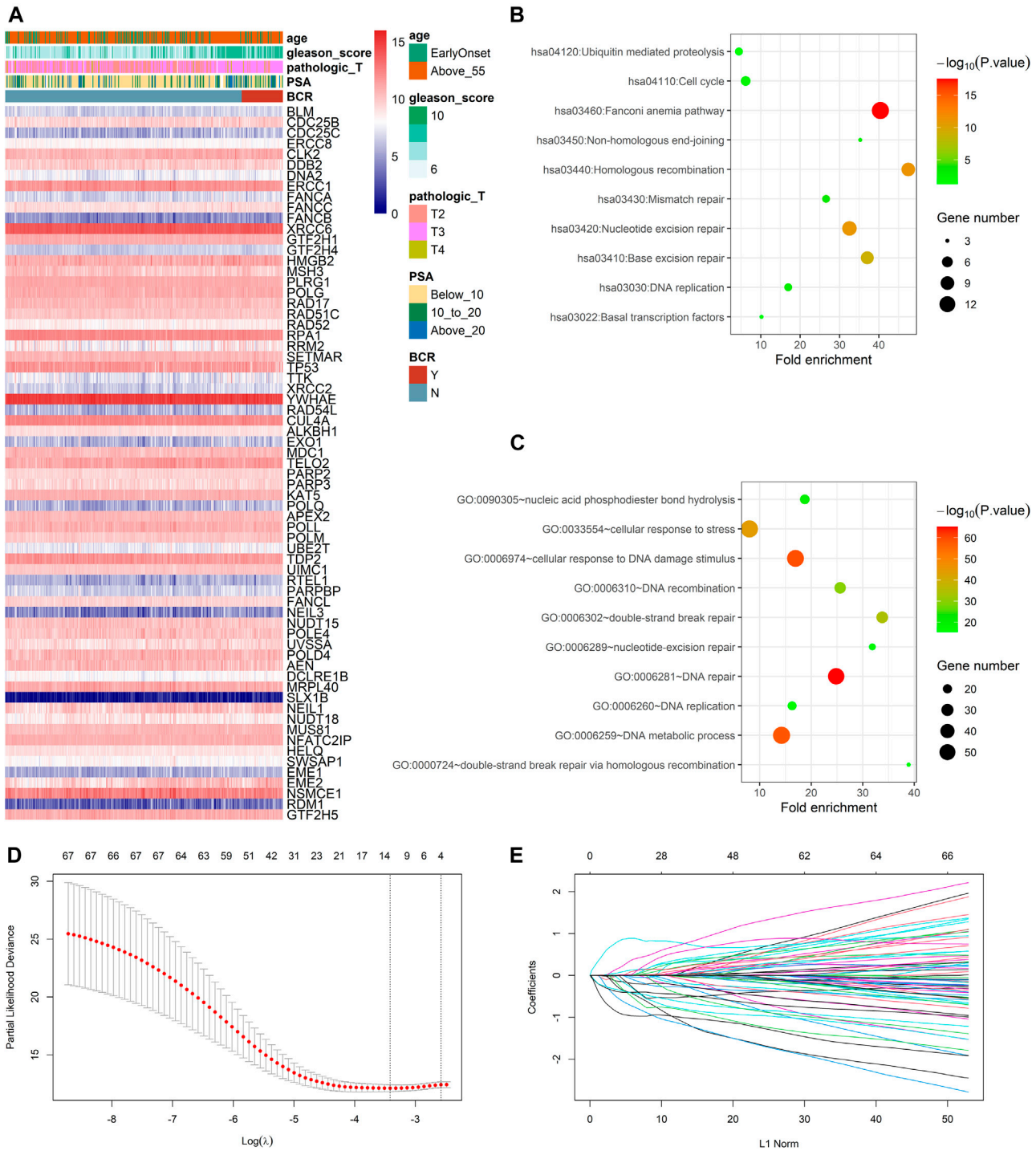

FIGURE 1 | Identification of prognostic DNA repair genes in prostate cancer **(A)** Univariate Cox regression analysis identified 67 DNA repair genes significantly associated with BCR **(B)** KEGG analysis of identified genes **(C)** GO analysis of identified genes **(D)** Parameter selection in the LASSO model **(E)** LASSO coefficient profiles of the prognostic genes.

Cox regression analyses were performed based on the prognostic gene signature and clinical parameters, including the age at diagnosis, pathologic T stage, Gleason score, and preoperative PSA. Parameters with $p < 0.05$ based on univariate analysis were further included in the multivariate Cox regression analysis. $p < 0.05$ was considered statistically significant.

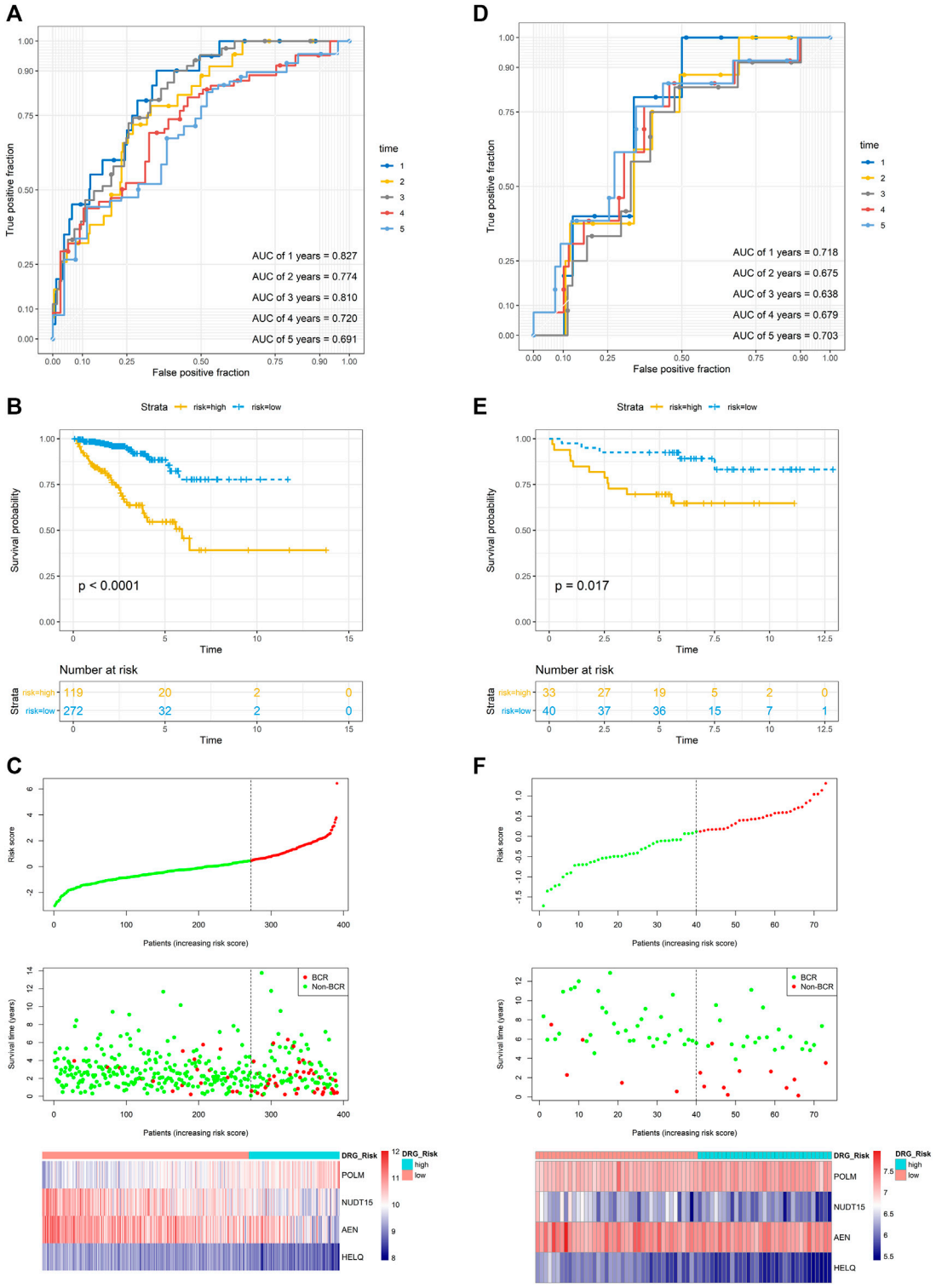

FIGURE 2 | Evaluation of the prognostic performance of the DRG signature in the training dataset and validation dataset **(A)** The time-dependent ROC for 1-, 2-, 3-, 4- and 5-years BCR predictions for the DRG signature in the training dataset **(B)** The Kaplan–Meier survival curves of the DRG signature. Patients from the training dataset were stratified into two groups according to the optimal cutoff value for the risk scores **(C)** The distribution of risk score, recurrence status, and gene expression panel in the training dataset **(D)** The time-dependent ROC for 1-, 2-, 3-, 4- and 5-years BCR predictions for the DRG signature in the validation dataset **(E)** The Kaplan–Meier survival curves of the DRG signature. Patients from the validation dataset were stratified into two groups according to the optimal cutoff values for the risk scores **(F)** The distribution of risk score, recurrence status, and gene expression panel in the validation dataset.

Establishment and Validation of a Predictive Nomogram.

After testing for collinearity, independent prognostic parameters and relevant clinical parameters were included to construct a prognostic nomogram to predict 1-, 3-, and 5-year progression-free survival for PCa patients. Calibration plots of 1-, 3-, and 5-year were plotted to assess the reliability of this nomogram. Kaplan-Meier analysis, the AUC of the ROC curve (using the timeROC package), and C index (using the survcomp package) were used to evaluate the performance of the nomogram. To evaluate the efficacy of the DRG signature in improving the nomogram model performance, we also generated a clinical model with only clinical parameters using the Cox stepwise regression. The decision curve analysis (DCA) was applied to compare the performance of the nomogram model and clinical model. Integrated discrimination improvement (IDI) and net reclassification improvement (NRI) were also calculated.

Statistical Analysis Softwares

Statistical analysis was performed using R software v4.0.2 and GraphPad Prism v8.01 (https://www.graphpad.com).

RESULTS

Construction of the DRG Signature in TCGA Cohort

In the TCGA dataset, three hundred and ninety one patients with the BCR survival information were selected to develop the DRG signature (**Supplementary Table S1**). The median (Interquartile range, IQR) follow-up duration was 2.4 (1.4–3.7) years. The univariate Cox regression analysis found that 67 DRGs were statistically significantly correlated with BCR survival ($p < 0.05$) (**Supplementary Table S2**). The detailed expression pattern of 67 DRG were shown in **Figure 1A**. KEGG and GO analyses were used to clarify the biological processes and pathways related to these significant genes (**Figures 1B,C**), which revealed that these genes were primarily involved in Fanconi anemia, DNA damage response, and DNA repair pathways. Next, a LASSO Cox regression model was used to calculate the most useful prognostic genes, and one SE above the minimum criteria was chosen, resulting in a model with four genes: POLM, NUDT15, AEN, and HELQ (**Figures 1D,E**). Additionally, a stepwise Cox proportional hazards regression model was used and it suggested that the 4-gene signature was already the optimal model. The detailed information of this signature was listed in **Supplementary Table S3**. Subsequently, a risk score was built: Risk Score = (0.9139 × POLM expression)−(0.7278 × NUDT15 expression)−(0.6761 × AEN expression)−(1.2567 × HELQ expression). The risk score for each patient was calculated using this formula. The ROC curve was plotted and the AUC values of different time points were calculated. Results showed that for predicting BCR-free survival in the TCGA dataset at 1st, 2nd, 3rd, 4th, and 5th year, the DRG risk score had AUC values of 0.827, 0.774, 0.810, 0.720, and 0.691 (**Figure 2A**). The C index of 0.777 (95% CI, 0.722–0.831) also suggested the fair performance of the DRG signature (**Table 1**). According to the optimal cutoff value of risk score, patients were assigned into high-risk group and low-risk group. Kaplan-Meier survival analyses showed that the rate of recurrence in the high-risk group was significantly higher than the low-risk group (**Figure 2B**, $p < 0.0001$). The distribution of risk score, recurrence status, and gene expression panel were illustrated in **Figure 2C**.

Validation of DRG Signature in GSE84042 Dataset

To validate the DRG signature, the GSE84042 dataset was used as a validation dataset and the relevant information was listed in **Supplementary Table S4**. The dataset comprised seventy three patients and the median (IQR) follow-up duration was 5.9 (5.1–7.6) years. Using the same formula, the risk scores of each patient were calculated and the cutoff value was also determined by the "surv_cutpoint" function. The AUCs for the 1-, 2-, 3-, 4-, and 5-years BCR-free survival were 0.718, 0.675, 0.638, 0.679, and 0.703, respectively (**Figure 2D**), and the C index was 0.634 (95% CI, 0.516–0.752) (**Table 1**). Kaplan-Meier survival analyses revealed that patients in the low-risk group had significantly better BCR-free survival than the high-risk group (**Figure 2E**, $p = 0.017$).

Clinical Relevance of DRG Signature

To investigate the association between clinical parameters and DRG signature, we compared the risk scores according to clinical status. Results suggested that the older age, high PSA, high pathologic T stage, and high Gleason score were related to a significantly higher DRG signature risk score (**Figures 3A–D**). These patients who experienced BCR also had a significantly higher risk score than those who did not recurrent (**Figure 3E**).

To explore the potential sensitivity to PARPi, we also compared the HRD scores in groups with different risks. The HRD status represents novel predictive biomarkers of response to PARPi (Ganguly et al., 2016) and the HRD scores could detect the HRD through its evaluation of genomic scarring based on next-generation sequencing. In our analysis, these patients who were identified as high risk by DRG signature had higher HRD scores (**Figure 3F**), indicating much more deficiency in homologous recombination repair in this subset of patients. In the detailed analysis, the TAI scores, LST scores, and LOH scores were all significantly higher in the DRG signature high-risk group (**Supplementary Figure S1**). Notably, the HRD score also presented a prognostic value in the TCGA dataset (**Supplementary Figure S2**).

Identification of Independent Prognostic Parameters

We performed univariate and multivariate Cox regression analyses to evaluate the prognostic significance of the DRG signature combined with various clinical parameters (**Table 2**). In the TCGA cohort, the Gleason score ($p = 0.004$) and DRG signature ($p < 0.001$) were significantly correlated with BCR-free survival. Additionally, the DRG signature showed a significant prognostic value in subgroups (**Supplementary Figure S3**). In the

TABLE 1 | Summary of performance of different models.

Parameters		TCGA dataset		GSE84042	
		Value and 95% CI	*p* value	Value and 95% CI	*p* value
C Index of DRG signature		0.777 (0.722–0.831)	< **0.001**	0.634 (0.516–0.752)	**0.026**
C Index of Nomogram,		0.780 (0.722–0.838)	< **0.001**	0.750 (0.630–0.870)	<**0.001**
C Index of Clinical model		0.711 (0.642–0.780)	< **0.001**	0.680 (0.548–0.811)	**0.007**
C Index of Walz's model		0.691 (0.620–0.762)	< **0.001**	0.678 (0.535–0.822)	**0.014**
Nomogram vs clinical model	IDI of 1 year	0.040 (0.014–0.083)	< **0.001**	0.066 (–0.028–0.230)	0.170
	NRI of 1 year	0.511 (0.159–0.662)	**0.016**	0.374 (–0.155–0.651)	0.106
	IDI of 2 years	0.046 (0.012–0.093)	< **0.001**	0.068 (–0.017–0.218)	0.128
	NRI of 2 years	0.452 (0.031–0.610)	**0.042**	0.335 (–0.091–0.584)	0.112
	IDI of 3 years	0.076 (0.017–0.144)	**0.010**	0.105 (–0.039–0.279)	0.138
	NRI of 3 years	0.477 (0.055–0.616)	**0.028**	0.357 (–0.094–0.576)	0.086
	IDI of 4 years	0.072 (-0.001–0.150)	0.056	0.113 (–0.031–0.280)	0.098
	NRI of 4 years	0.376 (-0.030–0.551)	0.068	0.396 (–0.005–0.618)	0.052
	IDI of 5 years	0.049 (-0.037–0.131)	0.276	0.124 (–0.012–0.295)	0.074
	NRI of 5 years	0.302 (-0.118–0.496)	0.128	0.424 (0.017–0.638)	**0.040**
Nomogram vs Walz's model	IDI of 1 year	0.053 (0.021–0.098)	< **0.001**	0.057 (–0.018–0.199)	0.129
	NRI of 1 year	0.052 (0.269–0.695)	< **0.001**	0.388 (–0.299–0.636)	0.378
	IDI of 2 years	0.057 (0.019–0.108)	**0.006**	0.068 (–0.013–0.196)	0.102
	NRI of 2 years	0.428 (0.220–0.596)	< **0.001**	0.350 (–0.134–0.587)	0.194
	IDI of 3 years	0.110 (0.039–0.195)	< **0.001**	0.078 (–0.042–0.193)	0.179
	NRI of 3 years	0.435 (0.208–0.579)	**0.002**	0.373 (–0.301–0.575)	0.289
	IDI of 4 years	0.139 (0.049–0.242)	< **0.001**	0.084 (–0.012–0.235)	0.090
	NRI of 4 years	0.380 (0.157–0.539)	**0.004**	0.413 (–0.205–0.608)	0.169
	IDI of 5 years	0.121 (0.009–0.231)	**0.038**	0.087 (–0.014–0.208)	0.090
	NRI of 5 years	0.309 (0.055–0.498)	**0.024**	0.424 (–0.202–0.637)	0.209

C index, Harrell's concordance index; DRG, DNA repair gene; IDI, Integrated discrimination improvement; NRI, Continuous net reclassification improvement.
p *value < 0.05 was considered statistically significant and highlighted in bold.*

GSE84042 dataset, the pathologic T stage ($p = 0.007$) and DRG signature ($p = 0.005$) were significantly correlated with BCR-free survival. Therefore, after adjustment for other clinical parameters, the DRG signature was still an independent prognostic factor for BCR-free survival in PRAD.

Nomogram Establishment and Its Performance

In the TCGA dataset, three hundred and seventy three patients with complete clinical data were included to establish the prognostic nomogram. Due to the insignificant prognostic value for BCR ($p = 0.819$), the age was excluded in the nomogram establishment. The Gleason score, pathologic T stage, PSA, and DRG signature were enrolled in this model (**Figure 4A**). No significant collinearity was detected for all the included factors (**Supplementary Table S5**). The calibration plots (**Supplementary Figure S4**) show excellent agreement between the nomogram prediction and actual observation in terms of the 1, 3 and 5-years BCR-free survival rates in both the TCGA dataset and the GSE84042 dataset. The AUCs for the 1-, 2-, 3-, 4-, and 5-years BCR survival in TCGA dataset were 0.806, 0.758, 0.793, 0.778, and 0.775, respectively (**Figure 4B**) and the C index was 0.780 (95% CI, 0.722–0.838). In the GSE84042 dataset, the AUCs were 0.859, 0.713, 0.775, 0.792, and 0.813 (**Figure 4C**), and the C index was 0.750 (95% CI, 0.630–0.870). In the TCGA dataset, the patients were divided into high-risk and low-risk groups based on the optimal cut-off value, and the low-risk group was associated with a better prognosis ($p < 0.0001$) (**Figure 4D**). In the GSE84042 dataset, patients were also perfectly stratified into high-risk group and low-risk group ($p < 0.0001$) (**Figure 4E**).

To evaluate the efficacy of the DRG signature in improving BCR prediction, a clinical model without the DRG signature was generated. We firstly input all the clinical parameters to build an initial Cox model. Then a stepwise Cox regression was applied to obtain the optimal model, which enrolled parameters including Gleason score, pathologic T stage, and PSA. Besides, we calculated the risk points of each patient using Walz's nomogram (Walz et al., 2009). The performance of the present nomogram model, clinical model, and Walz's model were compared. As shown in **Figure 5A**, the nomogram model outperformed the clinical model and Walz's model, especially at 1–3 years. The IDI and NRI outcomes also supported the better performance of the nomogram model (**Table 1**). The median (IQR) follow-up duration of the TCGA dataset was 2.4 (1.4–3.7) years, and this might be the reason for the relatively insignificant improvement in the 5th year. The superior performance of the nomogram was also confirmed in the GSE84042 dataset, but the advantage was more significant in the 4th and 5th years (**Figure 5C**). Considering the long follow-up duration of the GSE84042 dataset, we additionally plotted the ROC curves and DCA curves at the 6th and 7th years (**Supplementary Figure S5**) and the improvement turned more distinct. The DCA curves suggested that the DRG signature did not bring significant net benefit for patients with very high recurrence risk in short term, but the intermedia risk population might benefit from the DRG signature (**Figures 5B**,D). This alerted us that the clinical parameters including

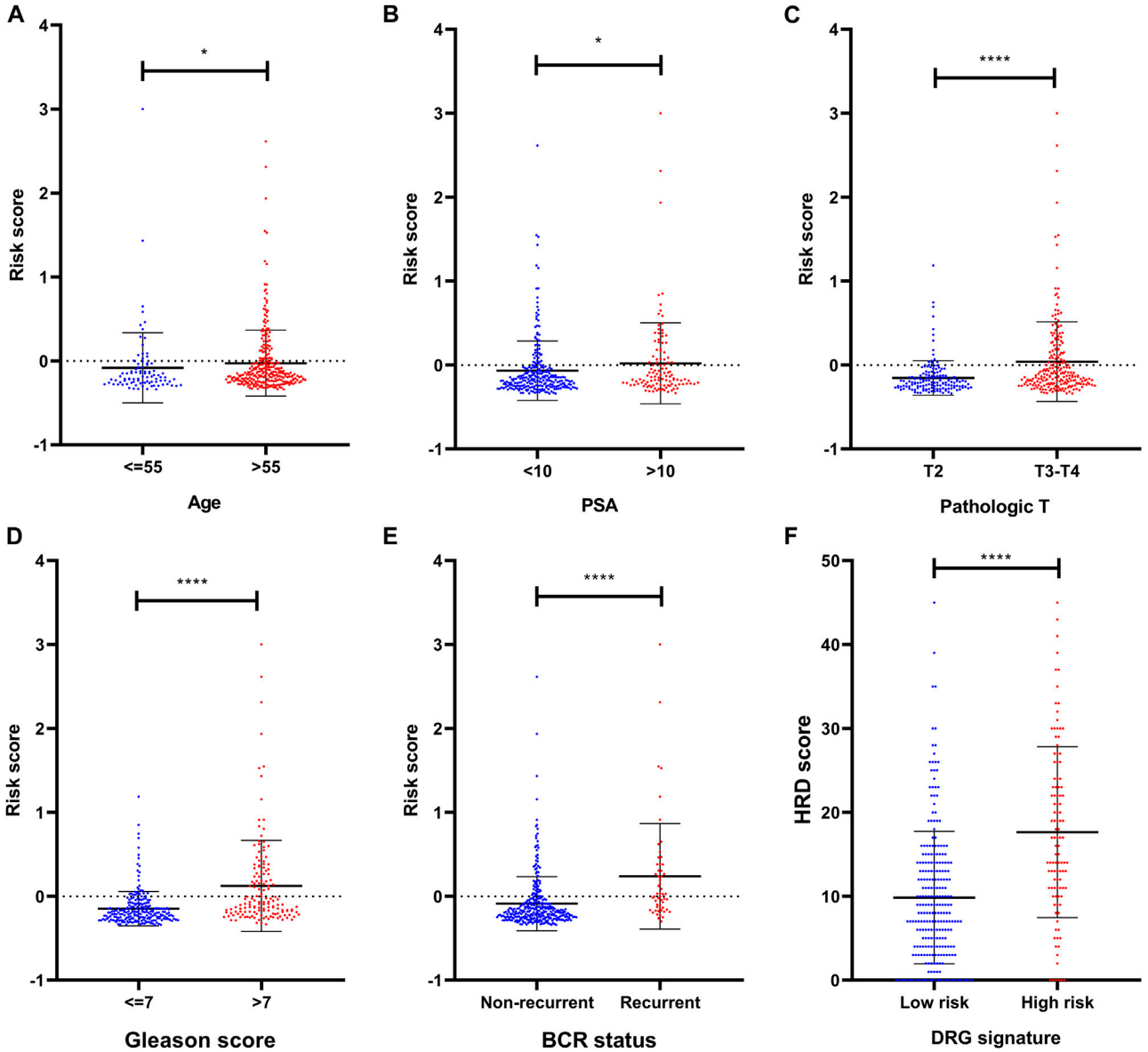

FIGURE 3 | Clinical relevance of the DRG signature **(A)** The distribution of the DRG signature risk score according to different ages **(B)** The distribution of the DRG signature risk score according to different PSA **(C)** The distribution of the DRG signature risk score according to different pathologic T stage **(D)** The distribution of the DRG signature risk score according to different Gleason scores **(E)** The distribution of the DRG signature risk score according to different BCR status **(F)** The association between DRG signature and HRD score. *$p < 0.05$, **$p < 0.01$, ***$p < 0.001$, ****$p < 0.0001$. Error bars were represented as Mean with SD.

pathologic stage, Gleason score, and PSA might be sufficient for very-high-risk groups, and we should select the patients to whom the DRG signature could be applied.

DISCUSSION

The cases of PCa is increasing worldwide, with sharp rises in incidence rates in Asia and Northern and Western Europe (Wong et al., 2016). Although the prognosis of PCa is relatively good, recurrent PCa after curative treatment may develop to progression and even metastasis. Randomized controlled trials have suggested the benefit of early androgen deprivation treatment (ADT) and radiotherapy after surgery for high-risk localized PCa (Messing et al., 2006; Gandaglia et al., 2017). The accurate prediction of prognosis will help to select patients that could benefit from further treatments. The traditional clinicopathological parameters such as TNM staging and Gleason scores can predict the prognosis of PCa, but the accuracy should be improved. Moreover, these parameters do not reflect the biological progression of PCa. Gene signatures can be measured by standardized detection systems, and dynamically describe the characteristics and progression of PCa.

TABLE 2 | Outcomes of univariate and multivariate cox regression analysis.

Variable	TCGA dataset				GSE84042			
	Univariate analysis		Multivariate analysis		Univariate analysis		Multivariate analysis	
	HR and 95% CI	*p* value	HR and 95% CI	*p* value	HR and 95% CI	*p* value	HR and 95% CI	*p* value
Age	0.995 (0.957–1.036)	0.819	NA	NA	0.980 (0.908–1.058)	0.612	NA	NA
Pathologic T (ref: T2)T3-T4	4.942 (2.233–10.940)	< **0.001**	2.280 (0.951–5.464)	0.065	3.251 (1.124–9.408)	**0.0296**	4.467 (1.520–13.130)	**0.007**
Gleason score	2.113 (1.613–2.768)	< **0.001**	1.541 (1.145–2.074)	**0.004**	2.208 (0.499–9.770)	0.296	NA	NA
PSA	1.021 (1.005–1.037)	**0.009**	1.008 (0.987–1.029)	0.465	1.030 (0.955–1.111)	0.442	NA	NA
DRG signature (ref: low risk) High risk	5.296 (3.013–9.310)	< **0.001**	3.462 (1.927–6.221)	< **0.001**	0.293 (0.101–0.850)	**0.024**	4.672 (1.580–13.810)	**0.005**

HR, Hazard ratio; DRG, DNA repair gene; NA, not applicable.

p value < 0.05 was considered statistically significant and highlighted in bold.In the multivariate Cox regression, only factors with a p value < 0.1 in the univariate analysis were included. In the TCGA dataset, the pathologic T stage, Gleason score, PSA and DRG signature were included. In the GSE84042 dataset, only pathologic T stage and DRG signature were included.

Additionally, these genes might represent potential therapeutic targets. Nomograms are widely used in oncology to evaluate clinical prognosis. A nomogram integrated multiple prognostic determinants including molecular biology and clinicopathological parameters, and it offers a more accurate prediction and a more intuitive view for patients. These advantages could contribute to clinical decision making and made nomogram an excellent tool for illustration of prognosis prediction (Balachandran et al., 2015).

There were many gene signatures based on different gene sets to predict the prognosis of PCa. Epigenetic alterations are frequently observed in tumors and several epigenetic biomarkers were developed including the GSTP1, APC, and RASSF1 (Trock et al., 2012; Van Neste et al., 2012; Stewart et al., 2013). Likewise, Prolaris, a gene signature consisting of thirty three cell cycle genes, was established and it was confirmed able to independently predict biochemical recurrence (Cuzick et al., 2011). Also, there were signatures comprising genes of different biological functions. The OncotypeDX Genomic Prostate Score (GPS) is based on a multi-gene assay consisting of seventeen genes related to androgen metabolism, cellular organization, proliferation, and stromal response (Klein et al., 2014). The GPS was designed to allow risk assessment for selecting candidates for active surveillance and generate valid results particularly for small tumor volumes in biopsy specimens by predicting adverse pathologic features at the time of RP, but its prognostic accuracy in predicting BCR was further confirmed (Cullen et al., 2015). The Decipher gene signature consists of a 22-gene panel and represents multiple biological pathways that are involved in aggressive PCa, including cell proliferation, cell structure, immune system modulation, cell cycle progression, and androgen signaling (Nakagawa et al., 2008). The Decipher gene signature could predict the BCR and metastasis in patients receiving postoperative radiotherapy (Den et al., 2014), and in patients following RP, it could also predict the early metastasis and even cancer-specific mortality (Erho et al., 2013; Ross et al., 2014; Klein et al., 2016; Nguyen et al., 2017; Karnes et al., 2018).

DNA repair genes play a critical role in the development of various cancer such as ovarian cancer, breast cancer, and PCa (Goodwin et al., 2013; Oktay et al., 2015; Majidinia and Yousefi, 2017). Due to the strong association between DDR defects and cancer progression, several gene signatures based on DRGs were established for cancers including ovarian cancer (Sun et al., 2019), colon cancer (Wang et al., 2020), and hepatic cancer (Li et al., 2019). In this study, we developed a DRG signature that could predict the BCR survival of PCa. Also, we built a nomogram that integrated clinicopathological parameters and the DRG signature, and the nomogram could efficiently stratify patients into a high-risk group and low-risk group. This model could provide valuable information to guide the further treatment of PCa patients who underwent RP.

Among these DDR defects, the HRD has been mostly explored. Using homologous recombination repair, a cell can efficiently perform the error-free repair of a double-strand break (DSB) in S phase. The HRD showed a double-edge property in cancer development. On the one hand, HRD resulted in genomic instability, which could a reason for the worse prognosis (Castro et al., 2013). Similar outcomes were also observed in our analysis. On the other hand, HRD is a predictor of response to specific treatment such as PARPi (Kaufman et al., 2015; Mateo et al., 2015; Robson et al., 2017; Mateo et al., 2020). The PARPi could block base excision repair, resulting in a conversion of a single strand break to a DSB. For HRD cancer cells, the accumulation of DSBs would eventually lead to cell death (D'Andrea, 2018). However, methods to identify HRD in tumors are varied and controversial (Hoppe et al., 2018). The somatic mutations in homologous recombination genes were focus biomarkers to identify HRD, and PARPi has been shown to have clinical activity in these subgroups (Mateo et al., 2015). To expand the group that suitable for PARPi treatment, a genomic-scar-based HRD score was developed, and it has been suggested as a promising predictor for response to Olaparib (Lheureux et al., 2017). In the present study, we found that the DRG signature high-risk group was related to a higher HRD score and the HRD could be a potential reason for the worse prognosis in this subset of patients. Notably, in the management of PCa, PARPi would only be considered in the castration-resistant PCa (CRPC) stage (de Bono et al., 2020; Hussain et al., 2020), and the present study was based on patients with hormone-sensitive PCa (HSPC). When the HSPC progressed to the ADT-insensitive CRPC, the genomic hallmarks also significantly changed and the proportion of HRD could also increase (van Dessel et al., 2019). In the present study, the HRD score only reflects the HRD situation at the HSPC stage, and the association between the DRG signature and HRD scores might provide information for treatment

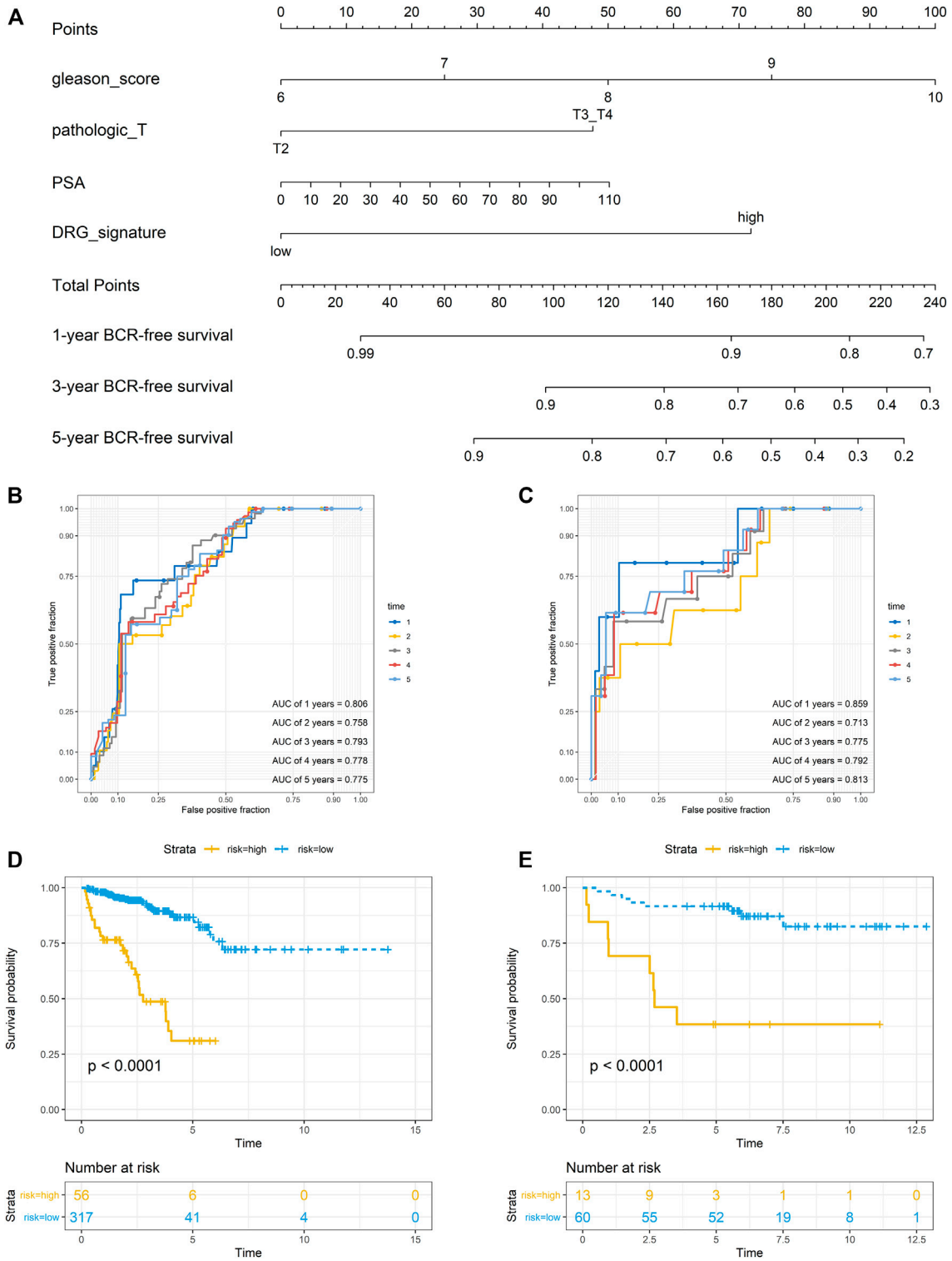

FIGURE 4 | Nomogram to predict BCR-free survival probability of patients with PCa **(A)** A prognostic nomogram predicting 1-, 3-, and 5-years BCR survival of PCa **(B)** The time-dependent ROC for 1-, 2-, 3-, 4- and 5-years BCR predictions for the nomogram in the training dataset **(C)** The time-dependent ROC for 1-, 2-, 3-, 4- and 5-years BCR predictions for the nomogram in the validation dataset **(D)** The Kaplan–Meier survival curves of the nomogram. Patients from the training dataset were stratified into two groups according to the optimal cutoff values for the risk scores **(E)** The Kaplan–Meier survival curves of the nomogram. Patients from the validation dataset were stratified into two groups according to the optimal cutoff values for the risk scores.

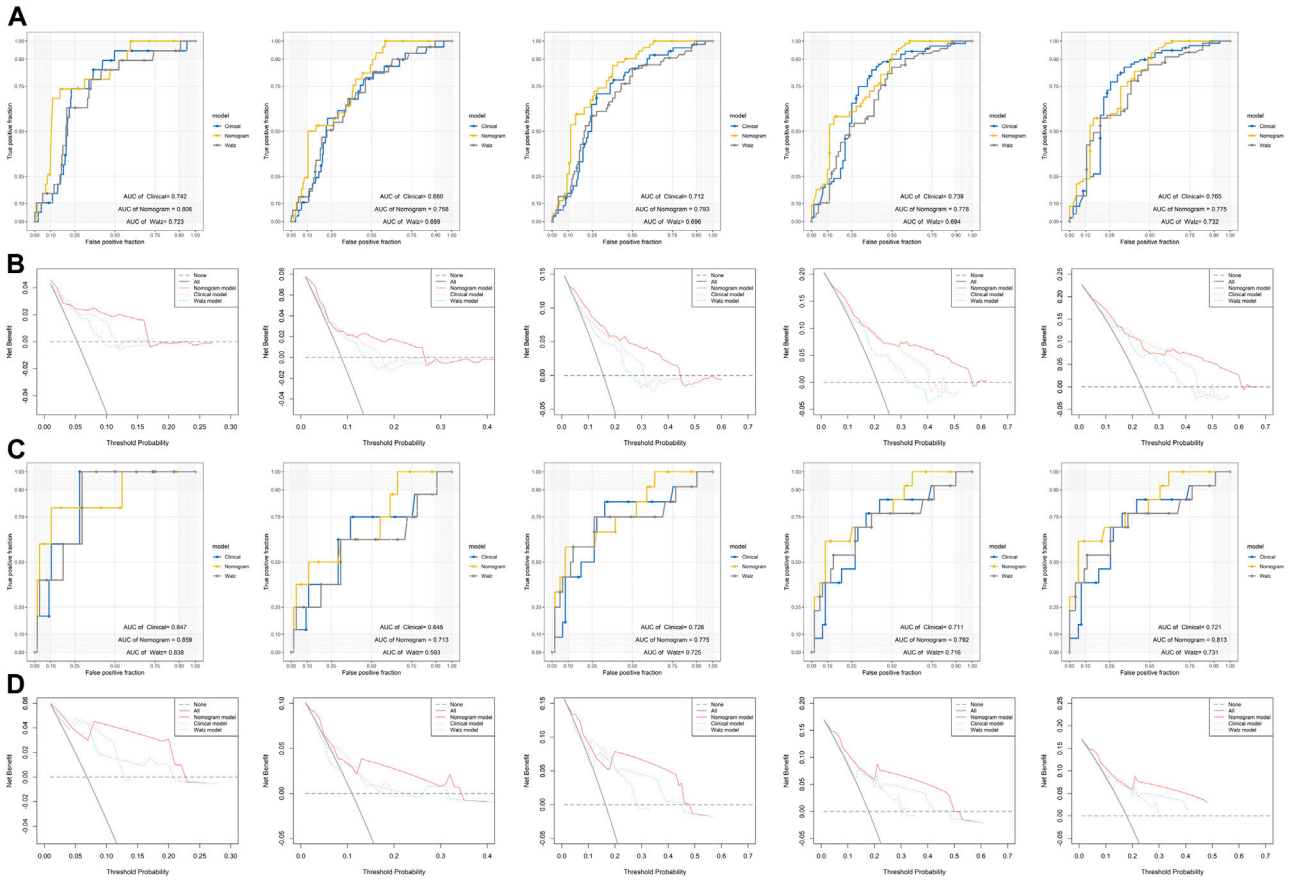

FIGURE 5 | Comparison of the performance of the nomogram model, Walz's model, and clinical model **(A)** ROC curves of the nomogram model, Walz's model, and clinical model at 1–5 years in the training dataset **(B)** DCA curve to compare the performance of the nomogram model, Walz's model, and clinical model at 1–5 years in the training dataset **(C)** ROC curves of the nomogram model, Walz's model, and clinical model at 1–5 years in the validation dataset **(D)** DCA curve to compare the performance of the nomogram model, Walz's model, and clinical model at 1–5 years in the validation dataset.

choosing when cancer progressed, but these results should be interpreted with caution.

The DRG signature consists of four genes including POLM, NUDT15, AEN, and HELQ. POLM, also known as polymerase μ (Pol μ), could promote the accuracy in the nonhomologous DNA end-joining (NHEJ), which is another solution for DSB (Waters et al., 2014). The POLM could be up-regulated in response to accumulated DSB (Mahajan et al., 2002). In our cases, the overexpression of POLM may infer the deficiency in homologous repair. NUDT15 played a role in DNA synthesis and cell cycle progression by stabilizing proliferating cell nuclear antigen (PCNA) (Yu et al., 2009). Mutations in this gene result in poor metabolism of thiopurines and are associated with thiopurine-induced early leukopenia (Yang et al., 2014). However, its role in the development of PCa was not explored. AEN (Apoptosis Enhancing Nuclease) is an autophagy-related protein-coding gene, and it is induced by p53 with various DNA damage, leading to cell apoptosis (Kawase et al., 2008; Eby et al., 2010). An association between the AEN and prognosis of hepatocellular carcinoma has been reported (Zhu et al., 2019). HELQ (Helicase POLQ-like), an ATP-dependent 3′-5′ DNA helicase, plays pivotal roles in DNA processing, including homologous recombination repair (Han et al., 2016). It has been reported to serve as an indicator of platinum-based chemoresistance for ovarian cancer (Long et al., 2018).

Besides the genomic biomarkers, several advanced examinations could also predict the prognosis of PCa. As an example, the PSMA PET/CT could predict progression-free survival in localized PCa (Roberts et al., 2020) and could even guide the use of salvage treatments such as radiotherapy (Emmett et al., 2020). However, due to the limitation of the dataset, the role of this kind of technique was unable to be adjusted in our study.

To the best of our knowledge, a prognostic model based on these five DNA repair-related genes and the associated nomogram in PCa have not been reported. A DRG signature in PCa has been previously reported to predict BCR-free, metastasis-free, and overall survival, but it is based on a profile of nine DDR pathways using seventeen gene sets for GSEA (Gene Set Enrichment Analysis) (Evans et al., 2016). Our gene signature is based on the expression of four genes. Therefore it is economical and clinically practicable to be used. Our nomogram combined with DRG signature and clinicopathological parameters presented an excellent performance in prognosis prediction. It could provide a straightforward and convenient graphical scoring system and help clinical decision making.

Our current study has some limitations. First, the training set was from the TCGA database and GSE84042 was served as the validation dataset. The majority of these patients are from North America, and thus, the expanding of our results to other ethnicities should be with caution. Second, the DCA analysis suggested that the signature did not bring significant net benefit for patients with very high risk and the signature might be more meaningful for patients who were thought moderate or low risk with traditional tools. Third, the salvage treatments could influence the BCR, and predictors such as PSMA PET could also prognosticate the BCR after salvage therapies in these patients with a rising PSA after RP (Emmett et al., 2020). While in our study, due to the lack of data, the prognostic value of the signature on patients after salvage therapies require further ascertainment. Besides, we identified four genes to construct a gene signature based on the mRNA sequencing data, but the protein expression of these genes and the underlying mechanism require further investigation. Last, the establishing and validation of this model were all conducted with publicly available data, and it needs to be further validated in original external datasets.

CONCLUSION

In conclusion, our study profiled DNA repair genes that are significantly related to the prognosis of PCa. The combination of these biomarkers may serve as a signature to stratify PCa patients into low-risk and high-risk groups for assessing BCR survival. We also constructed a nomogram based on clinical parameters and the DRG signature to predict the BCR, which could be helpful for precise and personalized treatment.

DATA AVAILABILITY STATEMENT

Publicly available datasets were analyzed in this study. This data can be found in The Cancer Genome Atlas (TCGA) and Gene Expression Omnibus (GEO) (GSE84042).

ETHICS STATEMENT

Ethical review and approval was not required for the study on human participants in accordance with the local legislation and institutional requirements. Written informed consent for participation was not required for this study in accordance with the national legislation and the institutional requirements.

AUTHOR CONTRIBUTIONS

GL and HL: conception and design. WO and YZ: development of methodology. GL, GS, and JG: analysis and interpretation of data. GL: writing of the manuscript. WO, GS, JG, and ZH: review of the manuscript. ZH and HL: study supervision.

FUNDING

This research was supported by the Natural Science Fund of Hubei Province (Grant Number: 2018CFB459). The funding sources had no role in the design and conduct of the study; collection, management, analysis, and interpretation of the data; and preparation, review, or approval of the manuscript.

SUPPLEMENTARY MATERIAL

The Supplementary Material for this article can be found online at: https://www.frontiersin.org/articles/10.3389/fmolb.2021.608369/full#supplementary-material.

ACKNOWLEDGMENTS

We would like to thank Jianbo Tian from the School of Public Health, Tongji Medical College, Huazhong University of Science and Technology for his assistance with the methodology.

REFERENCES

Abkevich, V., Timms, K. M., Hennessy, B. T., Potter, J., Carey, M. S., Meyer, L. A., et al. (2012). Patterns of genomic loss of heterozygosity predict homologous recombination repair defects in epithelial ovarian cancer. *Br. J. Cancer* 107 (10), 1776–1782. doi:10.1038/bjc.2012.451

Ali, R., Rakha, E. A., Madhusudan, S., and Bryant, H. E. (2017). DNA damage repair in breast cancer and its therapeutic implications. *Pathology* 49 (2), 156–165. doi:10.1016/j.pathol.2016.11.002

Balachandran, V. P., Gonen, M., Smith, J. J., and DeMatteo, R. P. (2015). Nomograms in oncology: more than meets the eye. *Lancet Oncol.* 16 (4), e173–e180. doi:10.1016/s1470-2045(14)71116-7

Birkbak, N. J., Wang, Z. C., Kim, J.-Y., Eklund, A. C., Li, Q., Tian, R., et al. (2012). Telomeric allelic imbalance indicates defective DNA repair and sensitivity to DNA-damaging agents. *Cancer Discov.* 2 (4), 366–375. doi:10.1158/2159-8290.Cd-11-0206

Brockman, J. A., Alanee, S., Vickers, A. J., Scardino, P. T., Wood, D. P., Kibel, A. S., et al. (2015). Nomogram predicting prostate cancer-specific mortality for men with biochemical recurrence after radical prostatectomy. *Eur. Urol.* 67 (6), 1160–1167. doi:10.1016/j.eururo.2014.09.019

Castro, E., Goh, C., Olmos, D., Saunders, E., Leongamornlert, D., Tymrakiewicz, M., et al. (2013). Germline BRCA mutations are associated with higher risk of nodal involvement, distant metastasis, and poor survival outcomes in prostate cancer. *J. Clin. Oncol.* 31 (14), 1748–1757. doi:10.1200/jco.2012.43.1882

Cullen, J., Rosner, I. L., Brand, T. C., Zhang, N., Tsiatis, A. C., Moncur, J., et al. (2015). A biopsy-based 17-gene genomic prostate score predicts recurrence after radical prostatectomy and adverse surgical pathology in a racially diverse population of men with clinically low- and intermediate-risk prostate cancer. *Eur. Urol.* 68 (1), 123–131. doi:10.1016/j.eururo.2014.11.030

Cuzick, J., Swanson, G. P., Fisher, G., Brothman, A. R., Berney, D. M., Reid, J. E., et al. (2011). Prognostic value of an RNA expression signature derived from cell cycle proliferation genes in patients with prostate cancer: a retrospective study. *Lancet Oncol.* 12 (3), 245–255. doi:10.1016/s1470-2045(10)70295-3

D'Andrea, A. D. (2018). Mechanisms of PARP inhibitor sensitivity and resistance. *DNA Repair (Amst)* 71, 172–176. doi:10.1016/j.dnarep.2018.08.021

de Bono, J., Mateo, J., Fizazi, K., Saad, F., Shore, N., Sandhu, S., et al. (2020). Olaparib for metastatic castration-resistant prostate cancer. *N. Engl. J. Med.* 382 (22), 2091–2102. doi:10.1056/NEJMoa1911440

Den, R. B., Feng, F. Y., Showalter, T. N., Mishra, M. V., Trabulsi, E. J., Lallas, C. D., et al. (2014). Genomic prostate cancer classifier predicts biochemical failure and metastases in patients after postoperative radiation therapy. *Int. J. Radiat. Oncol. Biol. Phys.* 89 (5), 1038–1046. doi:10.1016/j.ijrobp.2014.04.052

Eby, K. G., Rosenbluth, J. M., Mays, D. J., Marshall, C. B., Barton, C. E., Sinha, S., et al. (2010). ISG20L1 is a p53 family target gene that modulates genotoxic stress-induced autophagy. *Mol. Cancer* 9, 95. doi:10.1186/1476-4598-9-95

Emmett, L., Tang, R., Nandurkar, R., Hruby, G., Roach, P., Watts, J. A., et al. (2020). 3-Year freedom from progression after 68Ga-PSMA PET/CT-triaged management in men with biochemical recurrence after radical prostatectomy: results of a prospective multicenter trial. *J. Nucl. Med.* 61 (6), 866–872. doi:10.2967/jnumed.119.235028

Erho, N., Crisan, A., Vergara, I. A., Mitra, A. P., Ghadessi, M., Buerki, C., et al. (2013). Discovery and validation of a prostate cancer genomic classifier that predicts early metastasis following radical prostatectomy. *PLoS One* 8 (6), e66855. doi:10.1371/journal.pone.0066855

Evans, J. R., Zhao, S. G., Chang, S. L., Tomlins, S. A., Erho, N., Sboner, A., et al. (2016). Patient-level DNA damage and repair pathway profiles and prognosis after prostatectomy for high-risk prostate cancer. *JAMA Oncol.* 2 (4), 471–480. doi:10.1001/jamaoncol.2015.4955

Fraser, M., Sabelnykova, V. Y., Yamaguchi, T. N., Heisler, L. E., Livingstone, J., Huang, V., et al. (2017). Genomic hallmarks of localized, non-indolent prostate cancer. *Nature* 541 (7637), 359–364. doi:10.1038/nature20788

Gandaglia, G., Briganti, A., Clarke, N., Karnes, R. J., Graefen, M., Ost, P., et al. (2017). Adjuvant and salvage radiotherapy after radical prostatectomy in prostate cancer patients. *Eur. Urol.* 72 (5), 689–709. doi:10.1016/j.eururo.2017.01.039

Ganguly, B., Dolfi, S. C., Rodriguez-Rodriguez, L., Ganesan, S., and Hirshfield, K. M. (2016). Role of biomarkers in the development of PARP inhibitors. *Biomark Cancer* 8s1, 15–25. doi:10.4137/bic.S36679

Goodwin, J. F., Schiewer, M. J., Dean, J. L., Schrecengost, R. S., de Leeuw, R., Han, S., et al. (2013). A hormone-DNA repair circuit governs the response to genotoxic insult. *Cancer Discov.* 3 (11), 1254–1271. doi:10.1158/2159-8290.Cd-13-0108

Han, X., Zhao, L., and Li, X. (2016). HELQ in cancer and reproduction. *Neoplasma* 63 (6), 825–835. doi:10.4149/neo_2016_601

Hanahan, D., and Weinberg, R. A. (2011). Hallmarks of cancer: the next generation. *Cell* 144 (5), 646–674. doi:10.1016/j.cell.2011.02.013

Hoppe, M. M., Sundar, R., Tan, D. S. P., and Jeyasekharan, A. D. (2018). Biomarkers for homologous recombination deficiency in cancer. *J. Natl. Cancer Inst.* 110 (7), 704–713. doi:10.1093/jnci/djy085

Huang, D. W., Sherman, B. T., and Lempicki, R. A. (2009). Systematic and integrative analysis of large gene lists using DAVID bioinformatics resources. *Nat. Protoc.* 4 (1), 44–57. doi:10.1038/nprot.2008.211

Hussain, M., Mateo, J., Fizazi, K., Saad, F., Shore, N., Sandhu, S., et al. (2020). Survival with Olaparib in metastatic castration-resistant prostate cancer. *N. Engl. J. Med.* 383, 2345. doi:10.1056/NEJMoa2022485

Karnes, R. J., Choeurng, V., Ross, A. E., Schaeffer, E. M., Klein, E. A., Freedland, S. J., et al. (2018). Validation of a genomic risk classifier to predict prostate cancer-specific mortality in men with adverse pathologic features. *Eur. Urol.* 73 (2), 168–175. doi:10.1016/j.eururo.2017.03.036

Kaufman, B., Shapira-Frommer, R., Schmutzler, R. K., Audeh, M. W., Friedlander, M., Balmaña, J., et al. (2015). Olaparib monotherapy in patients with advanced cancer and a germline BRCA1/2 mutation. *J. Clin. Oncol.* 33 (3), 244–250. doi:10.1200/jco.2014.56.2728

Kawase, T., Ichikawa, H., Ohta, T., Nozaki, N., Tashiro, F., Ohki, R., et al. (2008). p53 target gene AEN is a nuclear exonuclease required for p53-dependent apoptosis. *Oncogene* 27 (27), 3797–3810. 0.1038/onc.2008.32

Klein, E. A., Cooperberg, M. R., Magi-Galluzzi, C., Simko, J. P., Falzarano, S. M., Maddala, T., et al. (2014). A 17-gene assay to predict prostate cancer aggressiveness in the context of gleason grade heterogeneity, tumor multifocality, and biopsy undersampling. *Eur. Urol.* 66 (3), 550–560. doi:10.1016/j.eururo.2014.05.004

Klein, E. A., Haddad, Z., Yousefi, K., Lam, L. L. C., Wang, Q., Choeurng, V., et al. (2016). Decipher genomic classifier measured on prostate biopsy predicts metastasis risk. *Urology* 15, 148–152. doi:10.1016/j.urology.2016.01.012

Knijnenburg, T. A., Wang, L., Zimmermann, M. T., Chambwe, N., Gao, G. F., Cherniack, A. D., et al. (2018). Genomic and molecular landscape of DNA damage repair deficiency across the cancer genome Atlas. *Cell Rep.* 23 (1), 239–254e6. doi:10.1016/j.celrep.2018.03.076

Lheureux, S., Lai, Z., Dougherty, B. A., Runswick, S., Hodgson, D. R., Timms, K. M., et al. (2017). Long-term responders on Olaparib maintenance in high-grade serous ovarian cancer: clinical and molecular characterization. *Clin. Cancer Res.* 23 (15), 4086–4094. doi:10.1158/1078-0432.Ccr-16-2615

Li, N., Zhao, L., Guo, C., Liu, C., and Liu, Y. (2019). Identification of a novel DNA repair-related prognostic signature predicting survival of patients with hepatocellular carcinoma. *Cell. Manage. Res.* 11, 7473–7484. doi:10.2147/cmar.S204864

Long, J., Zhu, J.-Y., Liu, Y.-B., Fu, K., Tian, Y., Li, P.-Y., et al. (2018). Helicase POLQ-like (HELQ) as a novel indicator of platinum-based chemoresistance for epithelial ovarian cancer. *Gynecol. Oncol.* 149 (2), 341–349. doi:10.1016/j.ygyno.2018.03.006

Mahajan, K. N., Nick McElhinny, S. A., Mitchell, B. S., and Ramsden, D. A. (2002). Association of DNA polymerase μ (pol μ) with Ku and ligase IV: role for pol μ in end-joining double-strand break repair. *Mol. Cell Biol.* 22 (14), 5194–5202. doi:10.1128/mcb.22.14.5194-5202.2002

Majidinia, M., and Yousefi, B. (2017). DNA repair and damage pathways in breast cancer development and therapy. *DNA Repair* 54, 22–29. doi:10.1016/j.dnarep.2017.03.009

Mateo, J., Boysen, G., Barbieri, C. E., Bryant, H. E., Castro, E., Nelson, P. S., et al. (2017). DNA repair in prostate cancer: biology and clinical implications. *Eur. Urol.* 71 (3), 417–425. doi:10.1016/j.eururo.2016.08.037

Mateo, J., Carreira, S., Sandhu, S., Miranda, S., Mossop, H., Perez-Lopez, R., et al. (2015). DNA-repair defects and Olaparib in metastatic prostate cancer. *N. Engl. J. Med.* 373 (18), 1697–1708. doi:10.1056/NEJMoa1506859

Mateo, J., Porta, N., Bianchini, D., McGovern, U., Elliott, T., Jones, R., et al. (2020). Olaparib in patients with metastatic castration-resistant prostate cancer with DNA repair gene aberrations (TOPARP-B): A multicentre, open-label, randomised, phase 2 trial. *Lancet Oncol.* 21 (1), 162–174. doi:10.1016/s1470-2045(19)30684-9

Messing, E. M., Manola, J., Yao, J., Kiernan, M., Crawford, D., Wilding, G., et al. (2006). Immediate versus deferred androgen deprivation treatment in patients with node-positive prostate cancer after radical prostatectomy and pelvic lymphadenectomy. *Lancet Oncol.* 7 (6), 472–479. doi:10.1016/s1470-2045(06)70700-8

Minchom, A., Aversa, C., and Lopez, J. (2018). Dancing with the DNA damage response: next-generation anti-cancer therapeutic strategies. *Ther. Adv. Med. Oncol.* 10, 175883591878665. doi:10.1177/1758835918786658

Mirza-Aghazadeh-Attari, M., Ostadian, C., Saei, A. A., Mihanfar, A., Darband, S. G., Sadighparvar, S., et al. (2019). DNA damage response and repair in ovarian cancer: potential targets for therapeutic strategies. *DNA Repair* 80, 59–84. doi:10.1016/j.dnarep.2019.06.005

Mottet, N., Bellmunt, J., Bolla, M., Briers, E., Cumberbatch, M. G., De Santis, M., et al. (2017). EAU-ESTRO-SIOG Guidelines on prostate cancer. Part 1: screening, diagnosis, and local treatment with curative intent. *Eur. Urol.* 71 (4), 618–629. doi:10.1016/j.eururo.2016.08.003

Nakagawa, T., Kollmeyer, T. M., Morlan, B. W., Anderson, S. K., Bergstralh, E. J., Davis, B. J., et al. (2008). A tissue biomarker panel predicting systemic progression after PSA recurrence post-definitive prostate cancer therapy. *PLoS One* 3 (5), e2318, doi:10.1371/journal.pone.0002318

Nguyen, P. L., Haddad, Z., Ross, A. E., Martin, N. E., Deheshi, S., Lam, L. L. C., et al. (2017). Ability of a genomic classifier to predict metastasis and prostate cancer-specific mortality after radiation or surgery based on Needle biopsy specimens. *Eur. Urol.* 72 (5), 845–852. doi:10.1016/j.eururo.2017.05.009

Oktay, K., Turan, V., Titus, S., Stobezki, R., and Liu, L. (2015). BRCA mutations, DNA repair deficiency, and ovarian Aging1. *Biol. Reprod.* 93 (3), 67. doi:10.1095/biolreprod.115.132290

Popova, T., Manié, E., Rieunier, G., Caux-Moncoutier, V., Tirapo, C., Dubois, T., et al. (2012). Ploidy and large-scale genomic instability consistently identify basal-like breast carcinomas with BRCA1/2 inactivation. *Cancer Res.* 72 (21), 5454–5462. doi:10.1158/0008-5472.Can-12-1470

Roberts, M. J., Morton, A., Donato, P., Kyle, S., Pattison, D. A., Thomas, P., et al. (2020). 68Ga-PSMA PET/CT tumour intensity pre-operatively predicts adverse pathological outcomes and progression-free survival in localised prostate cancerGa-PSMA PET/CT tumour intensity pre-operatively predicts adverse pathological outcomes and progression-free survival in localised prostate cancer. *Eur. J. Nucl. Med. Mol. Imaging* 48, 477. doi:10.1007/s00259-020-04944-2

Robinson, M. D., McCarthy, D. J., and Smyth, G. K. (2010). edgeR: a bioconductor package for differential expression analysis of digital gene expression data. *Bioinformatics* 26 (1), 139–140. doi:10.1093/bioinformatics/btp616

Robson, M., Im, S.-A., Senkus, E., Xu, B., Domchek, S. M., Masuda, N., et al. (2017). Olaparib for metastatic breast cancer in patients with a germline BRCA mutation. *N. Engl. J. Med.* 377 (6), 523–533. doi:10.1056/NEJMoa1706450

Ross, A. E., Feng, F. Y., Ghadessi, M., Erho, N., Crisan, A., Buerki, C., et al. (2014). A genomic classifier predicting metastatic disease progression in men with biochemical recurrence after prostatectomy. *Prostate Cancer Prostatic Dis.* 17 (1), 64–69. doi:10.1038/pcan.2013.49

Sanda, M. G., Cadeddu, J. A., Kirkby, E., Chen, R. C., Crispino, T., Fontanarosa, J., et al. (2018). Clinically localized prostate cancer: AUA/ASTRO/SUO Guideline. Part I: risk stratification, shared decision making, and care options. *J. Urol.* 199 (3), 683–690. doi:10.1016/j.juro.2017.11.095

Siegel, R. L., Miller, K. D., and Jemal, A. (2020). Cancer statistics, 2020. *CA A. Cancer J. Clin.* 70 (1), 7–30. doi:10.3322/caac.21590

Stewart, G. D., Van Neste, L., Delvenne, P., Delrée, P., Delga, A., McNeill, S. A., et al. (2013). Clinical utility of an epigenetic assay to detect occult prostate cancer in histopathologically negative biopsies: results of the MATLOC study. *J. Urol.* 189 (3), 1110–1116. doi:10.1016/j.juro.2012.08.219

Sun, H., Cao, D., Ma, X., Yang, J., Peng, P., Yu, M., et al. (2019). Identification of a prognostic signature associated with DNA repair genes in ovarian cancer. *Front. Genet.* 10, 839. doi:10.3389/fgene.2019.00839

Trock, B. J., Brotzman, M. J., Mangold, L. A., Bigley, J. W., Epstein, J. I., McLeod, D., et al. (2012). Evaluation of GSTP1 and APC methylation as indicators for repeat biopsy in a high-risk cohort of men with negative initial prostate biopsies. *BJU Int.* 110 (1), 56–62. doi:10.1111/j.1464-410X.2011.10718.x

Van den Broeck, T., van den Bergh, R. C. N., Arfi, N., Gross, T., Moris, L., Briers, E., et al. (2019). Prognostic value of biochemical recurrence following treatment with curative intent for prostate cancer: a systematic review. *Eur. Urol.* 75 (6), 967–987. doi:10.1016/j.eururo.2018.10.011

van Dessel, L. F., van Riet, J., Smits, M., Zhu, Y., Hamberg, P., van der Heijden, M. S., et al. (2019). The genomic landscape of metastatic castration-resistant prostate cancers reveals multiple distinct genotypes with potential clinical impact. *Nat. Commun.* 10 (1), 5251. doi:10.1038/s41467-019-13084-7

Van Neste, L., Herman, J. G., Otto, G., Bigley, J. W., Epstein, J. I., and Van Criekinge, W. (2012). The epigenetic promise for prostate cancer diagnosis. *Prostate* 72 (11), 1248–1261. doi:10.1002/pros.22459

Walz, J., Chun, F. K.-H., Klein, E. A., Reuther, A., Saad, F., Graefen, M., et al. (2009). Nomogram predicting the probability of early recurrence after radical prostatectomy for prostate cancer. *J. Urol.* 181 (2), 601–608. doi:10.1016/j.juro.2008.10.033

Wang, X., Tan, C., Ye, M., Wang, X., Weng, W., Zhang, M., et al. (2020). Development and validation of a DNA repair gene signature for prognosis prediction in colon cancer. *J. Cancer* 11 (20), 5918–5928. doi:10.7150/jca.46328

Waters, C. A., Strande, N. T., Wyatt, D. W., Pryor, J. M., and Ramsden, D. A. (2014). Nonhomologous end joining: a good solution for bad ends. *DNA Repair* 17, 39–51. doi:10.1016/j.dnarep.2014.02.008

Wong, M. C. S., Goggins, W. B., Wang, H. H. X., Fung, F. D. H., Leung, C., Wong, S. Y. S., et al. (2016). Global incidence and mortality for prostate cancer: analysis of temporal patterns and trends in 36 countries. *Eur. Urol.* 70 (5), 862–874. doi:10.1016/j.eururo.2016.05.043

Yang, S.-K., Hong, M., Baek, J., Choi, H., Zhao, W., Jung, Y., et al. (2014). A common missense variant in NUDT15 confers susceptibility to thiopurine-induced leukopenia. *Nat. Genet.* 46 (9), 1017–1020. doi:10.1038/ng.3060

Yu, Y., Cai, J.-P., Tu, B., Wu, L., Zhao, Y., Liu, X., et al. (2009). Proliferating cell nuclear antigen is protected from degradation by forming a complex with MutT Homolog2. *J. Biol. Chem.* 284 (29), 19310–19320. doi:10.1074/jbc.M109.015289

Zhu, Y., Zhou, C., and He, Q. (2019). High miR-139-3p expression predicts a better prognosis for hepatocellular carcinoma: a pooled analysis. *J. Int. Med. Res.* 47 (1), 383–390. doi:10.1177/0300060518802727

Conflict of Interest: The authors declare that the research was conducted in the absence of any commercial or financial relationships that could be construed as a potential conflict of interest.

frontiers in Cell and Developmental Biology

REVIEW
published: 23 March 2021
doi: 10.3389/fcell.2021.633305

Cell Metabolism and DNA Repair Pathways: Implications for Cancer Therapy

*Thais Sobanski[1], Maddison Rose[1], Amila Suraweera[1], Kenneth O'Byrne[1,2], Derek J. Richard[1] and Emma Bolderson[1,2]**

[1] Cancer and Ageing Research Program, Centre for Genomics and Personalised Health, Translational Research Institute (TRI), Queensland University of Technology (QUT), Brisbane, QLD, Australia, [2] Princess Alexandra Hospital, Brisbane, QLD, Australia

DNA repair and metabolic pathways are vital to maintain cellular homeostasis in normal human cells. Both of these pathways, however, undergo extensive changes during tumorigenesis, including modifications that promote rapid growth, genetic heterogeneity, and survival. While these two areas of research have remained relatively distinct, there is growing evidence that the pathways are interdependent and intrinsically linked. Therapeutic interventions that target metabolism or DNA repair systems have entered clinical practice in recent years, highlighting the potential of targeting these pathways in cancer. Further exploration of the links between metabolic and DNA repair pathways may open new therapeutic avenues in the future. Here, we discuss the dependence of DNA repair processes upon cellular metabolism; including the production of nucleotides required for repair, the necessity of metabolic pathways for the chromatin remodeling required for DNA repair, and the ways in which metabolism itself can induce and prevent DNA damage. We will also discuss the roles of metabolic proteins in DNA repair and, conversely, how DNA repair proteins can impact upon cell metabolism. Finally, we will discuss how further research may open therapeutic avenues in the treatment of cancer.

Keywords: warburg effect, tumor metabolic reprogramming, homologous recombination, non-homologous end-joining, DNA repair, glycolysis, cell metabolism

OPEN ACCESS

Edited by:
Cesare Indiveri, University of Calabria, Italy

Reviewed by:
William K. K. Wu, Chinese University of Hong Kong, China
Waldemar Wagner, Institute for Medical Biology (PAN), Poland

***Correspondence:**
Emma Bolderson
Emma.bolderson@qut.edu.au

Specialty section:
This article was submitted to Cellular Biochemistry, a section of the journal Frontiers in Cell and Developmental Biology

Received: *25 November 2020*
Accepted: *19 February 2021*
Published: *23 March 2021*

Citation:
Sobanski T, Rose M, Suraweera A, O'Byrne K, Richard DJ and Bolderson E (2021) Cell Metabolism and DNA Repair Pathways: Implications for Cancer Therapy. Front. Cell Dev. Biol. 9:633305. doi: 10.3389/fcell.2021.633305

INTRODUCTION

DNA repair and metabolic pathways are vital to maintain cellular homeostasis. Under normal cellular conditions, DNA repair proteins can maintain genomic stability following exposure to exogenous and endogenous genotoxic insults. When growing in normal physiological conditions, cells predominately rely on the TCA cycle to generate ATP and other essential precursors for cellular processes. However, it has been well established that tumor cells are more likely to generate energy via glycolysis and hyperactivate their DNA damage response pathways, both of which

Abbreviations: ACLY, ATP-citrate lyase; ATM, ataxia telangiectasia mutated; DDR, DNA damage response; DNA-PK, DNA-dependent kinases; 2DG, 2-Deoxy-D-glucose; FDG-PET, ^{18}F-deoxyglucose-positron emission tomography; FH, fumarate hydratase/fumarase; FLT3, FMS-like tyrosine kinase 3; GLUT4, glucose transporter 4; GS, glutamine synthetase; G6P, glucose-6-phosphate; G6PD, glucose-6-phosphate dehydrogenase; HK2, hexokinase 2; PFKB3, 6-phosphofructo-2-kinase/fructose-2,6-biphosphatase 3; PGAM, phosphoglycerate mutase enzyme; PKM2, pyruvate kinase M2; TCA, tricarboxylic acid cycle.

promote the uncontrolled proliferative, survival and cellular growth pathways (Warburg, 1925). It was initially proposed that these two mechanisms operate independently within the cell; however, recent studies suggest a link between DNA repair and glycolysis. For instance, several independent studies have suggested novel roles for glycolytic proteins in DNA repair pathways, largely based on the observation that several glycolytic proteins, including Hexokinase II, Fumarase and ATP-citrate lyase (ACLY), migrate to the nucleus following exposure to genomic stress (van Vugt, 2017; Ohba et al., 2020; Hitosugi et al., 2012; Yuan et al., 2010). Several studies have also suggested glycolysis may be involved in maintaining genome stability, given that the glycolytic pathway provides metabolites which play an essential role in DNA metabolism. For example, the pentose phosphate pathway (PPP) utilizes the glycolysis intermediate, glucose-6-phosphate, to ultimately enable the biosynthesis of nucleotides via the generation of ribose-5-phosphate. Despite this, the interaction between DNA repair pathways and glycolysis remains unclear. Metabolic products from glycolysis, such as L- and D-lactate also play a role in DNA repair by decreasing chromatin compaction and subsequently increasing transcription of key genes involved in DNA DSB (double-strand break) repair (Wagner et al., 2015). Here, we will review the peer-reviewed evidence linking metabolism and DNA repair and how these processes may lead to radio- and chemo-resistance in tumor cells.

The Warburg Effect and Tumor Metabolic Reprogramming

High glucose intake is a characteristic shared amongst most solid tumors, and this phenomenon was first described in 1920 by Otto Warburg (Warburg et al., 1927). This observation, referred to as the Warburg effect, describes how cancer cells shift their predominate metabolic pathway from oxidative phosphorylation to anaerobic glycolysis, consequently producing high levels of lactic acid via fermentation (Warburg et al., 1927; Warburg, 1956). Recently, studies have demonstrated that elevated lactic acid production may induce resistance to major anti-cancer therapies, including radiation and chemotherapy, via numerous mechanisms. Furthermore, the upregulated production of lactic acid contributes to the development of an acidic tumor microenvironment, which has been associated with increased metastatic capacity and growth rate in a subset of aggressive tumors (Turkcan et al., 2019).

In the early studies of Warburg's effect, it was thought that cancer cells experience mitochondrial dysfunction via the "irreversible injuring of respiration," as cancer cells downregulate oxidative phosphorylation during the tricarboxylic acid cycle (TCA, also known as the Krebs cycle) (Warburg, 1956). However, subsequent investigations of mitochondrial functionality in tumor cells revealed that the majority of tumor cells possess functional mitochondria, and can still undergo oxidative phosphorylation (Zong et al., 2016). This led to speculation as to why cancer cells with functional mitochondria preferentially convert excess pyruvate to lactate, instead of utilizing oxidative phosphorylation to more efficiently produce ATP.

As altered metabolic features are observed commonly across many cancer subtypes, reprogrammed metabolism is considered one of Pavlova and Thompson's hallmarks of cancer (Pavlova and Thompson, 2016). For example, increased glucose uptake has been observed in a variety of tumor contexts and has been shown to negatively correlate with tumor prognostic markers and be involved in chemo- and radio-resistance mechanisms. This has been clinically exploited using ^{18}F-deoxyglucose-positron emission tomography (FDG-PET) based imaging, where a radioactive fluorine-labeled glucose analog it utilized to diagnose and stage tumor progression (Spermon et al., 2002).

DNA Repair Pathways and Their Relationship to Tumor Therapies

In tumor cells that undergo metabolic reprogramming, there is an observable increase in the activation of the DNA damage response pathways, which subsequently trigger nucleotide synthesis and anabolic glucose metabolism (Tong et al., 2009). DNA damage response pathways are highly active in tumor cells, subsequently promoting their rapid growth and survival. The DNA damage response consists of several DNA repair pathways, and each pathway represents a specific mechanism to repair a specific type of DNA damage. The initiation and progression of repair pathways is considered a spatiotemporally regulated process in which proteins move toward DNA damage sites, following the remodeling of the chromatin (van Attikum and Gasser, 2009; Gospodinov and Herceg, 2013). DNA damage may be induced by several endogenous sources such as DNA double-strand breaks and oxidative stress induced by reactive oxygen species, resulting from cellular metabolism. DNA damage may also result from exogenous sources, for example nucleotide damage from UV light or oxidative damage and DNA strand breaks caused by ionizing radiation (Jackson and Bartek, 2009; Tubbs and Nussenzweig, 2017). In order to maintain the integrity of genome, in human cells there are several types of DNA repair processes, classified into five major pathways including base excision repair (BER), nucleotide excision repair (NER), mismatch repair (MMR), non-homologous end-joining (NHEJ), and homology-directed repair (HDR) (Kalluri, 2016; Roos et al., 2016; Chatterjee and Walker, 2017). In addition to having a critical role in maintenance of genome integrity, alterations in the expression, and function of DNA repair proteins are a major mediator of tumor responses to chemo- and radiotherapy, which commonly function by inducing DNA damage in tumor cells. Here, we will briefly discuss the relevance of each repair pathway on tumor sensitivity to chemo- and radiotherapies, but further detail can be found in the following review (Minchom et al., 2018).

In terms of chemo- and radiotherapy, DSB repair via NHEJ and HDR is an important consideration, since many therapies, including radiotherapy, topoisomerase inhibitors, such as doxorubicin, and PARP inhibitors, induce DNA DSBs. Therefore, the defective functioning of DSB repair pathways can significantly influence the tumor response to these therapies. For example mutations or decreased expression of the Breast Cancer Associated 1 and 2 (BRCA1 and BRCA2) proteins can lead to

defects in the HDR of DNA DSBs, sensitizing tumor cells to PARP inhibitors and radiotherapy that induce lesions that require HDR for repair (Rose et al., 2020). Conversely, upregulation of DNA DSB repair proteins in the NHEJ pathway can also induce resistance to these DSB-inducing therapies, due to the tumor cells ability to rapidly repair DNA damage and therefore avoid induction of cell death (Jensen and Rothenberg, 2020). BER removes and repairs damaged bases within the DNA. The capacity of cells to perform BER is also of relevance to tumor therapy as the anti-tumor agents temozolomide, pemetrexed, or floxuridine induce DNA lesions of N7mG, uracil, or 5-FU, respectively, all of which can be recognized and repaired by the BER pathway (Storr et al., 2011). Upregulation or down regulation of the BER pathway can lead to resistance or sensitivity, respectively, to these agents. Several inhibitors of the BER pathway are also in development (Grundy et al., 2020).

In the process of MMR, proteins recognize mismatched bases in DNA which arise from processes such as replication. MMR proteins identify, excise and replace these mismatched bases with the correct pairing base. Mutations in the MMR genes Mlh1 and Msh2 are associated with the human colon cancer-prone syndrome, Lynch Syndrome [also known as hereditary non-polyposis colorectal cancer (HNPCC)], but MMR genes are also frequently mutated in other cancers. Tumors with mutated Mlh1 and Msh2 in colon tumors were historically targeted with methotrexate, which leads to the accumulation of oxidative damage. However, due to the high number of somatic mutations found in MMR-deficient tumors, which can contribute to stimulation of the immune system, immunotherapy is showing potential to become the preferred therapy for tumors with defects in MMR (Le et al., 2015).

The nucleotide excision repair pathway recognizes damaged nucleotides including pyrimidine dimers, intrastrand crosslinks, and bulky adducts. Alkylating agents, such as platinum compounds like cisplatin are commonly used to treat many types of cancers and induce intrastrand crosslinks within the DNA, activating the NER pathway. Expression of the NER proteins, including ERCC1 are correlated with sensitivity to platinum agents in multiple tumor types due to an inability to resolve DNA crosslinks (Arora et al., 2010).

Therefore, although alterations in DNA repair pathways contribute to the development of tumors, and can lead to resistance to tumor therapies, they also hold huge potential as the next generation targets for the treatment of many cancer types. Due to the metabolic reprogramming in tumor cells, it is likely that targeting cellular metabolism may also be advantageous. The current literature supporting a link between metabolic reprogramming and the DNA damage response pathways will be further explored below.

The Requirement of the Pentose Phosphate Pathway (PPP) and G6PD Protein in DNA Damage Prevention and DNA Repair Processes

The pentose phosphate pathway is a parallel pathway to glycolysis and generates pentoses and NADPH, together with ribose-5-phosphate, a precursor for nucleotide synthesis (Patra and Hay, 2014). The PPP is upregulated in several tumor types and regulates various functions that promote tumor growth, including DNA metabolism and cell proliferation (Mori-Iwamoto et al., 2007; Chan et al., 2013; Catanzaro et al., 2015). In non-carcinogenic cells, the PPP pathway is responsible for generating the bulk of nucleotides through salvage pathways, which recycle existing nucleosides and nucleobases. Although, a portion of nucleotide synthesis also takes place via *de novo* synthesis pathways to produce purine and pyrimidine rings to sustain rapid DNA metabolism (Mori-Iwamoto et al., 2007). Supporting this, highly proliferative cells, such as tumor cells, are more likely to use *de novo* nucleotide synthesis pathways over the salvage pathways to maintain the increased production of nucleotides and other macromolecules. The *de novo* nucleotide synthesis pathways maintain nucleic acid and protein synthesis, along with other cellular activities, to meet the high metabolic requirements of cancer cells (Kilstrup et al., 2005; Villa et al., 2019).

The PPP pathway consists of an oxidative and a non-oxidative phase: the oxidative phase generates NADPH that is used for reductive biosynthetic reactions, such as fatty acid synthesis and the prevention of oxidative stress by detoxification of oxygen species (ROS). The non-oxidative arms of the PPP produce ribose-5-phosphatase, which is then further metabolized for the production of nucleotides (**Figure 1**). The PPP pathway occurs in parallel to glycolysis, diverging from glycolysis at glucose-6-phosphate (G6P), which is involved in the oxidation of glucose to provide the building blocks for anabolic pathways (D'Urso et al., 1983). Alternatively, under conditions of high reductive demand cancer cells have the capacity to divert glucose-6-phosphate dehydrogenase (G6PD) into the PPP pathway to maintain the constant generation of NADPH and nucleotides (Bokun et al., 1987). Downregulation of NADPH production renders tumor cells more susceptible to oxidative DNA damage, as NADPH functions as a major cofactor for glutathione (GS) and cytochrome p450 reductase, which is essential for maintaining the cellular redox balance.

Cells lacking G6PD are more sensitive to oxidative damage and therefore have increased sensitivity to ionizing radiation (IR), which in addition to inducing DNA strand breaks, also causes oxidative damage (Tuttle et al., 2000). G6PD is essential in sustaining a balanced pool of nucleotides in response to DNA damage and promotes PPP-mediated nucleotide synthesis. Furthermore, a study showed that Ataxia Telangiectasia Mutated (ATM), a key DNA damage protein, activates the PPP pathway through G6PD to promote antioxidant defense mechanisms and DNA repair activity via nucleotide production under stressed conditions (Cosentino et al., 2011). This suggests that G6PD activity is likely to also be required for the repair of DNA damage and maintaining DNA integrity (Zhang et al., 2016).

The wild type tumor suppressor protein, p53, has also been shown to downregulate the PPP via directly reducing G6PD activity (Jiang et al., 2011). However, inhibition of ATM is also known to downregulate p53 expression, subsequently promoting the constitutive upregulation of the PPP via G6PD upregulation too, consequently restoring dNTP levels in cancer

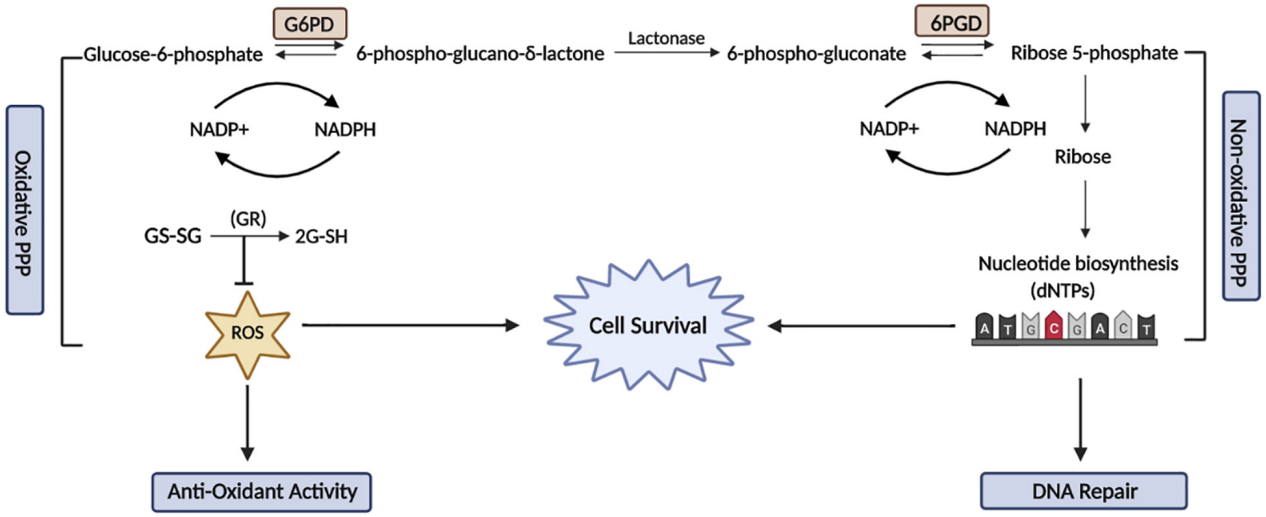

FIGURE 1 | The relationship between the Pentose Phosphate Pathway and DNA damage and repair. The PPP comprises of two phases known as the oxidative and non-oxidative phases. The oxidative phase is responsible for the conversion of glucose-6-phosphate to ribose-5-phosphate, which releases NADPH to maintain the cellular redox balance and also reduces oxidative damage. In the non-oxidative phase, the activity of a key enzyme, G6PD is stimulated by ATM to promote the production of NADPH and nucleotide synthesis. The activation of G6PD is essential to maintain a reduced cellular environment and also synthesises nucleotide precursors for DNA damage repair. This figure was created with BioRender.com.

cells and facilitating cellular proliferation (Aird et al., 2015). G6PD is the rate-limiting enzyme that regulates oxidative PPP and therefore controls the flux of dNTP production required for DNA replication and maintaining genome stability. As such, G6PD is also required to suppress dNTP-enhanced mutagenesis. Overall, the altered cellular metabolic flux induced by G6PD during metabolic reprogramming enables the more rapid repair of DNA lesions, promoting resistance to conventional therapies such as radiation, and cellular growth advantages (Leick and Levis, 2017).

Activating mutations of FMS-like tyrosine kinase 3 (FLT3) have been shown to drive the initiation and progression of acute myeloid leukemia (AML). As such, inhibition of FLT3 was suggested to be a promising treatment for AML; however, targeting FLT3 as a monotherapy did not achieve long term remission (Leick and Levis, 2017). In contrast, a genome-wide RNA interference (RNAi)-based screen found that inhibition of the ATM/G6PD pathway in combination with FLT3 inhibition was synthetically lethal (Gregory et al., 2016). Thus, the simultaneous targeting of ATM-mediated G6PD regulation and inhibition of up-regulated nucleotide synthesis following chemotherapy induced stress may offer a new treatment option by decreasing DNA repair capacity. Following this, the targeting of key enzymes that regulate PPP also potentiated the effect of conventional therapies to selectively suppress cancer cell growth. For example, treatment with the glycolysis inhibitors 2-Deoxy-D-glucose (2DG) and 6-aminonicotinamide (6AN) has been shown to increase radio-sensitivity in squamous carcinoma cell lines (Khaitan et al., 2006; Sharma et al., 2012). In addition, this suggests that the inhibition of PPP or G6PD in combination with DNA damage inducing chemotherapies, such as 5-fluorouracil (5-FU) and doxorubicin, may restore chemosensitivity in cancer cells.

ATM and DNA-PK Kinases Play a Key Role in Cellular Energy Sensing

Ataxia telangiectasia mutated and DNA-dependent kinases (DNA-PK) are key proteins that recognize DNA damage and initiate DNA damage repair signaling (Mirzayans et al., 2006; Marechal and Zou, 2013). Upon activation by DNA-damage, these kinases generate a cascade of phosphorylation events that regulate the recruitment and activity of many downstream effector proteins to repair DNA double-strand breaks (DSBs) (Cosentino et al., 2011; Aird et al., 2015). ATM is generally considered to form a homodimer, while the active DNA-PK complex is comprised of the DNA-PK catalytic subunit bound to the Ku70/80 heterodimer. Several studies have shown that both DNA-PK and ATM are also involved in cellular metabolism rewiring after DNA damage for energy supply by activating of glucose transporter (GLUT4) thought AKT, maintenance of mitochondrial homeostasis and increased nucleotide production for DNA metabolism (**Figure 2**). This is particularly evident in individuals with Ataxia-Telangiectasia syndrome (A-T), which results from mutations in the ATM gene. These individuals exhibit alterations in cellular metabolism, including the dysfunction of enzymes involved in glucose metabolism and mitochondrial function (Sharma et al., 2014; Volkow et al., 2014).

Besides its primary function in the recognition of DNA damage, ATM functions as a metabolic stress sensor, identifying reductions in the energy levels of tumor cells, subsequently promoting increased PPP activity, which can lead to increased

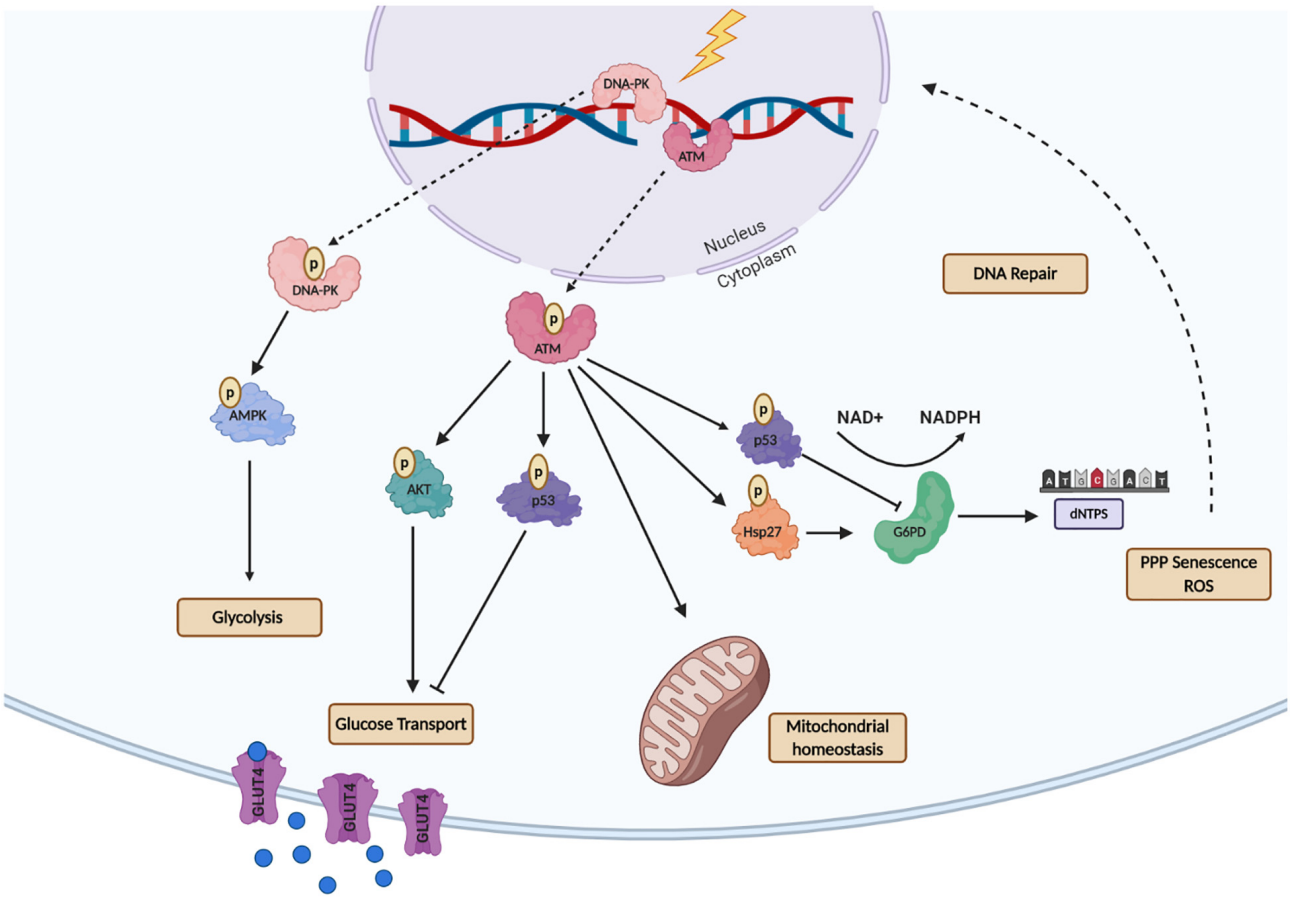

FIGURE 2 | A schematic representation of the Ataxia-Telangiectasia Mutated- (ATM) and DNA-Dependent Kinase- (DNA-PK) mediated regulation of metabolic processes after DNA Damage. ATM activates multiple downstream proteins regulating cell cycle arrest, DNA repair and cellular metabolism. ATM activates the tumor suppressor p53 which decreases GLUT recruitment, glycolysis, and dNTP production. ATM non-canonical function is essential for repairing mitochondrial genome defects to maintain mitochondrial homeostasis. For maintenance of energy production ATM activates AKT to promote glucose recruitment to the nucleus via GLUT4-mediated transport. ATM also activates G6PD though Hsp27, as an alternative mechanism to produce nucleotides for DNA metabolism. DNA-PK following energy depletion or metabolic rewiring promotes glycolysis through AMP signaling. This figure was created with BioRender.com.

cancer cell survival and resistance to conventional therapies (Krüger and Ralser, 2011). Additionally, there is a growing quantity of evidence showing that ATM also regulates the translocation of glucose transporter 4 (GLUT4), which in part explains why patients with A-T syndrome tend to present high incidences of type 2 diabetes mellitus (Halaby et al., 2008). It is known that cytoplasmic ATM is an insulin-responsive protein that activates AKT following insulin treatment, and inhibition of ATM leads to downregulation of AKT activity that in turn downregulates the GLUT4 glucose transporter protein (Halaby et al., 2008). A recent study found that loss of ATM-mediated p53 Ser18 (murine Ser15) phosphorylation led to increased metabolic stress and insulin resistance (Armata et al., 2010). Additionally, ATM was also shown to enhance glycolysis in breast cancer cells via GLUT1-phosphorylation and PKM2 up-regulation, increasing lactate production. High levels of lactate were found to promote tumor invasion through lactate-mediated metabolic coupling (Sun et al., 2019). These recent studies suggest that ATM is essential for glycolysis homeostasis as it regulates key metabolic proteins that are responsible for the maintenance of glucose levels such as glucose transporters.

DNA-dependent kinases is best known for recognizing DSBs and initiating DNA repair responses by activation of the NHEJ pathway. DNA-PK is an abundant, cytoplasmatic protein that migrates to the nucleus after DNA damage (Yang et al., 2014). There is also growing evidence indicating that DNA-PK may function to regulate metabolic homeostasis (Weterings and Chen, 2008; Lieber, 2010). Similar to ATM, DNA-PK also functions as a metabolic stress sensor and regulates AMPK (AMP-activated protein kinase) in response to energy depletion or metabolic stress in mammalian cells. AMPK is an essential protein that recognizes when energy production is low. It has been shown that inhibition of the DNA-PK catalytic subunit, decreases AMPK activity in response to energy deprivation.

Cell starvation leads to the phosphorylation of AMPKα (Thr172) and acetyl-CoA carboxylase (ACC). However, the inhibition of DNA-PKcs inhibits AMPK phosphorylation, thereby disrupting the sensing of glucose metabolism by AMPK.

In addition, it was shown that DNA-PKcs directly interacts with the energy monitoring regulatory subunit of AMPK (Amatya et al., 2012). This finding suggests that DNA-PK is essential for activating AMPK under low energy levels as a result of glucose deprivation in mammalian cells. Similarly, another study confirmed that DNA-PKcs is a positive regulator of AMPK activity and was found to phosphorylate two residues on AMPKγ (S192 and T284) (Puustinen et al., 2020). Conversely, another study showed that an aging-related increase in DNA-PKcs activity led to decreased AMPK activity, via phosphorylation-mediated inhibition of Hsp90 chaperone activity toward AMPKαα2 (Park et al., 2017). It is also possible that the interaction between DNA-PKcs and AMPK may depend on cellular context as DNA-PKcs itself is regulated by the cellular metabolic state and may decline as individuals' age.

Autophagy is the process by which damaged proteins or organelles are degraded by the lysosome, this provides a mechanism to recycle cellular components providing macromolecular precursors and energy for cellular metabolism. Autophagy is generally classified into five defined steps: initiation, vesicle nucleation, vesicle elongation, vesicle fusion and cargo degradation. The regulation of autophagy by metabolic proteins and vice versa have been well charactered but there is also mounting evidence that DNA repair is also regulated by autophagy [reviewed in Hewitt and Korolchuk (2017)]. Some studies suggest that DNA repair is inhibited by autophagy, but other studies propose that autophagy promotes DNA repair (Bae and Guan, 2011; Liu et al., 2015). In order to explain this discrepancy, it has been hypothesized that following low levels of DNA damage, autophagy may promote DNA repair, while severe DNA damage may lead to autophagy-dependent degradation of DNA repair proteins to promote apoptosis (Guo and Ying, 2020). Autophagy has been shown to be initiated by AMPK activation and/or inhibition of the metabolic sensor Mammalian Target of Rapamycin Complex 1 (mTORC1), establishing another link between metabolism and DNA repair pathways (Kim et al., 2011). As discussed above the DNA-PK-dependent regulation of AMPK may also provide a feedback loop to regulate autophagy in the context of DNA repair (Puustinen et al., 2020).

Key Metabolic Enzymes That Play a Role in DNA Repair and Resistance to Chemo- and Radiotherapies (Summarized in Table 1)

Phosphoglycerate Mutase Enzyme (PGAM)

The Phosphoglycerate mutase 1 (PGAM1) is a key glycolytic enzyme that coordinates different metabolic process including glycolysis, PPP, and serine biosynthesis in cancer cells. As a result of its dynamic role in metabolic coordination, PGAM1 is overexpressed in several cancer types, including gliomas, oral carcinomas and pancreatic cancers (Liu et al., 2008, 2018; Zhang et al., 2017). For example, PGAM1 activity directly regulates the PPP and the resulting production of nucleotides, promoting cancer cell proliferation and tumor resistance to conventional therapies. Indirectly, PGAM1 contributes to DNA repair activity in cancer cells by the upregulation of glycolysis and/or nucleotide synthesis (Ohba et al., 2020). However, it was also found that PGAM1 plays a direct role in DNA repair as its activity was required for the repair of DNA double-strand breaks via homologous recombination (HR). Its role in HR was shown to be through regulating the stability of CTBP-interacting protein (CtIP), which is essential for the recruitment of Rad51 to sites of damage to facilitate filament formation (Qu et al., 2017). Complementary studies in gliomas cells demonstrated that depletion of PGAM1 also led to defective DNA damage signaling, including ATM autophosphorylation and phosphorylation of its downstream substrates. This led to disrupted DSB repair and subsequent sensitivity to IR, suggesting that PGAM1 may be a potential therapeutic target in gliomas (Ohba et al., 2020).

Fumarase/Fumarate Hydratase (FH)

Under normal cellular conditions FH localizes mainly in the cellular cytosol and mitochondria (Kornberg and Krebs, 1957). A study in yeast demonstrated that following the induction of DNA damage, FH moves to the nucleus and functions as a DNA repair protein to promote the repair of DSBs (Yogev et al., 2010). In human cells, FH plays a similar role in DNA repair and was found to be a substrate of DNA-PK, which phosphorylates FH at Threonine 236. This stimulates the local generation of fumarate near DSBs, which inhibits the activity of the histone demethylase, KDM2B (Jiang et al., 2015). Subsequently, increasing the level of Histone H3 lysine 36 dimethylation which has been shown to facilitate the recruitment of DNA-PK to DSB sites and subsequently facilitate NHEJ activity (Fnu et al., 2011). A recently study showed that depletion of fumarase prolonged the interaction of Mre11 at sites of DSBs, delaying the progression of the HR pathway (Leshets et al., 2018). In addition, increased FH expression also disrupts HR by the inhibition of two key lysine demethylases (KDM4A and KDM4B) in Leiomyomatosis Renal Cell Cancer (HLRCC). This syndrome is classified as a familial DNA repair deficiency syndrome, as these patients carry a germline mutation in FH leading to defective responses to DNA damage and results in a higher predisposition for cancer development (Sulkowski et al., 2018).

Pyruvate Kinase M2 (PKM2)

Pyruvate kinase is an enzyme that converts phosphoenolpyruvate and ADP into pyruvate to generate ATP, and its activity is essential for the maintenance of glucose homeostasis. Pyruvate kinase M2 (PKM2) is highly expressed in cancer cells and a master regulator of tumor metabolic reprogramming (Wu et al., 2016; Zheng et al., 2018). Under normal conditions PKM2 is an abundant cytosolic protein that upon certain cellular stress, such as ultraviolet light (UV) or H_2O_2, migrates to the nucleus (Stetak et al., 2007). The migration of PKM2 to the nucleus has been associated with its non-metabolic functions, as PKM2 was found to phosphorylate several nuclear proteins, including histone H3 (Yang et al., 2014). It was also reported that nuclear PKM2 interacts with histone H2AX after DNA

TABLE 1 | The effects of metabolic proteins and metabolites on DNA repair.

Metabolic protein	Canonical function	Non-canonical function	Inhibitor	Clinical stage	Observations	DNA repair pathways	References
PGAM phosphoglycerate mutase enzyme	Catalyzes the conversion of 3-phosphoglycerate (3PG) to (2PG)	Maintains the stability of CTBP-interacting protein (CtIP) Activates DDR pathway via the regulation of WIP1 activity	PGM1-0004A	Preclinical data	Reduces tumor growth *in vitro*/vivo	HR	Hatzivassiliou et al., 2005; Wellen et al., 2009; Keller et al., 2014; Koerner et al., 2017
PKM2 pyruvate kinase M2	Pyruvate production	Binds to the promoter of HIF increasing its transcriptional activity Promotes DSB repair as ATM phosphorylates PKM2;	TLN-232 (Thallion)	Preclinical data	Decreases aerobic glycolysis in some tumor models	HR	Hatzivassiliou et al., 2005; Wellen et al., 2009; Keller et al., 2014; Koerner et al., 2017
FH fumarate hydratase/fumarase	Catalyzes the conversion of fumarate to malate	Produces fumarate inhibiting the demethylase KDM2B increasing H3 methylation Phosphorylates DNA-PK	Miconazole nitrate (MN)	Preclinical data	Reduces DNA repair activity Enhances the cytotoxicity of cisplatin (CDDP)	NHEJ	Hatzivassiliou et al., 2005; Wellen et al., 2009; Keller et al., 2014; Koerner et al., 2017
ACLY ATP-citrate lyase	Production of acetyl-CoA	Production of ACLY increases histone acetylation, promoting DNA repair Increases the expression of genes promoting cell cycle progression and cell proliferation	SB-204990 (Furan carboxylate derivatives)	Preclinical data	Anti-proliferative activity in several cancer cell lines Tumor growth inhibition	HR	Seltzer et al., 2010; Wang et al., 2010; Tardito et al., 2015; Fu et al., 2019
GS glutamine synthetase	Catalyzes the conversion of glutamate and ammonia into glutamine	Enhances DNA repair via *de novo* nucleotide synthesis	Glutaminase inhibitor (CB839)	Clinical data	Sensitizes malignant cells expressing mutant IDH1 to GLS1-targeting agents Studies in Leukemia and solid tumors	HR	Seltzer et al., 2010; Wang et al., 2010; Tardito et al., 2015; Fu et al., 2019
PFKB3 6-phosphofructo-2-kinase/fructose-2,6-Biphosphatase 3	PFKB catalyzes the synthesis of F6P to F2,6BP	Nuclear PFKB3 drives cancer cell proliferation Promotes recruitment of HR factors	KAN0438757	Preclinical data	Induces radiosensitivity in transformed cells	HR	Yalcin et al., 2009; Gustafsson et al., 2018
L/D-lactate	Cellular energy source	Promotes histone hyperacetylation and decreased chromatin compactness leading to enhanced DNA repair activity Induces the expression of genes involved in DNA repair, such as upregulation of DNA-PK	1-(phenylseleno)-4 (trifluoromethyl) benzene (PSTMB) Galloflavin	Preclinical data	Inhibits the cellular growth of several tumor cell lines; Blocks aerobic glycolysis and induces cell death by triggering apoptosis	HR and NHEJ	Hunt et al., 2007; Manerba et al., 2012; Sonveaux et al., 2012; Kim et al., 2019

damage, and that PKM2 could directly phosphorylate H2AX on serine 139, one of the first phosphorylation events following DNA damage. Furthermore, replacement of wild type PKM2 with a kinase dead form led to increased chromosomal aberrations following DNA damage. Collectively, this reveals PKM2 as a novel modulator for genomic instability in tumor cells (Xia et al., 2017). As part of its non-metabolic activity it was also recently uncovered that PKM2 directly promotes DSB repair, as ATM phosphorylates PKM2 at Threonine 328 (T328) to induce the nuclear accumulation of PKM2 (Matsuoka et al., 2007). This ATM-mediated phosphorylation of PKM2 was shown to be required for efficient homologous recombination (HR) through the recruitment of CtIP at the site of DSBs. Additionally, the disruption of the ATM-PKM2-CtIP axis interaction was shown to sensitize tumor cells to a variety of DNA-damaging agents, including PARP inhibitors (Sizemore et al., 2018).

ATP-Citrate Lyase (ACLY)

ATP-citrate lyase is a nuclear-cytoplasmic enzyme that utilizes acetyl-CoA to generate citrate, and plays a crucial role in conserving the global histone acetylation in mammalian cells (Wellen et al., 2009). ACLY deficiency has been shown to result in defective DSB repair, due to the depletion of acetyl-CoA pools and reduction in acetylated histones at sites of DSBs (Kumari et al., 2019). Supporting this Sivanand et al. showed that nuclear acetyl-CoA played a role in HR and following DNA damage ACLY was phosphorylated at Serine 455, in an ATM- and AKT-dependent manner. Additionally, ACLY

phosphorylation and nuclear localization were necessary to promote BRCA1 recruitment in order for HR to occur (Sivanand et al., 2017). Thus, acetyl-CoA production by ACLY is critical for the repair of DNA DSBs.

Glutamine Synthetase (GS)

Glutamine synthetase (GS) is an enzyme that catalyzes the conversion of glutamate and ammonia into glutamine. Transcriptome analyses revealed that GS is responsible for the metabolic reprogramming that occurs in tumor cells, as GS activity was shown to enhance DNA repair via *de novo* nucleotide synthesis (Kalluri, 2016). Further analyses revealed that knockdown of GS delayed DNA repair due to impaired nucleotide metabolism, which led to increased radio-sensitivity. HR was impaired in GS depleted cells further supporting a role for GS in DSB repair. Collectively, these findings suggest glutamine synthase plays a similar role to G6PD in DNA repair, as its upregulation increases nucleotide synthesis leading increased DSB repair capacity.

The Role of Metabolic Reprogramming in Tumor Cell Chemo- and Radio-Resistance

Radiotherapy remains a key anti-cancer therapy, with over 50% of patients undergoing radiation treatment as a monotherapy or in combination with other therapies (Kalluri, 2016). However, a significant proportion of patients experience resistance to conventional radiotherapy. Studies have demonstrated that the likelihood of radio-resistance is influenced by several factors, including metabolic changes and the upregulation of DNA repair pathways (Dwarkanath et al., 2001; Schwarz et al., 2008). Metabolic reprogramming may enable tumor cells to enhance nucleotide synthesis through the upregulation of the PPP, subsequently promoting resistance to traditional anti-cancer therapies (Zhao et al., 2016; Yin et al., 2017). Supporting this, several studies have shown that upregulation of metabolic enzymes or metabolic processes increases the activity of DNA repair pathways. For example, as a result of elevated glycolytic activity, some tumors generate a high level of lactate, which can promote cisplatin-resistance through increased DNA repair activity (Wagner et al., 2015). As previously discussed, several metabolic enzymes from glycolysis and PPP play a direct role in DNA repair pathways, and inhibition of key enzymes of both pathways not only inhibited cellular proliferation but also restored radio-sensitivity by decreasing DNA repair activity. The link between radio-resistance and altered metabolism is not fully understood but several studies suggest that decreasing the metabolic activity of the key enzymes involved in the PPP and glycolysis pathways could restore the sensitivity of resistant tumors to conventional therapies.

In ovarian cancer, three glycolytic enzymes, HK2, PFK, and PKM2, have been suggested to be promising targets due to their positive correlation with chemo- and radio-resistance via anti-apoptotic and cell survival mechanisms (Li et al., 2015; Zhang et al., 2018; Lin et al., 2019). There are four isoforms of PK; however, the PKM2 isoform is a key regulator of glycolysis in cancer cells and is thus the most prominent potential candidate for restoring sensitivity to therapies. Supporting this, the inhibition of PKM2 in cervical cancer cells leads to decreased cell viability, G2/M cell cycle arrest, and promotes apoptosis (Lin et al., 2019). Furthermore, inhibition of PKM2 may induce radio-sensitivity, as demonstrated by a study which found that PKM2 depletion decreases AKT and PDK1 phosphorylation to subsequently promote radio-sensitivity in NSCLCs (Yuan et al., 2016). Similar to LDHA, miR-133 overexpression inhibits the expression of PKM2, which restores the sensitivity of radio-resistant lung cancer cells, offering a potential new treatment option for these radio-resistant tumors (Liu et al., 2016).

Hexokinase 2 (HK2) is a key glycolytic enzyme that catalyzes the first essential step of glucose metabolism. Like many other glycolytic proteins, HK2 is highly expressed in several tumor types (Anderson et al., 2017; Wu et al., 2017). Similar to other metabolic proteins, inhibition of HK2 has been shown to increase radio-sensitivity in cancer cells (Vartanian et al., 2016). 2-deoxy-D-glucose (2-DG) is an inhibitor of glucose metabolism, that is phosphorylated by Hexokinase to produce 2-deoxyglucose-6-phosphate. The intracellular accumulation of this metabolite inhibits hexokinase activity and therefore ATP production via glycolysis. Significantly, the anti-proliferative effects of 2-DG have been demonstrated in numerous preclinical studies (Giammarioli et al., 2012; Zhang et al., 2015). 2-DG has also been shown to be an effective sensitizer in several tumor types, including gliomas and lung carcinomas (Dwarkanath et al., 2001; Singh et al., 2019). Additionally, combining 2-DG with chemotherapy has already shown promising results in its ability to restore the sensitivity of chemo-resistance cells. A recent study analyzed the effect of combination treatment with 2-DG and carboplatin chemotherapy in high stage and recurrent ovarian clear cell carcinoma (OCC), and found that 2-DG in combination with carboplatin and cisplatin chemotherapy increased efficacy in chemo-resistant ovarian tumor cell lines and patient-derived xenograft models (Zhang et al., 2015; Khan et al., 2020). Thus, the combination of 2-DG with both radio- and chemotherapy drugs improves tumor cell sensitivity; however, the underlying mechanism for the restoration of sensitivity to therapy remains largely unknown.

The glucose transporter GLUT1 is involved with the early steps of glucose uptake and metabolism. GLUT1 is overexpressed in many types of cancers and has been evaluated as a potential target for anti-cancer drugs (Wincewicz et al., 2010; Koch et al., 2015; Kim and Chang, 2019). Depletion of GLUT1 using small interfering RNA (siRNA) was shown to increase the radiosensitivity of laryngeal cancer cells and led to the downregulation of DNA repair. Similarly, restoration of radio-sensitivity was observed when antisense oligonucleotides (AS-ODNs) were used to inhibit GLUT1 activity in laryngeal carcinoma cells (Chan et al., 2004; Yan et al., 2013). In breast cancer, a synthetic inhibitor of GLUT1 known as WZB117, was demonstrated to radio-sensitize cancer by increasing the level of intracellular ROS, thereby inhibiting tumor growth (Zhao et al., 2016). Thus, inhibition of GLUT1 has therapeutic potential as an intervention to overcome cellular radio-resistance.

L-lactate is produced by glycolysis and is found to be expressed in high quantities in malignant tumors. High lactate levels have also been associated with resistance to clinical chemotherapeutics in numerous cancer subtypes. Recently, studies have shown that lactate can inhibit the activity of histone deacetylases (HDACs), which leads to changes in chromatin structure and transcription (Wagner et al., 2015, 2017). HDACs remove acetyl groups from histones, and their inhibition results in increased acetylation of histones, which are generally associated with a more open chromatin structure to promote transcription. This open chromatin state has also been suggested to increase accessibility of DNA repair proteins to sites of damage, in turn increasing the rates of DNA repair (Tamburini and Tyler, 2005). A study showed that lactate also modulates chromatin compaction in cervical cancer, leading to the up-regulation of DNA-PKcs (Wagner et al., 2015). Thus, the characteristic increase in lactate levels in tumor cells results in increased DNA repair activity, which has been shown to enhance radio-resistance in cervical carcinoma. Additionally, L/D-lactate was shown to increase the rate of γ-H2AX foci resolution after irradiation and induce cisplatin resistance, consistent with the up-regulation of DNA repair pathways (Wagner et al., 2015). Lactate dehydrogenase (LDHA) is a key metabolic protein found in almost all human tissues that is required for the conversion of pyruvate to lactic acid, playing an important role in the final steps of glycolysis. Increased expression of LDHA induces hypoxic environments that are associated with tumor metastases, poor overall survival, and radio-resistance in several tumor types, including prostate and bladder cancers (Koukourakis et al., 2009, 2014, 2016). Based on these findings, it can be suggested that the inhibition of LDHA activity may confer sensitivity in tumor cells to DNA damaging agents (Manerba et al., 2015). Supporting this, a soluble adenylate cyclase (sAC) that promotes the release of LDHA, led to the activation of the BRAF/ERK1/2 signaling pathway and consequently increased radio-resistance in prostate cancer cells (Flacke et al., 2013; Appukuttan et al., 2014). Treatment of prostate cancer cells with an LHDA-specific inhibitor, FX-11, reduced the activity of DNA repair proteins, improving cellular sensitivity to radiotherapy (Hao et al., 2016). Another study demonstrated that miR-34a overexpression inhibits LDHA and restored radio-sensitivity in hepatocellular carcinoma cells (Li et al., 2016). Based on these findings, it has been suggested that targeting LDHA via miR-34a may provide a mechanism to restore sensitivity to therapies in radio-resistant tumors (Li et al., 2016). Lactate influx and efflux is mediated by four members of the solute carrier 16a family Monocarboxylate transporters (MCT1-4). These proteins control the transport of lactate across the plasma membrane, effectively controlling lactate homeostasis. Given that high lactate levels confer chemo- and radioresistance, MCTs may also represent an effective mechanism to target lactate levels in tumor cells and increase sensitivity to DNA damaging agents (Halestrap, 2012).

CONCLUSION

Genomic instability and metabolic reprogramming are central components in cancer development and evolution. These changes in chromatin structure, DNA repair enzyme expression and mutation allow the cancer cells to develop genetic heterogeneity, which in turn can promote evolution and metastasis. The metabolic changes allow cancer cells to increase growth rates, adapt to the rapidly changing external environment and to reduce the reliance on oxygen. It has become increasingly apparent that these two processes do not exist in isolation, but instead are mutually dependent. This raises the notion that the cell must adapt more globally to small changes in metabolism. While the DNA damage signaling kinases regulate the metabolic state of the cell, the opposite is also true. This generates a regulatory loop that ensures that changes in one pathway have compensatory changes in the other pathways. It must be considered that this link, and the peer reviewed studies supporting the link, have predominantly occurred in cancer cell lines and studies. It is likely these studies sit at the extreme of changes that have occurred in genomic instability and metabolism, as these cells have adapted to a metabolic and genetic state that gives them a growth and survival advantage. Understanding how these processes function under normal physiological cell conditions and indeed how they may drive the process of aging and other age-related diseases needs to be further addressed. During the aging process, the DNA repair capacity of cells declines and also undergo metabolic changes induced by cellular and endocrine changes. Understanding, how these changes in metabolism and DNA repair capacity under the normal process of aging may shed further light on why cancers form in the first place. In cancer, further studies may also identify new therapeutic targets that can target both metabolism and DNA repair concurrently.

AUTHOR CONTRIBUTIONS

TS made the figures. All authors listed have made a substantial, direct and intellectual contribution to the work, and approved it for publication.

FUNDING

This work was supported by a Queensland Senior Clinical Research Fellowship (KO'B).

REFERENCES

Aird, K. M., Worth, A. J., Snyder, N. W., Lee, J. V., Sivanand, S., Liu, Q., et al. (2015). ATM couples replication stress and metabolic reprogramming during cellular senescence. *Cell Rep.* 11, 893–901. doi: 10.1016/j.celrep.2015.04.014

Amatya, P. N., Kim, H. B., Park, S. J., Youn, C. K., Hyun, J. W., Chang, I. Y., et al. (2012). A role of DNA-dependent protein kinase for the activation of AMP-activated protein kinase in response to glucose deprivation. *Biochim. Biophys. Acta* 1823, 2099–2108. doi: 10.1016/j.bbamcr.2012.08.022

Anderson, M., Marayati, R., Moffitt, R., and Yeh, J. J. (2017). Hexokinase 2 promotes tumor growth and metastasis by regulating lactate production in pancreatic cancer. *Oncotarget* 8, 56081–56094. doi: 10.18632/oncotarget.9760

Appukuttan, A., Flacke, J. P., Flacke, H., Posadowsky, A., Reusch, H. P., and Ladilov, Y. (2014). Inhibition of soluble adenylyl cyclase increases the radiosensitivity of prostate cancer cells. *Biochim. Biophys. Acta* 1842, 2656–2663. doi: 10.1016/j.bbadis.2014.09.008

Armata, H. L., Golebiowski, D., Jung, D. Y., Ko, H. J., Kim, J. K., and Sluss, H. K. (2010). Requirement of the ATM/p53 tumor suppressor pathway for glucose homeostasis. *Mol. Cell Biol.* 30, 5787–5794. doi: 10.1128/MCB.00347-10

Arora, S., Kothandapani, A., Tillison, K., Kalman-Maltese, V., and Patrick, S. M. (2010). Downregulation of XPF-ERCC1 Enhances Cisplatin Efficacy in Cancer Cells. *DNA Repair* 2010, 010. doi: 10.1016/j.dnarep.2010.03.010

van Attikum, H., and Gasser, S. M. (2009). Crosstalk between Histone Modifications during the DNA Damage Response. *Trends Cell Biol.* 2009:001. doi: 10.1016/j.tcb.2009.03.001

Bae, H., and Guan, J. L. (2011). Suppression of Autophagy by FIP200 Deletion Impairs DNA Damage Repair and Increases Cell Death upon Treatments with Anticancer Agents. *Mole. Cancer Res.* 2011:0098. doi: 10.1158/1541-7786.MCR-11-0098

Bokun, R., Bakotin, J., and Milasinovic, D. (1987). Semiquantitative cytochemical estimation of glucose-6-phosphate dehydrogenase activity in benign diseases and carcinoma of the breast. *Acta Cytol.* 31, 249–252.

Catanzaro, D., Gaude, E., Orso, G., Giordano, C., Guzzo, G., Rasola, A., et al. (2015). Inhibition of glucose-6-phosphate dehydrogenase sensitizes cisplatin-resistant cells to death. *Oncotarget* 6, 30102–30114. doi: 10.18632/oncotarget.4945

Chan, B., VanderLaan, P. A., and Sukhatme, V. P. (2013). 6-Phosphogluconate dehydrogenase regulates tumor cell migration in vitro by regulating receptor tyrosine kinase c-Met. *Biochem. Biophys. Res. Commun.* 439, 247–251. doi: 10.1016/j.bbrc.2013.08.048

Chan, K. K., Chan, J. Y., Chung, K. K., and Fung, K. P. (2004). Inhibition of cell proliferation in human breast tumor cells by antisense oligonucleotides against facilitative glucose transporter 5. *J. Cell Biochem.* 93, 1134–1142. doi: 10.1002/jcb.20270

Chatterjee, N., and Walker, G. C. (2017). Mechanisms of DNA Damage, Repair, and Mutagenesis. *Environ. Mol. Mutagen.* 58, 235–263. doi: 10.1002/em.22087

Cosentino, C., Grieco, D., and Costanzo, V. (2011). ATM activates the pentose phosphate pathway promoting anti-oxidant defence and DNA repair. *EMBO J.* 30, 546–555. doi: 10.1038/emboj.2010.330

D'Urso, M., Mareni, C., Toniolo, D., Piscopo, M., Schlessinger, D., and Luzzatto, L. (1983). Regulation of glucose 6-phosphate dehydrogenase expression in CHO-human fibroblast somatic cell hybrids. *Somatic. Cell Genet.* 9, 429–443. doi: 10.1007/BF01543044

Dwarkanath, B. S., Zolzer, F., Chandana, S., Bauch, T., Adhikari, J. S., Muller, W. U., et al. (2001). Heterogeneity in 2-deoxy-D-glucose-induced modifications in energetics and radiation responses of human tumor cell lines. *Int. J. Radiat. Oncol. Biol. Phys.* 50, 1051–1061. doi: 10.1016/s0360-3016(01)01534-6

Flacke, J.-P., Flacke, H., Appukuttan, A., Palisaar, R.-J., Noldus, J., Robinson, B. D., et al. (2013). Type 10 soluble adenylyl cyclase is overexpressed in prostate carcinoma and controls proliferation of prostate cancer cells. *J. Biol. Chem.* 288, 3126–3135. doi: 10.1074/jbc.M112.403279

Fnu, S., Williamson, E. A., De Haro, L. P., Brenneman, M., Wray, J., Shaheen, M., et al. (2011). Methylation of histone H3 lysine 36 enhances DNA repair by nonhomologous end-joining. *Proc. Natl. Acad. Sci. U S A* 108, 540–545. doi: 10.1073/pnas.1013571108

Fu, S., Li, Z., Xiao, L., Hu, W., Zhang, L., Xie, B., et al. (2019). Glutamine synthetase promotes radiation resistance via facilitating nucleotide metabolism and subsequent DNA damage repair. *Cell Rep.* 28, 1136–1143. doi: 10.1016/j.celrep.2019.07.002

Giammarioli, A. M., Gambardella, L., Barbati, C., Pietraforte, D., Tinari, A., Alberton, M., et al. (2012). Differential effects of the glycolysis inhibitor 2-deoxy-D-glucose on the activity of pro-apoptotic agents in metastatic melanoma cells, and induction of a cytoprotective autophagic response. *Int. J. Cancer* 131, E337–E347. doi: 10.1002/ijc.26420

Gospodinov, A., and Herceg, Z. (2013). Chromatin Structure in Double Strand Break Repair. *DNA Repair* 12:006. doi: 10.1016/j.dnarep.2013.07.006

Gregory, M. A., D'Alessandro, A., Alvarez-Calderon, F., Kim, J., Nemkov, T., Adane, B., et al. (2016). ATM/G6PD-driven redox metabolism promotes FLT3 inhibitor resistance in acute myeloid leukemia. *Proc. Natl. Acad. Sci. U S A* 113, E6669–E6678. doi: 10.1073/pnas.1603876113

Grundy, Gabrielle, J., Jason, L., and Parsons. (2020). Base excision repair and its implications to cancer therapy. *Essays Biochem.* 64, 831–843. doi: 10.1042/EBC20200013

Guo, C., and Ying Z. (2020). Autophagy and DNA Damage Repair. *Genome Instab. Dis.* 1, 172–183.

Gustafsson, N. M. S., Färnegårdh, K., Bonagas, N., Ninou, A. H., Groth, P., Wiita, E., et al. (2018). Targeting $PFKFB_3$ radiosensitizes cancer cells and suppresses homologous recombination. *Nat. Commun.* 9:3872. doi: 10.1038/s41467-018-06287-x

Halaby, M. J., Hibma, J. C., He, J., and Yang, D. Q. (2008). ATM protein kinase mediates full activation of Akt and regulates glucose transporter 4 translocation by insulin in muscle cells. *Cell Signal.* 20, 1555–1563. doi: 10.1016/j.cellsig.2008.04.011

Halestrap, A. P. (2012). The Monocarboxylate Transporter Family-Structure and Functional Characterization. *IUBMB Life* 64:573. doi: 10.1002/iub.573

Hao, J., Graham, P., Chang, L., Ni, J., Wasinger, V., Beretov, J., et al. (2016). Proteomic identification of the lactate dehydrogenase A in a radioresistant prostate cancer xenograft mouse model for improving radiotherapy. *Oncotarget* 7, 74269–74285. doi: 10.18632/oncotarget.12368

Hatzivassiliou, G., Zhao, F., Bauer, D. E., Andreadis, C., Shaw, A. N., Dhanak, D., et al. (2005). ATP citrate lyase inhibition can suppress tumor cell growth. *Cancer Cell* 8, 311–321. doi: 10.1016/j.ccr.2005.09.008

Hewitt, G., and Korolchuk, V. I. (2017). Repair, Reuse, Recycle: The Expanding Role of Autophagy in Genome Maintenance. *Trends Cell Biol.* 2017, 011. doi: 10.1016/j.tcb.2016.11.011

Hitosugi, T., Zhou, L., Elf, S., Fan, J., Kang, H. B., Seo, J. H., et al. (2012). Phosphoglycerate mutase 1 coordinates glycolysis and biosynthesis to promote tumor growth. *Cancer Cell* 22, 585–600. doi: 10.1016/j.ccr.2012.09.020

Hunt, T. K., Aslam, R. S., Beckert, S., Wagner, S., Ghani, Q. P., Hussain, M. Z., et al. (2007). Aerobically derived lactate stimulates revascularization and tissue repair via redox mechanisms. *Antioxid Redox Signal* 9, 1115–1124. doi: 10.1089/ars.2007.1674

Jackson, S. P., and Bartek, J. (2009). The DNA-Damage Response in Human Biology and Disease. *Nature* doi: 10.1038/nature08467

Jensen, R. B., and Rothenberg, E. (2020). Preserving Genome Integrity in Human Cells via DNA Double-Strand Break Repair. *Mole. Biol. Cell* 31, 859–865.

Jiang, P., Du, W., Wang, X., Mancuso, A., Gao, X., Wu, M., et al. (2011). p53 regulates biosynthesis through direct inactivation of glucose-6-phosphate dehydrogenase. *Nat. Cell Biol.* 13, 310–316. doi: 10.1038/ncb2172

Jiang, Y., Qian, X., Shen, J., Wang, Y., Li, X., Liu, R., et al. (2015). Local generation of fumarate promotes DNA repair through inhibition of histone H3 demethylation. *Nat. Cell Biol.* 17, 1158–1168. doi: 10.1038/ncb3209

Kalluri, R. (2016). The Biology and Function of Fibroblasts in Cancer. *Nat. Rev. Cancer* 16, 582–598. doi: 10.1038/nrc.2016.73

Keller, K. E., Doctor, Z. M., Dwyer, Z. W., and Lee, Y. S. (2014). SAICAR induces protein kinase activity of PKM2 that is necessary for sustained proliferative signaling of cancer cells. *Mol. Cell.* 53, 700–709. doi: 10.1016/j.molcel.2014.02.015

Khaitan, D., Chandna, S., Arya, M. B., and Dwarakanath, B. S. (2006). Differential mechanisms of radiosensitization by 2-deoxy-D-glucose in the monolayers and multicellular spheroids of a human glioma cell line. *Cancer Biol. Ther.* 5, 1142–1151. doi: 10.4161/cbt.5.9.2986

Khan, T., He, Y., Kryza, T., Harrington, B. S., Gunter, J. H., Sullivan, M. A., et al. (2020). Disruption of Glycogen Utilization Markedly Improves the Efficacy of Carboplatin against Preclinical Models of Clear Cell Ovarian Carcinoma. *Cancers* 12:cancers12040869. doi: 10.3390/cancers12040869

Kilstrup, M., Hammer, K., Ruhdal Jensen, P., and Martinussen, J. (2005). Nucleotide metabolism and its control in lactic acid bacteria. *FEMS Microbiol. Rev.* 29, 555–590. doi: 10.1016/j.femsre.2005.04.006

Kim, B. H., and Chang, J. H. (2019). Differential effect of GLUT1 overexpression on survival and tumor immune microenvironment of human papilloma virus

type 16-positive and -negative cervical cancer. *Sci. Rep.* 9:13301. doi: 10.1038/s41598-019-49928-x

Kim, E. Y., Chung, T. W., Han, C. W., Park, S. Y., Park, K. H., Jang, S. B., et al. (2019). A novel lactate dehydrogenase inhibitor, 1-(phenylseleno)-4-(trifluoromethyl) benzene, suppresses tumor growth through apoptotic cell death. *Sci. Rep.* 9:3969. doi: 10.1038/s41598-019-40617-3

Kim, J., Kundu, M., Viollet, B., and Guan, K. L. (2011). AMPK and MTOR Regulate Autophagy through Direct Phosphorylation of Ulk1. *Nat. Cell Biol.* 2011:ncb2152. doi: 10.1038/ncb2152

Koch, A., Lang, S. A., Wild, P. J., Gantner, S., Mahli, A., Spanier, G., et al. (2015). Glucose transporter isoform 1 expression enhances metastasis of malignant melanoma cells. *Oncotarget* 6, 32748–32760. doi: 10.18632/oncotarget.4977

Koerner, S. K., Hanai, J. I., Bai, S., Jernigan, F. E., Oki, M., Komaba, C., et al. (2017). Design and synthesis of emodin derivatives as novel inhibitors of ATP-citrate lyase. *Eur. J. Med. Chem.* 126, 920–928. doi: 10.1016/j.ejmech.2016.12.018

Kornberg, H. L., and Krebs, H. A. (1957). Synthesis of cell constituents from C2-units by a modified tricarboxylic acid cycle. *Nature* 179, 988–991. doi: 10.1038/179988a0

Koukourakis, M. I., Giatromanolaki, A., Panteliadou, M., Pouliliou, S. E., Chondrou, P. S., Mavropoulou, S., et al. (2014). Lactate dehydrogenase 5 isoenzyme overexpression defines resistance of prostate cancer to radiotherapy. *Br. J. Cancer* 110, 2217–2223. doi: 10.1038/bjc.2014.158

Koukourakis, M. I., Giatromanolaki, A., Winter, S., Leek, R., Sivridis, E., and Harris, A. L. (2009). Lactate dehydrogenase 5 expression in squamous cell head and neck cancer relates to prognosis following radical or postoperative radiotherapy. *Oncology* 77, 285–292. doi: 10.1159/000259260

Koukourakis, M. I., Kakouratos, C., Kalamida, D., Bampali, Z., Mavropoulou, S., Sivridis, E., et al. (2016). Hypoxia-inducible proteins HIF1alpha and lactate dehydrogenase LDH5, key markers of anaerobic metabolism, relate with stem cell markers and poor post-radiotherapy outcome in bladder cancer. *Int. J. Radiat. Biol.* 92, 353–363. doi: 10.3109/09553002.2016.1162921

Krüger, A., and Ralser, M. (2011). ATM is a redox sensor linking genome stability and carbon metabolism. *Sci. Signal* 4:e17. doi: 10.1126/scisignal.2001959

Kumari, R., Deshmukh, R. S., and Das, S. (2019). Caspase-10 inhibits ATP-citrate lyase-mediated metabolic and epigenetic reprogramming to suppress tumorigenesis. *Nat. Commun.* 10:4255. doi: 10.1038/s41467-019-12194-6

Le, D. T., Uram, J. N., Wang, H., Bartlett, B. R., Kemberling, H., Eyring, A. D., et al. (2015). PD-1 Blockade in Tumors with Mismatch-Repair Deficiency. *N. Engl. J. Med.* doi: 10.1056/nejmoa1500596

Leick, M. B., and Levis, M. J. (2017). The Future of Targeting FLT3 Activation in AML. *Curr. Hematol. Malig. Rep.* 12, 153–167. doi: 10.1007/s11899-017-0381-2

Leshets, M., Ramamurthy, D., Lisby, M., Lehming, N., and Pines, O. (2018). Fumarase is involved in DNA double-strand break resection through a functional interaction with Sae2. *Curr. Genet.* 64, 697–712. doi: 10.1007/s00294-017-0786-4

Li, Q., Zhang, D., Chen, X., He, L., Li, T., Xu, X., et al. (2015). Nuclear PKM2 contributes to gefitinib resistance via upregulation of STAT3 activation in colorectal cancer. *Sci. Rep.* 5:16082. doi: 10.1038/srep16082

Liu, E. Y., Xu, N., O'Prey, J., Lao, L. Y., Joshi, S., Long, J. S., et al. (2015). Loss of Autophagy Causes a Synthetic Lethal Deficiency in DNA Repair. *Proc. Natl. Acad. Sci. U S A* 2015, 1409563112. doi: 10.1073/pnas.1409563112

Li, X., Lu, P., Li, B., Yang, R., Chu, Y., Zhang, Z., et al. (2016). Sensitization of hepatocellular carcinoma cells to irradiation by miR-34a through targeting lactate dehydrogenase-A. *Mol. Med. Rep.* 13, 3661–3667. doi: 10.3892/mmr.2016.4974

Lieber, M. R. (2010). The mechanism of double-strand DNA break repair by the nonhomologous DNA end-joining pathway. *Annu. Rev. Biochem.* 79, 181–211. doi: 10.1146/annurev.biochem.052308.093131

Lin, Y., Zhai, H., Ouyang, Y., Lu, Z., Chu, C., He, Q., et al. (2019). Knockdown of PKM2 enhances radiosensitivity of cervical cancer cells. *Cancer Cell Int.* 19:129. doi: 10.1186/s12935-019-0845-7

Liu, G., Li, Y. I., and Gao, X. (2016). Overexpression of microRNA-133b sensitizes non-small cell lung cancer cells to irradiation through the inhibition of glycolysis. *Oncol. Lett.* 11, 2903–2908. doi: 10.3892/ol.2016.4316

Liu, L., Wang, S., Zhang, Q., and Ding, Y. (2008). Identification of potential genes/proteins regulated by Tiam1 in colorectal cancer by microarray analysis and proteome analysis. *Cell Biol. Int.* 32, 1215–1222. doi: 10.1016/j.cellbi.2008.07.004

Liu, X., Weng, Y., Liu, P., Sui, Z., Zhou, L., Huang, Y., et al. (2018). Identification of PGAM1 as a putative therapeutic target for pancreatic ductal adenocarcinoma metastasis using quantitative proteomics. *Onco Targets Ther.* 11, 3345–3357. doi: 10.2147/ott.S162470

Manerba, M., Di Ianni, L., Fiume, L., Roberti, M., Recanatini, M., and Di Stefano, G. (2015). Lactate dehydrogenase inhibitors sensitize lymphoma cells to cisplatin without enhancing the drug effects on immortalized normal lymphocytes. *Eur. J. Pharm. Sci.* 74, 95–102. doi: 10.1016/j.ejps.2015.04.022

Manerba, M., Vettraino, M., Fiume, L., Di Stefano, G., Sartini, A., Giacomini, E., et al. (2012). Galloflavin (CAS 568-80-9): a novel inhibitor of lactate dehydrogenase. *ChemMedChem* 7, 311–317. doi: 10.1002/cmdc.201100471

Marechal, A., and Zou, L. (2013). DNA damage sensing by the ATM and ATR kinases. *Cold Spr. Harb. Perspect. Biol.* 5:a012716. doi: 10.1101/cshperspect.a012716

Matsuoka, S., Ballif, B. A., Smogorzewska, A., McDonald, E. R. III, Hurov, K. E., Luo, J., et al. (2007). ATM and ATR substrate analysis reveals extensive protein networks responsive to DNA damage. *Science* 316, 1160–1166. doi: 10.1126/science.1140321

Minchom, A., Aversa, C., and Lopez, J. (2018). Dancing with the DNA Damage Response: Next-Generation Anti-Cancer Therapeutic Strategies. *Ther. Adv. Med. Oncol.* 2018:1758835918786658. doi: 10.1177/1758835918786658

Mirzayans, R., Severin, D., and Murray, D. (2006). Relationship between DNA double-strand break rejoining and cell survival after exposure to ionizing radiation in human fibroblast strains with differing ATM/p53 status: implications for evaluation of clinical radiosensitivity. *Int. Radiat. Oncol. Biol. Phys.* 66, 1498–1505. doi: 10.1016/j.ijrobp.2006.08.064

Mori-Iwamoto, S., Kuramitsu, Y., Ryozawa, S., Mikuria, K., Fujimoto, M., Maehara, S., et al. (2007). Proteomics finding heat shock protein 27 as a biomarker for resistance of pancreatic cancer cells to gemcitabine. *Int. J. Oncol.* 31, 1345–1350.

Ohba, S., Johannessen, T. A., Chatla, K., Yang, X., Pieper, R. O., and Mukherjee, J. (2020). Phosphoglycerate Mutase 1 Activates DNA Damage Repair via Regulation of WIP1 Activity. *Cell Rep.* 31:107518. doi: 10.1016/j.celrep.2020.03.082

Park, S. J., Gavrilova, O., Brown, A. L., Soto, J. E., Bremner, S., Kim, J., et al. (2017). DNA-PK Promotes the Mitochondrial. Metabolic, and Physical Decline that Occurs During Aging. *Cell Metab.* 113:e1137. doi: 10.1016/j.cmet.2017.04.008

Patra, K. C., and Hay, N. (2014). The pentose phosphate pathway and cancer. *Trends Biochem. Sci.* 39, 347–354. doi: 10.1016/j.tibs.2014.06.005

Pavlova, N. N., and Thompson, C. B. (2016). The Emerging Hallmarks of Cancer Metabolism. *Cell Metab.* 23, 27–47. doi: 10.1016/j.cmet.2015.12.006

Puustinen, P., Keldsbo, A., Corcelle-Termeau, E., Ngoei, K., Sonder, S. L., Farkas, T., et al. (2020). DNA-dependent protein kinase regulates lysosomal AMP-dependent protein kinase activation and autophagy. *Autophagy* 16, 1871–1888. doi: 10.1080/15548627.2019.1710430

Qu, J., Sun, W., Zhong, J., Lv, H., Zhu, M., Xu, J., et al. (2017). Phosphoglycerate mutase 1 regulates dNTP pool and promotes homologous recombination repair in cancer cells. *J. Cell Biol.* 216, 409–424. doi: 10.1083/jcb.201607008

Rose, M., Burgess, J. T., O'byrne, K., Richard, D. J., and Bolderson, E. (2020). PARP inhibitors: clinical relevance, mechanisms of action and tumor resistance. *Front. Cell Dev. Biol.* 8:564601. doi: 10.3389/fcell.2020.564601

Roos, W. P., Thomas, A. D., and Kaina, B. (2016). DNA Damage and the Balance between Survival and Death in Cancer Biology. *Nat. Rev. Cancer* 2016, 20–33. doi: 10.1038/nrc.2015.2

Schwarz, S. B., Schaffer, P. M., Kulka, U., Ertl-Wagner, B., Hell, R., and Schaffer, M. (2008). The effect of radio-adaptive doses on HT29 and GM637 cells. *Radiat. Oncol.* 3:12. doi: 10.1186/1748-717X-3-12

Seltzer, M. J., Bennett, B. D., Joshi, A. D., Gao, P., Thomas, A. G., Ferraris, D. V., et al. (2010). Inhibition of glutaminase preferentially slows growth of glioma cells with mutant IDH1. *Cancer Res.* 70, 8981–8987. doi: 10.1158/0008-5472.CAN-10-1666

Sharma, N. K., Lebedeva, M., Thomas, T., Kovalenko, O. A., Stumpf, J. D., Shadel, G. S., et al. (2014). Intrinsic mitochondrial DNA repair defects in Ataxia Telangiectasia. *DNA Rep.* 13, 22–31. doi: 10.1016/j.dnarep.2013.11.002

Sharma, P. K., Dwarakanath, B. S., and Varshney, R. (2012). Radiosensitization by 2-deoxy-D-glucose and 6-aminonicotinamide involves activation of redox sensitive ASK1-JNK/p38MAPK signaling in head and neck cancer cells.

Free Radic. Biol. Med. 53, 1500–1513. doi: 10.1016/j.freeradbiomed.2012.07.001

Singh, S., Pandey, S., Chawla, A. S., Bhatt, A. N., Roy, B. G., Saluja, D., et al. (2019). Dietary 2-deoxy-D-glucose impairs tumour growth and metastasis by inhibiting angiogenesis. *Eur. J. Cancer* 123, 11–24. doi: 10.1016/j.ejca.2019.09.005

Sivanand, S., Rhoades, S., Jiang, Q., Lee, J. V., Benci, J., Zhang, J., et al. (2017). Nuclear Acetyl-CoA Production by ACLY Promotes Homologous Recombination. *Mol. Cell* 67, 252–265e256. doi: 10.1016/j.molcel.2017.06.008

Sizemore, S. T., Zhang, M., Cho, J. H., Sizemore, G. M., Hurwitz, B., Kaur, B., et al. (2018). Pyruvate kinase M2 regulates homologous recombination-mediated DNA double-strand break repair. *Cell Res.* 28, 1090–1102. doi: 10.1038/s41422-018-0086-7

Sonveaux, P., Copetti, T., De Saedeleer, C. J., Végran, F., Verrax, J., Kennedy, K. M., et al. (2012). Targeting the lactate transporter MCT1 in endothelial cells inhibits lactate-induced HIF-1 activation and tumor angiogenesis. *PLoS One* 7:e33418. doi: 10.1371/journal.pone.0033418

Spermon, J. R., De Geus-Oei, L. F., Kiemeney, L. A., Witjes, J. A., and Oyen, W. J. (2002). The role of (18)fluoro-2-deoxyglucose positron emission tomography in initial staging and re-staging after chemotherapy for testicular germ cell tumours. *BJU Int.* 89, 549–556. doi: 10.1046/j.1464-410x.2002.02641.x

Stetak, A., Veress, R., Ovadi, J., Csermely, P., Keri, G., and Ullrich, A. (2007). Nuclear translocation of the tumor marker pyruvate kinase M2 induces programmed cell death. *Cancer Res.* 67, 1602–1608. doi: 10.1158/0008-5472.CAN-06-2870

Storr, S. J., Woolston, C. M., and Martin, S. G. (2011). Base Excision Repair, the Redox Environment and Therapeutic Implications. *Curr. Mole. Pharmacol.* 5, 88–101. doi: 10.2174/1874467211205010088

Sulkowski, P. L., Sundaram, R. K., Oeck, S., Corso, C. D., Liu, Y., Noorbakhsh, S., et al. (2018). Krebs-cycle-deficient hereditary cancer syndromes are defined by defects in homologous-recombination DNA repair. *Nat. Genet.* 50, 1086–1092. doi: 10.1038/s41588-018-0170-4

Sun, K., Tang, S., Hou, Y., Xi, L., Chen, Y., Yin, J., et al. (2019). Oxidized ATM-mediated glycolysis enhancement in breast cancer-associated fibroblasts contributes to tumor invasion through lactate as metabolic coupling. *EBioMed.* 41, 370–383. doi: 10.1016/j.ebiom.2019.02.025

Tamburini, B. A., and Tyler, J. K. (2005). Localized histone acetylation and deacetylation triggered by the homologous recombination pathway of double-strand DNA repair. *Mol. Cell Biol.* 25, 4903–4913. doi: 10.1128/MCB.25.12.4903-4913.2005

Tardito, S., Oudin, A., Ahmed, S. U., Fack, F., Keunen, O., Zheng, L., et al. (2015). Glutamine synthetase activity fuels nucleotide biosynthesis and supports growth of glutamine-restricted glioblastoma. *Nat. Cell Biol.* 17, 1556–1568. doi: 10.1038/ncb3272

Tong, X., Zhao, F., and Thompson, C. B. (2009). The Molecular Determinants of de Novo Nucleotide Biosynthesis in Cancer Cells. *Curr. Opin. Genet. Dev.* doi: 10.1016/j.gde.2009.01.002

Tubbs, A., and Nussenzweig, A. (2017). Endogenous DNA Damage as a Source of Genomic Instability in Cancer. *Cell* 2017:002. doi: 10.1016/j.cell.2017.01.002

Turkcan, S., Kiru, L., Naczynski, D. J., Sasportas, L. S., and Pratx, G. (2019). Lactic Acid Accumulation in the Tumor Microenvironment Suppresses (18)F-FDG Uptake. *Cancer Res.* 79, 410–419. doi: 10.1158/0008-5472.CAN-17-0492

Tuttle, S., Stamato, T., Perez, M. L., and Biaglow, J. (2000). Glucose-6-phosphate dehydrogenase and the oxidative pentose phosphate cycle protect cells against apoptosis induced by low doses of ionizing radiation. *Radiat. Res.* 153, 781–787. doi: 10.1667/0033-75872000153

van Vugt, M. A. T. M. (2017). Shutting down the power supply for DNA repair in cancer cells. *J. Cell Biol.* 216, 295–297. doi: 10.1083/jcb.201701026

Vartanian, A., Agnihotri, S., Wilson, M. R., Burrell, K. E., Tonge, P. D., Alamsahebpour, A., et al. (2016). Targeting hexokinase 2 enhances response to radio-chemotherapy in glioblastoma. *Oncotarget* 7, 69518–69535. doi: 10.18632/oncotarget.11680

Villa, E., Ali, E. S., Sahu, U., and Ben-Sahra, I. (2019). Cancer Cells Tune the Signaling Pathways to Empower de Novo Synthesis of Nucleotides. *Cancers* 11:11050688. doi: 10.3390/cancers11050688

Volkow, N. D., Tomasi, D., Wang, G. J., Studentsova, Y., Margus, B., and Crawford, T. O. (2014). Brain glucose metabolism in adults with ataxia-telangiectasia and their asymptomatic relatives. *Brain* 137(Pt 6), 1753–1761. doi: 10.1093/brain/awu092

Wagner, W., Ciszewski, W. M., and Kania, K. D. (2015). L- and D-lactate enhance DNA repair and modulate the resistance of cervical carcinoma cells to anticancer drugs via histone deacetylase inhibition and hydroxycarboxylic acid receptor 1 activation. *Cell Commun. Signal* 13:36. doi: 10.1186/s12964-015-0114-x

Wagner, W., Kania, K. D., and Ciszewski, W. M. (2017). Stimulation of lactate receptor (HCAR1) affects cellular DNA repair capacity. *DNA Repair* 52, 49–58. doi: 10.1016/j.dnarep.2017.02.007

Wang, J. B., Erickson, J. W., Fuji, R., Ramachandran, S., Gao, P., Dinavahi, R., et al. (2010). Targeting mitochondrial glutaminase activity inhibits oncogenic transformation. *Cancer Cell* 18, 207–219. doi: 10.1016/j.ccr.2010.08.009

Warburg, O. (1925). The Metabolism of Carcinoma Cells. *J.Cancer Res.* 9, 148–163. doi: 10.1158/jcr.1925.148

Warburg, O. (1956). On the origin of cancer cells. *Science* 123, 309–314. doi: 10.1126/science.123.3191.309

Warburg, O., Wind, F., and Negelein, E. (1927). The Metabolism of Tumors in the Body. *J. Gen. Physiol.* 8, 519–530. doi: 10.1085/jgp.8.6.519

Wellen, K. E., Hatzivassiliou, G., Sachdeva, U. M., Bui, T. V., Cross, J. R., and Thompson, C. B. (2009). ATP-citrate lyase links cellular metabolism to histone acetylation. *Science* 324, 1076–1080. doi: 10.1126/science.1164097

Weterings, E., and Chen, D. J. (2008). The endless tale of non-homologous end-joining. *Cell Res.* 18, 114–124. doi: 10.1038/cr.2008.3

Wincewicz, A., Baltaziak, M., Kanczuga-Koda, L., Koda, M., Sulkowska, U., and Sulkowski, S. (2010). GLUT1 and Bcl-xL in relation to erythropoietin in human colorectal adenocarcinomas. *Hepatogastroenterology* 57, 741–745.

Wu, J., Hu, L., Chen, M., Cao, W., Chen, H., and He, T. (2016). Pyruvate kinase M2 overexpression and poor prognosis in solid tumors of digestive system: evidence from 16 cohort studies. *Onco. Targets Ther.* 9, 4277–4288. doi: 10.2147/OTT.S106508

Wu, J., Hu, L., Wu, F., Zou, L., and He, T. (2017). Poor prognosis of hexokinase 2 overexpression in solid tumors of digestive system: a meta-analysis. *Oncotarget* 8, 32332–32344. doi: 10.18632/oncotarget.15974

Xia, L., Qin, K., Wang, X. R., Wang, X. L., Zhou, A. W., Chen, G. Q., et al. (2017). Pyruvate kinase M2 phosphorylates H2AX and promotes genomic instability in human tumor cells. *Oncotarget* 8, 109120–109134. doi: 10.18632/oncotarget.22621

Yalcin, A., Telang, S., Clem, B., and Chesney, J. (2009). Regulation of glucose metabolism by 6-phosphofructo-2-kinase/fructose-2,6-bisphosphatases in cancer. *Exp. Mol. Pathol.* 86, 174–179. doi: 10.1016/j.yexmp.2009.01.003

Yan, S. X., Luo, X. M., Zhou, S. H., Bao, Y. Y., Fan, J., Lu, Z. J., et al. (2013). Effect of antisense oligodeoxynucleotides glucose transporter-1 on enhancement of radiosensitivity of laryngeal carcinoma. *Int. J. Med. Sci.* 10, 1375–1386. doi: 10.7150/ijms.6855

Yang, W., Xia, Y., Hawke, D., Li, X., Liang, J., Xing, D., et al. (2014). PKM2 Phosphorylates Histone H3 and Promotes Gene Transcription and Tumorigenesis. *Cell* 158:1210. doi: 10.1016/j.cell.2014.08.003

Yin, X., Tang, B., Li, J. H., Wang, Y., Zhang, L., Xie, X. Y., et al. (2017). ID1 promotes hepatocellular carcinoma proliferation and confers chemoresistance to oxaliplatin by activating pentose phosphate pathway. *J. Exp. Clin. Cancer Res.* 36:166. doi: 10.1186/s13046-017-0637-7

Yogev, O., Yogev, O., Singer, E., Shaulian, E., Goldberg, M., Fox, T. D., et al. (2010). Fumarase: a mitochondrial metabolic enzyme and a cytosolic/nuclear component of the DNA damage response. *PLoS Biol.* 8:e1000328. doi: 10.1371/journal.pbio.1000328

Yuan, S., Qiao, T., Zhuang, X., Chen, W., Xing, N., and Zhang, Q. (2016). Knockdown of the M2 Isoform of Pyruvate Kinase (PKM2) with shRNA Enhances the Effect of Docetaxel in Human NSCLC Cell Lines In Vitro. *Yonsei Med. J.* 57, 1312–1323. doi: 10.3349/ymj.2016.57.6.1312

Yuan, W., Wu, S., Guo, J., Chen, Z., Ge, J., Yang, P., et al. (2010). Silencing of TKTL1 by siRNA inhibits proliferation of human gastric cancer cells in vitro and in vivo. *Cancer Biol. Ther.* 9, 710–716. doi: 10.4161/cbt.9.9.11431

Zhang, D., Wu, H., Zhang, X., Ding, X., Huang, M., Geng, M., et al. (2017). Phosphoglycerate Mutase 1 Predicts the Poor Prognosis of Oral Squamous

Cell Carcinoma and is Associated with Cell Migration. *J. Cancer* 8, 1943–1951. doi: 10.7150/jca.19278

Zhang, J., Cao, M., Yang, W., Sun, F., Xu, C., Yin, L., et al. (2016). Inhibition of Glucose-6-Phosphate Dehydrogenase Could Enhance 1,4-Benzoquinone-Induced Oxidative Damage in K562 Cells. *Oxidative Med. Cell. Long.* 2016:3912515. doi: 10.1155/2016/3912515

Zhang, L., Su, J., Xie, Q., Zeng, L., Wang, Y., Yi, D., et al. (2015). 2-Deoxy-d-Glucose Sensitizes Human Ovarian Cancer Cells to Cisplatin by Increasing ER Stress and Decreasing ATP Stores in Acidic Vesicles. *J. Biochem. Mol. Toxicol.* 29, 572–578. doi: 10.1002/jbt.21730

Zhang, X. Y., Zhang, M., Cong, Q., Zhang, M. X., Zhang, M. Y., Lu, Y. Y., et al. (2018). Hexokinase 2 confers resistance to cisplatin in ovarian cancer cells by enhancing cisplatin-induced autophagy. *Int. J. Biochem. Cell Biol.* 95, 9–16. doi: 10.1016/j.biocel.2017.12.010

Zhao, F., Ming, J., Zhou, Y., and Fan, L. (2016). Inhibition of Glut1 by WZB117 sensitizes radioresistant breast cancer cells to irradiation. *Cancer Chemother. Pharmacol.* 77, 963–972. doi: 10.1007/s00280-016-3007-9

Zheng, B., Liu, F., Zeng, L., Geng, L., Ouyang, X., Wang, K., et al. (2018). Overexpression of Pyruvate Kinase Type M2 (PKM2) Promotes Ovarian Cancer Cell Growth and Survival Via Regulation of Cell Cycle Progression Related with Upregulated CCND1 and Downregulated CDKN1A Expression. *Med. Sci. Monit.* 24, 3103–3112. doi: 10.12659/MSM.907490

Zong, W.-X., Rabinowitz, J. D., and White, E. (2016). Mitochondria and Cancer. *Mole. Cell* 61, 667–676. doi: 10.1016/j.molcel.2016.02.011

Conflict of Interest: KO and DR are founders of CARP Pharmaceuticals. EB, DR, and KO are founders of Carpe Vitae Pharmaceuticals. EB, KO, and DR are inventors on patent applications filed by Queensland University of Technology.

The remaining authors declare that the research was conducted in the absence of any commercial or financial relationships that could be construed as a potential conflict of interest.

frontiers in Molecular Biosciences

BRIEF RESEARCH REPORT
published: 29 April 2021
doi: 10.3389/fmolb.2021.633344

Veliparib Is an Effective Radiosensitizing Agent in a Preclinical Model of Medulloblastoma

Jessica Buck[1,2†], Patrick J. C. Dyer[1†], Hilary Hii[1], Brooke Carline[1], Mani Kuchibhotla[1], Jacob Byrne[1], Meegan Howlett[1,2], Jacqueline Whitehouse[1,2], Martin A. Ebert[3,4], Kerrie L. McDonald[5], Nicholas G. Gottardo[1,6] and Raelene Endersby[1,2]*

[1] Brain Tumour Research Program, Telethon Kids Cancer Centre, Telethon Kids Institute, Perth, WA, Australia, [2] Centre for Child Health Research, University of Western Australia, Perth, WA, Australia, [3] School of Physics, Mathematics and Computing, University of Western Australia, Perth, WA, Australia, [4] Radiation Oncology, Sir Charles Gairdner Hospital, Perth, WA, Australia, [5] Brain Cancer Consultancy, Sydney, NSW, Australia, [6] Department of Paediatric Oncology and Haematology, Perth Children's Hospital, Perth, WA, Australia

OPEN ACCESS

Edited by:
Amila Suraweera, Queensland University of Technology, Australia

Reviewed by:
Veronika Butin-Israeli, Northwestern University, United States
Diana Aguilar-Morante, Institute of Biomedicine of Seville (IBIS), Spain

***Correspondence:**
Raelene Endersby
raelene.endersby@telethonkids.org.au

† These authors have contributed equally to this work

Specialty section:
This article was submitted to Molecular Diagnostics and Therapeutics, a section of the journal Frontiers in Molecular Biosciences

Received: *25 November 2020*
Accepted: *30 March 2021*
Published: *29 April 2021*

Citation:
Buck J, Dyer PJC, Hii H, Carline B, Kuchibhotla M, Byrne J, Howlett M, Whitehouse J, Ebert MA, McDonald KL, Gottardo NG and Endersby R (2021) Veliparib Is an Effective Radiosensitizing Agent in a Preclinical Model of Medulloblastoma. Front. Mol. Biosci. 8:633344. doi: 10.3389/fmolb.2021.633344

Medulloblastoma is the most common malignant childhood brain tumor, and 5-year overall survival rates are as low as 40% depending on molecular subtype, with new therapies critically important. As radiotherapy and chemotherapy act through the induction of DNA damage, the sensitization of cancer cells through the inhibition of DNA damage repair pathways is a potential therapeutic strategy. The poly-(ADP-ribose) polymerase (PARP) inhibitor veliparib was assessed for its ability to augment the cellular response to radiation-induced DNA damage in human medulloblastoma cells. DNA repair following irradiation was assessed using the alkaline comet assay, with veliparib inhibiting the rate of DNA repair. Veliparib treatment also increased the number of γH2AX foci in cells treated with radiation, and analysis of downstream pathways indicated persistent activation of the DNA damage response pathway. Clonogenicity assays demonstrated that veliparib effectively inhibited the colony-forming capacity of medulloblastoma cells, both as a single agent and in combination with irradiation. These data were then validated *in vivo* using an orthotopic implant model of medulloblastoma. Mice harboring intracranial D425 medulloblastoma xenografts were treated with vehicle, veliparib, 18 Gy multifractionated craniospinal irradiation (CSI), or veliparib combined with 18 Gy CSI. Animals treated with combination therapy exhibited reduced tumor growth rates concomitant with increased intra-tumoral apoptosis observed by immunohistochemistry. Kaplan–Meier analyses revealed a statistically significant increase in survival with combination therapy compared to CSI alone. In summary, PARP inhibition enhanced radiation-induced cytotoxicity of medulloblastoma cells; thus, veliparib or other brain-penetrant PARP inhibitors are potential radiosensitizing agents for the treatment of medulloblastoma.

Keywords: Medulloblastoma, radiotherapy, veliparib, DNA repair, poly(ADP-ribose) polymerase

INTRODUCTION

Brain tumors represent one of the leading causes of mortality in children, with medulloblastoma the most common childhood brain cancer (Millard and De Braganca, 2016). Medulloblastoma is a heterogeneous group of cancers that can been divided into four core molecular subgroups: SHH, WNT, Group 3, and Group 4 (Thompson et al., 2006; Louis et al., 2016). These subgroups can be further classified into 13 subtypes based on genomic, epigenomic, proteomic, and clinical features (Hovestadt et al., 2020). Five-year overall survival rates for medulloblastoma range from 40 to 98%, depending on molecular subtype (Hovestadt et al., 2020), with *MYC*-amplified Group 3 medulloblastoma associated with very poor survival rates. Despite significant progress in our understanding of the underlying molecular drivers of these tumors, this has not yet been translated into improved outcomes.

The standard treatment regimen for medulloblastoma consists of maximal safe tumor resection followed by craniospinal irradiation (CSI) and multi-agent chemotherapy (Martin et al., 2014; Northcott et al., 2019). As radiotherapy and chemotherapy induce DNA damage, sensitizing medulloblastoma cells to these treatments through inhibiting DNA repair pathways is a potential therapeutic strategy (Carrassa and Damia, 2017). We recently performed a drug screen that identified kinase inhibitors of the DNA damage response (DDR) pathway and cell cycle machinery as potent agents against *MYC*-amplified Group 3 medulloblastoma in combination with chemotherapy (Endersby et al., 2021). The DDR is a carefully orchestrated network which allows cells to sense problems in their DNA, arrest cell cycle progression and repair DNA damage. The poly-(ADP-ribose) polymerase (PARP) family of proteins are important facilitators of DNA damage repair. While there are 18 members of the PARP family, PARP1 and PARP2 are the most important for DNA damage repair (Kamaletdinova et al., 2019). PARPs bind to DNA at various sites of damage which stimulates them to synthesize PAR chains (PARylation). These PAR chains act as docking sites for DNA repair proteins, facilitating their recruitment to sites of DNA damage (Pommier et al., 2016). A number of PARP inhibitors have been developed and may be used clinically to treat cancers with homologous recombination (HR) deficiency, such as those with mutations in *BRCA1*, *BRCA2*, and *PALB2*. In these cancers, PARP inhibitors can induce synthetic lethality, and this approach has had some success particularly in breast and ovarian cancer (Janysek et al., 2021). This synthetic lethality approach is unlikely to be widely successful in medulloblastoma, as very few patients harbor mutations in genes encoding HR machinery. However, PARP inhibitors have recently been investigated for their ability to sensitize brain cancer cells to chemotherapy and radiotherapy (Van Vuurden et al., 2011; Chornenkyy et al., 2015; Jue et al., 2017) and it is this approach that we sought to test in medulloblastoma.

There is evidence that PARP inhibition can sensitize cancer cell lines to radiation, including cells derived from pediatric brain tumors. PARP inhibition increased DNA damage, and reduced cell viability and proliferation when combined with irradiation in pediatric high-grade glioma, ependymoma, and diffuse intrinsic pontine glioma (DIPG) cell lines *in vitro* (Van Vuurden et al., 2011; Chornenkyy et al., 2015). Combined PARP inhibition and radiotherapy has also increased survival in mouse models of high-grade astrocytoma (Chornenkyy et al., 2015). In medulloblastoma, it has been demonstrated that PARP inhibition has the potential to sensitize cells to chemotherapy *in vivo* (Daniel et al., 2010). Radiosensitization of medulloblastoma cells has been demonstrated *in vitro* (Van Vuurden et al., 2011), however this has not yet been tested *in vivo* in orthotopic xenograft models.

Of the PARP inhibitors developed so far, veliparib is the most clinically advanced in children. A phase I trial has examined veliparib in combination with temozolomide for the treatment of recurrent CNS tumors in children, including two patients diagnosed with medulloblastoma (Su et al., 2014); where veliparib was well tolerated and stable disease was observed in four patients. A recent phase I/II clinical trial examined the use of veliparib in combination with temozolomide and radiotherapy for treatment of DIPG (Baxter et al., 2020). While veliparib was well-tolerated, no survival benefit was shown at interim analysis, and the trial was stopped. A further phase I/II clinical trial examining the use of veliparib in combination with temozolomide and radiotherapy for treatment of pediatric glioma is currently underway (clinicaltrials.gov ID#NCT03581292). Recently, veliparib in combination with radiation was shown to significantly increase survival of glioblastoma patient-derived xenograft (PDX) mouse models (Jue et al., 2017). Therefore, we sought to investigate methods that may improve treatment outcomes for high-risk medulloblastoma patients by preclinically evaluating the radiosensitizing potential of PARP inhibition in *MYC*-amplified Group 3 medulloblastoma models. Despite promising data from PARP inhibitors like niraparib and olaparib (Murai et al., 2012), given that veliparib is the most clinically tested PARP inhibitor for children with brain cancer, we investigated a potential role for veliparib in medulloblastoma to ensure rapid clinical translatability.

METHODS

Cell Culture

D425 and D283 human medulloblastoma cells were a gift from Prof. Darell Bigner of Duke University, United States (Friedman et al., 1985; Bigner et al., 1990). STR analysis and sequencing of previously reported genetic alterations confirmed the identity of all cell lines. All cultures were incubated at 37°C with 5% CO_2 and confirmed mycoplasma-free using a MycoAlert™ Mycoplasma Detection Kit (Lonza). D425 cells were cultured in modified IMEM (#A10489-01, Gibco) supplemented with GlutaMAX (#35050-061, Invitrogen), 10% fetal bovine serum (FBS, Cell Sera), and 10 μM HEPES (#15630-080, Gibco). D425 cells were transduced with pCL20-MSCV-GFP-ires-Luc2 lentiviral particles to drive expression of GFP and luciferase (referred to as D425GiL). D283 cells were cultured in MEMα (#12561072, Gibco) supplemented with GlutaMAX (Invitrogen) and 10% FBS. D283 were transduced with MSCV-ires-pacLuc2 retroviral particles to drive expression of a puromycin acetyltransferase and codon-optimized firefly luciferase fusion protein (referred to as

D283Luc2). Viral constructs and packaging plasmids were kindly provided by Drs. Richard Williams and Arthur Nienhuis of St. Jude Children's Research Hospital, United States.

In vitro Dose Response Assay

Veliparib (MedChem Express) was dissolved in DMSO (10 mM). D425Gil or D283Luc2 cells (5,000/well) were seeded into black-walled 384-well plates (Costar) and compounds were applied using a D300e digital dispenser (Tecan). Viability was assessed after 72 h using alamarBlue [0.6 mM resazurin, 1 mM potassium hexacyanoferrate (II) trihydrate, 1 mM potassium hexacyanoferrate (III), 2.5% methylene blue]. Resorufin fluorescence (excitation 570 nm, emission 590 nm) was used to calculate the percentage of viable cells relative to control (DMSO) wells. The effective dose that inhibits 50% of cells (ED50) was determined using data pooled from at least three independent experiments. For drug-radiation interaction assays, cells were treated with increasing concentrations of veliparib alone, X-ray radiation alone [1, 2.5, 5, or 7.5 Gy, delivered using an XRAD SmART 225-cx (Precision X-ray) (**Supplementary Methods**)], or the combination of both veliparib and radiation. The combinatorial treatment effects were assessed using Combenefit software (Di Veroli et al., 2016). At least three independent experiments were performed.

Comet Assays

D425Gil cells were treated with DMSO (0.1%) or veliparib (10 μM). After the addition of drug, cells were immediately placed on ice, then exposed to 10 Gy γ-radiation using a cesium source irradiator (Gammacell 3000, MDS Nordion) and returned to ice. Cells were either immediately resuspended in 1% low melting point agarose and spread onto a glass slide, or incubated at 37°C in 5% CO_2 for 10, 20, 40, 60, 80, 100, or 120 min prior to processing. Slides were immersed in lysis solution (2.5 M NaCl, 0.1 M EDTA, 10 mM Tris–HCl and 1% Triton X-100) at 4°C for 1 h, then washed twice in alkaline solution (0.3 M NaOH, 1 mM EDTA). DNA was separated via electrophoresis in alkaline solution for 20 min at 18 V, 4°C. A reference standard slide with pre-irradiated (10 Gy) cells was included in every electrophoresis run for standardization. Slides were washed for 10 min and propidium iodide added for visualization. OpenComet software (Gyori et al., 2014) was used to determine the proportion of damaged DNA in each cell by calculation of percentage tail DNA. A minimum of three experimental replicates were performed.

Immunofluorescence

D425 and D283 cells were seeded onto Matrigel (BD Biosciences) coated coverslips and then treated with DMSO (0.1%) or 10 μM veliparib, followed by either 0 or 2 Gy γ-radiation (Gammacell 3000, MDS Nordion). Cells were fixed 24 h post-irradiation and stained using the following antibodies: γH2AX [Cell Signaling Technologies (CST), #9718S, 1:400], RPA32/RPA2 (CST #2208S, 1:200), AlexaFluor488 anti-rabbit (Life Technologies, #A11008, 1:400) and AlexaFluor568 anti-rat (Life Technologies, #A11077, 1:200). Nuclei were stained using NucBlue (Life Technologies, #R37605), and coverslips mounted in VectorShield (Vector Labs). Images were taken using a Nikon Ti-E microscope and images analyzed using NIS Elements software (Nikon).

Flow Cytometry

Cell cycle distribution was analyzed using EdU (added 45 min before harvest) to label cells in S phase and DAPI to label DNA content. Cells were treated and harvested as indicated in the figure legends. Cells were stained using the Click-iT EdU AlexaFluor488 kit (Invitrogen). Samples were analyzed using an LSRFortessa X20 (BD) and results were visualized and quantified using FlowJo software as previously described (Andradas et al., 2021). Data are pooled from two independent experiments and show the mean with standard deviation (SD).

Protein Analysis by Immunoblotting

D425GiL and D283Luc2 cells were treated with DMSO (0.1%) or 10 μM veliparib, alone or combined with 10 Gy γ-radiation (Gammacell 3000, Nordion). Cells were lysed after 24 h with radioimmunoprecipitation assay (RIPA) buffer containing protease and phosphatase inhibitors (Roche). Protein (30 μg/lane) was separated using 4–12% NuPAGE Bis-Tris gels (Invitrogen) and transferred to nitrocellulose membranes. Membranes were immunoblotted with primary antibodies and horseradish peroxidase-conjugated secondary antibodies (1:5000, Cytiva) which were detected using Supersignal West Dura (Pierce) or Clarity Western ECL (Bio-Rad) and images collected using a ChemiDoc (Bio-Rad). Primary antibodies used were phosphorylated (p-) CHK1^{Ser345} (#2348), p-CHK2^{Thr68} (#2661), p53 (#9282), PAR (#83732), PARP (#9542), CHK1 (#2360), CHK2 (#6334), and γH2AX (#9718S) from CST, and β-actin (Sigma-Aldrich, #A1978). Data are representative of two independent experiments.

Colony-Forming Assays

Medulloblastoma cells were treated with DMSO (0.1%) or veliparib (10 μM), then either untreated or exposed to 2 Gy γ-radiation (Gammacell 3000, Nordion) prior to suspending in media containing 1.25% methylcellulose (STEMCELL Technologies) and plating. After 14 days, colonies at least 100 μm in diameter were counted. Three independent experiments were performed.

Orthotopic Xenograft Model of Medulloblastoma

D425Gil cells (5×10^5) suspended in Matrigel (BD Biosciences) were implanted into the right cerebral cortex of 7–10 weeks old NOD/Rag1$^{-/-}$ mice (Jackson Laboratories). Tumor growth was monitored weekly using bioluminescence imaging (BLI, IVIS Spectrum, Caliper). Mice were randomized into treatment groups with equivalent mean bioluminescence (photons per second per centimeter squared per steradian, abbreviated as p/s). Veliparib dissolved in 20% Captisol® was delivered *per os* (p.o.) twice daily (12.5 mg/kg/dose). When delivered in combination, veliparib was administered 1 h prior to radiotherapy. Radiotherapy was delivered using an X-RAD SmART (Precision X-ray) employing cone-beam CT guidance with fully assessed spatial

and dosimetric accuracy (Feddersen et al., 2019; **Supplementary Material**). For CSI, mice were anesthetized using isoflurane, and 18 Gy was delivered as nine 2 Gy fractions on sequential weekdays. Three sets of two lateral coplanar beams with 40 mm square collimation were delivered to three separate isocentres, with the first set of beams targeting the brain and cervical spine, the second targeting the thoracic spine, and the third targeting the lumbar spine. For Kaplan–Meier analyses an event was counted when mice required euthanasia due to tumor-related morbidity. Mice requiring euthanasia for non-tumor-related reasons (weight loss, physical trauma) were censored. Animal experiments were approved by the Animal Ethics Committee of the Telethon Kids Institute and performed in accordance with Australia's Code for the Care and Use of Animals for Scientific Purposes.

Immunohistochemistry

BALB/c$^{nu/nu}$ mice (Animal Resources Centre) bearing intracranial D425GiL xenografts were treated with either vehicle (20% Captisol®), veliparib (two 12.5 mg/kg doses, p.o., 8 h apart), 2 Gy radiotherapy alone (delivered using the XRAD SmART), or a combination of veliparib and 2 Gy radiotherapy (n = 3–4 per group). Mice were anesthetized after 24 h, perfused with PBS followed by 4% paraformaldehyde (PFA) in PBS and brains were further fixed in 4% PFA/PBS overnight at 4°C prior to paraffin embedding. Tissue sections (5 μm) underwent antigen retrieval in citrate buffer before immunostaining with the following primary antibodies: cleaved caspase-3 (BD, #559565, 1:500), γH2AX (CST, #9718S, 1:500), phospho-histone H3^{Thr3} (CST, #9714, 1:100), PARP-1 (Abcam, #32138, 1:500). Sections were developed using an Elite ABC kit and NovaRED substrate, then counterstained with Gill's hematoxylin (Vector Laboratories). Positively stained cells were quantified using a Nuance spectral unmixing camera and InForm software (Perkin Elmer).

Statistical Analysis

Prism v8.1.2 was used to analyze results. Comet assays were compared using unpaired two-tailed Student's t-tests for each timepoint, using Holm-Sidak correction for multiple comparisons. Comparison of treatments in colony forming assays, immunofluorescence and immunohistochemistry was performed using a one-way ANOVA with Holm-Sidak multiple testing correction. Comparison of Kaplan–Meier survival curves was performed using the Mantel–Cox test. Where multiple testing correction was carried out, adjusted p-values are reported.

RESULTS

PARP Inhibition Alone Does Not Reduce Medulloblastoma Cell Viability

To determine the effect of PARP inhibition on medulloblastoma cell viability *in vitro* drug sensitivity assays were performed using veliparib (**Supplementary Figures 1A,B**). Minimal effect on D425GiL and D283Luc2 medulloblastoma cell viability was observed over a large range of concentrations. The ED50 was estimated to be >25 μM.

Inhibition of PARP Delays Repair of Radiation-Induced DNA Damage

The alkaline comet assay was used to determine the effect of veliparib on radiation-induced DNA damage repair in D425GiL medulloblastoma cells. Veliparib did not induce DNA damage when used as a single agent (**Figure 1A**). Radiation-induced DNA strand breaks, detected as an increase in the percentage of DNA in the comet tail, were almost completely resolved within 2 h in cells treated with DMSO (**Figure 1A**). When the cells were exposed to veliparib in combination with radiation, a significant delay in DNA damage repair following irradiation was observed (**Figure 1A**). These results indicate that PARP inhibition reduces the repair rate of radiation-induced DNA damage in human medulloblastoma cells.

PARP Inhibition Increases DNA Damage Foci

The effect of veliparib, radiation or combination treatment on the number of γH2AX foci (indicating DNA damage) and RPA32/RPA2 foci (indicating DNA repair) in medulloblastoma cells was determined (**Figure 1B**). In D425 cells treated with DMSO or veliparib few γH2AX foci were present but foci were significantly increased upon irradiation (2 Gy) and then further increased upon co-treatment with veliparib and irradiation (**Figures 1B,C**). Cells treated with veliparib showed significantly fewer RPA32/RPA2 DNA repair foci compared to DMSO controls, however there were no significant differences in DNA repair foci between cells treated with 2 Gy irradiation alone and combination veliparib/irradiation at the timepoint examined (24 h, **Figure 1D**). These results were validated in a second medulloblastoma cell line. D283Luc2 cells treated with DMSO or veliparib had few γH2AX foci (**Supplementary Figure 2A**). Irradiation significantly increased γH2AX foci compared to DMSO controls, and cells treated with combination veliparib/irradiation had significantly increased γH2AX foci compared to irradiation alone (**Supplementary Figure 2B**). Furthermore, in these cells RPA32/RPA2 foci were also increased in combination veliparib/radiation-treated cells compared to irradiation alone (**Supplementary Figure 2C**). These data are consistent with the comet assays and suggest that PARP inhibition delays the ability of medulloblastoma cells to repair radiation-induced DNA damage.

DNA Damage Pathways Are Upregulated Following PARP Inhibition

The DDR following veliparib and/or radiation exposure was further assessed using immunoblotting (**Figures 1E–F**). In D425 cells treated with veliparib, either alone or in combination with irradiation, clear inhibition of PARP was observed as a reduction in PAR protein. As expected, DNA damage (as measured by γH2AX abundance) was increased in irradiated medulloblastoma cells, either alone or in combination with veliparib. Notably, although p53 abundance was increased in cells treated with irradiation alone, it was further increased in combination-treated cells indicating exacerbated cellular stress. Radiation induces cell cycle arrest via activation of ATM, ATR and

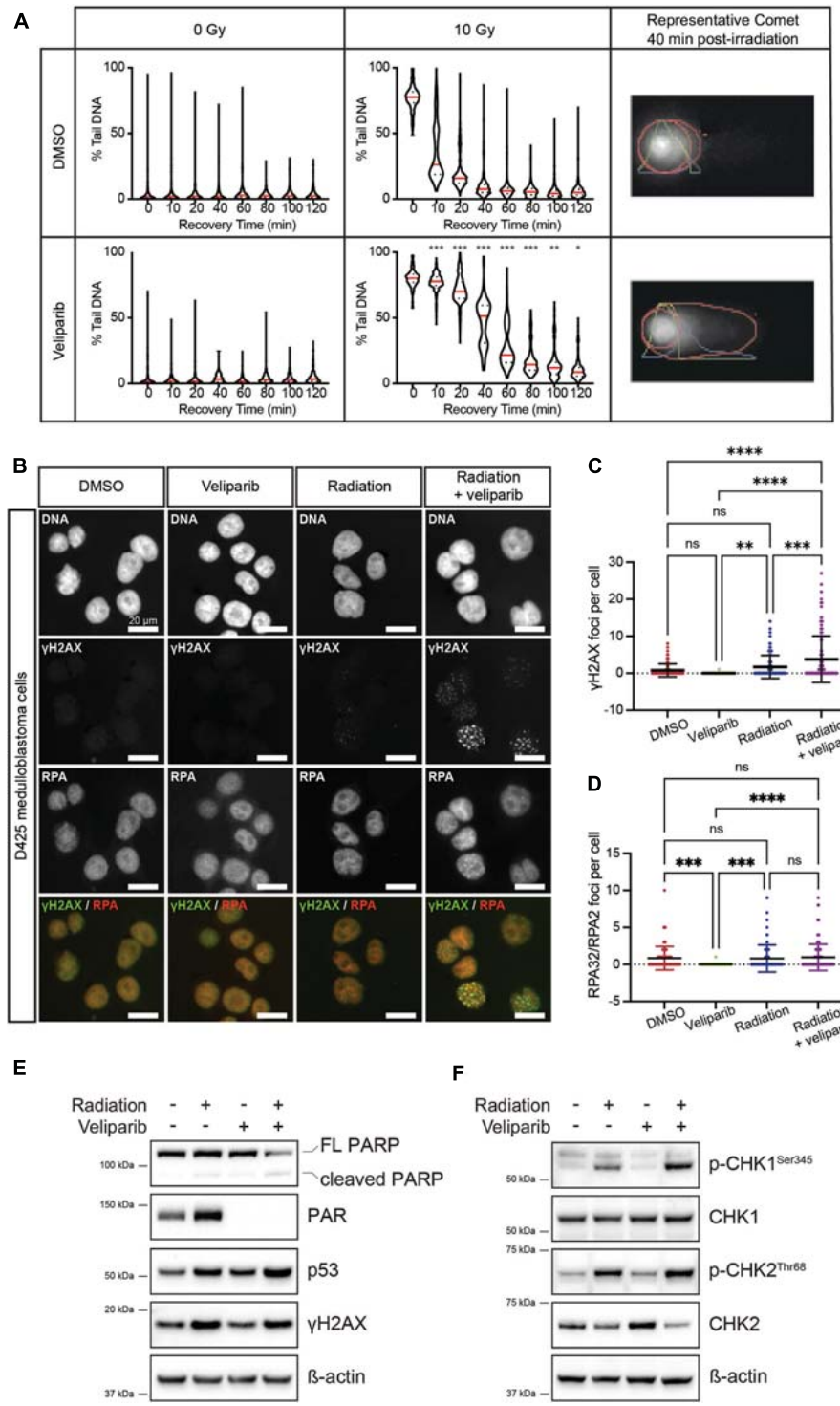

FIGURE 1 | PARP inhibition reduces the repair rate of radiation-induced DNA damage. **(A)** Comet assays were performed to detect DNA damage post-irradiation. Violin plots showing DNA damage (measured as the percent of DNA in the comet tail) for D425GiL medulloblastoma cells treated with DMSO or veliparib; and exposed to 0 or 10 Gy γ-radiation. Mean values for each timepoint are shown in red. $^{*}p < 0.05$, $^{**}p < 0.01$, $^{***}p < 0.001$. Shown are representative images of comets with the head and tail regions outlined in red for each treatment at 40 min recovery time post-irradiation. **(B)** Representative fluorescent microscopy images of D425 medulloblastoma cells stained for DNA damage foci (γH2AX, green) and DNA repair foci (RPA32/RPA2, red), shown as single channel and composite images. Scale bar represents 20 μm. **(C,D)** Quantification of γH2AX foci **(C)** or RPA32/RPA2 **(D)** foci per cell. Each point is an individual cell and mean ± SD is shown. $^{**}p < 0.01$, $^{***}p < 0.001$, $^{****}p < 0.0001$, ns indicates not significant. **(E,F)** Immunoblots for the indicated proteins in D425GiL medulloblastoma cells treated with DMSO (–) or veliparib and exposed to 0 or 10 Gy γ-radiation. Blots are representative of two independent experiments.

phosphorylation of the downstream regulators CHK1 and CHK2 (Huang and Zhou, 2020), which become dephosphorylated upon the completion of DNA repair. As expected, radiation induced both CHK1 and CHK2 phosphorylation, and this was increased by co-treatment with veliparib. Similar effects were observed in D283Luc2 medulloblastoma cells (**Supplementary Figure 2D**). Since CHK1 and CHK2 phosphorylation were increased following combination exposure of cells to veliparib and radiation we also investigated the effects of treatment on cell cycle progression using flow cytometry. D425 and D283 medulloblastoma cells were treated with DMSO, veliparib, radiation or both veliparib and radiation and cell cycle progression was assessed. Radiation induced a reduction in DNA synthesis and robust G2 arrest in both cell lines; however, no difference in cell cycle arrest or recovery was observed in the presence of veliparib (**Supplementary Figure 3**). Overall, the immunoblotting results indicate persistent activation of the DDR pathway when veliparib is combined with radiation and support our data suggesting veliparib delays DNA repair in medulloblastoma cells. Immunoblotting data also revealed that, in both cell lines, PARP cleavage was increased following combination treatment suggesting that apoptosis is induced.

PARP Inhibition Radiosensitizes Medulloblastoma Cells *in vitro*

Due to its effect on DNA damage repair, we investigated if there was a synergistic effect of combining veliparib and radiotherapy *in vitro* using three different mathematical models of measuring drug-radiation interactions (Bliss, 1939; Loewe, 1953; Tan et al., 2012): the Loewe Additivity method (**Figures 2A,B**), Bliss Independence model, and the highest single agent (HSA) model (both shown in **Supplementary Figure 4**). In D425Gil cells, veliparib and radiation was neither synergistic nor antagonistic across multiple different doses indicating an additive interaction (**Figure 2A**) and in D283Luc2 cells, most experimental conditions were additive, although the combination of 25 μM veliparib and 5 Gy radiation demonstrated significant synergy (**Figure 2B**). These results show that PARP inhibition in combination with radiotherapy reduces medulloblastoma cell viability *in vitro*.

The limitation of these interaction assays is that they are performed over a short time frame (72 h). To further investigate the ability of veliparib and radiation to impact medulloblastoma proliferative capacity, clonogenicity assays were performed (**Figures 2C,D**). Medulloblastoma cells treated with radiation (2 Gy) showed significantly reduced colony forming capacity compared to controls (D425, $p < 0.01$; D283, $p < 0.001$). Veliparib alone also significantly impaired colony forming capacity (D425Gil, $p < 0.01$; D283Luc2, $p < 0.001$), which was in contrast to the failure of veliparib to measurably reduce cell viability in the dose response assays. Of note, the combination of veliparib with radiation resulted in a further significant reduction in colony number compared to radiation alone (D425Gil, $p < 0.05$; D283Luc2, $p < 0.01$). These results indicate that veliparib has a radiosensitizing effect on medulloblastoma cells and impairs colony forming capacity.

Veliparib in Combination With Radiation Increases Medulloblastoma Cell Apoptosis *in vivo*

Given the effects of veliparib and radiotherapy co-treatment on medulloblastoma cells *in vitro*, we examined the effect of treatment on medulloblastomas *in vivo* by immunohistochemical analysis of orthotopic D425GiL xenografts grown in immune-deficient mice (**Figure 3**). Combined treatment of mice with veliparib and radiotherapy significantly increased the proportion of apoptotic medulloblastoma cells (marked by cleaved caspase 3) compared to controls or single agents. There was a trend toward increased DNA damage and decreased mitosis (marked using γH2AX and phospho-histone H3, respectively) in medulloblastomas treated with combination therapy, but these results were not statistically significant at the timepoint examined. Notably, no difference in PARP1 staining was observed in the tumors of veliparib-treated mice, likely due to the 24-h timepoint examined, at which point very little veliparib remains in the brain (Gupta et al., 2016).

Veliparib in Combination With Radiotherapy Increases Animal Survival

Given the increased apoptosis observed following combination veliparib/radiotherapy treatment, the effect of veliparib in combination with CSI on medulloblastoma growth and overall animal survival was assessed. Mice with D425GiL medulloblastomas were treated as shown in **Figure 4A** and monitored until the development of tumor-related morbidity (**Figure 4B**). Control mice had a median tumor-free survival of 17 days. Veliparib treatment alone had no impact on animal survival, with a median survival of 17.5 days. As expected, radiotherapy (CSI) increased median survival compared to control mice (34.5 versus 17 days, respectively). Combination treatment with veliparib and radiotherapy significantly increased survival compared to radiotherapy alone, with a median survival of 53 days ($p < 0.05$, **Figure 4B**). Two mice were censored during treatment, one in the veliparib alone group (diarrhea) and one in the radiotherapy alone group (anesthesia-associated death). In concordance with the survival data, bioluminescence flux in mice treated with vehicle or veliparib was similar, while CSI delayed tumor growth (**Figures 4C,D**). Tumor growth was further delayed in mice treated with veliparib in combination with CSI; however, tumor regression was not observed.

DISCUSSION

This study aimed to identify treatments to improve medulloblastoma patient outcomes. We tested inhibition of the DDR pathway in combination with radiotherapy in *MYC*-amplified Group 3 medulloblastoma. Veliparib, a small molecule inhibitor of PARP1/2, was assessed for its ability to inhibit DNA repair in two human medulloblastoma cell lines.

In vitro assays were performed to test the effect of veliparib on medulloblastoma cell viability. Doses of up to 25 μM had no effect on the viability of medulloblastoma cells over a

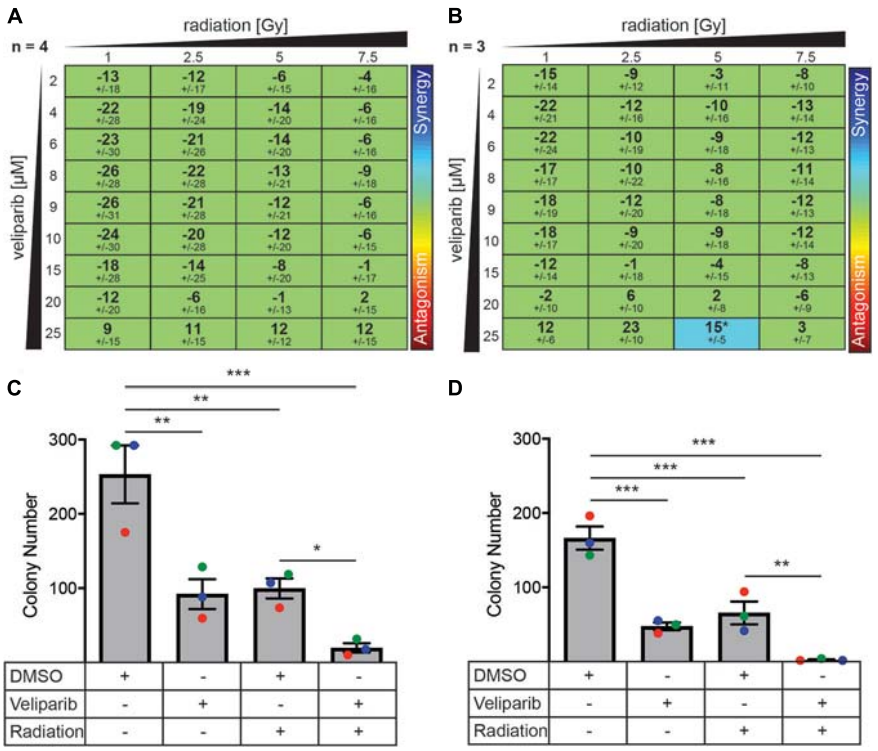

FIGURE 2 | PARP inhibitors enhance radiation-induced cytotoxicity and decrease colony forming ability in medulloblastoma cells. **(A)** D425GiL and **(B)** D283Luc2 cells were treated with increasing doses of radiation combined with veliparib and the mean ± SD synergy score for each combination was calculated using the Loewe Additivity model. Values greater than or less than zero indicate synergy or antagonism, respectively (indicated by the rainbow heat map). The number (*n*) of independent experiments used in the analysis is shown, and statistical comparisons were performed as described by Di Veroli et al., 2016. $^{*}p < 0.05$. **(C)** D425Gil and **(D)** D283Luc2 cells were treated with DMSO, veliparib, 2 Gy irradiation or a combination of veliparib and irradiation as indicated and plated in methylcellulose. The mean number of colonies formed ± SEM is shown from three independent experiments (indicated in different colors). Groups were compared using one-way ANOVA with Holm–Sidak multiple testing correction. $^{*}p < 0.05$, $^{**}p < 0.01$, $^{***}p < 0.001$.

short time course. Higher doses were not tested, as they are unlikely to be achieved *in vivo* in the brain or brain tumor. Recent studies have shown peak concentrations of 0.71 and 3.0 μmol/L were achieved in mouse brain and brain tumors respectively, using the same veliparib dosing schedule as this study (Donawho et al., 2007; Gupta et al., 2016). It is important to note that since these medulloblastoma cell lines are not deficient in HR, we did not expect to see synthetic lethality, and therefore did not expect veliparib alone to affect viability; although, veliparib exposure did inhibit the colony-forming ability of medulloblastoma cells over a longer experimental period *in vitro*. Despite showing minimal cytotoxicity using the metabolic reagent alamarBlue, veliparib significantly reduced medulloblastoma cell colony forming capacity to a similar extent as radiation. To test the potential of veliparib to act as a radiosensitizing agent, we examined the interaction between veliparib and radiotherapy using both alamarBlue and clonogenicity assays. The combination of veliparib and radiation was found to be mostly additive with some synergy, suggesting that it may be an efficient radiosensitizer in medulloblastoma. Notably, the combination of veliparib and radiation significantly reduced colony formation for both cell lines. This demonstrates the limitation of short-term metabolic assays in understanding the impact of drug treatment *in vitro*, and adds evidence to suggest that veliparib can enhance medulloblastoma control in combination with radiotherapy. This potential radiosensitizing ability of PARP inhibition is consistent with observations made with veliparib in other brain cancers such as glioblastoma (Jue et al., 2017), and the PARP inhibitor olaparib on D283 medulloblastoma cells (Van Vuurden et al., 2011).

Mechanistically, comet assays demonstrated that veliparib was able to delay repair of radiation-induced DNA damage in the medulloblastoma cells tested. This is consistent with PARP1 deficient cells, which also exhibit delayed but not ablated DDR activation (Haince et al., 2007). However, veliparib treated cells had not completely repaired the radiation-induced DNA damage by the end of the experiment, warranting further investigation on the lasting mutational burden in these cells. This may be of particular importance since pediatric brain tumors are known to have low mutational burden, partially contributing to the relative lack of success with some immunotherapies (Wang et al., 2019; Patel et al., 2020). In further support of a potential therapeutic benefit that may be achieved by combining veliparib and radiation is the increased γH2AX foci in medulloblastoma cells following combination treatment compared to radiation alone. Additionally, in the *TP53* mutant

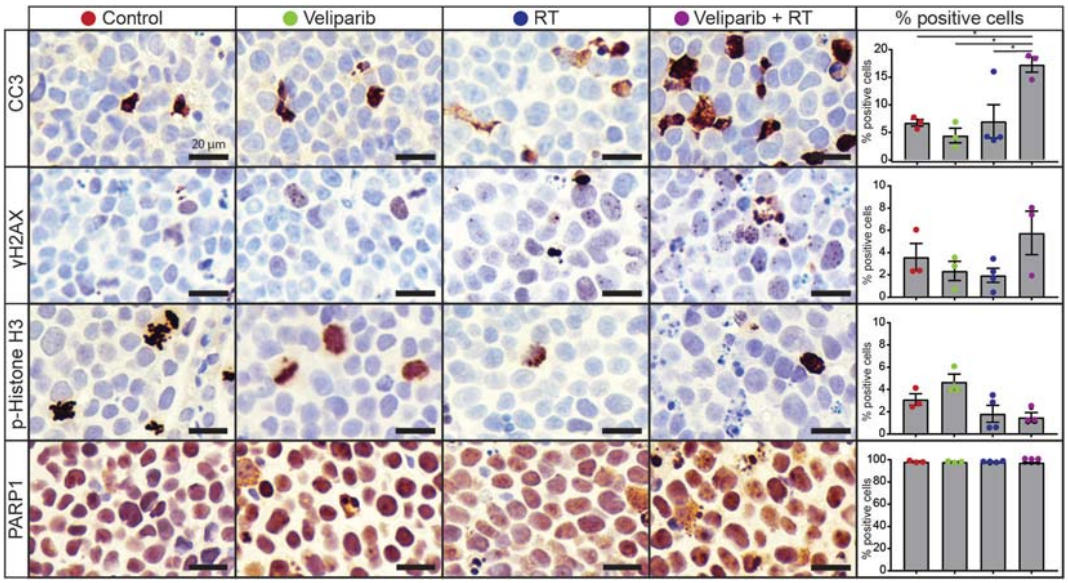

FIGURE 3 | Veliparib in combination with radiotherapy increases apoptosis in an orthotopic xenograft model of medulloblastoma. Representative images are shown of immunohistochemistry for cleaved caspase 3 (CC3), γH2AX, phospho(p)-histone H3, and PARP1 from D425GiL xenografts in mice treated with vehicle, veliparib, radiotherapy (RT) or the combination of both veliparib and RT. The percentage of positively stained medulloblastoma cells for each antibody were quantified from three independent fields of view per tumor from $n = 3$ or 4 mice per treatment group. Error bars represent SEM. Scale bar represents 20 μm. $^{*}p < 0.05$.

D425 cell line, veliparib markedly reduced the formation of DNA repair foci, and when combined with irradiation, no increase in DNA repair foci was seen in veliparib-treated cells despite increased DNA damage. This effect was not seen in the *TP53* wild-type D283Luc2 cells, suggesting that p53 deficient cells may show an increased response to PARP inhibition in combination with radiotherapy. In combination with radiation, veliparib also increased downstream activation of the DDR pathway, including increases in p53, phosphorylated CHK1^{Ser345} and phosphorylated CHK2^{Thr68}, suggesting the persistence of DNA damage in the combination treated cells.

Following these encouraging *in vitro* results, veliparib was tested as a radiosensitizing agent in a mouse model of medulloblastoma. Immunohistochemistry demonstrated that a single dose of veliparib in combination with radiotherapy significantly increased intratumoral apoptosis, suggesting that veliparib improves radiation-induced medulloblastoma cell death *in vivo*. A trend toward increased DNA damage and decreased mitosis was observed in combination treatment groups, although this was limited by the small number of animals examined and was not statistically significant. PARP-1 expression was high in D425Gil tumors, consistent with a previous study showing high expression in D283 medulloblastoma cells and clinical samples (Van Vuurden et al., 2011), although this expression remained high in groups treated with veliparib. Veliparib has been shown to cross the blood–brain barrier (Donawho et al., 2007) and our observed increase in apoptosis confirms intratumoral drug penetration in this model. However, pharmacokinetic studies in brain tissue show veliparib concentrations peak shortly after administration but are almost absent 6 h thereafter (Gupta et al., 2016), likely explaining why no change in PARP-1 expression was observed in our samples examined 24 h post-treatment. Due to the short half-life of veliparib, we chose twice daily administration to assess the impact of treatment on animal survival, similar to Jue et al. (2017).

The potential of veliparib to extend survival was examined *in vivo* using an orthotopic xenograft mouse model of Group 3 medulloblastoma. Veliparib had no effect on survival compared to controls, further confirming the *in vitro* findings that veliparib monotherapy was insufficient to induce medulloblastoma cell death. CSI alone increased survival over control groups but did not cure mice, consistent with clinical outcomes. The addition of veliparib to CSI significantly increased survival beyond that of radiotherapy alone, confirming our *in vitro* and immunohistochemical findings, and demonstrating the radiosensitizing potential of veliparib in an orthotopic xenograft model of medulloblastoma for the first time.

While veliparib was studied due to its clinical advancement at the time, many other PARP inhibitors with greater PARP trapping abilities and more favorable pharmacokinetics have since been investigated (Pommier et al., 2016). Several adult clinical trials have examined, or are in the process of examining the safety of PARP inhibitors such as olaparib (NCT03212742), rucaparib (NCT03542175), and niraparib (NCT03076203) in combination with radiotherapy. Other PARP inhibitors have also moved into clinical trial for pediatric brain cancers. Olaparib has been tested as a single agent (Pediatric MATCH, NCT03233204) (Takagi et al., 2019) in pediatric solid tumors, and was well tolerated. One patient with pediatric high-grade glioma who was treated with olaparib and temozolomide demonstrated a 2 year durable response (Valiakhmetova et al., 2020). Talazoparib has

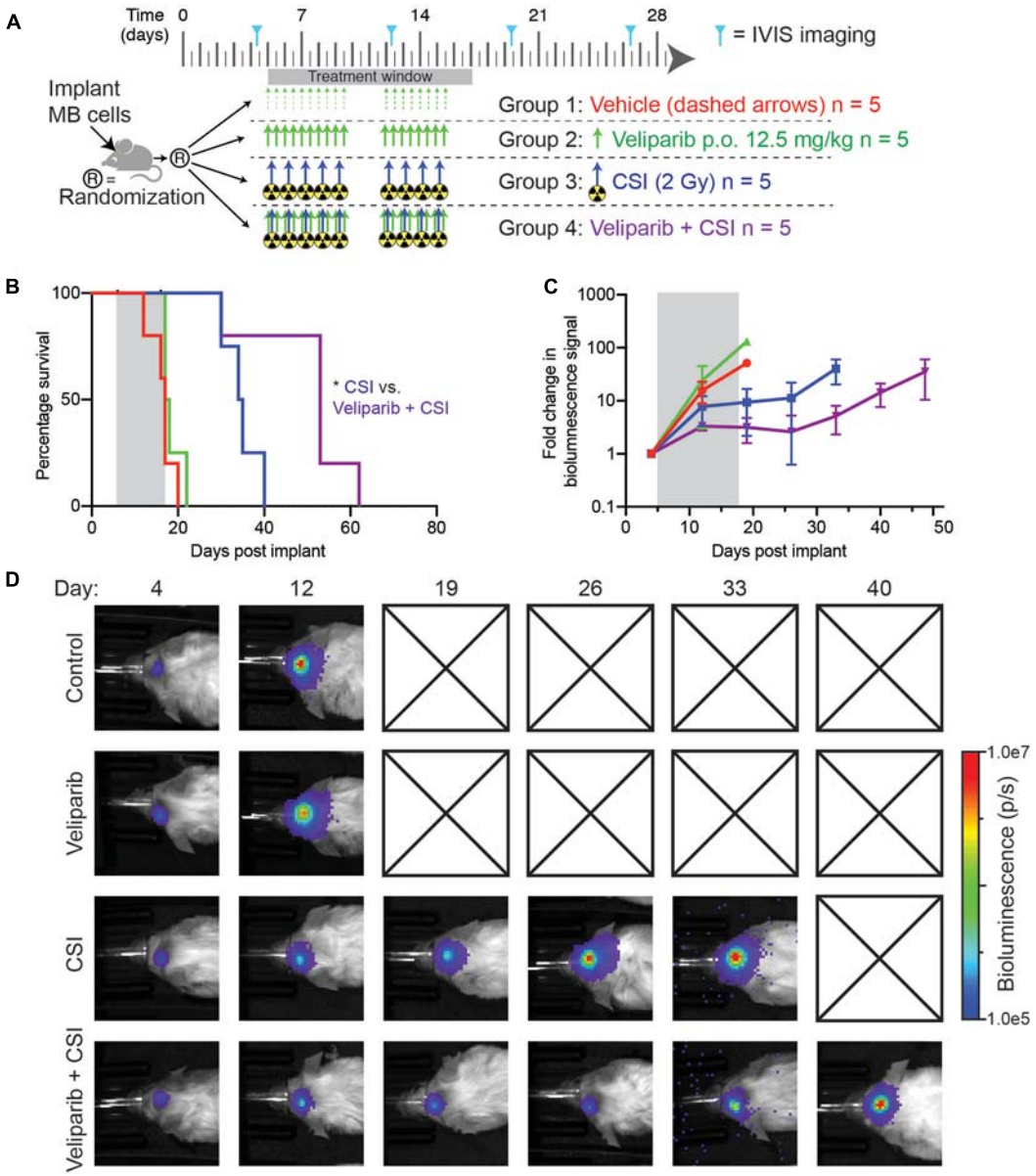

FIGURE 4 | Combination veliparib and CSI extends survival of mice with medulloblastoma. **(A)** Preclinical mouse treatment protocol for mice with orthotopic D425GiL Group 3 medulloblastoma for data shown in **(B-D)**, $n = 5$ mice per group. **(B)** Survival curves for mice treated as indicated in **(A)**. Mantel–Cox tests compared the combination-treated group with CSI alone: $^*p < 0.05$. **(C)** Bioluminescence measurements from the animals shown in **(B)**. Data are represented as the fold change in mean ± SD bioluminescence flux measured over time with a representative mouse from each group shown in **(D)**. Checked boxes indicate that the animal was euthanized prior to the timepoint shown.

also been tested with temozolomide in pediatric solid tumors, though limited anti-tumor activity was observed in CNS tumors (Schafer et al., 2020), likely due to poor blood-brain barrier penetrance (Kizilbash et al., 2017).

Collectively our preclinical data demonstrate that PARP inhibition can improve animal survival in combination with radiotherapy. Although veliparib may not be the optimal PARP inhibitor to take forward clinically, we provide evidence that radiosensitization through PARP inhibition shows promise for improving the efficacy of radiotherapy in medulloblastoma.

DATA AVAILABILITY STATEMENT

The raw data supporting the conclusions of this article will be made available by the authors, without undue reservation.

ETHICS STATEMENT

The animal study was reviewed and approved by the Telethon Kids Institute Animal Ethics Committee.

AUTHOR CONTRIBUTIONS

RE, ME, KM, and NG designed the study. JBu, PD, HH, BC, MK, JBy, JW, and RE performed the experiments. JBu, PD, MH, and RE analyzed the data. JBu, PD, MH, NG, and RE prepared and intellectually assessed the manuscript. All authors read and approved the final version of the manuscript.

FUNDING

Funding for this work was provided by the National Health and Medical Research Council (APP1164804) and from the Pirate Ship Foundation. JBu was funded by a Forrest Fellowship (Forrest Foundation), NG was supported by a Cancer Council of Western Australia Fellowship and the Stan Perron Chair of Paediatric Haematology and Oncology, and RE had support from the Brainchild Fellowship.

ACKNOWLEDGMENTS

We thank all members of the Telethon Kids Institute Brain Tumour Research team for their advice, suggestions and discussions during the course of this project. We would like to thank Darell Bigner of Duke University and Arthur Nienhuis and Richard Williams of St. Jude Children's Research Hospital for providing reagents. We also thank the Telethon Kids Institute Bioresources team for their assistance with animal husbandry, and Blake Klyen and Tamara Abel for their assistance with the XRAD SmART.

SUPPLEMENTARY MATERIAL

The Supplementary Material for this article can be found online at: https://www.frontiersin.org/articles/10.3389/fmolb.2021.633344/full#supplementary-material

REFERENCES

Andradas, C., Byrne, J., Kuchibhotla, M., Ancliffe, M., Jones, A. C., Carline, B., et al. (2021). Assessment of Cannabidiol and Δ9-Tetrahydrocannabiol in Mouse Models of Medulloblastoma and Ependymoma. *Cancers* 13:330. doi: 10.3390/cancers13020330

Baxter, P. A., Su, J. M., Onar-Thomas, A., Billups, C. A., Li, X.-N., Poussaint, T. Y., et al. (2020). A phase I/II study of veliparib (ABT-888) with radiation and temozolomide in newly diagnosed diffuse pontine glioma: a Pediatric Brain Tumor Consortium study. *Neuro Oncol.* 22, 875–885. doi: 10.1093/neuonc/noaa016

Bigner, S. H., Friedman, H. S., Vogelstein, B., Oakes, W. J., and Bigner, D. D. (1990). Amplification of the c-myc gene in human medulloblastoma cell lines and xenografts. *Cancer Res.* 50, 2347–2350.

Bliss, C. I. (1939). The toxicity of poisons applied jointly. *Ann. Appl. Biol.* 26, 585–615. doi: 10.1111/j.1744-7348.1939.tb06990.x

Carrassa, L., and Damia, G. (2017). DNA damage response inhibitors: mechanisms and potential applications in cancer therapy. *Cancer Treat. Rev.* 60, 139–151. doi: 10.1016/j.ctrv.2017.08.013

Chornenkyy, Y., Agnihotri, S., Yu, M., Buczkowicz, P., Rakopoulos, P., Golbourn, B., et al. (2015). Poly-ADP-Ribose Polymerase as a Therapeutic Target in Pediatric Diffuse Intrinsic Pontine Glioma and Pediatric High-Grade Astrocytoma. *Mol. Cancer Ther.* 14:2560. doi: 10.1158/1535-7163.mct-15-0282

Daniel, R. A., Rozanska, A. L., Mulligan, E. A., Drew, Y., Thomas, H. D., Castelbuono, D. J., et al. (2010). Central nervous system penetration and enhancement of temozolomide activity in childhood medulloblastoma models by poly(ADP-ribose) polymerase inhibitor AG-014699. *Br. J. Cancer* 103, 1588–1596. doi: 10.1038/sj.bjc.6605946

Di Veroli, G. Y., Fornari, C., Wang, D., Mollard, S., Bramhall, J. L., Richards, F. M., et al. (2016). Combenefit: an interactive platform for the analysis and visualization of drug combinations. *Bioinformatics* 32, 2866–2868. doi: 10.1093/bioinformatics/btw230

Donawho, C. K., Luo, Y., Luo, Y., Penning, T. D., Bauch, J. L., Bouska, J. J., et al. (2007). ABT-888, an orally active poly(ADP-ribose) polymerase inhibitor that potentiates DNA-damaging agents in preclinical tumor models. *Clin. Cancer Res.* 13, 2728–2737.

Endersby, R., Whitehouse, J., Pribnow, A., Kuchibhotla, M., Hii, H., Carline, B., et al. (2021). Small-molecule screen reveals synergy of cell cycle checkpoint kinase inhibitors with DNA-damaging chemotherapies in medulloblastoma. *Sci. Transl. Med.* 13:eaba7401. doi: 10.1126/scitranslmed.aba7401

Feddersen, T. V., Rowshanfarzad, P., Abel, T. N., and Ebert, M. A. (2019). Commissioning and performance characteristics of a pre-clinical image-guided radiotherapy system. *Australas. Phys. Eng. Sci. Med.* 42, 541–551. doi: 10.1007/s13246-019-00755-4

Friedman, H. S., Burger, P. C., Bigner, S. H., Trojanowski, J. Q., Wikstrand, C. J., Halperin, E. C., et al. (1985). Establishment and Characterization of the Human Medulloblastoma Cell Line and Transplantable Xenograft D283 Med. *J. Neuropathol. Exper. Neurol.* 44, 592–605. doi: 10.1097/00005072-198511000-00005

Gupta, S. K., Kizilbash, S. H., Carlson, B. L., Mladek, A. C., Boakye-Agyeman, F., Bakken, K. K., et al. (2016). Delineation of MGMT Hypermethylation as a Biomarker for Veliparib-Mediated Temozolomide-Sensitizing Therapy of Glioblastoma. *J. Natl. Cancer Inst.* 108:djv369. doi: 10.1093/jnci/djv369

Gyori, B. M., Venkatachalam, G., Thiagarajan, P. S., Hsu, D., and Clement, M. V. (2014). OpenComet: an automated tool for comet assay image analysis. *Redox Biol.* 2, 457–465. doi: 10.1016/j.redox.2013.12.020

Haince, J.-F., Kozlov, S., Dawson, V. L., Dawson, T. M., Hendzel, M. J., Lavin, M. F., et al. (2007). Ataxia Telangiectasia Mutated (ATM) Signaling Network Is Modulated by a Novel Poly(ADP-ribose)-dependent Pathway in the Early Response to DNA-damaging Agents. *J. Biol. Chem.* 282, 16441–16453. doi: 10.1074/jbc.m608406200

Hovestadt, V., Ayrault, O., Swartling, F. J., Robinson, G. W., Pfister, S. M., and Northcott, P. A. (2020). Medulloblastomics revisited: biological and clinical insights from thousands of patients. *Nat. Rev. Cancer* 20, 42–56. doi: 10.1038/s41568-019-0223-8

Huang, R.-X., and Zhou, P.-K. (2020). DNA damage response signaling pathways and targets for radiotherapy sensitization in cancer. *Signal Transduct. Target. Ther.* 5:60.

Janysek, D. C., Kim, J., Duijf, P. H. G., and Dray, E. (2021). Clinical use and mechanisms of resistance for PARP inhibitors in homologous recombination-deficient cancers. *Transl. Oncol.* 14:101012. doi: 10.1016/j.tranon.2021.101012

Jue, T. R., Nozue, K., Lester, A. J., Joshi, S., Schroder, L. B., Whittaker, S. P., et al. (2017). Veliparib in combination with radiotherapy for the treatment of MGMT unmethylated glioblastoma. *J. Transl. Med.* 15:61.

Kamaletdinova, T., Fanaei-Kahrani, Z., and Wang, Z.-Q. (2019). The Enigmatic Function of PARP1: from PARylation Activity to PAR Readers. *Cells* 8:1625. doi: 10.3390/cells8121625

Kizilbash, S. H., Gupta, S. K., Chang, K., Kawashima, R., Parrish, K. E., Carlson, B. L., et al. (2017). Restricted Delivery of Talazoparib Across the Blood-Brain Barrier Limits the Sensitizing Effects of PARP Inhibition on Temozolomide Therapy in Glioblastoma. *Mol. Cancer Ther.* 16, 2735–2746. doi: 10.1158/1535-7163.mct-17-0365

Loewe, S. (1953). The problem of synergism and antagonism of combined drugs. *Arzneimittel Forschung* 3, 285–290.

Louis, D. N., Perry, A., Reifenberger, G., Von Deimling, A., Figarella-Branger, D., Cavenee, W. K., et al. (2016). The 2016 World Health Organization classification of tumors of the central nervous system: a summary. *Acta Neuropathol.* 131, 803–820. doi: 10.1007/s00401-016-1545-1

Martin, A. M., Raabe, E., Eberhart, C., and Cohen, K. J. (2014). Management of pediatric and adult patients with medulloblastoma. *Curr. Treat. Options Oncol.* 15, 581–594. doi: 10.1007/s11864-014-0306-4

Millard, N. E., and De Braganca, K. C. (2016). Medulloblastoma. *J. Child Neurol.* 31, 1341–1353.

Murai, J., Huang, S. Y., Das, B. B., Renaud, A., Zhang, Y., Doroshow, J. H., et al. (2012). Trapping of PARP1 and PARP2 by Clinical PARP Inhibitors. *Cancer Res.* 72, 5588–5599. doi: 10.1158/0008-5472.can-12-2753

Northcott, P. A., Robinson, G. W., Kratz, C. P., Mabbott, D. J., Pomeroy, S. L., Clifford, S. C., et al. (2019). Medulloblastoma. *Nat. Rev. Dis. Primers* 5:11.

Patel, R. R., Ramkissoon, S. H., Ross, J., and Weintraub, L. (2020). Tumor mutational burden and driver mutations: characterizing the genomic landscape of pediatric brain tumors. *Pediatr. Blood Cancer* 67:e28338.

Pommier, Y., O'connor, M. J., and De Bono, J. (2016). Laying a trap to kill cancer cells: PARP inhibitors and their mechanisms of action. *Sci. Transl. Med.* 8:362ps17. doi: 10.1126/scitranslmed.aaf9246

Schafer, E. S., Rau, R. E., Berg, S. L., Liu, X., Minard, C. G., Bishop, A. J. R., et al. (2020). Phase 1/2 trial of talazoparib in combination with temozolomide in children and adolescents with refractory/recurrent solid tumors including Ewing sarcoma: a Children's Oncology Group Phase 1 Consortium study (ADVL1411). *Pediatr. Blood Cancer* 67:e28073.

Su, J. M., Thompson, P., Adesina, A., Li, X. N., Kilburn, L., Onar-Thomas, A., et al. (2014). A phase I trial of veliparib (ABT-888) and temozolomide in children with recurrent CNS tumors: a pediatric brain tumor consortium report. *Neuro Oncol.* 16, 1661–1668. doi: 10.1093/neuonc/nou103

Takagi, M., Ogawa, C., Aoki-Nogami, Y., Iehara, T., Ishibashi, E., Imai, M., et al. (2019). Phase I clinical study of oral olaparib in pediatric patients with refractory solid tumors: study protocol. *BMC Pediatr.* 19:31. doi: 10.1186/s12887-019-1409-7

Tan, X., Hu, L., Luquette, L. J. III, Gao, G., Liu, Y., Qu, H., et al. (2012). Systematic identification of synergistic drug pairs targeting HIV. *Nat. Biotechnol.* 30, 1125–1130. doi: 10.1038/nbt.2391

Thompson, M. C., Fuller, C., Hogg, T. L., Dalton, J., Finkelstein, D., Lau, C. C., et al. (2006). Genomics Identifies Medulloblastoma Subgroups That Are Enriched for Specific Genetic Alterations. *J. Clin. Oncol.* 24, 1924–1931. doi: 10.1200/jco.2005.04.4974

Valiakhmetova, A., Gorelyshev, S., Konovalov, A., Trunin, Y., Savateev, A., Kram, D. E., et al. (2020). Treatment of Pediatric Glioblastoma with Combination Olaparib and Temozolomide Demonstrates 2-Year Durable Response. *Oncologist* 25, e198–e202.

Van Vuurden, D. G., Hulleman, E., Meijer, O. L. M., Wedekind, L. E., Kool, M., Witt, H., et al. (2011). PARP inhibition sensitizes childhood high grade glioma, medulloblastoma and ependymoma to radiation. *Oncotarget* 2, 984–996. doi: 10.18632/oncotarget.362

Wang, S. S., Bandopadhayay, P., and Jenkins, M. R. (2019). Towards Immunotherapy for Pediatric Brain Tumors. *Trends Immunol.* 40, 748–761. doi: 10.1016/j.it.2019.05.009

Conflict of Interest: KM was employed by company Brain Cancer Consultancy.

The remaining authors declare that the research was conducted in the absence of any commercial or financial relationships that could be construed as a potential conflict of interest.

frontiers in Cell and Developmental Biology

ORIGINAL RESEARCH
published: 10 June 2021
doi: 10.3389/fcell.2021.666376

MCM4 Is a Novel Biomarker Associated With Genomic Instability, BRCAness Phenotype, and Therapeutic Potentials in Soft-Tissue Sarcoma

Qi Liu[1‡], Qiyuan Bao[1‡], Yiqi Xu[1‡], Yucheng Fu[1], Zhijian Jin[1], Jun Wang[2], Weibin Zhang[1,2†] and Yuhui Shen[1,2*†]*

[1] Department of Orthopedics, Ruijin Hospital, Shanghai Jiao Tong University School of Medicine, Shanghai, China, [2] Shanghai Institute of Orthopedics and Traumatology, Ruijin Hospital, Shanghai Jiao Tong University School of Medicine, Shanghai, China

Soft-tissue sarcoma (STS) is represented by a heterogeneous group of rare malignancies with various molecular oncogenesis. Therapies targeting DNA repair pathways in STS have achieved minimal progress, potentially due to the lack of molecular biomarker(s) beyond the histology subtype. In this report, we comprehensively analyzed the expression profiles of 100 liposarcomas (LPSs), the most common STS subtype, in comparison with 21 adipose tissues from multiple GEO datasets to identify the potential prognostic and therapeutic biomarker for LPS. Furthermore, we investigated TCGA database, our archived tumor samples, and patient-derived tumor cell cultures (PTCCs) as a validation. We identified a total of 69 common differentially expressed genes (DEGs) among public datasets, with mini-chromosome maintenance protein 4 (MCM4) identified as a novel biomarker correlated with patients' clinical staging and survival outcome. MCM4-high expression LPS was characterized by MCM4 copy number increase, genomic instability, and BRCAness phenotype compared with the MCM4-low expression counterpart. In contrast, the mutational and the immune landscape were minimally different between the two groups. Interestingly, the association of MCM4-high expression with genomic instability and BRCAness were not only validated in LPS samples from our institution (n = 66) but also could be expanded to the pan-sarcoma cohort from TCGA database (n = 263). Surprisingly, based on four sarcoma cell lines and eight PTCCs (three LPS and five other sarcoma), we demonstrated that MCM4 overexpression tumors were therapeutically sensitive to PARP inhibitor (PARPi) and platinum chemotherapy, independent of the histology subtypes. Our study, for the first time, suggested that MCM4 might be a novel prognostic biomarker, associated with dysregulated DNA repair pathways and potential therapeutic vulnerability in STS.

Keywords: mini-chromosome maintenance protein 4 (MCM4), soft-tissue sarcoma, liposarcoma, genome instability, BRCAness phenotype

OPEN ACCESS

Edited by:
Amila Suraweera, Queensland University of Technology, Australia

Reviewed by:
Richard Chahwan, University of Zurich, Switzerland
Santosh Panjikar, Australian Synchrotron, Australia

****Correspondence:***
Weibin Zhang
zhangweibin10368@163.com
Yuhui Shen
yuhuiss@163.com

†ORCID:
Weibin Zhang
orcid.org/0000-0002-5247-3438
Yuhui Shen
orcid.org/0000-0002-9220-6473

‡These authors have contributed equally to this work and share first authorship

Specialty section:
This article was submitted to Cellular Biochemistry, a section of the journal Frontiers in Cell and Developmental Biology

Received: *10 February 2021*
Accepted: *11 May 2021*
Published: *10 June 2021*

Citation:
Liu Q, Bao Q, Xu Y, Fu Y, Jin Z, Wang J, Zhang W and Shen Y (2021) MCM4 Is a Novel Biomarker Associated With Genomic Instability, BRCAness Phenotype, and Therapeutic Potentials in Soft-Tissue Sarcoma. Front. Cell Dev. Biol. 9:666376. doi: 10.3389/fcell.2021.666376

INTRODUCTION

Soft-tissue sarcoma (STS) is represented by a heterogeneous group (>70 subtypes) of rare malignancies with a variety of molecular oncogenesis. The metastasis rate of STS in patients with intermediate- or high-grade tumors that are large and deeply seated to the fascia is approximated 50% despite local curative therapy, leading to dismal survival outcome. Currently, the prognostic and predictive biomarker(s) beyond histology-based classification is still lacking.

For example, liposarcoma (LPS) is one of the most common types of STS in the extremities and retroperitoneum with a variety of molecular pathogenesis (Crago and Brennan, 2015). Studies have shown that the primary pathological assessment of LPS results in a 25% misclassification of the histologic subtypes, indicating a pathological and morphological continuum of LPS tumor cells (de Vreeze et al., 2010). Furthermore, due to the inter-tumor heterogeneity, the biological behavior of the same LPS tumor could be drastically varied from proportion to another (Swanton, 2012; Bill et al., 2016). It was estimated that 20–40% of relapsed well-differentiated LPS (WDLS) could be identified with a dedifferentiated LPS (DDLS) component (Singer et al., 2003; Fabre-Guillevin et al., 2006). In contrast, tumor cells of different subtypes of LPS could also share common signaling pathways (Bill et al., 2016), epigenetic aberration (Chen et al., 2019), and intra-tumoral immune microenvironment (Tseng et al., 2015). Therefore, patient stratification based on histology alone is insufficient for the prognostication and management of sarcoma. Unfortunately, the molecular biomarkers for most of the STS have been minimally improved over the past decades (Patel et al., 2017). Therefore, novel histology-independent biomarker(s) for tailored prognosis and therapeutic regimen is as-yet to be exploited in LPS as well as in other histology subtypes.

In this report, we comprehensively analyzed the transcriptome of 100 LPS and 21 adipose tissue samples from multiple Gene Expression Omnibus (GEO) datasets, and identified mini-chromosome maintenance protein 4 (MCM4) as a novel biomarker associated with patient prognosis, as well as the genomic instability and BRCAness phenotype. We then investigated the MCM4 expression profiles from our archived tumor samples, nine histology subtypes of STS in TCGA, and patient-derived tumor cell cultures (PTCCs) as a validation (**Figure 1A**).

MATERIALS AND METHODS

Gene Expression Omnibus Datasets and Microarray Data Analysis

To study the gene expression profiles, we obtained three LPS cohorts from the GEO database (**Supplementary Table 1**): (1) GSE21124 (89 LPS and 9 adipose tissues), (2) GSE51049 (4 LPS and 4 adipose tissues), and (3) GSE62747 (7 LPS and 8 adipose tissues). The online tool GEO2R (Davis and Meltzer, 2007) was used to screen for the differentially expressed genes (DEGs) between cancer and normal samples, according to the criteria of false discovery rate (FDR) < 0.05 and $|$ fold-change (FC)$| \geq 2$. The results were then overlapped to identify the common DEGs among three cohorts (**Figures 1A,B**). For multiple probes mapping to the same gene, we exhibited those with the max $|$ log2FC$|$ in the heatmap. Besides, to explore the gene expression between cell lines with different therapeutic sensitivity, we downloaded the raw RNA-seq data of sarcoma cell lines from GSE76981, comprising four STS cell lines (HT1080, SW684, DMR, and 402.91) and two bone sarcoma cell lines (TC106 and SJSA1).

Prioritization of the Prognostic Biomarker of Liposarcoma

To prioritize the gene of interest from common DEGs, a protein–protein interaction network was constructed using STRING database (**Supplementary Table 1**). The Molecular Complex Detection (MCODE) app in Cytoscape software v3.7.1 (confidence score $\geq$ 0.4) (Shannon et al., 2003) was used to remove the separated nodes in network, thereby leaving the key hub genes.

Using the clinical data of 60 patients with LPS in GDC TCGA-SARC cohort (**Supplementary Table 1**), the hub genes were then assessed by univariate and multivariate Cox regression analysis via the "survival" R package to prioritize the gene with the greatest prognostic significance. In univariate Cox regression analysis, we computed the hazard ratio of the hub genes contributing to the worse survival outcome (death). The hazard ratio is defined as the ratio of (hazard rate in study group)/(hazard rate in control group), while the hazard rate is the chance of a hazardous event occurring at a given time (Blagoev et al., 2012). The gene expression values were dichotomized according to the median expression into high-expression subset and low-expression subset. Furthermore, to identify the independent prognostic biomarker in LPS, multivariate analysis was performed among genes with hazard ratio > 1 and $p < 0.05$ in the univariate analysis. Results were demonstrated using "forestplot" and "survival" package in R. The receiver operating characteristic (ROC) curves were plotted to predict the 1-, 3-, and 5-year survival of patients based on MCM4 expression, via "survivalROC" package in R.

Multi-Omics Analysis of MCM4-High Liposarcoma

Multi-Omics data of the aforementioned 60 LPS specimens were obtained from the GDC data portal as well (**Supplementary Table 1**). LPS were classified into MCM4-high ($n = 30$) vs. MCM4-low ($n = 30$) subset using the median MCM4 expression level as the cutoff. For somatic mutations, we compared the difference of mutation frequencies and tumor mutation burden (TMB) between these two groups, and visualized the results by "maftools" package in R. The TMB was calculated as the total mutation frequency/megabase (Mb) for each sample. Then, we analyzed the association of MCM4 copy number and MCM4 methylation with MCM4 expression. The test results were visualized by "ggplot2" and "ggpubr" package in R. Finally, the transcriptome and immune landscape between the

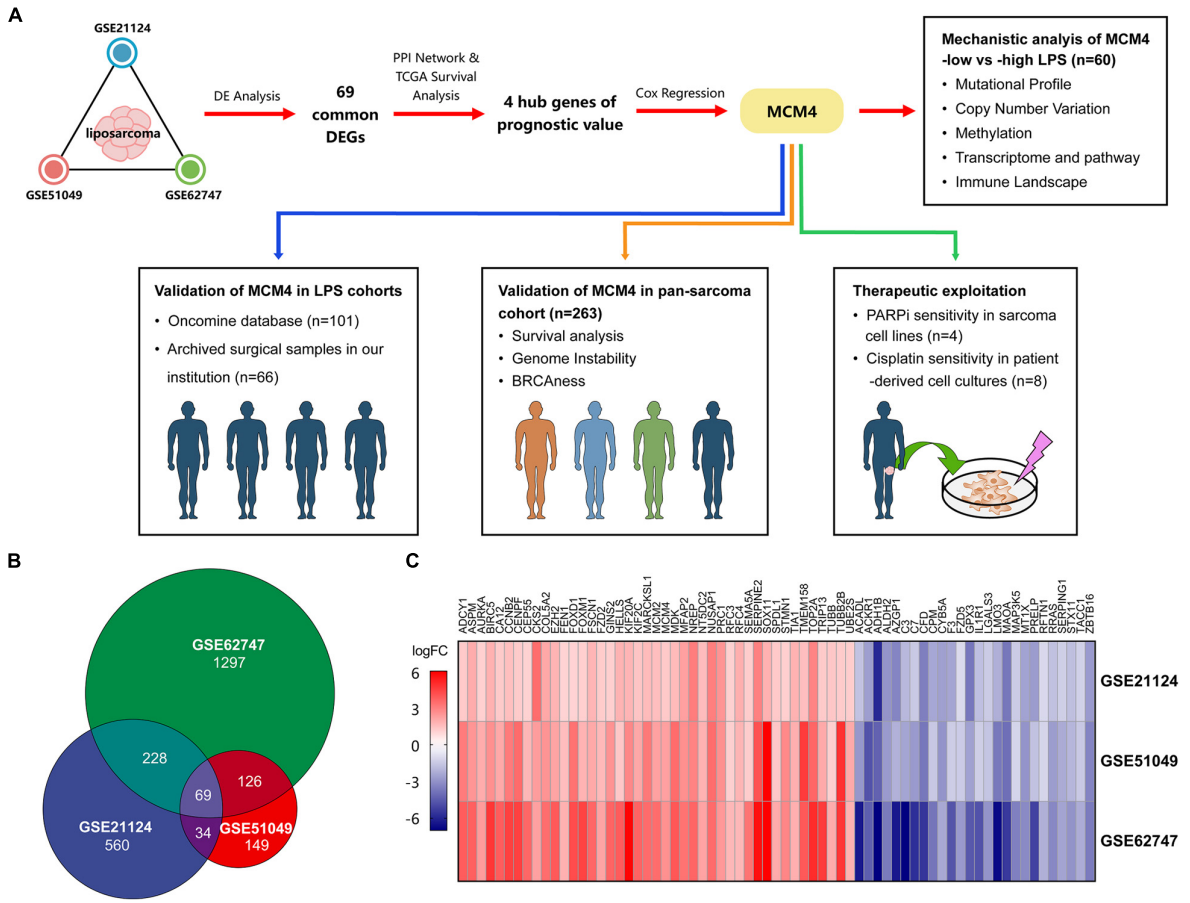

FIGURE 1 | The overall study design and the identification of the potential biomarkers. The schematic graph represents the overall design of the study. Mini-chromosome maintenance protein 4 (MCM4) was prioritized from multiple Gene Expression Omibus (GEO) datasets, and validated in liposarcoma (LPS) and pan-sarcoma cohorts. The therapeutic potential of the MCM4-high expression subgroup was explored in cell lines and patient-derived tumor cell cultures **(A)**. A total of 69 common differentially expressed genes (DEGs) among three datasets of LPS **(B)**, with the corresponding gene expression level shown in the heatmap **(C)**.

subgroups were compared using Gene Set Enrichment Analysis (GSEA) (Subramanian et al., 2005) (gene set permutations of 1,000 times, $P < 0.05$ and FDR < 0.05) and EPIC software (Racle et al., 2017), respectively. Wilcoxon test was used to compare the difference in immune cell infiltration between two groups.

Calculation of Genomic Instability and BRCAness

The proportion of the copy number variations (CNVs) across the whole genome (genome-wide CNVs) and weighted genome instability index (wGII) across 22 autosomal chromosomes were measured to estimate the genomic instability of sarcoma (Dewhurst et al., 2014). Moreover, to assess the function loss of homologous recombination (HR) pathway, we calculated the BRCAness (BRCA-like phenotypes shared by non-BRCA-mutated tumors) score on the transcriptome level based on the 60 gene signature (Konstantinopoulos et al., 2010), in addition to the PARP1 expression, which was reportedly associated with HR deficiency and therapeutic efficiency in sarcoma (Pignochino et al., 2017).

Validation of MCM4 Expression of Liposarcoma and Other Soft-Tissue Sarcoma in Oncomine Database

Oncomine database (**Supplementary Table 1**) was used to assess the gene mRNA expression for common types of sarcoma and the corresponding normal tissues. In this study, "MCM4" was searched with the following filter criteria: (1) threshold ($P < 1E-4$, FC > 2, gene rank: top 10%), (2) data type: mRNA, (3) analysis type: cancer vs. normal analysis, and (4) cancer type: sarcoma.

Validation of the MCM4 as a Biomarker in Pan-Sarcoma Cohort

The UCSC Xena database (**Supplementary Table 1**) was utilized to acquire the Genotype-Tissue Expression (GTEx; **Supplementary Table 1**) and TCGA gene expression data, so as to explore whether MCM4 transcripts were distinguishable between STS and 36 types of normal tissues (n = 8,425).

Meanwhile, we used cBioPortal database (**Supplementary Table 1**) to retrieve the additional clinical information of 263 STS specimens, including cancer subtype classification, MCM4 copy number, metastasis, mitotic count, tumor necrosis rate, and survival outcome, thus, broadening our findings derived from LPS to a wider pan-sarcoma population.

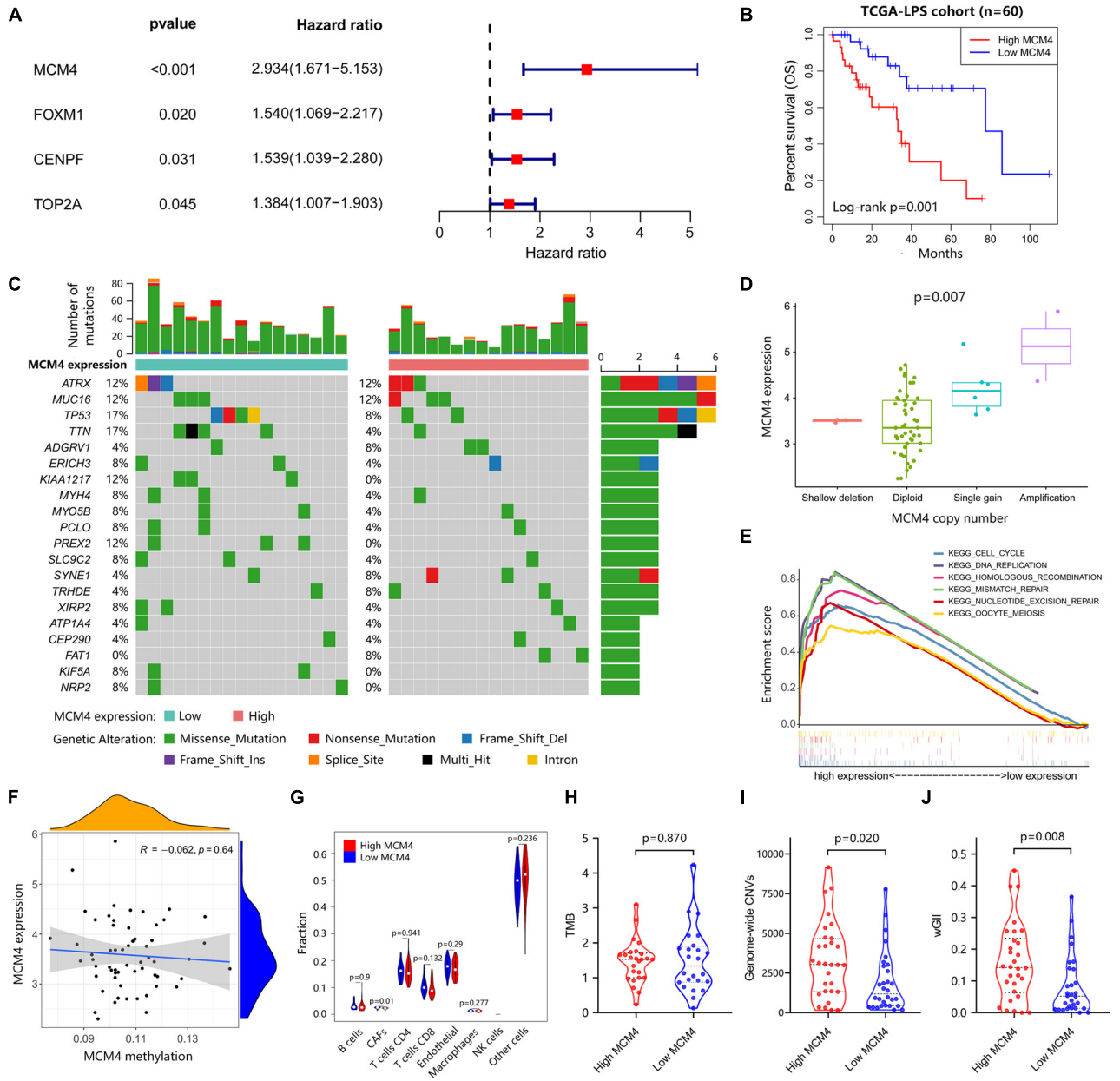

FIGURE 2 | Integrated genomic characterization of the MCM4-high and MCM4-low expression subgroup of LPS in TCGA (n = 60). **(A)** The four hub genes were investigated using the univariate Cox-regression analysis. The hazard ratio and the 95% confidence interval of each gene were shown in forest map. **(B)** The overall survival of the MCM4-high subgroup is significantly worse than that of the MCM4-low subgroup in LPS with Log-rank test $p < 0.001$. **(C)** The landscape of somatic mutations between MCM4 high- and low-expression LPS demonstrated recurrent mutations in ATRX, MUC16, TP53, etc. There was no significant difference in the frequency of the somatic mutations between the two groups (t-test, $p > 0.05$). **(D)** The MCM4 expression of LPS tumor samples was significantly affected by the copy-number variations of MCM4 (Kruskal–Wallis, $p = 0.007$). **(E)** The KEGG pathways enrichment analysis indicated that the transcriptome of the MCM4-high vs. the MCM4-low subset was different in several pathways, including the cell cycle, DNA replication and multiple DNA damage repair gene sets. **(F–H)** The tumor mutation burden (TMB) (t-test, $p = 0.870$), MCM4 methylation (Spearman's correlation, $p = 0.640$), and immune cell infiltration (Wilcoxon test, $p > 0.05$; except for CAFs) were minimally different between the MCM4-high and MCM4-low LPS. In contrast, the MCM4-high LPS exhibited a higher level of genomic instability than the MCM4-low counterpart, as indicated by genome-wide copy number variations (CNV) burden [**(I)**; Wilcoxon test, $p = 0.020$] as well as the weighted Genome Instability Index score [**(J)**; Wilcoxon test, $p = 0.008$].

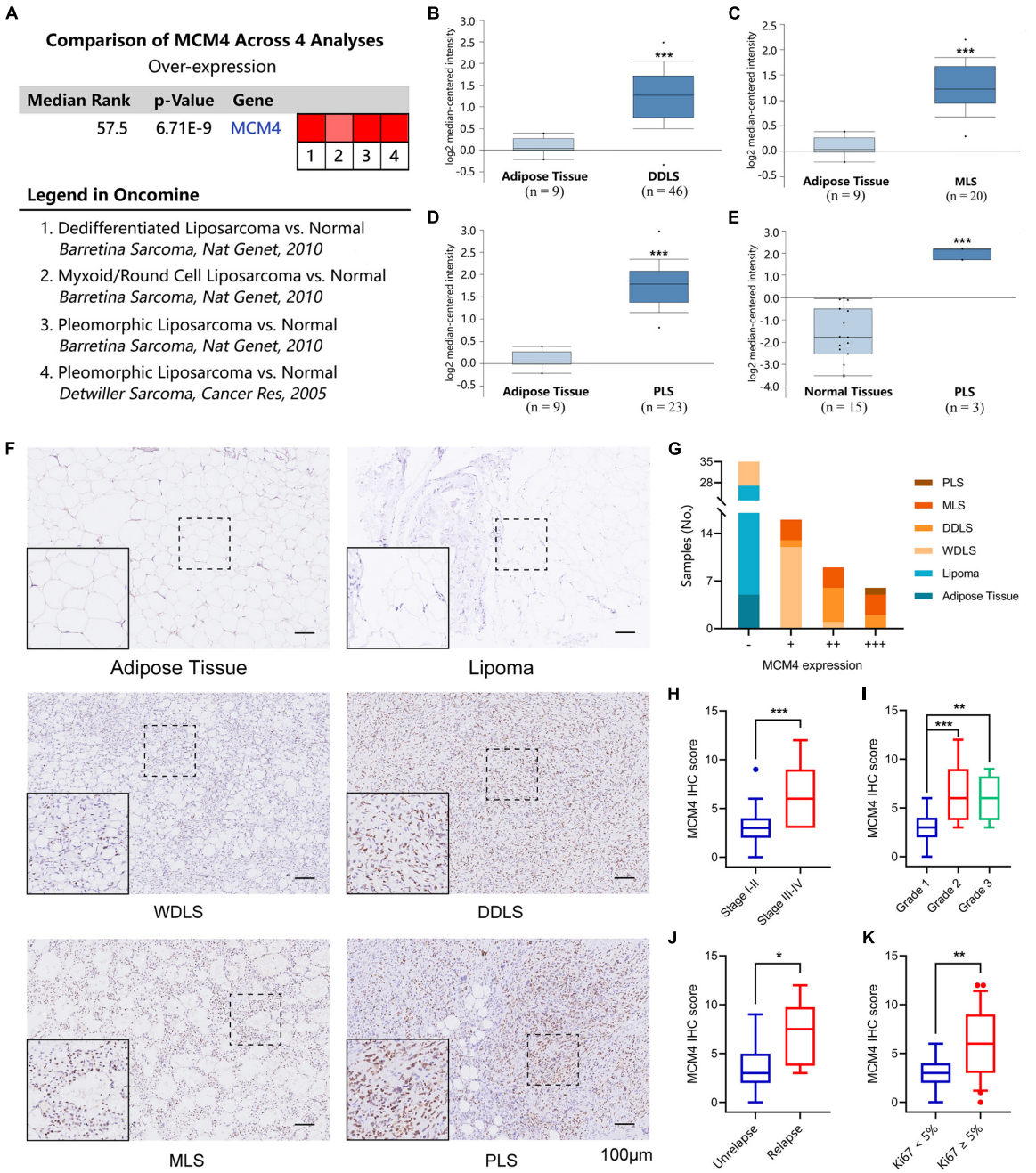

FIGURE 3 | Validation of MCM4 as a biomarker of LPS by Oncomine database and archived surgical specimens. A total of four registries supporting the high tumoral expression of MCM4 vs. normal, while no studies supported the MCM4-high expression in normal tissues **(A)**. MCM4 was found to be consistently overexpressed in dedifferentiated LPS (DDLS) **(B)**, Myxoid LPS (MLS) **(C)**, and Pleomorphic LPS (PLS) **(D,E)** compared to the adipose control. Using 66 archived surgical specimens, we confirmed the overexpression of MCM4 in LPS, but not the adipose tissue or benign lipoma **(F,G)**. MCM4 Immunohistochemistry (IHC) scores significantly correlated with AJCC stage, histological grade, tumor relapse-free survival, and Ki67 index (*t*-test, $p < 0.05$) **(H–K)**. $^{*}p < 0.05$, $^{**}p < 0.01$, $^{**}p < 0.001$,scale bar = 100 um.

Immunohistochemistry Validation of the Archived Sarcoma Specimens

As a validation, 66 MCM4 protein expressions from the surgical specimens of lipomatous neoplasms and normal adipose tissues were collected from patients diagnosed at Ruijin Hospital, affiliated to Shanghai Jiao Tong University School of Medicine. Among them were 39 LPS samples (malignant), 22 lipoma samples (benign), and five adipose tissue samples (normal). The pathological analysis was independently done by two expert pathologists, who identified tumor stages and grades according

to the AJCC STS s staging system (8th) (Tanaka and Ozaki, 2019). The malignant group comprised 20 cases of WDLS, 9 cases of DDLS, 9 cases of myxoid LPS (MLS), and 1 case of pleomorphic LPS (PLS). All malignant samples were equipped with the information of Ki67 labeling index and S-100.

Paraffin-embedded tissues were cut into slices of 4 μm thickness. After heat-induced antigen retrieval, we incubated sections in a rabbit anti-MCM4 antibody (monoclonal; D3H6N, 1:200; CST) at 4°C overnight. Breast cancer sections with MCM4 expression were used as the positive control, while samples without primary antibody incubation were selected as the negative control. We graded the intensity of nuclear staining for MCM4 (0, no staining; 1, yellow; 2, pale brown; 3, dark brown), and scored the extent of staining based on the rate of the positive cell (0, < 5%; 1, 5–25%; 2, 26–50%; 3, 51–75%; 4, 76–100%). By multiplying the color value with positive cell rate, we got the final IHC score: 0–2 (–), 3–4 (+), 5–8 (++), and 9–12 (+++).

Establishing Patient-Derived Tumor Cell Cultures From Sarcoma Specimens

Eight STS specimens were collected from the tumor biopsy (the corresponding clinical data was shown in **Supplementary Table 2**), which were cut into 1–3 mm^3 pieces after PBS washing. The tissue pieces were digested in 10 mL of Dulbecco's modified Eagle's medium (DMEM) supplemented with 10% fetal bovine serum (FBS), 1% penicillin–streptomycin, 5 μg/mL Amphotericin B (V900919, Sigma), and 1 mg/mL collagenase I (17100017, Thermo Fisher Scientific) on a constant temperature (37°C) water bath shaker for 1 h. We collected the digested cells by centrifugation at 1,500 rpm for 5 min. The pellet was then resuspended in 4 mL of fresh cell culture medium and filtered through a 70 μm filter. Afterward, dead or non-adherent cells were removed by medium change after 2 days, and adherent live cells were kept in culture medium. To explore the corresponding tumoral MCM4 expression, adherent cell cultures were digested and centrifugated into pellets, followed by 4% paraformaldehyde fixation and histological study, including HE staining and IHC labeling for MCM4.

Therapeutic Investigation of MCM4-High Soft-Tissue Sarcoma

PTCCs were treated with DMEM supplemented with 10% FBS and cisplatin (P4394, sigma) at 0.1, 0.5, 1.0, 5.0, and 10.0 μM for 24 h. To confirm the cytotoxicity of cisplatin for sarcoma cells, cell viability was measured by CCK-8 assay (CK04, Dojindo). Then we used built-in equations from Graphpad prism 8.0 (inhibitor vs. normalized response with Variable slope) to assess IC50, and compared the difference of IC50 between two groups via unpaired *t*-test. Also, Western blotting (WB) was performed as previously described (Peng et al., 2020). Briefly, we separated the proteins by 10% SDS-PAGE gel, and transferred them onto the polyvinyl difluoride (PVDF) membranes. The membranes were blocked by 5% bovine serum albumin (BSA) for 2 h at room temperature and incubated with primary antibodies overnight at 4°C. All primary and secondary antibodies can be found in **Supplementary Table 3**. Additionally, the gene expression profiles of four STS cell lines (Pignochino et al., 2017) were retrieved from GEO database to validate the association of MCM4 expression with therapeutic vulnerabilities.

RESULTS

Identifying Common Differentially Expressed Genes in Liposarcoma

LPS is one of the most common types of STS with a rich source of public data. We therefore started by analyzing a total of 121 samples, including 100 LPS and 21 adipose tissues in our study (**Figures 1A,B**). Based on the criteria of FDR < 0.05 and $|FC| \geq 2$, we totally screened 339, 221, and 760 DEGs from GSE21124, GSE51049, and GSE62747 datasets, respectively. Sixty-nine DEGs were commonly found among three datasets, including 43 upregulated and 26 downregulated genes (**Figure 1C**).

MCM4-High Expression as a Robust Prognosticator in Liposarcoma Patients

Based on the STRING database, we constructed a protein–protein interaction network complex of 48 genes and 285 edges (average local clustering coefficient: 0.579; the enrichment $p < 1.0e{-}16$) (**Supplementary Figure 1A**) from the 69 DEGs, resulting in 22 "hub" genes hypothetically of great importance in LPS (**Supplementary Figure 1B**). We then asked whether these hub genes correlated with the patients' survival outcome in LPS. Interestingly, in univariate Cox regression analysis, a total of four hub genes (CENPF, FOXM1, MCM4, and TOP2A) were found to have prognostic significance in terms of the overall survival, with MCM4 associated with the greatest hazard ratio of 2.934 (95% CI, 1.671–5.153, $p < 0.001$) (**Figure 2A**). Multivariate analysis further resulted in MCM4 as the only independent risk factor in LPS. After dichotomizing 60 LPS cases into MCM4-high ($n = 30$) and low ($n = 30$) expression subsets, we found that the overall survival was drastically worse in MCM4-high patients than the MCM4-low counterpart (**Figure 2B**). The ROC curve suggested a high predictive value of MCM4 for the 1–, 3–, and 5-year survival, respectively (**Supplementary Figure 1C**).

TABLE 1 | Mini-chromosome maintenance protein 4 (MCM4) expression in adipose tissues and lipomatous tumors.

Groups	Cases	Low		High		Positive rate (%)	*P*-value
		(–)	(+)	(++)	(+++)		
Malignant	39	8	16	9	6	79.5	<0.001*
Benign	22	22	0	0	0	0	
Normal	5	5	0	0	0	0	

**P < 0.05 was regarded as statistically significant.*

Integrated Multi-Omic Comparison of MCM4-High vs. MCM4-Low Liposarcoma

Whether MCM4-high LPS represents a mechanistically distinct entity with its own therapeutic potential remains an open question. We, therefore, investigated the genomic, epigenomic, transcriptomic, and immunological profiles between MCM4-high and MCM4-low LPS from TCGA cohort. As previously reported (Cancer Genome Atlas Research Network, 2017), recurrent mutations were found in TP53, ATRX, MUC16, etc., in both MCM4-high and -low subsets. However, we did not notice any statistical significance in any mutated genes (**Figure 2C**), total mutational burden (**Figure 2H**) or MCM4 gene methylation level (**Figure 2F**) between the two subsets ($p > 0.05$). The immune cell infiltration (**Figure 2G** and **Supplementary Figures 2A,B**) and immune checkpoints molecules expression such as PD-1, LAG3, CTLA4, etc. (**Supplementary Figure 2C**) were also minimally different between the MCM4-high and MCM4-low LPS. In contrast, copy number alteration analysis demonstrated that MCM4 expression was significantly affected by gene copy number ($p = 0.007$; **Figure 2D**).

The dysfunction of MCMs has been associated with double-strand DNA unwinding, DNA replication control, and DNA damage repair in several epithelial cancers (Yu et al., 2020). Consistently, GSEA demonstrated that the MCM4-high subgroup demonstrated an overexpression of cell cycle, DNA replication, as well as the HR pathways (**Figure 2E** and **Supplementary Figure 3**). In parallel, we observed that MCM4-high LPS more frequently harbored copy number loss in genes of HR pathway (**Supplementary Figure 4**). Furthermore, the MCM4-high LPS exhibited a higher level of genomic instability than the MCM4-low counterpart, as indicated by genome-wide CNV burden ($p = = 0.019$; **Figure 2I**) as well as the wGII score ($P = 0.008$; **Figure 2J**). In contrast, neither MCM4 copy number ($P = 0.268$) nor CNV burden ($P = 0.636$) was predictive of the patients' overall survival (**Supplementary Figures 1D,E**).

Validation of MCM4 Expression With Oncomine Database

By searching a total of 75 significant unique analysis records from the Oncomine database, we noticed four LPS studies supporting the high tumoral expression of MCM4 compared with the normal, while no studies supported the MCM4-high expression

TABLE 2 | Correlation between MCM4 expression and pathological parameters in liposarcoma (LPS).

Characteristics	Cases	Low		High		High positive rate (%)	*P*-value
		(–)	(+)	(++)	(+++)		
Gender							
Male	24 (61.5%)	3	13	5	3	33.33	0.405
Female	15 (38.5%)	5	3	4	3	46.67	
Age (years)							
<60	22 (56.4%)	3	10	6	3	40.91	0.721
≥60	17 (43.6%)	5	6	3	3	35.29	
Tumor size (cm)							
≤ 10	7 (17.9%)	2	2	2	1	42.86	0.792
> 10	32 (82.1%)	6	14	7	5	37.50	
Location							
Trunk and extremity	30 (76.9%)	5	13	6	6	40.00	0.718
Retroperitoneum	9 (23.1%)	3	3	3	0	33.33	
Stage							
I + II	24 (61.5%)	8	12	3	1	16.67	<0.001*
III + IV	15 (38.5%)	0	4	6	5	73.33	
Grade							
G1	23 (58.9%)	8	12	3	0	13.64	<0.001*
G2	12 (30.8%)	0	3	4	5	75.00	
G3	4 (10.3%)	0	1	2	1	75.00	
Relapse[#]							
No	9 (47.4%)	3	4	1	1	22.22	0.037*
Yes	10 (52.6%)	0	3	2	5	70.00	
Ki67 labeling index							
<5%	18 (46.2%)	5	11	2	0	11.11	0.001*
≥5%	21 (53.8%)	3	5	7	6	61.90	
S-100 expression							
Negative	9 (23.1%)	2	4	2	1	33.33	0.718
Positive	30 (76.9%)	6	12	7	5	40.00	

**P < 0.05 was regarded as statistically significant. [#]Due to incomplete follow-up data, 19 samples were included in the tumor relapse comparison.*

in normal tissues (**Figure 3A**). Specifically, MCM4 was found to be consistently overexpressed in DDLS (222036_s_at), MLS (222036_s_at), and PLS (222036_s_at and 212141_at) compared with the adipose control (**Figures 3B–E**).

Validation of MCM4 Signature With Archived Liposarcoma Samples From Our Institution

Next, we performed IHC staining of MCM4 for 66 archived surgical specimens in our institution, including 39 LPS, 22 lipomas, and 5 normal adipose tissues (**Figure 3F**). We found that MCM4 expression was positive in 79.5% of the LPS specimens across multiple histology subtypes, but not in the benign or normal tissues (**Figure 3G** and **Table 1**). For LPS, MCM4 was significantly correlated with AJCC stage, histological grade, tumor relapse-free survival, and Ki67 index ($p < 0.05$), but not gender, age, tumor location, etc. (**Figures 3H–K** and **Table 2**). These results confirmed that MCM4-high LPS as a potentially aggressive subset with poor clinical prognosis across the histology subtypes.

Validation of MCM4 Signature in Pan-Sarcoma Cohort

Using the UCSC Xena database (Goldman et al., 2020), we found that MCM4 overexpression was found almost exclusively in STS and testis, but not in other types of normal tissue (**Figure 4A**). Interestingly, the abundance of different MCM4 transcripts was distinguishable between STS and testis (**Supplementary Figure 6C**). A survey of all STS registries in Oncomine database confirmed a consistent overexpression of MCM4 not only in LPS but also in leiomyosarcoma, fibrosarcoma, synovial sarcoma, and undifferentiated pleomorphic sarcoma, compared with the normal (**Supplementary Figure 5**). To explore whether our

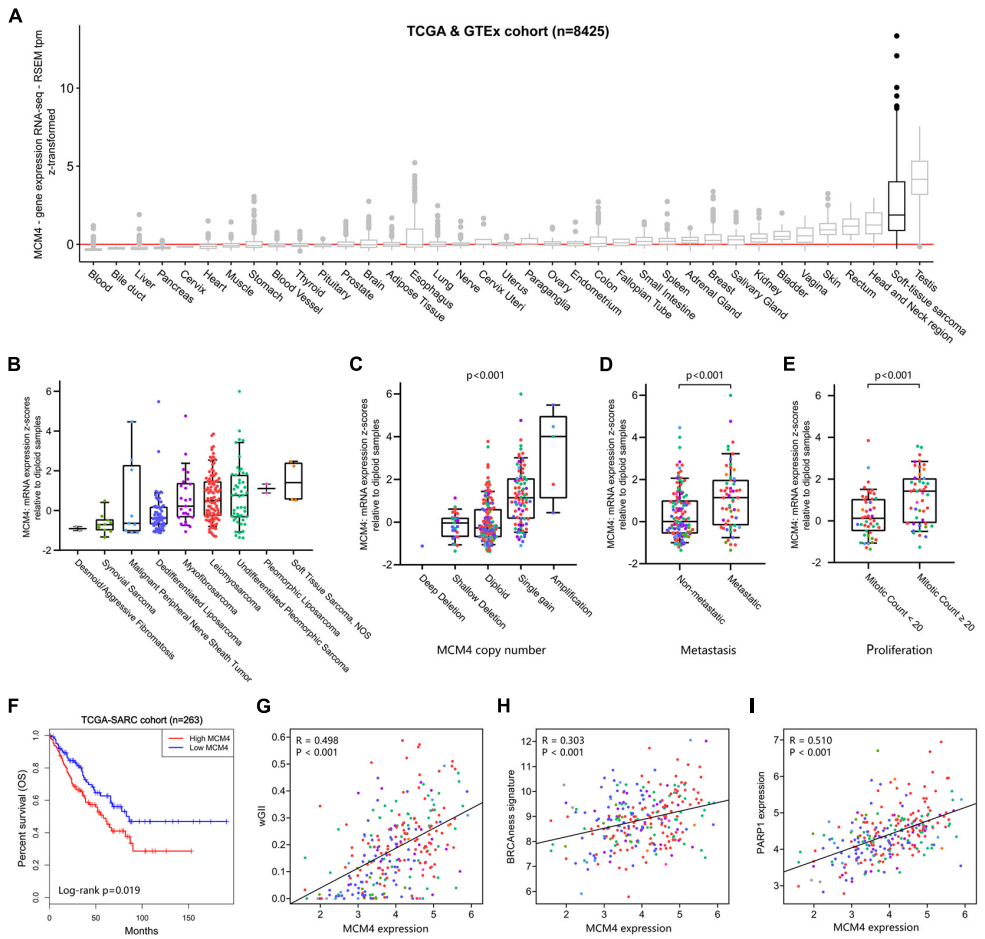

FIGURE 4 | Validation of MCM4 signature in pan-sarcoma cohorts. **(A)** MCM4 is highly expressed in soft-tissue sarcoma and testis, compared with the normal tissues. **(B)** The landscape of MCM4 expression in various soft-tissue sarcoma (STS) subtypes from TCGA database. **(C–F)** MCM4 expression was correlated with MCM4 copy-number (Kruskal-Wallis, $p < < 0.001$, $n = 255$), metastatic state (Wilcoxon test, $p < 0.001$, $n = 179$), proliferation index (Wilcoxon test, $p < 0.001$, $n = 93$), and patient overall survival (Log-rank test, $p < 0.019$, $n = 263$) across multiple histology subtypes in STS. **(G–I)** The tumoral expression of MCM4 was observed to be positively correlated with genome instability (weighted Genome Instability Index (wGII) score; $p < 0.001$, $R = 0.498$, $n = 263$), BRCAness signature ($p < 0.001$, $R = 0.303$, $n = 263$), and PARP1 expression ($p < 0.001$, $R = 0.510$, $n = 263$) in STS, via Spearman's correlation analysis.

findings derived from LPS could be broadened to a wider pan-sarcoma population, 263 STS specimens from TCGA-SARC (Cerami et al., 2012), including 104 leiomyosarcoma, 58 DDLS, 49 undifferentiated pleomorphic sarcoma, 25 myxofibrosarcoma, 10 synovial sarcoma, 9 malignant peripheral nerve sheath tumor, 4 sarcoma NOS (not otherwise specified), 2 PLS, and 2 desmoid fibromatosis, were assessed for MCM4 expression (**Figure 4B**). Surprisingly, the MCM4 expression was also found to be associated with MCM4 copy number ($p < 0.001$; **Figure 4C**), higher metastasis potential ($p < 0.001$; **Figure 4D**), tumor mitotic count ($p < 0.001$; **Figure 4E**), and worse survival outcome ($p = 0.019$; **Figure 4F**), but not tumor necrosis rate (**Supplementary Figure 6A**). In parallel with what we found in LPS, the MCM4 expression was positively correlated with genomic instability (wGII score) in STS ($R = 0.498$, $p < 0.001$; **Figure 4G**). Despite the lack of deleterious mutation in HR pathway (**Supplementary Figure 6B**), MCM4 overexpression STS also harbored an HR-deficiency (BRCAness) phenotype ($R = 0.303$, $p < 0.001$) as well as PARP1 overexpression ($R = 0.510$, $p < 0.001$) in a histology-agnostic fashion (**Figures 4H,I**).

Therapeutic Exploitation of MCM4 as a Predictive Biomarker of Sarcoma

Both of the genomic instability (Andor et al., 2017) and BRCAness (Konstantinopoulos et al., 2010) have been associated with increased sensitivity of tumor to DNA-damaging agents (such as cisplatin) and PARPi. To test this hypothesis in MCM-high STS, we first retrieved the expression profiles of four STS cell lines known to have a distinct vulnerability to PARPi or trabectedin, according to Pignochino et al. (2017). Interestingly, MCM4 was drastically overexpressed in the PARPi/trabectedin-sensitive cell lines compared with the PARPi/trabectedin-resistant cell lines ($p = 0.007$; **Figure 5A**). Next, PTCCs were established from the biopsy of eight STS patients (**Figure 5B**) and ranked from a to h according to the MCM4 IHC expression

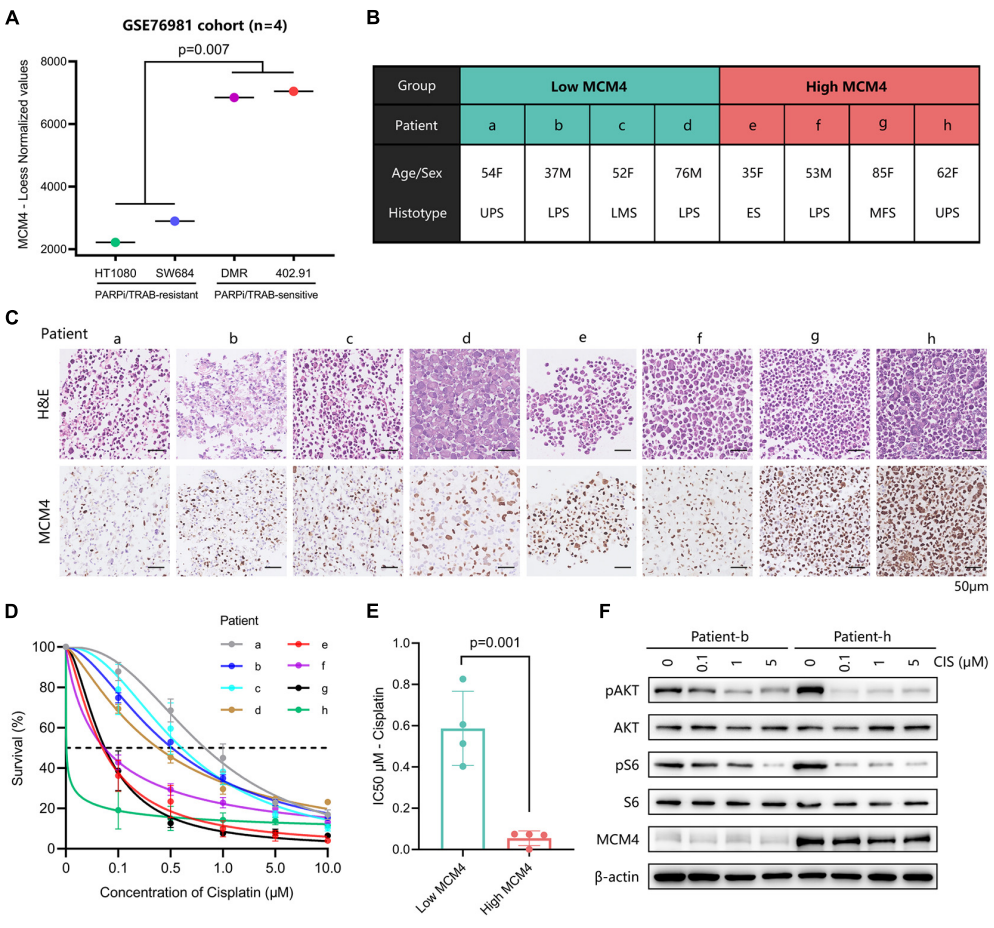

FIGURE 5 | Evaluation of the therapeutic potential in MCM4-high STS cell lines and patient-derived tumor cell cultures (PTCCs). **(A)** By comparing the gene expression profiles of four STS cell-lines, we found that MCM4 was drastically overexpressed in the PARPi/Trabectedin-sensitive cell lines compared with the PARPi/Trabectedin-resistant cell lines (*t*-test, $p = 0.007$, $n = 4$). **(B,C)** Patient-derived tumor cell cultures (PTCCs) were established from the biopsy of eight STS patients, ranked by the corresponding tumoral MCM4 expression. After treated with cisplatin, the MCM4-high PTCCs (patient e–h) demonstrated less cell proliferation **(D)**, with a lower half inhibitory concentration (IC50) than the MCM4-low subset (a–d) (*t*-test, $p = 0.001$, $n = 8$) **(E)**. Additionally, the levels of p-AKT and p-S6 were significantly reduced when cell growth was inhibited **(F)**.

(**Figure 5C**). After treatment with cisplatin, the MCM4-high PTCCs (e–h) demonstrated inhibited cell proliferation (**Figure 5D**), with a lower half inhibitory concentration (IC50, 0.001–0.075 μM) than the MCM4-low subset (a–d) (0.403–0.827 μM, $p = 0.001$; **Figure 5E**). Additionally, the levels of p-AKT and p-S6 were also reduced when cell growth was inhibited (**Figure 5F**).

DISCUSSION

DDLS, high-grade MLS, and PLS are high-grade adipose sarcoma with disease-specific survival (DSS) of 44, 74, and 59%, respectively (Dalal et al., 2006). Although rarely metastasizing, WDLS, and low-grade MLS are at high risk of local failure, leading to poor general performance, and self-reported outcomes (De Vita et al., 2016). In this study, we selected multiple large publicly available datasets composed of 100 LPS tumor samples and 21 adipose tissues. We have discovered four genes of prognostic value (CENPF, FOXM1, MCM4, and TOP2A), and further prioritized MCM4 as a key biomarker of LPS associated with tumor invasiveness (tumor stage, grade, and Ki67 labeling index) and prognostication. These findings were validated by the data registries from Oncomine as well as the clinicopathological data from our institution. However, the underlying mechanism of MCM4 related to a worse prognosis remains unclear. Previous literature has suggested the MCM gene as a direct index of tumor (Choy et al., 2016) and replicative stress responder of genome instability (Ibarra et al., 2008). MCMs have also been implicated in the epithelial–mesenchymal transition (Zhang et al., 2019) and other well-known cancer cell signaling pathways, such WNT, CDK, MYCN, etc. (Shohet et al., 2002; Yu et al., 2020). More interestingly, we found that such prognostic significance of MCM4 could be further expanded to the pan-sarcoma population at a broader scale, and the association of genomic instability and HR deficiency (BRCAness) with MCM4 expression might be a common genomic and transcriptomic portrait shared among different sarcoma histologies. To our knowledge, there are no studies reporting such prognostic significance of MCM4 and its associated genomic/transcriptomic signature in LPS as well as in STS.

Genome instability and HR deficiency have been recently postulated as key molecular characteristics of dysregulated DNA repair pathways in STS with potential therapeutic implications. In addition to the traditional knowledge of BRCAness as the Achilles' heel of cancer cells to PARPi and platinum-based chemotherapy, it is suggested that DNA-damaging agents could aggravate the copy number aberration in the chromosomal unstable tumor, surpassing the tolerance limit of the genome and leading to tumor cell death (Andor et al., 2017). Besides, targeting the HR and non-homologous end-joining (NHEJ) mechanism of cancer cell might further enhance such therapeutic sensitivity of the cancer cells with high levels of CNVs (Gregg et al., 1993; Zhang et al., 2014). However, previous clinical trials of PARPi and DNA-damaging agents mostly failed to confirm such vulnerability in unselected sarcoma population (Kalofonos et al., 2004; Choy et al., 2014). Interestingly, our study demonstrated that genomic instability and BRCAness phenotype could vary tremendously, both inter- and intra-in STS subtypes, which were correlative with tumoral MCM4 expression. On the basis of such observations, we speculated that DNA repair defect-targeted therapies might be implicated for MCM4-high subset, rather than the total population, of STS. Surprisingly, in accordance with our hypothesis, the therapeutic exploitation assay of PTCCs in our study clearly showed that the MCM4-high subset of STS owns a remarkably higher sensitivity to cisplatin treatment than MCM-low tumors. These findings warrant further elucidation of MCM4 as a biomarker for patient-tailored management of STS using DNA-damaging chemotherapy. The activity of PARPi and PARPi/chemotherapy combination therapy in MCM4-high STS is an even more attractive potential, although requiring more translational as well as mechanistic investigations in the future.

DATA AVAILABILITY STATEMENT

The datasets presented in this study can be found in online repositories. The names of the repository/repositories and accession number(s) can be found in the article/**Supplementary Material**.

ETHICS STATEMENT

The studies involving human participants were reviewed and approved by Ruijin Hospital Ethics Committee. The patients/participants provided their written informed consent to participate in this study.

AUTHOR CONTRIBUTIONS

QL, QB, and YX conducted experiments and analyzed the data and wrote the manuscript. YF, ZJ, and JW helped with the experiments. WZ and YS were co-corresponding authors. All authors contributed to the article and approved the submitted version.

FUNDING

This work was supported by the National Natural Science Foundation of China (Grant No. 82072957) and Chinese Society of Clinical Oncology (Grant No. Y-HR2019-0442).

SUPPLEMENTARY MATERIAL

The Supplementary Material for this article can be found online at: https://www.frontiersin.org/articles/10.3389/fcell.2021.666376/full#supplementary-material

REFERENCES

Andor, N., Maley, C. C., and Ji, H. P. (2017). Genomic instability in cancer: teetering on the limit of tolerance. *Cancer Res.* 77, 2179–2185. doi: 10.1158/0008-5472.can-16-1553

Bill, K. L., Casadei, L., Prudner, B. C., Iwenofu, H., Strohecker, A. M., and Pollock, R. E. (2016). Liposarcoma: molecular targets and therapeutic implications. *Cell. Mol. Life Sci.* 73, 3711–3718. doi: 10.1007/s00018-016-2266-2

Blagoev, K. B., Wilkerson, J., and Fojo, T. (2012). Hazard ratios in cancer clinical trials–a primer. *Nat. Rev. Clin. Oncol.* 9, 178–183. doi: 10.1038/nrclinonc.2011.217

Cancer Genome Atlas Research Network (2017). Comprehensive and integrated genomic characterization of adult soft tissue sarcomas. *Cell* 171, 950–965.e28.

Cerami, E., Gao, J., Dogrusoz, U., Gross, B. E., Sumer, S. O., Aksoy, B. A., et al. (2012). The cBio cancer genomics portal: an open platform for exploring multidimensional cancer genomics data. *Cancer Discov.* 2, 401–404. doi: 10.1158/2159-8290.cd-12-0095

Chen, Y., Xu, L., Mayakonda, A., Huang, M. L., Kanojia, D., Tan, T. Z., et al. (2019). Bromodomain and extraterminal proteins foster the core transcriptional regulatory programs and confer vulnerability in liposarcoma. *Nat. Commun.* 10:1353.

Choy, B., LaLonde, A., Que, J., Wu, T., and Zhou, Z. (2016). MCM4 and MCM7, potential novel proliferation markers, significantly correlated with Ki-67, Bmi1, and cyclin E expression in esophageal adenocarcinoma, squamous cell carcinoma, and precancerous lesions. *Hum. Pathol.* 57, 126–135. doi: 10.1016/j.humpath.2016.07.013

Choy, E., Butrynski, J. E., Harmon, D. C., Morgan, J. A., George, S., Wagner, A. J., et al. (2014). Phase II study of olaparib in patients with refractory Ewing sarcoma following failure of standard chemotherapy. *BMC Cancer* 14:813. doi: 10.1186/1471-2407-14-813

Crago, A. M., and Brennan, M. F. (2015). Principles in management of soft tissue sarcoma. *Adv. Surg.* 49, 107–122. doi: 10.1016/j.yasu.2015.04.002

Dalal, K. M., Kattan, M. W., Antonescu, C. R., Brennan, M. F., and Singer, S. (2006). Subtype specific prognostic nomogram for patients with primary liposarcoma of the retroperitoneum, extremity, or trunk. *Ann. Surg.* 244, 381–391. doi: 10.1097/01.sla.0000234795.98607.00

Davis, S., and Meltzer, P. S. (2007). GEOquery: a bridge between the gene expression omnibus (GEO) and bioconductor. *Bioinformatics* 23, 1846–1847. doi: 10.1093/bioinformatics/btm254

De Vita, A., Mercatali, L., Recine, F., Pieri, F., Riva, N., Bongiovanni, A., et al. (2016). Current classification, treatment options, and new perspectives in the management of adipocytic sarcomas. *Onco Targets Ther.* 9, 6233–6246. doi: 10.2147/ott.s112580

de Vreeze, R. S., de Jong, D., Nederlof, P. M., Ariaens, A., Tielen, I. H., Frenken, L., et al. (2010). Added value of molecular biological analysis in diagnosis and clinical management of liposarcoma: a 30-year single-institution experience. *Ann. Surg. Oncol.* 17, 686–693. doi: 10.1245/s10434-009-0806-9

Dewhurst, S. M., McGranahan, N., Burrell, R. A., Rowan, A. J., Gronroos, E., Endesfelder, D., et al. (2014). Tolerance of whole-genome doubling propagates chromosomal instability and accelerates cancer genome evolution. *Cancer Discov.* 4, 175–185. doi: 10.1158/2159-8290.cd-13-0285

Fabre-Guillevin, E., Coindre, J. M., Somerhausen, N. D. S., Bonichon, F., Stoeckle, E., and Bui, N. B. (2006). Retroperitoneal liposarcomas: follow-up analysis of dedifferentiation after clinicopathologic reexamination of 86 liposarcomas and malignant fibrous histiocytomas. *Cancer* 106, 2725–2733. doi: 10.1002/cncr.21933

Goldman, M. J., Craft, B., Hastie, M., Repecka, K., McDade, F., Kamath, A., et al. (2020). Visualizing and interpreting cancer genomics data via the Xena platform. *Nat. Biotechnol.* 38, 675–678. doi: 10.1038/s41587-020-0546-8

Gregg, C. M., Beals, T. E., McClatchy, K. M., Fisher, S. G., and Wolf, G. T. (1993). DNA content and tumor response to induction chemotherapy in patients with advanced laryngeal squamous cell carcinoma. *Otolaryngol. Head Neck Surg.* 108, 731–737. doi: 10.1177/019459989310800616

Ibarra, A., Schwob, E., and Mendez, J. (2008). Excess MCM proteins protect human cells from replicative stress by licensing backup origins of replication. *Proc. Natl. Acad. Sci. U.S.A.* 105, 8956–8961. doi: 10.1073/pnas.0803978105

Kalofonos, H. P., Bafaloukos, D., Kourelis, T. G., Karamouzis, M. V., Megas, P., Iconomou, G., et al. (2004). Adriamycin and cis-platinum as first-line treatment in unresectable locally advanced or metastatic adult soft-tissue sarcomas. *Am. J. Clin. Oncol.* 27, 307–311. doi: 10.1097/01.coc.0000071467.96942.2f

Konstantinopoulos, P. A., Spentzos, D., Karlan, B. Y., Taniguchi, T., Fountzilas, E., Francoeur, N., et al. (2010). Gene expression profile of BRCAness that correlates with responsiveness to chemotherapy and with outcome in patients with epithelial ovarian cancer. *J. Clin. Oncol.* 28, 3555–3561. doi: 10.1200/jco.2009.27.5719

Patel, R. B., Li, T., Liao, Z., Jaldeepbhai, J. A., Perera, H., Muthukuda, S. K., et al. (2017). Recent translational research into targeted therapy for liposarcoma. *Stem Cell Investig.* 4:21.

Peng, C., Wang, J., Bao, Q., Wang, J., Liu, Z., Wen, J., et al. (2020). Isolation of extracellular vesicle with different precipitation-based methods exerts a tremendous impact on the biomarker analysis for clinical plasma samples. *Cancer Biomark.* 29, 373–385. doi: 10.3233/cbm-201651

Pignochino, Y., Capozzi, F., D'Ambrosio, L., Dell'Aglio, C., Basirico, M., Canta, M., et al. (2017). PARP1 expression drives the synergistic antitumor activity of trabectedin and PARP1 inhibitors in sarcoma preclinical models. *Mol. Cancer* 16, 86.

Racle, J., de Jonge, K., Baumgaertner, P., Speiser, D. E., and Gfeller, D. (2017). Simultaneous enumeration of cancer and immune cell types from bulk tumor gene expression data. *Elife* 6:e26476.

Shannon, P., Markiel, A., Ozier, O., Baliga, N. S., Wang, J. T., Ramage, D., et al. (2003). Cytoscape: a software environment for integrated models of biomolecular interaction networks. *Genome Res.* 13, 2498–2504. doi: 10.1101/gr.1239303

Shohet, J. M., Hicks, M. J., Plon, S. E., Burlingame, S. M., Stuart, S., Chen, S. Y., et al. (2002). Minichromosome maintenance protein MCM7 is a direct target of the MYCN transcription factor in neuroblastoma. *Cancer Res.* 62, 1123–1128.

Singer, S., Antonescu, C. R., Riedel, E., and Brennan, M. F. (2003). Histologic subtype and margin of resection predict pattern of recurrence and survival for retroperitoneal liposarcoma. *Ann. Surg.* 238, 358–370; discussion 370–371.

Subramanian, A., Tamayo, P., Mootha, V. K., Mukherjee, S., Ebert, B. L., Gillette, M. A., et al. (2005). Gene set enrichment analysis: a knowledge-based approach for interpreting genome-wide expression profiles. *Proc. Natl. Acad. Sci. U.S.A.* 102, 15545–15550. doi: 10.1073/pnas.0506580102

Swanton, C. (2012). Intratumor heterogeneity: evolution through space and time. *Cancer Res.* 72, 4875–4882. doi: 10.1158/0008-5472.can-12-2217

Tanaka, K., and Ozaki, T. (2019). New TNM classification (AJCC eighth edition) of bone and soft tissue sarcomas: JCOG bone and soft tissue tumor study group. *Jpn. J. Clin. Oncol.* 49, 103–107. doi: 10.1093/jjco/hyy157

Tseng, W. W., Malu, S., Zhang, M., Chen, J., Sim, G. C., Wei, W., et al. (2015). Analysis of the intratumoral adaptive immune response in well differentiated and dedifferentiated retroperitoneal liposarcoma. *Sarcoma* 2015:547460.

Yu, S., Wang, G., Shi, Y., Xu, H., Zheng, Y., and Chen, Y. (2020). MCMs in cancer: prognostic potential and mechanisms. *Anal. Cell. Pathol.* 2020:3750294.

Zhang, R. R., Pointer, K. B., Kuo, J. S., and Dempsey, R. J. (2014). Mutational analysis reveals the origin and therapy-driven evolution of recurrent glioma. *Neurosurgery* 75, N9–N10.

Zhang, Y., Xu, L., Wang, P., Jian, H., Shi, X., Jia, M., et al. (2019). Phenotypic transition of tumor cells between epithelial- and mesenchymal-like state during adaptation to acidosis. *Cell Cycle* 18, 1938–1947. doi: 10.1080/15384101.2019.1635868

Conflict of Interest: The authors declare that the research was conducted in the absence of any commercial or financial relationships that could be construed as a potential conflict of interest.

frontiers in Molecular Biosciences

REVIEW
published: 07 July 2021
doi: 10.3389/fmolb.2021.685440

Epigenetic Mechanisms in DNA Double Strand Break Repair: A Clinical Review

Alejandra Fernandez[1], *Connor O'Leary*[1,2], *Kenneth J O'Byrne*[1,2], *Joshua Burgess*[1,2]*, *Derek J Richard*[1,2]* *and Amila Suraweera*[1,2]*

[1]*Centre for Genomics and Personalised Health, School of Biomedical Sciences and Translational Research Institute, Queensland University of Technology (QUT), Brisbane, QLD, Australia,* [2]*Princess Alexandra Hospital, Woolloongabba, QLD, Australia*

Upon the induction of DNA damage, the chromatin structure unwinds to allow access to enzymes to catalyse the repair. The regulation of the winding and unwinding of chromatin occurs via epigenetic modifications, which can alter gene expression without changing the DNA sequence. Epigenetic mechanisms such as histone acetylation and DNA methylation are known to be reversible and have been indicated to play different roles in the repair of DNA. More importantly, the inhibition of such mechanisms has been reported to play a role in the repair of double strand breaks, the most detrimental type of DNA damage. This occurs by manipulating the chromatin structure and the expression of essential proteins that are critical for homologous recombination and non-homologous end joining repair pathways. Inhibitors of histone deacetylases and DNA methyltransferases have demonstrated efficacy in the clinic and represent a promising approach for cancer therapy. The aims of this review are to summarise the role of histone deacetylase and DNA methyltransferase inhibitors involved in DNA double strand break repair and explore their current and future independent use in combination with other DNA repair inhibitors or pre-existing therapies in the clinic.

Keywords: DNA double strand breaks, DNA repair, epigenetic mechanisms, histone deacetylase inhibitors, DNA methyltransferase inhibitors

OPEN ACCESS

Edited by:
Megha Agrawal,
University of Illinois at Chicago, United States

Reviewed by:
Praveen Rajendran,
Texas A&M Health Science Center, United States
Kaushlendra Tripathi,
University of Alabama at Birmingham, United States

***Correspondence:**
Amila Suraweera
amila.suraweera@qut.edu.au
Derek J Richard
derek.richard@qut.edu.au
Joshua Burgess
j6.burgess@qut.edu.au

Specialty section:
This article was submitted to Molecular Diagnostics and Therapeutics, a section of the journal Frontiers in Molecular Biosciences

Received: *31 March 2021*
Accepted: *24 June 2021*
Published: *07 July 2021*

Citation:
Fernandez A, O'Leary C, O'Byrne KJ, Burgess J, Richard DJ and Suraweera A (2021) Epigenetic Mechanisms in DNA Double Strand Break Repair: A Clinical Review. Front. Mol. Biosci. 8:685440. doi: 10.3389/fmolb.2021.685440

INTRODUCTION

According to the World Health Organization (WHO), approximately 9.6 million people were estimated to die from cancer in 2018. The WHO defines cancer as an event involving abnormal cell growth that can occur in any part of the body and later invade adjoining sections or spread to other organs (World Health Organization, 2019). Cancer develops at a molecular level and requires specific management strategies to achieve efficient treatment (Hanahan and Weinberg, 2000). This genomic disease often results as a consequence of normal cellular processes. For example, events such as DNA double strand breaks (DSBs), which have been classified as the most detrimental damage to DNA, usually occur in the chromosome due to environmental exposure to irradiation, ultraviolet light, or other chemical agents. These adverse genomic breakages can lead to imbalanced expression of proteins that are crucial for genomic stability (e.g., BRCA1/2, TP53, RAD51C). However, DSBs can be repaired by either one of the two conserved DSB repair pathways; homologous recombination (HR) and non-homologous end joining (NHEJ) (Mavaddat et al., 2013; Brown et al., 2017).

Changes in an organism can also be caused by modifications of gene expression, rather than alterations in the genetic code itself, a phenomenon defined as epigenetics. The epigenome

comprises chemical compounds that are usually inherited, but that can also be altered by environmental influences such as diet and pollutants. These epigenetic modifications are described as a chemical layer on top of the DNA, which influences the way cells read genes. For instance, epigenetic modifications play a significant role in regulating several cellular processes involved in DNA damage/repair and thus, influence transcription, DNA damage response signaling and genomic stability, which are all hallmarks of cancer.

With the purpose of understanding the many genetic abnormalities that comprise cancer as a disease, epigenetics has been shown to be involved in altered gene function and malignant cellular transformation in the development of both solid tumors and hematological malignancies (Brower, 2011; Maeda et al., 2018; Rosenquist et al., 2018). The major epigenetic modifications involved in gene regulation are histone tail modifications, DNA methylation, chromatin remodeling and post translational ATP-dependent modifications, such as small non-coding RNA expression and gene imprinting (Wilson et al., 2010; Chervona and Costa, 2012; Werner et al., 2017; Zhou et al., 2020; Alexandrova et al., 2020; Zhou et al., 2018).

Histone tail modifications involving deacetylation and DNA methylation are the two epigenetic modifications most widely explored to date. Histone deacetylation is catalyzed by histone deacetylases (HDACs). On the other hand, DNA methylation is catalyzed by DNA methyltranferases (DNMTs) (Tu et al., 2020; Narayan et al., 2020; Ghasemi, 2020; Li et al., 2018; Mazzone et al., 2017; Werner et al., 2017; Villanueva et al., 2020). These discoveries have paved the way for targeted epigenetic therapy used in the clinic for the treatment of cancer. The inhibition of histone deacetylation and DNA methylation epigenetic mechanisms are a highly desirable target for novel drugs. The U.S Food and Drug Administration (FDA) has approved histone deacetylase inhibitors (HDACi) and DNA methyltransferase inhibitors (DNMTi) that are currently being used independently, or in combination with other cancer therapies (Narayan et al., 2020; FDA, 2020a; Mann et al., 2007). In this review, we investigate the mechanisms and effects of HDAC-HDACi and DNMT-DNMTi in DSB repair and their impact and/or potential as therapeutic agents.

CANCER, DNA DAMAGE AND EPIGENETIC CHANGES

DNA Damage as a Hallmark of Cancer

DNA damage has been defined as a hallmark of cancer (Hanahan and Weinberg, 2000; Andor et al., 2017). To remain guarded, the genome is reliant on stable DNA damage responses (DDR). Depending on the type of DNA damage, a signaling network is activated upon the detection of the DNA lesion to coordinate DNA repair, the cell cycle, senescence or apoptosis, in order to restore the genetic information (Falck et al., 2005). Hence, cancer cells can develop dysfunctional DNA repair mechanisms which further promote oncogenesis; however, this genomic instability can be exploited in cancer therapy (Jeggo and Löbrichf, 2015; Sokol et al., 2020; Caracciolo et al., 2021).

DNA damage may also lead to failures in cell cycle checkpoint activation, dysfunctional redox homeostasis and telomere attrition (Gad et al., 2014; Huber et al., 2014). Despite DNA being able to easily repair such lesions through DNA repair mechanisms, when these processes fail, mutations occur and this can predispose individuals to cancer (Hanahan and Weinberg, 2000; Andor et al., 2017). There are different types of DNA damage, including abasic sites (DNA base is missing), mismatches (replication errors), modified bases (changes to the bases), inter-strand crosslinks (covalent linkage between the two strands), single-strand breaks (a break in the sugar-phosphate backbone of one strand) or DSBs (both strand backbones are broken) (Ward, 1985; Vaz et al., 2017). A multiplicity of DNA repair systems has evolved in order to counteract these lesions. Some of these repair mechanisms involve base excision repair (BER), mismatch repair (MMR), post-replication repair and error-prone repair systems (Iyama and Wilson, 2013; Vaz et al., 2017; Rajapakse et al., 2019). BER features three steps: excision of the damaged base; use of the undamaged DNA strand as a template to fill in the gap via DNA polymerase; and DNA ligase to seal the process (Sancar, 1994). MMR, proofreads and corrects mismatched nucleotides (Kunkel and Erie, 2005). Post-replication repair involves modification of existing gaps in newly synthesized strands. The two most predominant post-replication repair systems are translation synthesis and template switching (Kaufmann, 1989). Lastly, homologous recombination (HR) and non-homologous recombination (NHEJ) pathways are involved in DSB repair, the most cytotoxic type of DNA backbone damage (Rodgers and Mcvey, 2016), which is discussed in more detail below.

DNA Double Strand Breaks

In contrast to single strand breaks, DSBs involve the breakage of the two strains of the double helix, making it more difficult to repair. These lesions bring alongside severe mutagenic consequences that promote oncogenesis. DNA DSBs occur spontaneously or are caused by both exogenous and endogenous agents (Takata et al., 1998; Moroni et al., 2013; Moloney and Cotter, 2018; Schwartz et al., 2005) (**Figure 1**). In response to this genetic insult, cells have evolved to recognize the damage and signal for DNA DSB repair mechanisms. The proteins responsible of signaling these events are PIKKs (phosphatidykinositol 3-kinase-related kinases), DNA-PKcs (DNA-dependent serine/threonine protein kinase catalytic subunit), ATM (ataxia telangiectasia mutated), and ATR (ataxia telangiectasia and Rad3-related protein). Unrepaired or incorrect repaired DSBs often lead to the loss of genetic information, chromosomal aberrations, unregulated cell division or cell death proceeding with genomic instability, which is a hallmark of cancer (Johnston et al., 1961; Antonarakis et al., 2004; Jackson and Bartek 2009; Jekimovs et al., 2014).

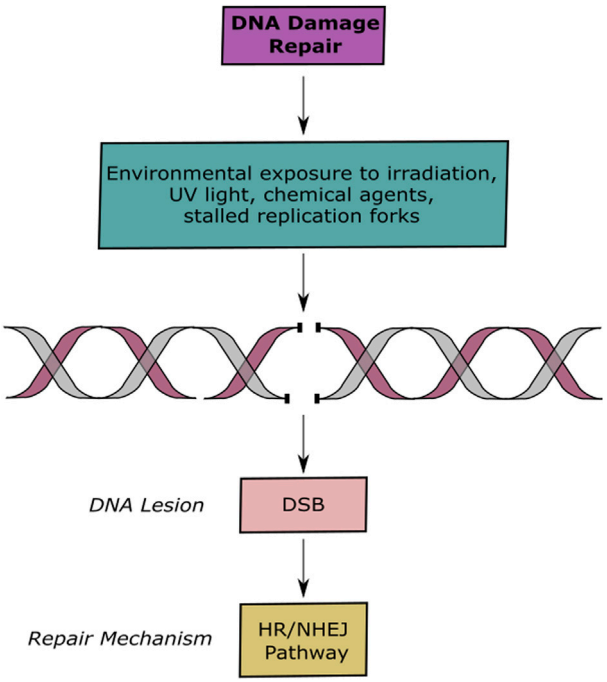

FIGURE 1 | DNA Lesions and Repair Pathways. Schematic representation of DNA damage and repair. Exogenous and endogenous agents induce DSBs, which are repaired by the HR or NHEJ pathways.

DNA Double Strand Break Repair Mechanisms

The two most conserved repair pathways are homologous recombination (HR) and non-homologous end joining (NHEJ) (Schwartz et al., 2005; Takata et al., 1998; Essers et al., 2000). These two pathways work collaboratively but can also compete with each other (**Figure 1**) (Decottignies, 2013). Cells undergo a regulated mechanism to choose between these two pathways, the progressive 5–3′ resection of DNA ends promotes HR dependent repair and blocks NHEJ (Escribano-Díaz et al., 2013). On the other hand, binding of the Ku70/Ku80 complex enables repair of the damage site via NHEJ by protecting DNA ends from exonucleases and by preventing HR pathway mechanisms. Additionally, it has been reported that RIF1 and 53BP1 play an important role in promoting NHEJ mechanisms, while, BRCA1 and RBBP8 promote HR mechanisms (Chapman et al., 2012; Escribano-Díaz et al., 2013).

Homologous Recombination

HR is a strand invasion mechanism that occurs during the late S to G2 phase of the cell cycle and is known to be unerring as it uses the presence of a homologous chromosome or sister chromatid as a template for the repair (**Figure 2A**) (Essers et al., 2000). Human single stranded DNA binding protein 1 (hSSB1) has shown to be an essential protein to signal for DNA DSB repair through HR by recruiting the MRN (Mre11/Rad50/NBS1) complex to the lesion site (Lawson et al., 2020; El-Kamand et al., 2020; Ashton et al., 2017; Croft et al., 2017; Touma et al., 2016; Paquet et al., 2016; Richard et al., 2011a; Richard et al., 2011b; Richard et al. 2008). The MRN complex is responsible for activating the ATM kinase activity and binding the DNA ends at the break site (D'Amours and Jackson 2002). This complex also plays an important role in the DSB repair pathway selection. This occurs depending on the cell type, cell cycle stage and by competing with the binding of the Ku70/80 complex, which favors NHEJ, at the damage site (Lamarche et al., 2010). Once HR has been selected as the pathway to proceed with, for lesion repair, the ATM kinase initiates a cascade of events that signal for DSB resection to produce single-stranded DNA (ssDNA), that later acts as a substrate for recombinase Rad51 (Jazayeri et al., 2008). The process continues with resection of the DNA by exposing the ssDNA through the binding of replication protein A (RPA) (Garcia et al., 2011; Tomimatsu et al., 2012). RPA also aids in protecting DNA from inappropriate annealing that could alter the genome (Bolderson et al., 2010). BRCA1 ensures that RPA remains bounded to the lesion site (Chen et al., 2008). BRCA2 removes RPA exposing ssDNA and stimulating the activity of the Rad51. Rad51 creates a helical filament on ssDNA which hunts for nearby homologous double-stranded DNA facilitating strand invasion of the sister chromatid to finally repair the damage site. The final stage is resolution of the Holliday junction and ligation of the broken phosphate backbone (**Figure 2A**) (Yuan et al., 1999; Helleday et al., 2007; Jekimovs et al., 2014).

Non-homologous End Joining

The NHEJ (also known as classical non-homologous or C-NHEJ) pathway takes place during all cell cycle stages, where it repairs DSBs through direct ligation (**Figure 2B**). NHEJ is the only available pathway in the G0 to G1 phases of the cell cycle. In contrast to HR, it does not use a homologous sister chromatin to fix DSBs, making it a potentially error-prone mechanism (Shrivastav et al., 2008; Jekimovs et al., 2014).

NHEJ follows a system involving recognition of the damage at site, DNA processing and ligation. Ku (Ku70 and Ku80 heterodimers) and DNA-PK are the most relevant protein complexes involved in this pathway (Dobbs et al., 2010). Ku recognizes the DNA DSB and it is responsible for protecting the DSB ends from degradation and attack of exonucleases. Similarly, it is in charge of recruiting other DNA damage repair proteins (Takata et al., 1998). DNA-PKcs, is a holoenzyme which functions to link the DNA ends together and DNA-PK is auto-phosphorylated either before or after the processing stage (Boldogh et al., 2003). These ends are processed by enzymes like the MRN complex. The DNA damage repair is finalized by stimulating end-joining. This occurs by the interaction of XLF and the XRCC4/DNA ligase IV complex (**Figure 2B**) (Ahnesorg et al., 2006).

Histone Acetylation and DNA Methylation as Epigenetic Regulator Mechanisms Involved in DNA Double Strand Break Repair

DNA is wrapped around histone proteins that are grouped into nucleosomes, which are coiled into a fiber that is later condensed into chromatin. When histones are modified, they affect gene

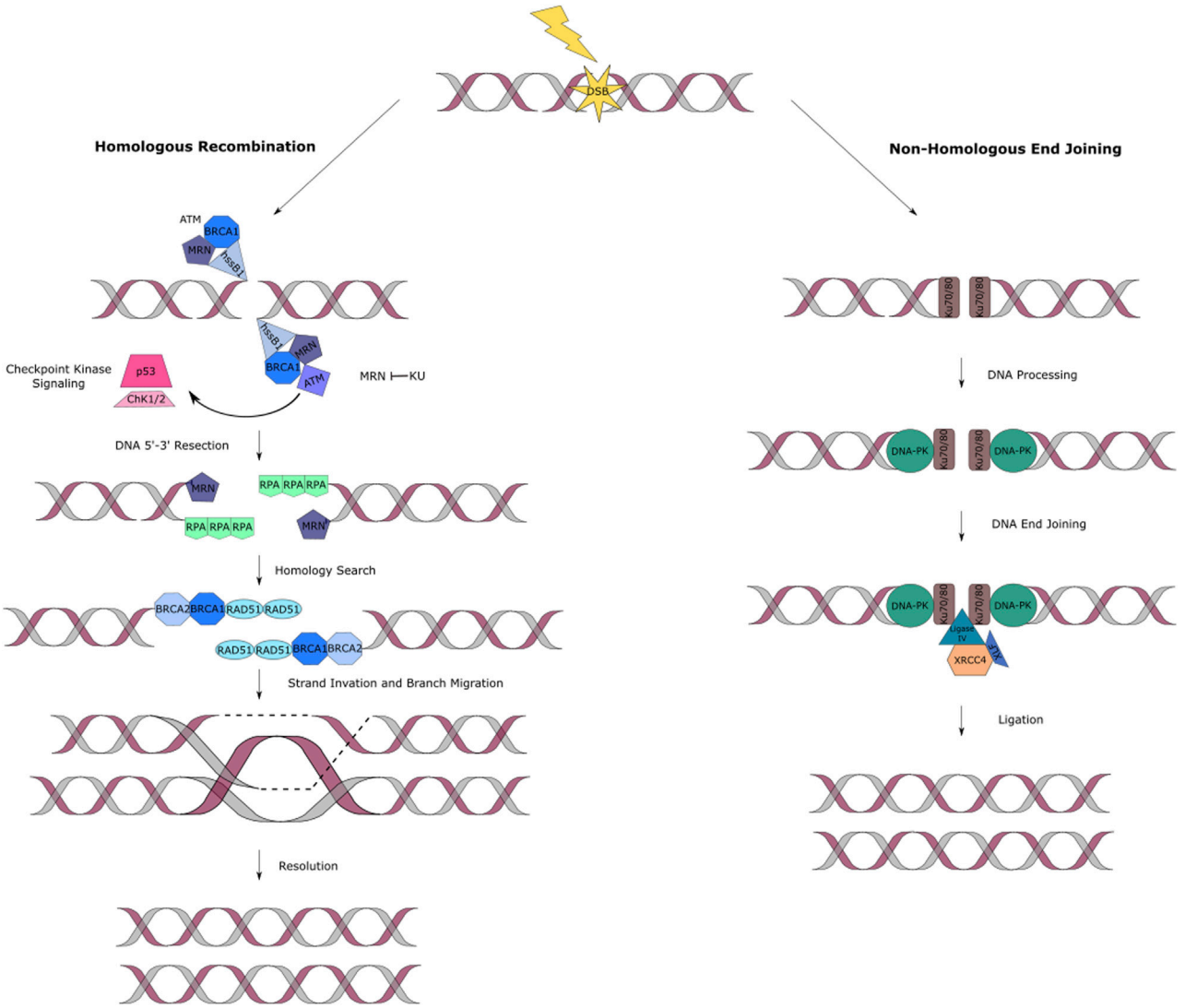

FIGURE 2 | DNA double strand break repair pathways. **(A)** HR fixes two-ended DSBs by a resection process. A recombinase will then induce strand invasion. The single strand is then extended, using the complementary strand as template. Recapture of the second end occurs followed by ligation. The main proteins involved in this pathway are hSSB1, MRN complex, RPA, BRACA1/2 and Rad51. **(B)** NHEJ of DSBs in DNA is accomplished by a series of proteins that work together to carry out the synapsis, preparation, and ligation of the broken DNA ends. The main proteins involved in NHEJ eukaryotes are Ku and DNA-PK complexes, XLF and the XRCC4/ DNA ligase IV complex.

expression regulation, protein activation and stability and can also enable or disable the access of transcription factors to the nucleotides (Mercurio et al., 2012) (**Figure 3A**). This can occur via epigenetic events known as histone modifications that are catalyzed through enzymatic activities that trigger reversible post-translational modifications such as: ADP-ribosylation (modification of histone ribosylation sites Aspartic/Glutamic acid) (Karch et al., 2017); ubiquitination (addition of a ubiquitin protein usually in histone H2A, lysine 119, and histone H2B, lysine 120) (Mercurio et al., 2012); sumoylation (addition of a small ubiquitin-related modifier SUMO, 11 kDa protein, at a lysine site) (Nathan et al., 2003); phosphorylation (mostly occurs in histone H2A(X), also known as γH2AX, at serine 139) (Jeggo and Löbrichf, 2015; Nair et al., 2017); methylation (a methyl group is added to a lysine or arginine residue in the histone tails) (Gupta et al., 2016); or acetylation.

However, in this review, we are mainly focusing on histone acetylation and DNA methylation as these have been the most widely studied epigenetic mechanisms due to their ability to modify chromatin and regulate transcriptional activity (Shinjo and Kondo 2015; Thakore et al., 2015; Podolsky et al., 2016). It has also been shown that histone modifications such as histone deacetylation and histone methylation can interact with DNA methylation to achieve long-term transcriptional repression (Freitag and Selker, 2005). It is important to mention that the deregulation of either of these epigenetic mechanisms during

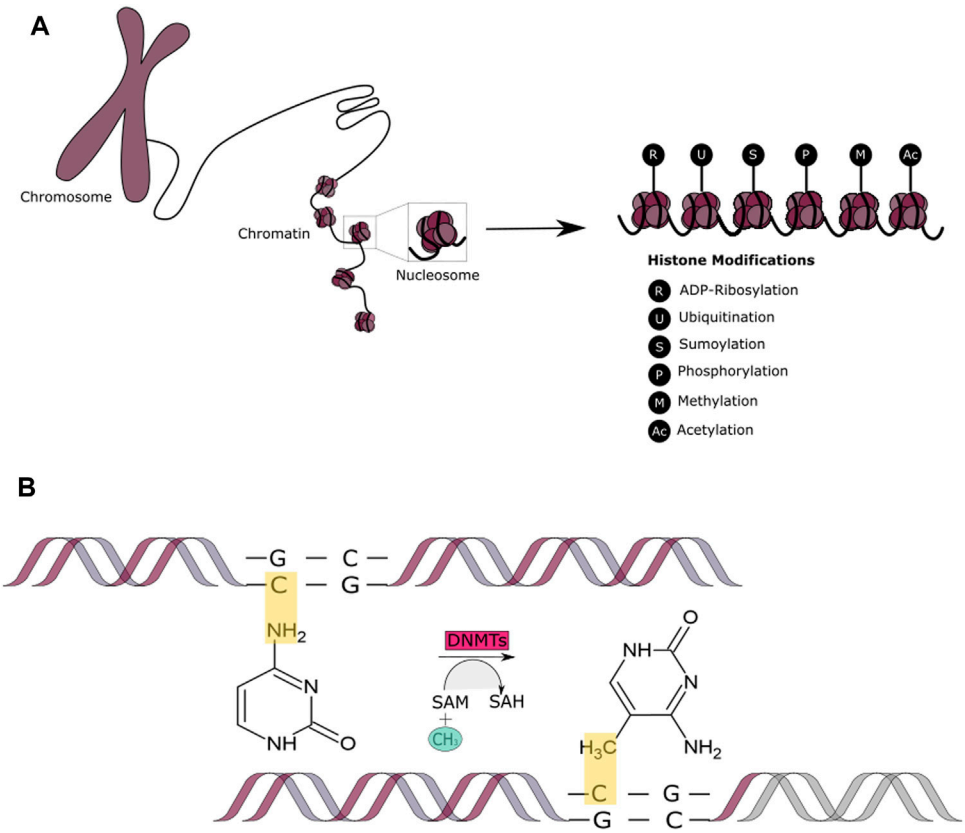

FIGURE 3 | Epigenetic Mechanisms - Histone Modifications and DNA methylation. **(A)** A schematic representation of the covalent post-translational modifications to histone proteins. These include ADP-ribosylation, ubiquitination, sumoylation, methylation, acetylation, and phosphorylation. **(B)** A schematic representation of the DNA methylation process that occurs by addition of the methyl (CH_3) group to the DNA, thereby often modifying the function of certain genes and affecting gene expression.

cancer initiation or progression can lead to resistance to therapy (Emran et al., 2019; Zhu et al., 2019).

Histone acetylation occurs through the addition of an acetyl group via acetyl-CoA to a lysine site at the N-terminal tail of the histone. Histone acetyl transferases (HATs) and histone deacetylases (HDAC) are the enzymes responsible of controlling the addition and removal of the acetyl group to histones, in an ATP-dependent manner (Verdone et al., 2005; Lakshmaiah et al., 2014). The addition of the acetyl group results in a charge change between histones and DNA. The acetyl group neutralizes lysine's positive charge while unwinding the chromatin and hence reducing the affinity between histones and DNA. On the other hand, the removal of the acetyl group condenses the chromatin and promotes the binding of histones and DNA (Görisch et al., 2005). This usually occurs in histones H3 and H4 as they contain several lysine residues.

HDACs play a role in preparing the chromatin to promote the repair of DSBs via HR and NHEJ. One of the mechanisms in which this occurs is through the activation of potent poly (ADP-ribose) polymerse1 (PARP1), a protein abundantly present in the nucleus, that is responsible for post-translational changes by attaching a negatively charged polymer, poly (ADP-ribose) (PAR), to itself and multiple proteins. This activity is known as PARylation (Meter et al., 2016; Mao et al., 2011). PARP1 and the PAR chain signal for the recruitment of the nucleosome remodeling deacetylation (NuRD) complex, which consists of HDAC1, HDAC2, RBBP4, RBBP7, MTA1/2/3, MBD3/2 and CHD3/4, that are essential for DSB repair. HDAC1 and HDAC2 deacetylase target sites at histone H4, which stimulate the RNF8/RNF168-dependent ubiquitination at DSB, promoting repair through NHEJ (Verreault et al., 1998; Chou et al., 2010; Polo et al., 2010; Millard et al., 2016). It has also been reported that the acetylation/deacetylation of specific sites in both histones H4 and H2 can create a switch from NHEJ to HR through the regulation of 53BP1 binding at the DSB site (Tang et al., 2013; Chapman et al., 2013).

A recent player in the DSB repair pathway, COMMD4, has shown promise as a potential prognostic marker and therapeutic target in non-small cell lung cancer. The authors demonstrated that COMMD4 depletion resulted in the induction of mitotic catastrophe and apoptosis of non-small cell lung cancer cells (Suraweera et al., 2020). COMMD4 has additionally been shown to regulate chromatin remodeling at sites of DSBs (Suraweera et al., 2021). COMMD4 is initially recruited to sites of DSBs by hSSB1 and here COMMD4 functions to protect H2B from ubiquitination by the RNF20/40 E3 ligase complex. In

undamaged cells, COMMD4 remains bound to H2B. However, upon the induction of DNA damage and subsequent phosphorylation, followed by disruption of the H2A-H2B dimer, COMMD4 preferentially binds to H2A. This switching of COMMD4 from H2B to H2A, enables RNF20/40 access to H2B and proceed with chromatin remodeling for DSB repair. Thus, highlighting the interplay between epigenetic regulatory mechanisms and DSB repair.

In addition to histone modifications, DNA itself can be modified by methylation. Methyl groups are added to the DNA molecule at specific sites known as CpG islands (**Figure 3B**). Methylation has the ability of changing the activity of a DNA segment without altering its sequence and is suggested to be the most stable of all epigenetic markers, contributing to more sustainable genetic changes. This epigenetic mechanism involves three players: the DNA, the enzyme (DNMTs) and cofactors and the S-adenosyl-L-methionine (SAM) of the cytosines at protected CpG (cystosine-phosphate-guanine sites, 5′-3′) sites of the genome (Lande-Diner and Cedar, 2005). DNA methylation occurs in approximately 60–90 CpG islands located at the promoter regions of the many genes. DNMTs are responsible for DNA methylation in early development. DNMTs obtain the methyl group from an activated S-adenosylmethionine (SAM) which leads to the release of S-adenosylhomocysteine (SAH) as a bi-product (Finkelstein, 1990; Mato et al., 1997). This allows for a cytosine structural change to 5-methylcytosine. Demethylation, comprises the involvement of human ten-eleven translocation (TET) enzymes. These enzymes are responsible of adding a hydroxyl group to the 5-methylcytosine, which leads to the formation of 5-hydroxymethil cytosine that is later transformed back into cytosine with the intervention of other TET enzymes during different pathways (Pastor et al., 2013; Cimmino et al., 2017). Hypomethylation and hypermethylation contribute to genomic instability and it is a characteristic present in cancer tumors. DNA methylation affects gene expression through a "writer," "reader" and "eraser" system. The writer and eraser proteins are the ones in charge of creating or deleting genomic modifications, meanwhile, readers oversee the recognizing of such changes (Kass et al., 1997). DNA methylation allows for the permanent silencing of a gene allowing for the transcriptional machinery to focus on the essential genes needed for the expression and continuity of a differentiated phenotype. It has been shown that DNA methylation plays an important role in early somatic cell differentiation and may also play a role in DNA damage repair (Khavari et al., 2010). Studies have indicated that DSBs can induce hypermethylation and therefore downregulate gene expression. Similarly, DNA damage and repair can lead to an accumulation of aberrant DNA methylation (O'Haganet al., 2008). Additional literature suggests that a balanced intake of nutrients contributes to the maintenance of an effective DNA repair machinery through DNA methylation. For example, dietary folate deficiency is linked with an increased risk of cancer development through DNA damage, hypomethylation and through the inhibition of DNA methyltransferases (Steevens et al., 2011; Kadayifci et al., 2018; Ferrari et al., 2019). Similarly, it has been observed that cancer patients with a low vitamin C diet can lead to an acceleration in cancer progression (Cimmino et al., 2017; Sant et al., 2018; Gillberg et al., 2019). This is because vitamin C can enhance the activity of DNMTs. In terms of its influence in chromatin structure, high levels of methyl-CpG have been associated with transcriptional inactivity and nuclear resistance in endogenous chromosomes (Antequera et al., 1999).

Mechanisms of Histone Deacetylases and Their Inhibitors

HDACs are not redundant in function and have been classified into four groups, based on their homology to yeast. Class I includes HDAC 1, 2, 3 and 8 (yeast RPD3 deacetylase related) which are highly homologous in their catalytic sites and are often ubiquitously expressed in the nucleus. Class II includes HDAC 4, −5, −6, −7, −9 and −10 (yeast Hda1 related), they are usually found in the cytoplasm, but they can also be found in the nucleus. They share homology in the C-terminal catalytic domain and the N-terminal regulatory domain. Class III HDACs are also known as "sirtuins", which enzymatic activity is NAD + dependent (Vaquero et al., 2007). Class IV HDACs (yeast Hda1 related) include HDAC11 and share conserved residues in the catalytic region with class I and II HDACs (Voelter-Mahlknecht et al., 2005).

Due to the different roles in which HDACs are involved; histone deacetylase inhibitors (HDACi) are currently playing an important part in cancer therapy. As the name describes, their function is to inhibit HDAC activity. This occurs by promoting chromatin relaxation through acetylation and therefore, endorsing transcriptional activation (**Figure 4A**). HDACi have been classified into groups which include hydroxamates, cyclic peptides, aliphatic acids, benzamides and electrophilic ketones (Voelter-Mahlknecht et al., 2005). For example, Class I and II HDACs are often inhibited by trichostatin A (TSA), suberoylanilide hydroxamic (SAHA) and related compounds (Ruijter et al., 2003). HDACi have been reported to induce cancer cell cycle arrest, differentiation and cell death, reduce angiogenesis and modulate immune response (Eckschlager et al., 2017). In the context of DSB repair, one of the observed outcomes indicates that HDAC inhibition or knockdown leads to the downregulation of RAD51 or Mre11 of the HR pathway. Similarly, it has been demonstrated that inhibition of HDAC1/2/3 leads to high levels of acetylated Ku 70/80, decreasing its bonding affinity to the DSB ends and therefore decreasing DSB repair via NHEJ. It has additionally been shown that the use of HDACi can increase sensitivity to DSB inducing chemotherapeutics (Koprinarova et al., 2011; Zhao et al., 2017), which occurs through their ability to alter the expression of the most critical proteins involved in the DNA DSB repair pathways.

HDAC1, 2 and 3 are involved in the direct regulation of non-histone proteins that play a critical role in DSB repair pathways. This occurs via acetylation/deacetylation of proteins, such as Ku70. Studies have reported a histone acetylation-independent mechanism by which the HDAC inhibitors; trichostatin A, suberoylanilide hydroxamic acid, MS-275, and OSU-HDAC42,

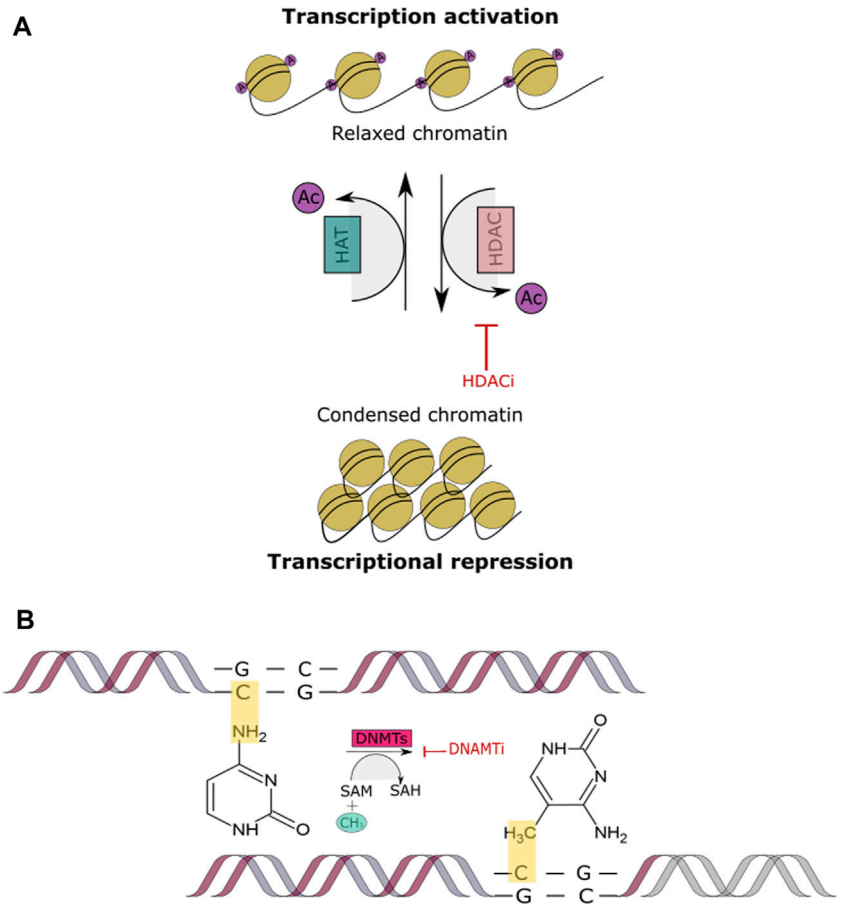

FIGURE 4 | Histone Acetylation and DNA methylation. **(A)** This figure shows the acetylation mechanism of adding an acetyl coenzyme A (acetyl CoA) to the N-terminal tail of a histone through the HAT enzyme, leading to a relaxed chromatin. Conversely, histone deacetylation removes the acetyl CoA through the HDAC enzyme, leading to a condensed chromatin and transcriptional repression. When a HDACi is added the acetyl CoA group cannot be removed and therefore, the chromatin remains relaxed and transcription remains active. **(B)** This figure depicts DNA methylation process being blocked by a DNMTI. The inhibitor prevents the addition of the methyl group to the CpG island site in DNA, inhibiting transcriptional repression.

are able to sensitize prostate cancer cells to DNA damaging agents through the regulation of Ku70 acetylation (Chen et al., 2007). Similarly, it has been shown that during HR, ATM is required for DSB-induced RAD52 acetylation through HATs (p300/CBP) (Yasuda et al., 2018). Rad52 acetylation is important for RAD51 colocalization at the DSB site, therefore, it plays an intrinsic role in the HR repair pathway. It has also been found that human SIRT6-dependent CtIP deacetylation promotes DNA resection, a crucial step in DNA DSB repair by HR (Kaidi et al., 2010). These approaches by which HATs/HDACs lead to mechanisms such as cell sensitization and or the regulation of RAD52 acetylation have been recognized as promising targets for cancer therapy. The use of epigenetic agents can be quite complex. A study showed that the inhibition of HDAC1 and HDAC2 was consistent with a decreased survival of cells upon induction of DSB, suggesting that these lysine deacetylases could potentially promote DSB repair by removing histone marks at the DNA damaged site (Miller et al., 2010). Further studies have revealed the existence of a DNA DSB-induced monoubiquitination-to-acetylation switch on histone H2B, regulated through the SAGA complex, as well as higher-ordering signaling at HR repaired DSBs whereby histone H1 is evicted, while ubiquitin and 53BP1 accumulate over γH2AX domains (Clouaire et al., 2018).

Mechanisms of DNA Methyltransferases and Their Inhibitors

DNMTs are enzymes that interact directly with the chromatin through chromatin-associated proteins, which bind to the histone tails at specific unmethylated sites, e.g., ADD, PWWP domains, H3K4 (Zhang et al., 2010). They are part of a family consisting of a conserved set of DNA-modifying enzymes. DNMT1, DNMT2, DNMT3A, DNMT3B and DNMT3L are the five encoded human DNMTs from which only DNMT1, DNM3A and DNMT3B are canonical cytosine-5 that catalyze the addition of methyl groups to the DNA (**Figure 4B**). Whenever there is a dysregulation in the expression of genes that encode for DNA methylation there are also implications in the regulation of DNMT activity. These regulations can be affected by molecular interactions, post-translational modifications, alternative splicing and through

gene loss and duplication (Li and Zhang, 2014; Robertson et al., 1999; Jeltsch and Jurkowska 2016; Aapola et al., 2000). These alterations often lead to the hypermethylation of tumors, however, the explanation behind such events still needs to be explored. In contrast to methylation of the CpG islands which leads to gene silencing, demethylation promotes gene activation. Studies have shown that DNMTi are able to reactivate tumor suppressor genes. In order to inhibit methylation, any of the three parts that comprise the catalytic pocket can be targeted, which is a promising approach for cancer treatment (**Figure 4B**) (Gros et al., 2015; Kim et al., 2012; Mair et al., 2014; Daskalakis et al., 2002).

Histone Deactylase Inhibitors and DNA Methyltransferase Inhibitors as Epigenetic Drugs Used in the Clinic

Studies have shown that modulation of HAT and HDAC are promising approaches to treat malignant gliomas, T-cell lymphoma, multiple myeloma, breast cancer and other malignancies (Werner et al., 2017; Eyüpoglu and Savaskan, 2016). Understanding how these modulations work has helped improve cancer classification schemes, identify markers for early cancer detection and/or monitoring metastatic disease, improve therapy response and dictate prognosis.

HDACi and DNMTi are the most predominantly approved epigenetic drugs (epi-drugs) by the FDA (**Tables 1**,**2**). Preclinical studies have recently started testing DNMTi and HDACi in combination with immunotherapies and have shown promising clinical responses in cancers such as lung adenocarcinoma, myeloid-derived carcinomas, melanoma and lymphomas (Mazzone et al., 2017) (**Tables 1**,**2**).

Vorinostat was the first HDACi approved by the FDA in 2006 for the treatment of T-cell lymphoma. Seventy-four patients were part of the clinical trial from which 61 had at least stage IIB disease. The overall response rate (ORR) was 29.7% overall; 29.5% in stage IIB or higher patients. Median time to response in stage IIB or higher patients was 56 days. Median duration of response (DoR) was estimated to be ≥ 185 days. Median time to progression was 4.9 months overall and ≥9.8 months for stage IIB or higher responders. Overall, 32% of patients had pruritus relief. Adverse effects included diarrhea (49%), fatigue (46%), nausea (43%), and anorexia (26%); most were grade ≤2. Those grade ≥3 included fatigue (5%), pulmonary embolism (5%), thrombocytopenia (5%), and nausea (4%) (Olsen et al., 2007). Vorinostat clinical trials are ongoing for the treatment of other cancers such as breast cancer, high grade glioma and acute lymphoblastic leukemia (**Table 1**). This drug can be used by itself or in combination with other therapies such as narrowband UVB. This approach has been successful for the treatment of different types of cutaneous T-cell lymphoma (CTCL) (Geskin, 2007; Mann et al., 2007; Ragheb et al., 2017).

Vorinostat in combination with the chemotherapy drug, etoposide, is currently undergoing phase I/II clinical trials for the treatment of solid tumors and relapsed refractory sarcomas in pediatric patients (ClinicalTrials.gov Identifier: NCT01294670). It is also being tested in combination with pembrolizumab to treat patients with advanced lung cancer (ClinicalTrials.gov Identifier: NCT02638090). Valproate (valproic acid) was approved by the FDA in 2008 for seizure treatment in gliomas. It is currently undergoing clinical trials (phase I/II) in combination with neratinib (tyrosine kinase inhibitor) to treat patients with advanced solid tumors (ClinicalTrials.gov Identifier: NCT03919292). Romidepsin was approved in 2009 for the treatment of CTCL and in 2011 for the treatment of peripheral T-cell lymphoma (PTCL). Romidepsin is currently undergoing clinical trials for the treatment of cancers such as relapsed/refractory T-cell lymphoma and peripheral T-cell lymphoma (**Table 1**). Ongoing studies involving romidepsin in combination with tenalisib (PI3K inhibitor) are currently on phase I/II for the treatment of patients with relapsed/refractory T-cell lymphoma (ClinicalTrials.gov Identifier: NCT03770000).

Belinostat was approved by the FDA in 2014 for the treatment of peripheral T-cell lymphoma. The clinical trial was a single-arm, open-label, multicentre trial in relapsed or refractory peripheral T-cell lymphoma (PTCL) patients. One hundred and twenty-nine patients were involved in the trial (range, 29–81 years old) from which the majority of patients had stage III or stage IV disease. The overall response rate (ORR) was 25.8% with a complete response (CR) of rate of 13% and partial response (PR) rate of 18%. Among responding patients treated with belinostat, probability of maintaining response was 57.7% at 6 months, 48.8% at 1 year and 32.6% at 2 years. The probability of surviving and being progression free at 1 year was 19.3%. One hundred and thirteen patients out of 129 tolerated belinostat well, median treatment duration was 7 weeks. The adverse events occurred in 96.9% of patients being generally mild to moderate in severity. These included nausea (41.9%), fatigue (37.2%), and pyrexia (34.9%). Grade 3–4 thrombocytopenia occurred in only 7.0% (O'Connor et al., 2015). Belinostat is currently undergoing studies to be used in the clinic for unresectable/metastatic conventional chondrosarcoma; glioblastoma multiforme and T-cell leukemia-lymphoma (**Table 1**). Clinical studies on belinostat in combination with SGI-110 (guadecitabine/hypomethylating agent) are currently in phase II trials for the treatment of unresectable and metastatic conventional chondrosarcoma (ClinicalTrials.gov Identifier: NCT04340843).

Panobinostat, was approved by the FDA in 2015 and has shown to be effective against Multiple Myeloma. The clinical trial consisted of combining panobinostat, bortezomib and dexamethasone with placebo, bortzomib and dexamethasone. This was a multicentre, randomized, placebo-controlled, double-blind phase III trial of relapsed or relapsed and refractory multiple myeloma who were randomly assigned 1:1. Seven hundred and eighty-six patients participated in the study. The median follow-up was 6.47 months in the panobinostat group and 5.59 months in the placebo group. The median progression-free survival was significantly longer in the panobinostat group than in the placebo group (11.99 vs 8.08 months, $p < 0.0001$). At the time of the study the overall survival was not yet mature. Serious adverse responses were reported in 60% of the 381 patients in the panobinostat group

TABLE 1 | Most common clinically used histone deacetylase inhibitors that have been approved by the FDA or are currently undergoing clinical trials for the treatment of cancer.

HDAC inhibitor	HDAC class	Maximum phase of therapy	Cancer type	Status	FDA approval	DNA damage impact: Proteins regulated or involved/pathway impact/cellular response
Romidepsin	Cyclic tetrapeptide	Phase III	Peripheral T cell lymphoma	Active, not recruiting	No	DNA damage and apoptotic cell death through caspase activation; accumulation of DNA-RNA hybrids (R-loops); radiosensitiser; activation of ATM pathway, increased production of reactive oxygen species (ROS), decreased mitochondrial membrane potential Valdez et al., (2018); Miles et al., (2019); Paillas et al., (2020); Rossetti et al., (2021); Safari et al., (2021)
		Phase II	Cutaneous T-cell lymphoma; peripheral T-cell lymphoma; T-cell non-Hodgkin lymphoma	Completed	Yes	
		Phase I/II	Relapsed/refractory T-cell lymphoma; peripheral T-cell lymphoma; relapsed/refractory lymphoid malignancies; multiple myeloma, non- Hodgkin's lymphoma; recurrent or metastatic triple negative breast cancer	Active, not recruiting	No	
Panobinostat	Hydroxamates	Phase III	Multiple myeloma	Completed	Yes	Pleiotropic antitumour effects and autophagy; induces clastogenicity, aneugenicity, oxidative damages and hypomethylation; increased G2/M arrest and production of ROS, enhanced proton-induced DNA damage A. Wilson et al., (2020); Choi et al., (2021); Al-Hamamah et al., (2019); Medon et al., (2017)
		Phase III	Acute myeloid leukemia; myelodysplastic syndromes	Completed	No	
		Phase II	Multiple myeloma; recurrent plasma cell myeloma; refractory/relapsed multiple myeloma; relapsed/refractory non-Hodgkin lymphoma; diffuse intrinsic pontine glioma	Active, not recruiting	No	
Mocetinostat	Benzamide	Phase II	Non-small cell lung carcinoma	Active, not recruiting	No	Potentially regulates RAD51 through HDAC2 in some cancers; maintains chromatin state; chemosensitizer; tumor suppression; increases tumor antigen presentation; cell cycle progression; suppresses cell proliferation; induces apoptosis through the upregulation of miR-31 (pro-apoptotic microRNA) (Briere et al., (2018); Q. Zhang et al., (2016b; Mondal et al., (2020); Headley et al., (2019); Shan et al., (2017); Yan and Efferth (2020)
		Phase I/II	Hodgkin lymphoma; lymphoma; relapsed/refractory hodgkin lymphoma; relapsed and refractory diffuse large B-cell lymphoma and follicular lymphoma	Active, not recruiting	No	
MS-275	Miscellaneous	Phase III	Advanced/metastatic breast cancer	Active, not recruiting	No	Inhibits RAD51/FANCD2 mediated HR; increases radiosensitization by prolongation of γH2AX Yao et al., (2018); Christmann and Kaina (2019); Kaina and Christmann (2019)
		Phase II	Renal cell carcinoma; male breast carcinoma, recurrent breast carcinoma; endometrial endometrioid adenocarcinoma; cholangiocarcinoma and pancreatic cancer; metastatic pancreatic cancer; metastatic uveal melanoma; bladder cancer; advanced or recurrent breast cancer	Active, not recruiting	No	
		Phase I/II	Epithelial ovarian cancer; peritoneal cancer; fallopian tube cancer; CNS tumor; solid tumor; non-small cell lung cancer; melanoma; mismatch repair-proficient colorectal cancer; clear renal cell carcinoma; metastatic kidney carcinoma; stage III, IV renal cell cancer; breast neoplasm	Active, not recruiting	No	
Abexinostat	Hydroxamates	Phase III	Renal cell carcinoma	Active, not recruiting	No	Regulates RAD51 (Kashyap et al., (2020)
		Phase II	Relapsed/refractory follicular lymphoma	Active, not recruiting	No	
Belinostat	Hydroxamates	Phase II	Peripheral T-cell lymphoma	Completed	Yes	Upregulates the expression of several genes in DNA damage pathway (PARP1, Gadd45a, Mpg); downregulates the expression of several genes involved in DNA damage pathway (Cdc25c, RAD 18, 51, 9, 1, TRP53, XRCC1); radiosensitizing through the induction of oxidative stress
		Phase II	Unresectable/metastatic conventional chondrosarcoma; glioblastoma multiform of brain; T-cell leukemia-lymphoma	Active, not recruiting	No	

(Continued on following page)

TABLE 1 | (*Continued*) Most common clinically used histone deacetylase inhibitors that have been approved by the FDA or are currently undergoing clinical trials for the treatment of cancer.

HDAC inhibitor	HDAC class	Maximum phase of therapy	Cancer type	Status	FDA approval	DNA damage impact: Proteins regulated or involved/pathway impact/cellular response
						and DNA damage; interferes with mitotic spindle assembly; promotes stem cell differentiation and inhibits MYC pathways (García-Giménez et al.,; To et al., (2017); F. Chi et al., (2021; Marijon et al., (2018); Attia et al., (2018)
Valproic acid	Short-chain fatty acid	Phase IV	Seizure treatment in glioma	Completed	Yes	Upregulates gadd45a; radiosensitizer via increase of γH2AX phosphorylation; alters cell proliferation, cell survival, cell migration and hormone receptor expression; increases cell cycle arrest by increasing the expression of cyclin dependent kinase inhibitor (CDKN1A) Jang et al. (2020); Gao et al., (2020); Yan et al., (2021); Bhatti et al., (2021); Ding et al., (2020)
		Phase II	High-grade glioma; myelodysplastic syndromes	Active, not recruiting	No	
		Phase I/II	Solid tumors; acute myeloid leukemia	Active, not recruiting	No	
Vorinostat	Hydroxamates	Phase III	Multiple myeloma; relapsed/refractory cutaneous T-cell lymphoma	Active, not recruiting	No	Downregulates the expression of genes involved in DNA repair pathway (BIRP1, CDC25C, RAD proteins, TRP53, XRCC1); upregulates mRNA transcripts of repair genes implicated in DNA damage (Gadd45a, PARP1, BAX); induces chromosomal aberrations, oxidative damages, apoptosis and hypomethylation; decreases cellular viability and ROS (Singh et al., (2021); Sher et al., (2020); Zhang et al., (2020); Attia et al., (2020)
		Phase II	Cutaneous T-cell lymphoma	Completed	Yes	
			Breast cancer; neuroblastoma; adenomas in Cushing's disease; cutaneous T-cell lymphoma/mycosis fungoides; myelodysplastic syndromes or chronic myelomonocytic leukemia	Active, not recruiting	No	
		Phase II/III	High grade glioma	Active, not recruiting	No	
		Phase I/II	Recurrent squamous cell head and neck cancer or salivary gland cancer; melanoma, skin neoplasms; multiple myeloma; advanced sarcoma; diffuse large B-cell lymphoma (stage II, III or IV); glioblastoma; glioblastoma multiforme; HIV-related diffuse large B-cell non-hodgkin lymphoma; acute myeloid leukemia in remission; myelodysplastic syndromes or acute myeloid leukemia	Active, not recruiting	No	
Nicotinamide	Sirtuins inhibitors	Phase III	Head and neck cancer; skin cancer	Completed	Yes	Represses genes involved in DNA damage and repair (FANCD2, BRCA1, RAD51; increases levels of phosphorylated DDR markers (γH2AX, pChk1 and p53) leading to cellular sensitivity (Pillay et al., (2021); Ogino et al., (2019); Magalhaes et al., (2021); Singh et al., (2021)
		Phase II	Non-melanoma skin cancer, squamous cell carcinoma, basal cell carcinoma; breast cancer metastatic, platinum resistant recurrent ovarian cancer; metastatic lung carcinoma; chronic myeloid leukemia	Active, not recruiting	No	
		Phase II/III	Non-small cell lung carcinoma	Active, not recruiting	No	

Source: U.S. National Library of Medicine, U.S. Food and Drug Administration, NIH Clinical Trial database: www.clinicaltrials.gov

and 42% of 377 patients in the placebo group. Common grade 3–4 laboratory abnormalities and adverse events included thrombocytopenia (67% panobinostat group vs 31% placebo group), lymphopenia (53 vs 40%), diarrhea (26 vs 8%), asthenia or fatigue (24 vs 12%) and peripheral neuropathy (18 vs 15%) (San-Miguel et al., 2014). Other studies suggest that panobinostat may also be effective against triple negative breast cancer, non-small cell lung cancer and head and neck squamous cell carcinoma (HNSCC) (Raedler, 2016; Suraweera et al., 2018) (**Table1**). Additionally, panobinostat in combination with carfilzomib (proteasome inhibitor) is currently in phase I/II clinical trials for the treatment of patients with relapsed/refractory MM (ClinicalTrials.gov Identifier: NCT01496118).

DNMTis can be nucleoside, non-nucleoside or oligonucleotide. Nucleoside DNMTis are integrated into the DNA and are prone to toxicity (e.g. 5-azacytidine, azacytosine and zebularine) (**Table 2**) (Zhou et al., 2002; Stresemann and Frank 2008; Gnyszka et al., 2013). On the other hand, non-nucleoside DNMTis are less toxic and usually more effective because they are not integrated into DNA (e.g., epigallocatechin-

TABLE 2 | Most common DNA methyltransferase inhibitors that have been approved by the FDA or are currently undergoing clinical trials for the treatment of cancer.

DNMT inhibitor	DNMT class	Maximum phase of therapy	Cancer type	Status	FDA approval	DNA damage impact: Proteins regulated or involved/pathway impact/cellular response
5-Azacitidine	Nucleoside	Phase III	Continued treatment of acute myeloid leukemia and treatment of all subtypes of myelodysplastic syndrome	Completed	Yes	Cytotoxicity caused by genomic instability and DNA damage as a result of hypomethylation; reactivation of tumor suppressor genes (TSG); apoptosis through the reduction of MCL-1 expression levels (Guo et al., 2021; Guirguis, Liddicoat, and Dawson 2020; Goel et al., 2021; Zhou, Li, and Liu 2018)
			Acute myeloid leukemia; myelodysplastic syndromes	Active, not recruiting	No	
		Phase II/III	Acute myeloid leukemia or high-risk myelodysplastic syndrome	Active, not recruiting	No	
		Phase II	Advanced solid tumors; male breast carcinoma; recurrent breast cancer, stage IIIC breast cancer; stage IV breast cancer, triple negative breast carcinoma; neoplasms; pancreatic cancer; epithelial ovarian cancer; advanced/metastatic non-small cell lung cancer; prostate cancer; ovarian, primary peritoneal, or fallopian tube cancer; peripheral T-cell lymphoma; Chronic myeloid leukemia; relapsed/refractory acute myeloid leukemia or relapsed/high-risk myelodysplastic syndrome	Active, not recruiting	No	
		Phase I/II	Mutant myeloid neoplasm; solid tumors, gliomas; acute myeloid leukemia; myelodysplastic syndrome; non-Hodgkin lymphoma, multiple myeloma, lymphocytic leukemia; recurrent ovarian, fallopian tube or primary peritoneal cancer	Active, not recruiting	No	
Decitabine (analogues: 5-Aza-fluoro-2-deoxycytidine; zebularine)	Nucleoside	Phase IV	Acute myeloid leukemia	Active, not recruiting	No	Increases DSB frequency; reduces proliferation through PARP binding; invasion and adhesion; activation of tumor suppressor genes (VHL, CDKN2A, GATA4, MLH1) Sato, et al. (2017); Dellomo et al. (2019); Kashyap et al. (2020); Nigris et al. (2021)
		Phase III	Myelodysplastic syndromes (MDS) including myelomonocytic leukemia	Completed	Yes	
		Phase III	Acute myeloid leukemia; myelodysplastic syndromes	Active, not recruiting	No	
		Phase II/III	Acute myeloid leukemia or high-risk myelodysplastic syndrome	Active, not recruiting	No	
		Phase II	Non-small cell lung cancer; acute myeloid leukemia; leukemia; myelodysplastic syndromes	Active, not recruiting	No	
		Phase I/II	Advanced solid tumors; acute myeloid leukemia; acute myelogenous leukemia; diffuse large B cell lymphoma	Active, not recruiting	No	
MG98	Oligonucleotide	Phase I	Solid tumors	Completed	No	Cellular sensitization, growth inhibition concomitant with re-expression of TSGs P16ink4a and RUNX3 Beaulieu et al. (2004); Reu et al. (2004); Ramezankhani et al. (2021)
S110	Miscellaneous	Phase III	Acute myeloid leukemia; myelodysplastic syndromes, chronic myelomonocytic leukemia	Completed	No	Suggested to be a damaging variant of the NHEJ pathway through XRCC4; retards tumor growth Voorde et al. (2012); Singh et al. (2018)
		Phase II	Small cell lung cancer; myeloproliferative neoplasms; recurrent ovarian carcinoma, primary peritoneal or fallopian tube cancer; urothelial cancer; high-risk myelodysplastic syndrome	Active, not recruiting	No	
		Phase I/II	Advanced kidney cancer; recurrent ovarian, fallopian tube or primary peritoneal cancer	Active, not recruiting	No	

Source: U.S. National Library of Medicine, U.S. Food and Drug Administration, NIH Clinical Trial database: www.clinicaltrials.gov

3-gallate EGCG, RG108 and procaine) (Y. C. Li et al., 2018; Rondelet et al., 2017; Zhang et al., 2016a). Oligonucleotides comprise antisense molecules such as MG98 (Davis et al., 2003) (**Table 2**). 5-Azacytidine (Vidaza) was the first DNMTi approved by the FDA in 2008 to be used in the clinic for the treatment of patients with myelodysplastic syndromes (MDS) (**Table 2**). In a phase III, international, multicentre, controlled, parallel-group, open-label trial, 358 patients with higher-risk myelodysplastic syndromes were randomly assigned 1:1 to receive azacytidine (n = 179) or conventional care (n = 179). With a median follow-up of 21.1 months the median overall survival was 24.5 months for the azacitadine group vs 15.0 months for the conventional care group. At 2 years the estimated overall survival was 50.8% for patients in the azacitadine group and 26.2% in the conventional care group ($p < 0.0001$). Peripheral cytopenias were the most common grade 3–4 adverse events for all treatments (Fenaux et al., 2009). Azacitidine is currently undergoing phase IV clinical trials in combination with HAG (Homoharringtonine, Cytarabine, G-CSF) regimen for the treatment of elderly patients with newly diagnosed myeloid malignancy (ClinicalTrials.gov Identifier: NCT03873311). It is also being studied in combination with the mutant p53 reactivating compound APR-246 (phase I/II) for the treatment of MDS and acute myeloid leukemia (ClinicalTrials.gov Identifier: NCT03588078). Another DNMTi known as decitabine (DACOGEN) has recently been approved by the FDA in combination with cedazuridine for the treatment of previously treated/untreated, *de novo* and secondary MDS as well as intermediate 1, 2 and high-risk International Prognostic Scoring System groups (FDA n. d.). Decitabine, alone, was initially approved in 2006 for the treatment of MDS. A total of 170 patients with MDS were randomized to receive either decitabine or best supportive care. Patients treated with decitabine achieved a significantly higher ORR (17%), including 9% CR, compared with supportive care (0%) ($p < 0.001$). Responses were durable (median, 10.3 months) and a trend toward a longer median time to acute myelogenous leukemia progression or death compared with patients who received supportive care alone was observed (Kantarjlan et al., 2006). Decitabine's efficacy has led to continuous studies for the treatment of different cancers such as primary malignant neoplasm of ovary, metastatic renal cell carcinoma and non-small cell lung cancer (**Table 2**). Hydralazine is a vasodilator initially approved by the FDA in 1997 for the treatment of high blood pressure and heart failure. However, recent studies have shown that it also acts as a DNMTi by inducing caspase-dependent apoptotic cell death in p53-mutant leukemic T lymphocytes (Ruiz-Magaña et al., 2016).

Despite, the promising outcomes of these epigenetic mechanisms in cancer patients, the anti-tumour activity achieved by HDACi and DNMTi are still limited. For instance, an alternative approach has been the use of combination therapy. Two or more therapeutic agents that individually produce similar or additive effects will often display enhanced efficacy, referred to as synergy, when given in combination (e.g., drug 1 + drug 2 = synergy). In this review we will mainly focus on the combination of HDACi and/or DNMTi together with DNA repair inhibitors and/or immune checkpoint inhibitors. The purpose behind this combination treatment approach is to target the blocking of several key pathways. Thus, to reshape the tumor microenvironment and potentially obtain a synergistic ani-tumour response that would be greater than that predicted by their individual potencies (Zeng et al., 2016; Villanueva et al., 2020; Zhou et al., 2018).

Histone Deactylase Inhibitors and DNA Methyltransferase Inhbitors in Combination With DNA Repair Inhibitors in the Clinic

The advent of PARP inhibitors has pinpointed DNA repair inhibitors as predominant targets for cancer therapy (Tangutoori et al., 2015). Olaparib (Lynparza), is a PARP inhibitor (PARPi) that targets the DNA damage response as a single agent for the treatment of breast and ovarian cancers in patients harboring BRCA1 or BRCA2 germline mutations (Kim et al., 2015). PARP anti-tumour activity is based on inducing defects in genes/pathways leading to genomic instability. PARPi induce apoptosis caused by the aggregation of DNA damage which favors the flow of T-cells into the tumor microenvironment, triggering the upregulation of PD-1/PD-L1 pathway. At present there are several clinical trials underway combining HDACi in combination with olaparib. A phase I clinical trial combining olaparib and vorinostat, busulfan, gemcitabine and melphalan with or without rituximab, has started for patients suffering from refractory lymphomas (ClinicalTrial.gov identifier: NCT03259503). There are additionally several clinical trials underway combining olaparib and entinostat for the treatment of ovarian carcinoma, peritoneal carcinoma fallopian tube carcinoma (ClinicalTrial.gov identifier: NCT03924245) and olaparib in combination with vorinostat for the treatment of relapsed, refractory and/or metastatic breast cancer (ClinicalTrial.gov identifier: NCT03742245).

Other approaches include a study conducted by (Kim et al., 2012), which suggests that DNMTi are able to induce radiosensitivity in a cell line model with A549 and U373MG cells together with an extended activity of γH2AX, which is believed to be achieved through DNA repair inhibition. However, more studies are needed to identify other additional mechanisms that can also be associated with radiosensitivity and to confirm the synergistic effects on radiosensitivity with other epigenetic drugs such as HDACi. It is expected that further investigation on this method will help determine whether the combination of DNMTi and radiation has potential as a future clinical approach for cancer treatment. Another approach involves using DNMTi in multiple myeloma cells through an ataxia telangiectasia and Rad3-related protein mediated manner that induces DNA DSBs, leading to apoptosis. (Kiziltepe et al., 2007). This study suggests significant relevance into pursuing more in-depth clinical trials involving 5-AzaC alone and in combination with other chemotherapy drugs for the treatment of multiple myelomas (**Table 2**). More recent examples of drug combinations are, the dual DNMTi and HDACi 208, which has shown to instigate antiproliferative activity against histiocytic lymphoma (U937) cells (Zhou et al., 2018). This occurs by

inducing G1 cell cycle arrest and apoptosis through the upregulation of CDK inhibitor p16, combined with the downregulation of cyclin-dependent kinases and their activators. Proteome and bioinformatic analyses showed that 208 inhibitor combinations affected the expression of a series of proteins involved in DNA repair. Similarly, PARPi has been studied in combination with DNMTi (e.g. guadecitabine or 5-azacitidine) with the purpose of being able to resensitize tumors to primary therapies or reprogramming DNA damage repair responses in cancers such as breast, ovarian and non-small cell lung cancers (Abbotts et al., 2019; Zhou et al., 2018; Muvarak et al., 2017).

Previous literature also indicates that CRISPR/dCAS9 can induce histone acetylation/deacetylation and methylation by catalyzing direct covalent modifications or via the recruitment of complexes that mediate such mechanisms (Tang et al., 2019; Thakore et al., 2015; Hilton et al., 2015). Similarly, DNA methylation/demethylation mechanisms can be programmed for the methyl groups to be added or removed from specific CpG island sites using CRISPR/dCas9. This epigenetic editing approach has been under continuous investigation as it proves to be more effective than modifications previously attempted by ZINC finger nucleases and TALENs modifications (Zhou et al., 2018; Thakore et al., 2015; Hilton et al., 2015; Zhang et al., 2017; Chi et al., 2021b). The use of CRISPR/dCas9 is a powerful candidate to manipulate the expression of therapeutic target genes, via epigenetic mechanisms, in cancer cells. (Jiang et al., 2015; Momparler et al., 2017; Wang et al., 2018).

Histone Deactylase Inhibitors and DNA Methyltransferase Inhibitors in Combination With Immune Checkpoint Inhibitors

Immune checkpoint inhibitors (ICis) are one of the most recent effective methods at reactivating anti-tumour responses in immune-oncology. They fulfill the role of keeping effector T-cells active in order to fight tumor cells. The first checkpoint inhibitor to be approved by the FDA was ipilimumab (targeting T-lymphocyte antigen-4, CTLA-4) for the treatment of melanoma patients (Hodi et al., 2010; Robert et al., 2011). Other ICis that have already been approved to be used in treatment are pembrolizumab and nivolumab as well as, atezolizumab, durvalumab and avelumab, used for the treatment of different carcinomas including metastatic melanoma, non-small cell lung cancer, renal cell carcinoma and neck squamous carcinoma (Kim, 2017; Syed, 2017; Horn et al., 2018; Ferris et al., 2016; Reck et al., 2016; Khoja et al., 2015). The latest monoclonal antibody approved by the FDA is cemiplimab for the treatment of metastatic cutaneous squamous cell carcinoma (Markham and Duggan, 2018). There have been several studies of HDACi and DNMTi in combination with ICis as an innovative approach in immunotherapy. Studies have shown that bladder tumors carry upregulated levels of HDACs. Pre-clinical trials are currently ongoing for using the HDACi, romidepsin and SAHA, in combination with HR-DNA repair genes and PARPi for the treatment of bladder cancer (Criscuolo et al., 2019). Additionally, DNMTi 5-aza-2′-deoxycytidine is currently undergoing trials to be used together with CTLA-4 for the treatment of mammary carcinoma and mesothelioma (Covre et al., 2015). PD-1/PD-L1 ICis have also been commenced in combination with alterations of DDR genes to treat urothelial carcinoma. It is expected that further studies involving HDACi, DNMTi and ICis will reveal novel ways of targeting genes involved in DDR, that can potentially be used as personalized immunotherapies (Daver et al., 2019; Gray et al., 2019).

Histone Deactylase Inhibitors and DNA Methyltransferase Inhibitors: Challenges to Overcome

Often, a single approach, such as adjuvant chemotherapy, is not effective in every patient and therefore leads to disease recurrence (Mamounas et al., 2017). Combination therapy is an approach designed to reinvigorate a drug's effect against a specific type of cancer, however, this path is also not always a safe bet. For example, the clinical use of atezolizumab in combination with paclitaxel protein-bound (abraxane) has been approved by the FDA for the treatment of metastatic triple negative breast cancer (mTNBC) in adult patients expressing PD-L1 (Narayan et al., 2020). The FDA has raised awareness about recent clinical studies showing that atezolizumab + paclitaxel combination has no effect in previously untreated inoperable locally advanced or mTNBC (FDA 2020b). It would therefore be recommended that abraxane should not be replaced with paclitaxel in clinical practice. Consequently, these results will require further testing and the potential update of current prescribing information. It is also well known that cancer cells develop drug resistance and therefore, cells can develop DNMTi and HDACi resistance (Maeda et al., 2018). This can lead to an increase or decrease in activity of important pathways such as HR and NHEJ. Some epi-drugs such as nucleoside DNMTi, are introduced into the DNA and have a toxic effect and future research should focus on finding epi-drugs that are more effective and less toxic. Similarly, it can be challenging to identify an epigenetic target that remains stable when tested *in vivo*. The emergence of nanotechnology in cancer therapy has shown to be an encouraging strategy to enhance the effectiveness of HDACi (Tangutoori et al., 2015).

CRISPR/dCAS9 is a novel promising approach to achieve programmable histone modifications and DNA methylation. However, this mechanism is still in its early stages and it requires further research before it can be used in the clinic as an epigenetic therapy. Currently, there are still risks of off-target effects, and potential secondary effects caused by unintended factors (Tang et al., 2019; Zhang et al., 2017; Thakore et al., 2015; Hilton et al., 2015). Additionally, when not used appropriately, CRISPR is prone to non-specific binding. Regardless of the mechanism, if successful, an epigenetic drug may be effective in one type of cancer but not in others. This means that it will require further clinical studies. It is also important to consider that the effect of an epigenetic change may vary in different phases of the trial.

CONCLUSION

DSBs are the most cytotoxic type of DNA backbone damage. In response to this genetic lesion, cells have evolved to recognize the

damage and signal for DNA DSB repair mechanisms. Failing to repair DNA via HR or NHEJ pathways can lead to cancer and/or tumorigenesis. Investigating how cancer works from an epigenetic perspective has helped improve cancer classification schemes, identify markers for early cancer detection and/or monitoring metastatic disease, improve therapy response, dictate prognosis as well as helping in identifying epigenetic patterns associated to a cell's transcriptional activity. DNMTi and HDACi have been shown to have positive effects in cancer treatment, especially when combined with traditional therapies or other epigenetic drugs. However, epigenetic drugs are just at the beginning of their apogee and there are still many factors to consider. Attention must be focused in finding epi-drugs that are more effective and less toxic; it is challenging to identify epigenetic targets that remain stable when tested *in vivo*. The CRISPR/dCAS9 approach to program the addition/removal of methyl groups still needs to be fine-tuned in terms of specificity. There are challenges in identifying epigenetic targets that remain equally effective in a type of cancer across all clinical trial phases. Taken together, epigenetic treatments are promising independent, combination treatment and potential personalized treatments in cancer therapy.

AUTHOR CONTRIBUTIONS

All authors were involved in the conception of the manuscript, the drafting and critically reviewing of the manuscript and have approved the final version for publication.

FUNDING

This work was supported by the Cancer and Ageing Research Program, a QUT Postgraduate Research Award (International) granted by the Queensland University of Technology (AF), a Chenhall Research Trust Award (DR) and a Yancoal Grant (KO).

REFERENCES

Aapola, U., Shibuya, K., Scott, H. S., Ollila, J., Vihinen, M., Heino, M., et al. (2000). Isolation and Initial Characterization of a Novel Zinc Finger Gene, DNMT3L, on 21q22.3, Related to the Cytosine-5- Methyltransferase 3 Gene Family. *Genomics* 65, 293–298. doi:10.1006/geno.2000.6168

Abbotts, R., Topper, M. J., Biondi, C., Fontaine, D., Goswami, R., Stojanovic, L., et al. (2019). DNA Methyltransferase Inhibitors Induce a BRCAness Phenotype that Sensitizes NSCLC to PARP Inhibitor and Ionizing Radiation. *Proc. Natl. Acad. Sci. USA* 116 (45), 22609–22618. doi:10.1073/pnas.1903765116

Ahnesorg, P., Smith, P., and Jackson, S. P. (2006). XLF Interacts with the XRCC4-DNA Ligase IV Complex to Promote DNA Nonhomologous End-Joining. *Cell* 124 (2), 301–313. doi:10.1016/J.CELL.2005.12.031

Al-Hamamah, M. A., Alotaibi, M. R., Ahmad, S. F., Ansari, M. A., Attia, M. S. M., Nadeem, A., et al. (2019). Genetic and Epigenetic Alterations Induced by the Small-Molecule Panobinostat: A Mechanistic Study at the Chromosome and Gene Levels. *DNA Repair* 78 (June), 70–80. doi:10.1016/j.dnarep.2019.03.008,

Alexandrova, E., Lamberti, J., Saggese, P., Pecoraro, G., Memoli, D., Valeria Mirici, C., et al. (2020). Small Non-coding RNA Profiling Identifies MiR-181a-5p as a Mediator of Estrogen Receptor Beta-Induced Inhibition of Cholesterol Biosynthesis in Triple-Negative Breast Cancer. *Cells* 9 (4), 874. doi:10.3390/cells9040874

Andor, N., Maley, C. C., and Ji, H. P. (2017). Genomic Instability in Cancer: Teetering on the Limit of Tolerance. *Cancer Res.* 77 (9), 2179–2185. doi:10.1158/0008-5472.CAN-16-1553

Antequera, F., Macleod, D., and Bird', A. P. (1999). Specific Protection of Methylated CpGs in Mammalian Nuclei. *Cell* 59.

Antonarakis, S. E., Lyle, R., Dermitzakis, E. T., Reymond, A., and Deutsch, S. (2004). Chromosome 21 and Down Syndrome: From Genomics to Pathophysiology. *Nat. Rev. Genet.* 5, 725–738. doi:10.1038/nrg1448

Ashton, N. W., Paquet, N., Shirran, S. L., Bolderson, E., Kariawasam, R., Touma, C., et al. (2017). HSSB1 Phosphorylation Is Dynamically Regulated by DNA-PK and PPP-Family Protein Phosphatases. *DNA Repair* 54 (June), 30–39. doi:10.1016/j.dnarep.2017.03.006

Attia, S. M., Al-Hamamah, M. A., Alotaibi, M. R., Harisa, G. I., Attia, M. M., Ahmad, S. F., et al. (2018). Investigation of Belinostat-Induced Genomic Instability by Molecular Cytogenetic Analysis and Pathway-Focused Gene Expression Profiling. *Toxicol. Appl. Pharmacol.* 350 (July), 43–51. doi:10.1016/j.taap.2018.05.002

Attia, S. M., Al-Khalifa, M. K., Al-Hamamah, M. A., Alotaibi, M. R., Attia, M. S. M., Ahmad, S. F., et al. (2020). Vorinostat Is Genotoxic and Epigenotoxic in the Mouse Bone Marrow Cells at the Human Equivalent Doses. *Toxicology* 441 (August), 152507. doi:10.1016/j.tox.2020.152507,

Beaulieu, N., Dupont, I., and Robert Macleod, A. (2004). Antitumor Activity of MG98, an Antisense Oligodeoxynucleotide Targeting DNA Methyltransferase-1 (DNMT1) in Gastric Carcinoma. *Cancer Res.* 64 (7 Supplment).

Bhatti, U. F., Remmer, H., Williams, A. M., Biesterveld, B. E., Russo, R., Wakam, G., et al. (2021). Assessment of the Cytoprotective Effects of High-Dose Valproic Acid Compared to a Clinically Used Lower Dose. *J. Surg. Res.* 266 (October), 125–141. doi:10.1016/j.jss.2021.03.025

Bolderson, E., Tomimatsu, N., Richard, D. J., Boucher, D., Kumar, R., Pandita, T. K., et al. (2010). Phosphorylation of Exo1 Modulates Homologous Recombination Repair of DNA Double-Strand Breaks. *Nucleic Acids Res.* 38 (6), 1821–1831. doi:10.1093/nar/gkp1164

Boldogh, I., Roy, G., Lee, M.-S., Bacsi, A., Hazra, T. K., Bhakat, K. K., et al. (2003). Reduced DNA Double Strand Breaks in Chlorambucil Resistant Cells Are Related to High DNA-PKcs Activity and Low Oxidative Stress. *Toxicology* 193 (1–2), 137–152. doi:10.1016/J.TOX.2003.08.013

Briere, D., Sudhakar, N., Woods, D. M., Hallin, J., Engstrom, L. D., Aranda, R., et al. (2018). The Class I/IV HDAC Inhibitor Mocetinostat Increases Tumor Antigen Presentation, Decreases Immune Suppressive Cell Types and Augments Checkpoint Inhibitor Therapy. *Cancer Immunol. Immunother.* 67 (3), 381–392. doi:10.1007/s00262-017-2091-y

Brower, V. (2011). Epigenetics: Unravelling the Cancer Code. *Nature* 471 (7339 Suppl. L), S12–S13. doi:10.1038/471S12a

Brown, J. S., O'Carrigan, B., Jackson, S. P., and Yap, T. A. (2017). Targeting DNA Repair in Cancer: Beyond PARP Inhibitors. *Cancer Discov.* 7, 20–37. doi:10.1158/2159-8290.CD-16-0860

Caracciolo, D., Scionti, F., Juli, G., Altomare, E., Golino, G., Todoerti, K., et al. (2021). Exploiting MYC-Induced PARPness to Target Genomic Instability in Multiple Myeloma. *Haematol.* 106 (1), 185–195. doi:10.3324/haematol.2019.240713

Chapman, J. R., Barral, P., Vannier, J.-B., Borel, V., Steger, M., Tomas-Loba, A., et al. (2013). RIF1 Is Essential for 53BP1-dependent Nonhomologous End Joining and Suppression of DNA Double-Strand Break Resection. *Mol. Cel.* 49 (5), 858–871. doi:10.1016/j.molcel.2013.01.002

Chapman, J. R., Taylor, M. R. G., and Boulton, S. J. (2012). Playing the End Game: DNA Double-Strand Break Repair Pathway Choice. *Mol. Cel.* 47 (4), 497–510. doi:10.1016/j.molcel.2012.07.029

Chen, C.-S., Wang, Y.-C., Yang, H.-C., Huang, P.-H., Kulp, S. K., Yang, C.-C., et al. (2007). Histone Deacetylase Inhibitors Sensitize Prostate Cancer Cells to Agents that Produce DNA Double-Strand Breaks by Targeting Ku70 Acetylation. *Cancer Res.* 67, 5318–5327. doi:10.1158/0008-5472.CAN-06-3996

Chen, L., Nievera, C. J., Lee, A. Y.-L., and Wu, X. (2008). Cell Cycle-dependent Complex Formation of BRCA1·CtIP·MRN Is Important for DNA Double-Strand Break Repair. *J. Biol. Chem.* 283 (12), 7713–7720. doi:10.1074/jbc.M710245200

Chervona, Y., and Costa., M. (2012). Histone Modifications and Cancer: Biomarkers of Prognosis? *Am. J. Cancer Res.* 2 (5), 589–597. Available at: http://www.ncbi.nlm.nih.gov/pubmed/22957310.

Chi, F., Liu, J., Brady, S. W., Cosgrove, P. A., Nath, A., McQuerry, J. A., et al. (2021a). A `one-Two Punch' Therapy Strategy to Target Chemoresistance in Estrogen Receptor Positive Breast Cancer. *Translational Oncol.* 14 (1), 100946. doi:10.1016/j.tranon.2020.100946

Chi, J., Zhao, J., Wei, S., Li, Y., Zhi, J., Wang, H., et al. (2021b). A CRISPR-Cas9-Based Near-Infrared Upconversion-Activated DNA Methylation Editing System. *ACS Appl. Mater. Inter.* 13 (5), 6043–6052. doi:10.1021/acsami.0c21223

Choi, C., Lee, G. H., Son, A., Yoo, G. S., Yu, J. I., and Park, H. C. (2021). Downregulation of Mcl-1 by Panobinostat Potentiates Proton Beam Therapy in Hepatocellular Carcinoma Cells. *Cells* 10 (3), 554. doi:10.3390/cells10030554

Chou, D. M., Adamson, B., Dephoure, N. E., Tan, X., Nottke, A. C., Hurov, K. E., et al. (2010). A Chromatin Localization Screen Reveals Poly (ADP Ribose)-Regulated Recruitment of the Repressive Polycomb and NuRD Complexes to Sites of DNA Damage. *Proc. Natl. Acad. Sci.* 107 (43), 18475–18480. doi:10.1073/pnas.1012946107

Christmann, M., and Kaina, B. (2019). Epigenetic Regulation of DNA Repair Genes and Implications for Tumor Therapy. *Mutat. Research/Reviews Mutat. Res.* 780, 15–28. doi:10.1016/j.mrrev.2017.10.001

Cimmino, L., Dolgalev, I., Wang, Y., Yoshimi, A., Martin, G. H., Wang, J., et al. (2017). Restoration of TET2 Function Blocks Aberrant Self-Renewal and Leukemia Progression. *Cell* 170 (6), 1079–1095.e20. doi:10.1016/j.cell.2017.07.032

Clouaire, T., Rocher, V., Lashgari, A., Arnould, C., Aguirrebengoa, M., Biernacka, A., et al. (2018). Comprehensive Mapping of Histone Modifications at DNA Double-Strand Breaks Deciphers Repair Pathway Chromatin Signatures. *Mol. Cel.* 72 (2), 250–262.e6. doi:10.1016/j.molcel.2018.08.020

Covre, A., Coral, S., Nicolay, H., Parisi, G., Fazio, C., Colizzi, F., et al. (2015). Antitumor Activity of Epigenetic Immunomodulation Combined with CTLA-4 Blockade in Syngeneic Mouse Models. *OncoImmunology* 4 (8), e1019978. doi:10.1080/2162402X.2015.1019978

Criscuolo, D., Morra, F., Giannella, R., Visconti, R., Cerrato, A., and Celetti, A. (2019). New Combinatorial Strategies to Improve the PARP Inhibitors Efficacy in the Urothelial Bladder Cancer Treatment. *J. Exp. Clin. Cancer Res.* 38 (1), 91. doi:10.1186/s13046-019-1089-z

Croft, L. V., Ashton, N. W., Paquet, N., Bolderson, E., O'Byrne, K. J., and Richard, D. J. (2017). HSSB1 Associates with and Promotes Stability of the BLM Helicase. *BMC Mol. Biol.* 18 (1), 1–10. doi:10.1186/s12867-017-0090-3

D'Amours, D., and Jackson, S. P. (2002). The MRE11 Complex: At the Crossroads of DNA Repair and Checkpoint Signalling. *Nat. Rev. Mol. Cel. Biol.* 3 (5), 317–327. doi:10.1038/nrm805

Daskalakis, M., Nguyen, T. T., Nguyen, C., Guldberg, P., Köhler, G., Wijermans, P., et al. (2002). "Demethylation of a Hypermethylated P15/INK4B Gene in Patients with Myelodysplastic Syndrome by 5-Aza-2′-Deoxycytidine (Decitabine) Treatment. *Blood* 100 (8), 2957–2964. doi:10.1182/blood.V100.8.2957

Daver, N., Garcia-Manero, G., Basu, S., Boddu, P. C., Alfayez, M., Cortes, J. E., et al. (2019). Efficacy, Safety, and Biomarkers of Response to Azacitidine and Nivolumab in Relapsed/Refractory Acute Myeloid Leukemia: A Nonrandomized, Open-Label, Phase II Study. *Cancer Discov.* 9 (3), 370–383. doi:10.1158/2159-8290.CD-18-0774

Davis, A. J., Gelmon, K. A., Siu, L. L., Moore, M. J., Britten, C. D., Mistry, N., et al. (2003). Phase I and Pharmacologic Study of the Human DNA Methyltransferase Antisense Oligodeoxynucleotide MG98 Given as a 21-Day Continuous Infusion Every 4 Weeks. *Investig. New Drugs* 21, 85–97. doi:10.1023/A:1022976528441,

Decottignies, A. (2013). Alternative End-Joining Mechanisms: A Historical Perspective. *Front. Genet.* 4, 48. doi:10.3389/fgene.2013.00048

Dellomo, A. J., Baer, M. R., and Rassool, F. V. (2019). Partnering with PARP Inhibitors in Acute Myeloid Leukemia with FLT3-ITD. *Cancer Lett.* 454, 171–178. doi:10.1016/j.canlet.2019.03.048

Ding, W., Lim, D., Wang, Z., Cai, Z., Liu, G., Zhang, F., et al. (2020). 2-Hexyl-4-Pentynoic Acid, a Potential Therapeutic for Breast Carcinoma by Influencing RPA2 Hyperphosphorylation-Mediated DNA Repair. *DNA Repair* 95 (November), 102940. doi:10.1016/j.dnarep.2020.102940

Dobbs, T. A., Tainer, J. A., and Lees-Miller, S. P. (2010). A Structural Model for Regulation of NHEJ by DNA-PKcs Autophosphorylation. *DNA Repair* 9 (12), 1307–1314. doi:10.1016/j.dnarep.2010.09.019

Eckschlager, T., Plch, J., Stiborova, M., and Hrabeta, J. (2017). Histone Deacetylase Inhibitors as Anticancer Drugs. *IjmsMDPI AG* 18, 1414. doi:10.3390/ijms18071414

El-Kamand, S., Jergic, S., Lawson, T., Kariawasam, R., Richard, D. J., Cubeddu, L., et al. (2020). A Biophysical and Structural Analysis of DNA Binding by Oligomeric HSSB1 (NABP2/OBFC2B). *BioRxiv* August 2020, 269084. doi:10.1101/2020.08.26.269084

Emran, A. A., Chatterjee, A., Rodger, E. J., Tiffen, J. C., Gallagher, S. J., Eccles, M. R., et al. (2019). Targeting DNA Methylation and EZH2 Activity to Overcome Melanoma Resistance to Immunotherapy. *Trends Immunol.* 40, 328–344. doi:10.1016/j.it.2019.02.004

Escribano-Díaz, C., Orthwein, A., Fradet-Turcotte, A., Xing, M., Young, J. T. F., Tkáč, J., et al. (2013). A Cell Cycle-dependent Regulatory Circuit Composed of 53BP1-RIF1 and BRCA1-CtIP Controls DNA Repair Pathway Choice. *Mol. Cel.* 49 (5), 872–883. doi:10.1016/J.MOLCEL.2013.01.001

Essers, J., van Steeg, H., de Wit, J., Swagemakers, S. M., Vermeij, M., Hoeijmakers, J. H., et al. (2000). Homologous and Non-homologous Recombination Differentially Affect DNA Damage Repair in Mice. *EMBO J.* 19 (7), 1703–1710. doi:10.1093/emboj/19.7.1703,

Eyüpoglu, I. Y., and Savaskan, Nicolai. E. (2016). Epigenetics in Brain Tumors: HDACs Take Center Stage. *Curr. Neuropharmacology* 14 (1), 48–54. doi:10.2174/1570159X13666151030162457

Falck, J., Coates, J., and Jackson, S. P. (2005). Conserved Modes of Recruitment of ATM, ATR and DNA-PKcs to Sites of DNA Damage. *Nature* 434 (7033), 605–611. doi:10.1038/nature03442

Fenaux, P., Mufti, G. J., Hellstrom-Lindberg, E., Santini, V., Finelli, C., Giagounidis, A., et al. (2009). Efficacy of Azacitidine Compared with that of Conventional Care Regimens in the Treatment of Higher-Risk Myelodysplastic Syndromes: A Randomised, Open-Label, Phase III Study. *Lancet Oncol.* 10 (3), 223–232. doi:10.1016/S1470-2045(09)70003-8

Ferrari, A., Torrezan, G. T., Carraro, D. M., and Aguiar Junior, S. (2019). Association of Folate and Vitamins Involved in the 1-Carbon Cycle with Polymorphisms in the Methylenetetrahydrofolate Reductase Gene (MTHFR) and Global DNA Methylation in Patients with Colorectal Cancer. *Nutrients* 11 (6), 1368. doi:10.3390/nu11061368

Ferris, R. L., Blumenschein, G., Fayette, J., Guigay, J., Colevas, A. D., Licitra, L., et al. (2016). George Blumenschein, Jerome Fayette, Joel Guigay, A. Dimitrios Colevas, Lisa Licitra, Kevin Harrington, et al.Nivolumab for Recurrent Squamous-Cell Carcinoma of the Head and Neck. *N. Engl. J. Med.* 375 (19), 1856–1867. doi:10.1056/nejmoa1602252

Finkelstein, J. D. (1990). Methionine Metabolism in Mammals. *J. Nutr. Biochem.* 1, 228–237. doi:10.1016/0955-2863(90)90070-2

Freitag, M., and Selker, E. U. (2005). Controlling DNA Methylation: Many Roads to One Modification. *Curr. Opin. Genet. Develop.* 15, 191–199. doi:10.1016/j.gde.2005.02.003

Gad, H., Koolmeister, T., Jemth, A.-S., Eshtad, S., Jacques, S. A., Ström, C. E., et al. (2014). MTH1 Inhibition Eradicates Cancer by Preventing Sanitation of the DNTP Pool. *Nature* 508 (7495), 215–221. doi:10.1038/nature13181

Gao, Y., Gao, J., Mu, G., Zhang, Y., Huang, F., Zhang, W., et al. (2020). Selectively Enhancing Radiosensitivity of Cancer Cells via *In Situ* Enzyme-Instructed Peptide Self-Assembly. *Acta Pharmaceutica Sinica B* 10 (12), 2374–2383. doi:10.1016/j.apsb.2020.07.022

Garcia, V., Phelps, S. E. L., Gray, S., and Neale, M. J. (2011). Bidirectional Resection of DNA Double-Strand Breaks by Mre11 and Exo1. *Nature* 479 (7372), 241. doi:10.1038/nature10515

García-Giménez, J.-L., Garcés, C., Romá-Mateo, C., and Pallardó, F. V. (2021). Oxidative Stress-Mediated Alterations in Histone Post-Translational Modifications. *Free Radic. Biol. Med.* 170, 6–18. doi:10.1016/j.freeradbiomed.2021.02.027

Geskin, L. J. (2007). Vorinostat in Combination with Other Agents for Therapy of Cutaneous T-Cell Lymphomas: A Case Series. *Blood* 110 (11), 4482. doi:10.1182/blood.v110.11.4482.4482

Ghasemi, S. (2020). Cancer's Epigenetic Drugs: where Are They in the Cancer Medicines? *Pharmacogenomics J.* 20, 367–379. doi:10.1038/s41397-019-0138-5

Gillberg, L., Ørskov, A. D., Nasif, A., Ohtani, H., Madaj, Z., Hansen, J. W., et al. (2019). Oral Vitamin C Supplementation to Patients with Myeloid Cancer on Azacitidine Treatment: Normalization of Plasma Vitamin C Induces Epigenetic Changes. *Clin. Epigenet.* 11 (1), 1–11. doi:10.1186/s13148-019-0739-5

Gnyszka, A.Z., and Flis, S. (2013). DNA Methyltransferase Inhibitors and Their Emerging Role in Epigenetic Therapy of Cancer. *Anticancer Res.* 33 (8), 2989–2996.Jastrzebski

Goel, S., Bhatia, V., Biswas, T., and Ateeq, B. (2021). Epigenetic Reprogramming during Prostate Cancer Progression: A Perspective from Development. *Semin. Cancer Biol.* doi:10.1016/j.semcancer.2021.01.009

Görisch, S. M., Wachsmuth, M., Tóth, K. F., Lichter, P., and Rippe, K. (2005). Histone Acetylation Increases Chromatin Accessibility. *J. Cel. Sci.* 118 (24), 5825–5834. doi:10.1242/jcs.02689

Gray, J. E., Saltos, A., Tanvetyanon, T., Haura, E. B., Creelan, B., Antonia, S. J., et al. (2019). Phase I/Ib Study of Pembrolizumab Plus Vorinostat in Advanced/Metastatic Non–small Cell Lung Cancer. *Clin. Cancer Res.* 25 (22), 6623–6632. doi:10.1158/1078-0432.CCR-19-1305

Gros, C., Fleury, L., Nahoum, V., Faux, C., Valente, S., Labella, D., et al. (2015). New Insights on the Mechanism of Quinoline-Based DNA Methyltransferase Inhibitors. *J. Biol. Chem.* 290 (10), 6293–6302. doi:10.1074/jbc.M114.594671

Guirguis, A. A., Liddicoat, B. J., and Dawson, M. A. (2020). The Old and the New: DNA and RNA Methylation in Normal and Malignant Hematopoiesis. *Exp. Hematol.* 90 (October), 1–11. doi:10.1016/j.exphem.2020.09.193

Guo, L., Lee, Y.-T., Zhou, Y., and Huang, Y. (2021). Targeting Epigenetic Regulatory Machinery to Overcome Cancer Therapy Resistance. *Semin. Cancer Biol.* doi:10.1016/j.semcancer.2020.12.022

Gupta, S., Weston, A., Bearrs, J., Thode, T., Neiss, A., Soldi, R., et al. (2016). Reversible Lysine-specific Demethylase 1 Antagonist HCI-2509 Inhibits Growth and Decreases C-MYC in Castration- and Docetaxel-Resistant Prostate Cancer Cells. *Prostate Cancer Prostatic Dis.* 19 (4), 349–357. doi:10.1038/pcan.2016.21

Hanahan, D., and Weinberg, R. A. (2000). The Hallmarks of Cancer. *Cell* 100 (1), 57–70. doi:10.1016/S0092-8674(00)81683-9

Headley, K. M., Kedziora, K. M., Alejo, A., Lai, E. Z.-X., Purvis, J. E., and Hathaway, N. A. (2019). Chemical Screen for Epigenetic Barriers to Single Allele Activation of Oct4. *Stem Cel. Res.* 38 (July), 101470. doi:10.1016/j.scr.2019.101470

Helleday, T., Lo, J., Vangent, D., Engelward, B., and Engelward, Bevin. P. (2007). DNA Double-Strand Break Repair: From Mechanistic Understanding to Cancer Treatment. *DNA Repair* 6 (7), 923–935. doi:10.1016/J.DNAREP.2007.02.006

Hilton, I. B., D'Ippolito, A. M., Vockley, C. M., Thakore, P. I., Crawford, G. E., Reddy, T. E., et al. (2015). Epigenome Editing by a CRISPR-Cas9-Based Acetyltransferase Activates Genes from Promoters and Enhancers. *Nat. Biotechnol.* 33 (5), 510–517. doi:10.1038/nbt.3199,

Hodi, F. S., O'Day, S. J., McDermott, D. F., Weber, R. W., McDermott, D. F., Sosman, J. A., et al. (2010). Improved Survival with Ipilimumab in Patients with Metastatic Melanoma. *N. Engl. J. Med.* 363 (8), 711–723. doi:10.1056/nejmoa1003466,

Horn, L., Mansfield, A. S., Szczęsna, A., Havel, L., Krzakowski, M., Hochmair, M. J., et al. (2018). First-Line Atezolizumab Plus Chemotherapy in Extensive-Stage Small-Cell Lung Cancer. *N. Engl. J. Med.* 379 (23), 2220–2229. doi:10.1056/nejmoa1809064

Huber, K. V. M., Salah, E., Radic, B., Gridling, M., Elkins, J. M., Stukalov, A., et al. (2014). Eidarus Salah, Branka Radic, Manuela Gridling, Jonathan M. Elkins, Alexey Stukalov, Ann Sofie Jemth, et al.Stereospecific Targeting of MTH1 by (S)-Crizotinib as an Anticancer Strategy. *Nature* 508 (7495), 222–227. doi:10.1038/nature13194

Iyama, T., and Wilson, D. M. (2013). DNA Repair Mechanisms in Dividing and Non-dividing Cells. *DNA Repair* 12 (8), 620–636. doi:10.1016/J.DNAREP.2013.04.015

Jackson, S. P., and Bartek., J. (2009). The DNA-Damage Response in Human Biology and Disease. *Nature* 461, 1071–1078. doi:10.1038/nature08467

Jang, Y.-G., Ko, E.-B., and Choi, K.-C. (2020). Gallic Acid, a Phenolic Acid, Hinders the Progression of Prostate Cancer by Inhibition of Histone Deacetylase 1 and 2 Expression. *J. Nutr. Biochem.* 84 (October), 108444. doi:10.1016/j.jnutbio.2020.108444

Jazayeri, A., Balestrini, A., Garner, James E., Costanzo, V., and Costanzo, J. E. (2008). Mre11-Rad50-Nbs1-dependent Processing of DNA Breaks Generates Oligonucleotides that Stimulate ATM Activity. *Embo. J.* 27 (14), 1953–1962. doi:10.1038/emboj.2008.128E

Jeggo, P. A., and Löbrich, M. (2015). How Cancer Cells Hijack DNA Double-Strand Break Repair Pathways to Gain Genomic Instability. *Biochem. J.* 471 (1), 1–11. doi:10.1042/BJ20150582

Jekimovs, C., Bolderson, E., Suraweera, A., Adams, M., O'Byrne, K. J., and Richard, D. J. (2014). Chemotherapeutic Compounds Targeting the DNA Double-Strand Break Repair Pathways: The Good, the Bad, and the Promising. *Front. Oncol.* 4, 86. doi:10.3389/fonc.2014.00086Richard

Jeltsch, A., and Jurkowska, R. Z. (2016). Allosteric Control of Mammalian DNA Methyltransferases - a New Regulatory Paradigm. *Nucleic Acids Res.* 44 (18), 8556–8575. doi:10.1093/nar/gkw723

Jiang, Y., Qian, X., Shen, J., Wang, Y., Li, X., Liu, R., et al. (2015). Local Generation of Fumarate Promotes DNA Repair through Inhibition of Histone H3 Demethylation. *Nat. Cel. Biol.* 17 (9), 1158–1168. doi:10.1038/ncb3209

Johnston, A. W., Ferguson-Smith, M. A., Handmaker, S. D., Jones, H. W., and Jones, G. S. (1961). The Triple-X Syndrome. *Bmj* 2 (5259), 1046–1052. doi:10.1136/bmj.2.5259.1046

Kadayifci, F. Z., Zheng, S., and Pan, Y.-X. (2018). Molecular Mechanisms Underlying the Link between Diet and DNA Methylation. *Ijms* 19, 4055. doi:10.3390/ijms19124055

Kaidi, A., Weinert, B. T., Choudhary, C., and Jackson, S. P. (2010). Human SIRT6 Promotes DNA End Resection through CtIP Deacetylation. *Science* 329 (5997), 1348–1353. doi:10.1126/science.1192049

Kaina, B., and Christmann, M. (2019). DNA Repair in Personalized Brain Cancer Therapy with Temozolomide and Nitrosoureas. *DNA Repair* 78, 128–141. doi:10.1016/j.dnarep.2019.04.007

Kantarjlan, H., Issa, J. P., Rosenfeld, Craig. S., Bennett, J. M., Maher, A., DiPersio, J., et al. (2006). Decitabine Improves Patient Outcomes in Myelodysplastic Syndromes: Results of a Phase III Randomized Study. *Cancer* 106 (8), 1794–1803. doi:10.1002/cncr.21792

Karch, K. R., Langelier, M.-F., Pascal, J. M., Garcia, B. A., and Garcia, B. A. (2017). The Nucleosomal Surface Is the Main Target of Histone ADP-Ribosylation in Response to DNA Damage. *Mol. Biosyst.* 13, 2660–2671. doi:10.1039/c7mb00498b

Kashyap, M. P., Sinha, R., Mukhtar, M. S., and Athar, M. (2020). Epigenetic Regulation in the Pathogenesis of Non-melanoma Skin Cancer. *Semin. Cancer Biol.* doi:10.1016/j.semcancer.2020.11.009

Kass, Stefan. U., Pruss, Dmitry., and Wolffe, Alan. P. (1997). How Does DNA Methylation Repress Transcription? *Trends Genet.* 13 (11), 444–449. doi:10.1016/S0168-9525(97)01268-7

Kaufmann, W. K. (1989). Pathways of Human Cell Post-Replication Repair. *Carcinogenesis* 10 (1), 1–11. doi:10.1093/carcin/10.1.1

Khavari, D. A., Sen, G. L., and Rinn, J. L. (2010). DNA Methylation and Epigenetic Control of Cellular Differentiation. *Cell Cycle* 9, 3880–3883. doi:10.4161/cc.9.19.13385

Khoja, L., Butler, M. O., Kang, S. P., Ebbinghaus, S., and Joshua, A. M. (2015). Pembrolizumab. *J. Immunotherapy Cancer* 3. doi:10.1186/s40425-015-0078-9

Kim, E. S. (2017). Avelumab: First Global Approval. *Drugs* 77 (8), 929–937. doi:10.1007/s40265-017-0749-6

Kim, G., Ison, G., McKee, A. E., Zhang, H., Tang, S., Gwise, T., et al. (2015). FDA Approval Summary: Olaparib Monotherapy in Patients with Deleterious Germline BRCA-Mutated Advanced Ovarian Cancer Treated with Three or More Lines of Chemotherapy. *Clin. Cancer Res.* 21 (19), 4257–4261. doi:10.1158/1078-0432.CCR-15-0887

Kim, H. J., Kim, J. H., Chie, E. K., DaYoung, P., Kim, I., and Kim, I. (2012). DNMT (DNA Methyltransferase) Inhibitors Radiosensitize Human Cancer Cells by Suppressing DNA Repair Activity. *Radiat. Oncol.* 7 (1), 39. doi:10.1186/1748-717X-7-39

Kiziltepe, T., Hideshima, T., Catley, L., Raje, N., Yasui, H., Shiraishi, N., et al. (2007). 5-Azacytidine, a DNA Methyltransferase Inhibitor, Induces ATR-Mediated DNA Double-Strand Break Responses, Apoptosis, and Synergistic Cytotoxicity with Doxorubicin and Bortezomib against Multiple Myeloma

Cells. *Mol. Cancer Ther.* 6 (6), 1718–1727. doi:10.1158/1535-7163.MCT-07-0010

Koprinarova, M., Botev, P., and Russev, G. (2011). Histone Deacetylase Inhibitor Sodium Butyrate Enhances Cellular Radiosensitivity by Inhibiting Both DNA Nonhomologous End Joining and Homologous Recombination. *DNA Repair* 10 (9), 970–977. doi:10.1016/j.dnarep.2011.07.003

Kunkel, T. A., and Erie, D. A. (2005). DNA Mismatch Repair. *Annu. Rev. Biochem.* 74 (1), 681–710. doi:10.1146/annurev.biochem.74.082803.133243

Lakshmaiah, K. C., Jacob, L. A., Aparna, S., Lokanatha, D., and Saldanha, Smitha. C. (2014). Epigenetic Therapy of Cancer with Histone Deacetylase Inhibitors. *J. Cancer Res. Ther.* 10 (3), 469–478. doi:10.4103/0973-1482.137937,

Lamarche, B. J., Orazio, N. I., and Weitzman, M. D. (2010). The MRN Complex in Double-Strand Break Repair and Telomere Maintenance. *FEBS LettersNIH Public Access* 584, 3682–3695. doi:10.1016/j.febslet.2010.07.029

Lande-Diner, L., and Cedar, H. (2005). Silence of the Genes - Mechanisms of Long-Term Repression. *Nat. Rev. Genet.* 6, 648–654. doi:10.1038/nrg1639

Lawson, T., El-Kamand, S., Boucher, D., Duong, D. C., Kariawasam, R., Bonvin, A. M. J. J., et al. (2020). The Structural Details of the Interaction of Single-stranded DNA Binding Protein hSSB2 (NABP1/OBFC2A) with UV-damaged DNA. *Proteins* 88 (2), 319. doi:10.1002/prot.25806

Li, E., and Zhang, Y. (2014). DNA Methylation in Mammals. *Cold Spring Harbor Perspect. Biol.* 6 (5), a019133. doi:10.1101/cshperspect.a019133

Li, Y. C., Wang, Y., Li, D. D., Zhang, Y., Zhao, T. C., and Li, C. F. (2018). Procaine Is a Specific DNA Methylation Inhibitor with Anti-tumor Effect for Human Gastric Cancer. *J. Cel. Biochem.* 119 (2), 2440–2449. doi:10.1002/jcb.26407

Maeda, M., Yamashita, S., Shimazu, T., Iida, N., Takeshima, H., Nakajima, T., et al. (2018). Novel Epigenetic Markers for Gastric Cancer Risk Stratification in Individuals after Helicobacter Pylori Eradication. *Gastric Cancer* 21 (5), 745–755. doi:10.1007/s10120-018-0803-4

Magalhaes, Y. T., Farias, J. O., Silva, L. E., and Forti, F. L. (2021). GTPases, Genome, Actin: A Hidden Story in DNA Damage Response and Repair Mechanisms. *DNA Repair* 100 (April), 103070. doi:10.1016/j.dnarep.2021.103070

Mair, B., Kubicek, S., Nijman, S. M. B., and Nijman, B. (2014). Exploiting Epigenetic Vulnerabilities for Cancer Therapeutics. *Trends Pharmacol. Sci.* 35, 136–145. doi:10.1016/j.tips.2014.01.001

Mamounas, E. P., Liu, Q., Paik, S., Baehner, F. L., Jeong, J-H., Tang, G., et al. (2017). 21-Gene Recurrence Score and Locoregional Recurrence in Node-Positive/ER-Positive Breast Cancer Treated with Chemo-Endocrine Therapy. *JNCI J. Natl. Cancer Inst.* 109, djw259. doi:10.1093/jnci/djw259

Mann, B. S., Johnson, J. R., Cohen, M. H., Justice, R., and Pazdur, R. (2007). FDA Approval Summary: Vorinostat for Treatment of Advanced Primary Cutaneous T-Cell Lymphoma. *Oncol.* 12, 1247–1252. doi:10.1634/theoncologist.12-10-1247

Mao, Z., Hine, C., Tian, X., Van Meter, M., Au, M., Vaidya, A., et al. (2011). SIRT6 Promotes DNA Repair under Stress by Activating PARP1. *Science* 332 (6036), 1443–1446. doi:10.1126/science.1202723

Marijon, H., Lee, D. H., Ding, L., Sun, H., Gery, S., de Gramont, A., et al. (2018). Co-Targeting Poly(ADP-Ribose) Polymerase (PARP) and Histone Deacetylase (HDAC) in Triple-Negative Breast Cancer: Higher Synergism in BRCA Mutated Cells. *Biomed. Pharmacother.* 99 (March), 543–551. doi:10.1016/j.biopha.2018.01.045

Markham, A., and Duggan, S. (2018). Cemiplimab: First Global Approval. *Drugs* 78 (17), 1841–1846. doi:10.1007/s40265-018-1012-5

Mato, José. M., Alvarez, Luis., Ortiz, Pablo., and Pajares, María. A. (1997). S-adenosylmethionine Synthesis: Molecular Mechanisms and Clinical Implications. *Pharmacol. Ther.* 73 (3), 265–280. doi:10.1016/S0163-7258(96)00197-0

Mavaddat, N., Peock, S., Frost, D., Ellis, S., Platte, R., Fineberg, E., et al. (2013). Cancer Risks for BRCA1 and BRCA2 Mutation Carriers: Results from Prospective Analysis of EMBRACE. *JNCI: J. Natl. Cancer Inst.* 105 (11), 812–822. doi:10.1093/jnci/djt095

Mazzone, R., Zwergel, C., Mai, A., and Valente, S. (2017). Epi-Drugs in Combination with Immunotherapy: A New Avenue to Improve Anticancer Efficacy. *Clin. Epigenet* 9, 59. doi:10.1186/s13148-017-0358-y

Medon, M., Vidacs, E., Vervoort, S. J., Li, J., Jenkins, M. R., Ramsbottom, K. M., et al. (2017). HDAC Inhibitor Panobinostat Engages Host Innate Immune Defenses to Promote the Tumoricidal Effects of Trastuzumab in HER2+ Tumors. *Cancer Res.* 77 (10), 2594–2606. doi:10.1158/0008-5472.CAN-16-2247

Mercurio, C., Plyte, S., and Minucci, S. (2012). Alterations of Histone Modifications in Cancer. *Epigenetics Hum. Dis.* 2012, 53–87. doi:10.1016/B978-0-12-388415-2.00004-4

Meter, Michael. Van., Simon, Matthew., Gregory, Tombline., May, Alfred., Morello, Timothy. D., Hubbard, Basil. P., et al. (2016). JNK Phosphorylates SIRT6 to Stimulate DNA Double-Strand Break Repair in Response to Oxidative Stress by Recruiting PARP1 to DNA Breaks. *Cel. Rep.* 16 (10), 2641–2650. doi:10.1016/j.celrep.2016.08.006

Miles, M. A., Harris, M. A., and Hawkins, C. J. (2019). Proteasome Inhibitors Trigger Mutations via Activation of Caspases and CAD, but Mutagenesis Provoked by the HDAC Inhibitors Vorinostat and Romidepsin Is Caspase/CAD-independent. *Apoptosis* 24 (5–6), 404–413. doi:10.1007/s10495-019-01543-x

Millard, C. J., Varma, N., Saleh, A., Morris, K., Watson, P. J., Bottrill, A. R., et al. (2016). The Structure of the Core NuRD Repression Complex Provides Insights into its Interaction with Chromatin. *ELife* 5 (April), e13941. doi:10.7554/eLife.13941

Miller, K. M., Tjeertes, J. V., Coates, J., Legube, G., Polo, S. E., Britton, S., et al. (2010). Human HDAC1 and HDAC2 Function in the DNA-Damage Response to Promote DNA Nonhomologous End-Joining. *Nat. Struct. Mol. Biol.* 17 (9), 1144–1151. doi:10.1038/nsmb.1899

Moloney, J. N., and Cotter., T. G. (2018). ROS Signalling in the Biology of Cancer. *Semin. Cel. Develop. Biol.* 80 (August), 50–64. doi:10.1016/J.SEMCDB.2017.05.023

Momparler, R. L., Côté, S., Momparler, L. F., and Idaghdour, Y. (2017). Inhibition of DNA and Histone Methylation by 5-Aza-2′-Deoxycytidine (Decitabine) and 3-Deazaneplanocin-A on Antineoplastic Action and Gene Expression in Myeloid Leukemic Cells. *Front. Oncol.* 7 (FEB), 19. doi:10.3389/fonc.2017.00019

Mondal, P., Natesh, J., Penta, D., and Meeran, S. M. (2020). Progress and Promises of Epigenetic Drugs and Epigenetic Diets in Cancer Prevention and Therapy: A Clinical Update. *Semin. Cancer Biol.* S1044-579X, 30266–30272. doi:10.1016/j.semcancer.2020.12.006

Moroni, M., Maeda, D., Whitnall, M., Bonner, W., Redon, C., Moroni, Maria., et al. (2013). Evaluation of the Gamma-H2ax Assay for Radiation Biodosimetry in a Swine Model. *Ijms* 14 (7), 14119–14135. doi:10.3390/ijms140714119

Muvarak, N., Chowdhury, K., Robert, C., Limin, X., Choi, E. Y., Cai, Y., et al. (2017). Abstract IA13: Combination of DNA Methyltransferase and PARP Inhibitors as a Novel Therapy Strategy for Multiple Cancers: Key Data in AML and Triple Negative Breast Cancer. *DNA Repair* 77, IA13. doi:10.1158/1538-7445.newfront17-ia13

Nair, N., Shoaib, M., Sørensen, C. S., Shoaib, M., and Sørensen, C. S. (2017). Chromatin Dynamics in Genome Stability: Roles in Suppressing Endogenous DNA Damage and Facilitating DNA Repair. *Ijms* 18 (7), 1486. doi:10.3390/ijms18071486

Narayan, P., Wahby, S., Gao, J. J., Amiri-Kordestani, L., Ibrahim, A., Bloomquist, E., et al. (2020). FDA Approval Summary: Atezolizumab Plus Paclitaxel Protein-Bound for the Treatment of Patients with Advanced or Metastatic TNBC Whose Tumors Express PD-L1. *Clin. Cancer Res.* 26 (10), 2284–2289. doi:10.1158/1078-0432.CCR-19-3545

Nathan, D., Sterner, D. E., and Berger, S. L. (2003). Histone Modifications: Now Summoning Sumoylation. *Proc. Natl. Acad. Sci.* 100, 13118–13120. doi:10.1073/pnas.2436173100

Nigris, F., Ruosi, C., and Napoli, C. (2021). Clinical Efficiency of Epigenetic Drugs Therapy in Bone Malignancies. *Bone* 143 (February), 115605. doi:10.1016/j.bone.2020.115605

O'Connor, O. A., Horwitz, S., Masszi, T., Van Hoof, A., Brown, P., Doorduijn, J., et al. (2015). Belinostat in Patients with Relapsed or Refractory Peripheral T-Cell Lymphoma: Results of the Pivotal Phase II BELIEF (CLN-19) Study. *J. Clin. Oncol.* 33 (23), 2492–2499. doi:10.1200/JCO.2014.59.2782

Ogino, Y., Sato, A., Uchiumi, F., and Tanuma, S.-i. (2019). Genomic and Tumor Biological Aspects of the Anticancer Nicotinamide Phosphoribosyltransferase Inhibitor FK866 in Resistant Human Colorectal Cancer Cells. *Genomics* 111 (6), 1889–1895. doi:10.1016/j.ygeno.2018.12.012

O'Hagan, H. M., Mohammad, H. P., and Baylin, S. B. (2008). "Double Strand Breaks Can Initiate Gene Silencing and SIRT1-dependent Onset of DNA

Methylation in an Exogenous Promoter CpG Island." Edited by Jeannie T. Lee. *PLoS Genet.* 4 (8), e1000155. doi:10.1371/journal.pgen.1000155

Olsen, E. A., Kim, Y. H., Kuzel, T. M., Pacheco, T. R., Foss, F. M., Parker, S., et al. (2007). Phase IIB Multicenter Trial of Vorinostat in Patients with Persistent, Progressive, or Treatment Refractory Cutaneous T-Cell Lymphoma. *Jco* 25, 3109–3115. doi:10.1200/JCO.2006.10.2434

Paillas, S., Then, C. K., Kilgas, S., Ruan, J.-L., Thompson, J., Elliott, A., et al. (2020). Then, Susan Kilgas, Jia Ling Ruan, James Thompson, Amy Elliott, Sean Smart, and Anne E. Kiltie.the Histone Deacetylase Inhibitor Romidepsin Spares Normal Tissues while Acting as an Effective Radiosensitizer in Bladder Tumors *In Vivo*. *Int. J. Radiat. Oncology*Biology*Physics* 107 (1), 212–221. doi:10.1016/j.ijrobp.2020.01.015

Paquet, N., Adams, M. N., Ashton, N. W., Touma, C., Gamsjaeger, R., Cubeddu, L., et al. (2016). HSSB1 (NABP2/OBFC2B) Is Regulated by Oxidative Stress. *Sci. Rep.* 6 (1), 1–13. doi:10.1038/srep27446

Pastor, W. A., Aravind, L., and Rao., A. (2013). TETonic Shift: Biological Roles of TET Proteins in DNA Demethylation and Transcription. *Nat. Rev. Mol. Cel. Biol.* 14, 341–356. doi:10.1038/nrm3589

Pillay, N., Brady, R. M., Dey, M., Morgan, R. D., and Taylor, S. S. (2021). DNA Replication Stress and Emerging Prospects for PARG Inhibitors in Ovarian Cancer Therapy. *Prog. Biophys. Mol. Biol.* 163 (August), 160–170. doi:10.1016/j.pbiomolbio.2021.01.004

Podolsky, M. D., Barchuk, A. A., Kuznetcov, V. I., Gusarova, N. F., Gaidukov, V. S., and Tarakanov, S. A. (2016). Evaluation of Machine Learning Algorithm Utilization for Lung Cancer Classification Based on Gene Expression Levels. *Asian Pac. J. Cancer Prev.* 17 (2), 835–838. doi:10.7314/APJCP.2016.17.2.835,

Polo, S. E., Kaidi, A., Baskcomb, L., Galanty, Y., and Jackson, S. P. (2010). Regulation of DNA-Damage Responses and Cell-Cycle Progression by the Chromatin Remodelling Factor CHD4. *Embo J.* 29 (18), 3130–3139. doi:10.1038/emboj.2010.188

Raedler, L. A. (2016). Farydak (Panobinostat): First HDAC Inhibitor Approved for Patients with Relapsed Multiple Myeloma. *Am. Health Drug Benefits* 9 (Spec Feature), 84–87. Available at: http://www.ncbi.nlm.nih.gov/pubmed/27668050.

Ragheb, R., Venton, G., Chelbi, R., Bonnet, N., Le Treut, T., Ivanov, V., et al. (2017). Vorinostat and Mithramycin A in Combination Therapy as an Interesting Strategy for the Treatment of Sézary T Lymphoma: a Transcriptomic Approach. *Arch. Dermatol. Res.* 309 (8), 611–623. doi:10.1007/s00403-017-1761-0

Rajapakse, A., Suraweera, A., Boucher, D., Naqi, A., O'Byrne, K., Richard, D. J., et al. (2020). Redox Regulation in the Base Excision Repair Pathway: Old and New Players as Cancer Therapeutic Targets. *Cmc* 27 (12), 1901–1921. doi:10.2174/0929867326666190430092732

Ramezankhani, R., Solhi, R., Es, H. A., Vosough, M., and Hassan, M. (2021). Novel Molecular Targets in Gastric Adenocarcinoma. *Pharmacol. Ther.* 220, 107714. doi:10.1016/j.pharmthera.2020.107714

Reck, M., Rodríguez-Abreu, D., Robinson, A. G., Hui, R., Csőszi, T., Fülöp, A., et al. (2016). Pembrolizumab versus Chemotherapy for PD-L1-Positive Non-small-cell Lung Cancer. *N. Engl. J. Med.* 375 (19), 1823–1833. doi:10.1056/nejmoa1606774

Reu, F. J., Fox, M. W., Chawla-Sarkar, M., Beaulieu, N., Leaman, D. W., Macleod, A. R., et al. (2004). Genes Involved in Sensitization of Renal Cancer Cells to Interferon-Induced Apoptosis after Selective Depletion of DNA Methyltransferase-1 by Antisense Oligonucleotide (MG98). *Cancer Res.* 64 (7 Suppl. ment).

Richard, D. J., Bolderson, E., CubedduWadsworth, L., Wadsworth, R. I. M., Savage, K., Sharma, G. G., et al. (2008). Single-Stranded DNA-Binding Protein HSSB1 Is Critical for Genomic Stability. *Nature* 453 (7195), 677–681. doi:10.1038/nature06883

Richard, D. J., Cubeddu, L., Urquhart, A. J., Bain, A., Bolderson, E., Menon, D., et al. (2011a). HSSB1 Interacts Directly with the MRN Complex Stimulating its Recruitment to DNA Double-Strand Breaks and its Endo-Nuclease Activity. *Nucleic Acids Res.* 39 (9), 3643–3651. doi:10.1093/nar/gkq1340

Richard, D. J., Savage, K., Bolderson, E., Cubeddu, L., So, S., Ghita, M., et al. (2011b). HSSB1 Rapidly Binds at the Sites of DNA Double-Strand Breaks and Is Required for the Efficient Recruitment of the MRN Complex. *Nucleic Acids Res.* 39 (5), 1692–1702. doi:10.1093/nar/gkq1098

Robert, C., Thomas, L., Bondarenko, I., O'Day, S., Weber, J., Garbe, C., et al. (2011). Ipilimumab Plus Dacarbazine for Previously Untreated Metastatic Melanoma. *N. Engl. J. Med.* 364 (26), 2517–2526. doi:10.1056/nejmoa1104621

Robertson, K. D., Uzvolgyi, E., Liang, G., Talmadge, C., Sumegi, J., Gonzales, F. A., et al. (1999). The Human DNA Methyltransferases (DNMTs) 1, 3a and 3b: Coordinate MRNA Expression in Normal Tissues and Overexpression in Tumors. *Nucleic Acids Res.* 27 (11), 2291–2298. Available at: https://academic.oup.com/nar/article/27/11/2291/1254660. doi:10.1093/nar/27.11.2291

Rodgers, K., and Mcvey, M. (2016). Error-Prone Repair of DNA Double-Strand Breaks. *J. Cel. Physiol.* 231 (1), 15–24. doi:10.1002/jcp.25053

Rondelet, G., Fleury, L., Faux, C., Masson, V., Dubois, J., Arimondo, P. B., et al. (2017). Inhibition Studies of DNA Methyltransferases by Maleimide Derivatives of RG108 as Non-nucleoside Inhibitors. *Future Med. Chem.* 9 (13), 1465–1481. doi:10.4155/fmc-2017-0074

Rosenquist, R., Esteller, M., and Plass, C. (2018). Introduction: Epigenetics in Cancer, *Semin. Cancer Biol.* 51:iv–v. doi:10.1016/j.semcancer.2018.07.002

Rossetti, A., Petragnano, F., Milazzo, L., Vulcano, F., Macioce, G., Codenotti, S., et al. (2021). Romidepsin (FK228) Fails in Counteracting the Transformed Phenotype of Rhabdomyosarcoma Cells but Efficiently Radiosensitizes, *In Vitro* and *In Vivo*, the Alveolar Phenotype Subtype. *Int. J. Radiat. Biol.* 1–15. doi:10.1080/09553002.2021.1928786

Ruijter, A. J. M. d., Gennip, A. H. v., Caron, H. N., Kemp, S., and Kuilenburg, A. B. P. v. (2003). Histone Deacetylases (HDACs): Characterization of the Classical HDAC Family. *Biochem. J.* 370, 737–749. doi:10.1042/BJ20021321

Ruiz-Magaña, M. J., Martínez-Aguilar, R., Lucendo, E., Campillo-Davo, D., Schulze-Osthoff, K., Ruiz-Ruiz, C., et al. (2016). The Antihypertensive Drug Hydralazine Activates the Intrinsic Pathway of Apoptosis and Causes DNA Damage in Leukemic T Cells. *Oncotarget* 7 (16), 21875–21886. doi:10.18632/oncotarget.7871

Safari, M., Litman, T., Robey, R. W., Aguilera, A., Chakraborty, A. R., Reinhold, W. C., et al. (2021). R-Loop-Mediated SsDNA Breaks Accumulate Following Short-Term Exposure to the HDAC Inhibitor Romidepsin. *Mol. Cancer Res.* doi:10.1158/1541-7786.MCR-20-0833

San-Miguel, J. F., Hungria, V. T. M., Yoon, S.-S., Beksac, M., Dimopoulos, M. A., Elghandour, A., et al. (2014). Panobinostat Plus Bortezomib and Dexamethasone versus Placebo Plus Bortezomib and Dexamethasone in Patients with Relapsed or Relapsed and Refractory Multiple Myeloma: A Multicentre, Randomised, Double-Blind Phase 3 Trial. *Lancet Oncol.* 15 (11), 1195–1206. doi:10.1016/S1470-2045(14)70440-1

Sancar, A. (1994). Mechanisms of DNA Excision Repair. *Science* 266 (5193), 1954–1956. doi:10.1126/science.7801120

Sant, D. W., Mustafi, S., Gustafson, C. B., Chen, J., Slingerland, J. M., and Wang, G. (2018). Vitamin C Promotes Apoptosis in Breast Cancer Cells by Increasing TRAIL Expression. *Sci. Rep.* 8 (1), 1–11. doi:10.1038/s41598-018-23714-7

Sato, T., Issa, J.-P. J., and Kropf, P. (2017). DNA Hypomethylating Drugs in Cancer Therapy. *Cold Spring Harb Perspect. Med.* 7 (5), a026948. doi:10.1101/cshperspect.a026948

Schwartz, M., Zlotorynski, E., Goldberg, M., Ozeri, E., Rahat, A., Carlos le Sage, B. P., et al. (2005). Homologous Recombination and Nonhomologous End-Joining Repair Pathways Regulate Fragile Site Stability. *Genes Develop.* 19 (22), 2715–2726. doi:10.1101/GAD.340905

Shan, W., Jiang, Y., Yu, H., Huang, Q., Liu, L., Guo, X., et al. (2017). HDAC2 Overexpression Correlates with Aggressive Clinicopathological Features and DNA-Damage Response Pathway of Breast Cancer. *Am. J. Cancer Res.* 7 (5), 1213–1226. Available at: /pmc/articles/PMC5446485/.

Sher, G., Salman, N. A., Khan, A. Q., Prabhu, K. S., Raza, A., Kulinski, M., et al. (2020). Epigenetic and Breast Cancer Therapy: Promising Diagnostic and Therapeutic Applications. *Semin. Cancer Biol.* S1044-579X (20), 30181–30184. doi:10.1016/j.semcancer.2020.08.009

Shinjo, K., and Kondo, Y. (2015). Targeting Cancer Epigenetics: Linking Basic Biology to Clinical Medicine. *Adv. Drug Deliv. Rev.* 95, 56–64. doi:10.1016/j.addr.2015.10.006

Shrivastav, M., De Haro, L. P., and Nickoloff, J. A. (2008). Regulation of DNA Double-Strand Break Repair Pathway Choice. *Cell Res.* 18 (1), 134–147. doi:10.1038/cr.2007.111

Singh, M., Kumar, V., Sehrawat, N., Yadav, M., Chaudhary, M., Upadhyay, S. K., et al. (2021). Current Paradigms in Epigenetic Anticancer Therapeutics and Future Challenges. *Semin. Cancer Biol.* doi:10.1016/j.semcancer.2021.03.013

Singh, P. K., Mistry, K. N., Chiramana, H., Rank, D. N., and Joshi, C. G. (2018). Exploring the Deleterious SNPs in XRCC4 Gene Using Computational Approach and Studying Their Association with Breast Cancer in the Population of West India. *Gene* 655 (May), 13–19. doi:10.1016/j.gene.2018.02.040

Sokol, E. S., Pavlick, D., Khiabanian, H., Frampton, G. M., Ross, J. S., Gregg, J. P., et al. (2020). Pan-Cancer Analysis of BRCA1 and BRCA2 Genomic Alterations and Their Association with Genomic Instability as Measured by Genome-wide Loss of Heterozygosity. *JCO Precision Oncol.* 4 (4), 442–465. doi:10.1200/po.19.00345

Steevens, J., Schouten, L. J., Goldbohm, R. A., and Van Den Brandt, P. A. (2011). Vegetables and Fruits Consumption and Risk of Esophageal and Gastric Cancer Subtypes in the Netherlands Cohort Study. *Int. J. Cancer* 129 (11), 2681–2693. doi:10.1002/ijc.25928

Stresemann, C., and Lyko, F. (2008). Modes of Action of the DNA Methyltransferase Inhibitors Azacytidine and Decitabine. *Int. J. Cancer* 123, 8–13. doi:10.1002/ijc.23607

Suraweera, A., Duff, A., Adams, M. N., Jekimovs, C., Duijf, P. H. G., Liu, C., et al. (2020). Defining COMMD4 as an Anti-cancer Therapeutic Target and Prognostic Factor in Non-small Cell Lung Cancer. *Br. J. Cancer* 123 (4), 591–603. doi:10.1038/s41416-020-0899-2

Suraweera, A., Gandhi, N. S., Beard, S., Burgess, J. T., Croft, L. V., Bolderson, E., et al. (2021). COMMD4 Functions with the Histone H2A-H2b Dimer for the Timely Repair of DNA Double-Strand Breaks. *Commun. Biol.* 4 (1), 1–11. doi:10.1038/s42003-021-01998-2

Suraweera, A., O'Byrne, K. J., and Richard, D. J. (2018). Combination Therapy with Histone Deacetylase Inhibitors (HDACi) for the Treatment of Cancer: Achieving the Full Therapeutic Potential of HDACi. *Front. Oncol.* 8, 92. doi:10.3389/fonc.2018.00092

Syed, Y. Y. (2017). Durvalumab: First Global Approval. *Drugs* 77 (12), 1369–1376. doi:10.1007/s40265-017-0782-5

Takata, M., Sasaki, M. S., Sonoda, E., Morrison, C., Hashimoto, M., Utsumi, H., et al. (1998). Homologous Recombination and Non-homologous End-Joining Pathways of DNA Double-Strand Break Repair Have Overlapping Roles in the Maintenance of Chromosomal Integrity in Vertebrate Cells. *Embo J.* 17 (18), 5497–5508. doi:10.1093/emboj/17.18.5497

Tang, J., Cho, N. W., Cui, G., Manion, E. M., Shanbhag, N. M., Botuyan, M. V., et al. (2013). Acetylation Limits 53BP1 Association with Damaged Chromatin to Promote Homologous Recombination. *Nat. Struct. Mol. Biol.* 20, 317–325. doi:10.1038/nsmb.2499

Tang, M., Li, Z., Zhang, C., Lu, X., Tu, B., Cao, Z., et al. (2019). SIRT7-Mediated ATM Deacetylation Is Essential for its Deactivation and DNA Damage Repair. *Sci. Adv.* 5 (3), eaav1118. doi:10.1126/sciadv.aav1118

Tangutoori, S., Baldwin, P., and Sridhar, S. (2015). PARP Inhibitors: A New Era of Targeted Therapy, *Maturitas*, 81, 5–9. doi:10.1016/j.maturitas.2015.01.015

Thakore, P. I., D'Ippolito, A. M., Song, L., Safi, A., Shivakumar, N. K., Kabadi, A. M., et al. (2015). Highly Specific Epigenome Editing by CRISPR-Cas9 Repressors for Silencing of Distal Regulatory Elements. *Nat. Methods* 12 (12), 1143–1149. doi:10.1038/nmeth.3630

To, K. K.-W., Tong, W.-S., and Fu, L.-w. (2017). Reversal of Platinum Drug Resistance by the Histone Deacetylase Inhibitor Belinostat. *Lung Cancer* 103 (January), 58–65. doi:10.1016/j.lungcan.2016.11.019

Tomimatsu, N., Mukherjee, B., Deland, K., Kurimasa, A., Bolderson, E., Khanna, K. K., et al. (2012). Exo1 Plays a Major Role in DNA End Resection in Humans and Influences Double-Strand Break Repair and Damage Signaling Decisions. *DNA Repair* 11 (4), 441–448. doi:10.1016/J.DNAREP.2012.01.006

Touma, C., Kariawasam, R., Gimenez, A. X., Bernardo, R. E., Ashton, N. W., Adams, M. N., et al. (2016). A Structural Analysis of DNA Binding by HSSB1 (NABP2/OBFC2B) in Solution. *Nucleic Acids Res.* 44 (16), 7963–7973. doi:10.1093/nar/gkw617

Tu, B., Zhang, M., Liu, T., and Huang, Y. (2020). Nanotechnology-Based Histone Deacetylase Inhibitors for Cancer Therapy. *Front. Cel. Dev. Biol.* 8 (June), 400. doi:10.3389/fcell.2020.00400

U.S. Food & Drug Administration (FDA) (2020a). *FDA Issues Alert about Efficacy and Potential Safety Concerns with Atezolizumab in Combination with Paclitaxel for Treatment of Breast Cancer*. Maryland, USA: FDA Government. Available at: https://www.fda.gov/drugs/resources-information-approved-drugs/fda-issues-alert-about-efficacy-and-potential-safety-concerns-atezolizumab-combination-paclitaxel.

U.S. Food & Drug Administration (FDA) (2020b). *FDA Issues Alert about Efficacy and Potential Safety Concerns with Atezolizumab in Combination with Paclitaxel for Treatment of Breast Cancer*. Maryland, USA: FDA Government.

Valdez, B. C., Li, Y., Murray, D., Liu, Y., Nieto, Y., Champlin, R. E., et al. (2018). Combination of a Hypomethylating Agent and Inhibitors of PARP and HDAC Traps PARP1 and DNMT1 to Chromatin, Acetylates DNA Repair Proteins, Down-Regulates NuRD and Induces Apoptosis in Human Leukemia and Lymphoma Cells. *Oncotarget* 9 (3), 3908–3921. doi:10.18632/oncotarget.23386

Vaquero, A., Sternglanz, R., and Reinberg, D. (2007). NAD+-Dependent Deacetylation of H4 Lysine 16 by Class III HDACs. *Oncogene* 26, 5505–5520. doi:10.1038/sj.onc.1210617

Vaz, B., Popovic, M., and Ramadan, K. (2017). DNA-protein Crosslink Proteolysis Repair. *Trends Biochem. Sci.* 42 (6), 483–495. doi:10.1016/J.TIBS.2017.03.005

Verdone, L., Caserta, M., and Mauro, E. D. (2005). Role of Histone Acetylation in the Control of Gene Expression. *Biochem. Cel. Biol.* 83, 344–353. doi:10.1139/o05-041

Verreault, A., Kaufman, P. D., Kobayashi, R., and Stillman, B. (1998). Nucleosomal DNA Regulates the Core-Histone-Binding Subunit of the Human Hat1 Acetyltransferase. *Curr. Biol.* 8 (2), 96–108. doi:10.1016/S0960-9822(98)70040-5

Villanueva, L., Álvarez-Errico, D., and Esteller, M. (2020). The Contribution of Epigenetics to Cancer Immunotherapy, *Trends Immunol.* 41. 676–691. doi:10.1016/j.it.2020.06.002

Voelter-Mahlknecht, S., Ho, A. D., and Mahlknecht, U. (2005). Chromosomal Organization and Localization of the Novel Class IV Human Histone Deacetylase 11 Gene. *Int. J. Mol. Med.* 16 (4), 589–598. doi:10.3892/ijmm.16.4.589

Voorde, L. V. D., Speeckaert, R., Van Gestel, D., Bracke, M., De Neve, W., Delanghe, J., et al. (2012). "DNA Methylation-Based Biomarkers in Serum of Patients with Breast Cancer." 751(2):304–325. doi: doi:10.1016/j.mrrev.2012.06.001

Wang, H., Guo, R., Du, Z., Bai, L., Li, L., Cui, J., et al. (2018). Epigenetic Targeting of Granulin in Hepatoma Cells by Synthetic CRISPR DCas9 Epi-Suppressors. *Mol. Ther. - Nucleic Acids* 11 (June), 23–33. doi:10.1016/j.omtn.2018.01.002

Ward, J. F. (1985). Biochemistry of DNA Lesions. *Radiat. Res.* 104 (2), S103. doi:10.2307/3576637

Werner, R. J., Kelly, A. D., and Issa, J.-P. J. (2017). Epigenetics and Precision Oncology. *Cancer J.* 23, 262. doi:10.1097/PPO.0000000000000281

Wilson, A. J., Dai, X., Liu, Q., Hiebert, S., Crispens, M., and Khabele, D. (2020). Abstract A32: Combination Panobinostat and Olaparib Treatment Promotes DNA Damage and Antitumor Immunity in Ovarian Cancer. *Clin. Cancer Res.* 26, A32. doi:10.1158/1557-3265.ovca19-a32

Wilson, B. G., Wang, X., Shen, X., McKenna, E. S., Lemieux, M. E., Cho, Y.-J., et al. (2010). Epigenetic Antagonism between Polycomb and SWI/SNF Complexes during Oncogenic Transformation. *Cancer Cell* 18 (4), 316–328. doi:10.1016/j.ccr.2010.09.006,

World Health Organization (2019). Cancer. Www.Who.Int. 2019. Available at: https://www.who.int/cancer/en/.

Yan, G., and Efferth, T. (2020). Identification of Chemosensitizers by Drug Repurposing to Enhance the Efficacy of Cancer Therapy. *Drug Repurposing Cancer Ther.* 295–310. doi:10.1016/b978-0-12-819668-7.00011-7

Yan, S., Chen, R., Wang, M., and Zha, J. (2021). Carbamazepine at Environmentally Relevant Concentrations Caused DNA Damage and Apoptosis in the Liver of Chinese Rare Minnows (Gobiocypris Rarus) by the Ras/Raf/ERK/P53 Signaling Pathway. *Environ. Pollut.* 270 (February), 116245. doi:10.1016/j.envpol.2020.116245

Yao, M., Rogers, L., Suchowerska, N., Choe, D., Al-Dabbas, M. A., Narula, R. S., et al. (2018). Sensitization of Prostate Cancer to Radiation Therapy: Molecules and Pathways to Target. *Radiother. Oncol.* 128, 283–300. doi:10.1016/j.radonc.2018.05.021

Yasuda, T., Kagawa, W., Ogi, T., Kato, T. A., Suzuki, T., Dohmae, N., et al. (2018). Novel Function of HATs and HDACs in Homologous Recombination through Acetylation of Human RAD52 at Double-Strand Break Sites. *Plos Genet.* 14 (3), e1007277. doi:10.1371/journal.pgen.1007277

Yuan, S. S., Lee, S. Y., Chen, G., Song, M., Tomlinson, G. E., and Lee, E. Y. (1999). BRCA2 Is Required for Ionizing Radiation-Induced Assembly of Rad51 Complex *In Vivo*. *Cancer Res.* 59 (15), 3547–3551. Available at: http://www.ncbi.nlm.nih.gov/pubmed/10446958.

Zeng, H., Qu, J., Jin, N., Xu, J., Lin, C., Chen, Y., et al. (2016). Feedback Activation of Leukemia Inhibitory Factor Receptor Limits Response to Histone Deacetylase Inhibitors in Breast Cancer. *Cancer Cell* 30 (3), 459–473. doi:10.1016/j.ccell.2016.08.001

Zhang, B., Lyu, J., Yang, E. J., Liu, Y., Wu, C., Pardeshi, L., et al. (2020). Class I Histone Deacetylase Inhibition Is Synthetic Lethal with BRCA1 Deficiency in Breast Cancer Cells. *Acta Pharmaceutica Sinica B* 10 (4), 615–627. doi:10.1016/j.apsb.2019.08.008

Zhang, J., Lei, Z., Huang, Z., Zhang, X., Zhou, Y., Luo, Z., et al. (2016a). Epigallocatechin-3-Gallate(EGCG) Suppresses Melanoma Cell Growth and Metastasis by Targeting TRAF6 Activity. *Oncotarget* 7 (48), 79557–79571. doi:10.18632/oncotarget.12836

Zhang, Q., Sun, M., Zhou, S., and Guo, B. (2016b). Class I HDAC Inhibitor Mocetinostat Induces Apoptosis by Activation of MiR-31 Expression and Suppression of E2F6. *Cel. Death Discov.* 2 (1), 1–7. doi:10.1038/cddiscovery.2016.36

Zhang, Y., Jurkowska, R., Soeroes, S., Rajavelu, A., Dhayalan, A., Bock, I., et al. (2010). Chromatin Methylation Activity of Dnmt3a and Dnmt3a/3L Is Guided by Interaction of the ADD Domain with the Histone H3 Tail. *Nucleic Acids Res.* 38 (13), 4246–4253. doi:10.1093/nar/gkq147

Zhang, Y. W., Wang, Z., Xie, W., Cai, Y., Xia, L., Easwaran, H., et al. (2017). Acetylation Enhances TET2 Function in Protecting against Abnormal DNA Methylation during Oxidative Stress. *Mol. Cel.* 65 (2), 323–335. doi:10.1016/j.molcel.2016.12.013

Zhao, J., Xie, C., Edwards, H., Wang, G., Taub, J. W., and Ge, Y. (2017). Histone Deacetylases 1 and 2 Cooperate in Regulating BRCA1, CHK1, and RAD51 Expression in Acute Myeloid Leukemia Cells. *Oncotarget* 8 (4), 6319–6329. doi:10.18632/oncotarget.14062

Zhou, J., Cheng, T., Li, X., Pineda, J. P., Lu, S., Yu, H., et al. (2020). Epigenetic Imprinted Gene Biomarkers Significantly Improve the Accuracy of Presurgical Bronchoscopy Diagnosis of Lung Cancer. *Jco* 38 (15_Suppl. l), e21055. doi:10.1200/jco.2020.38.15_suppl.e21055

Zhou, L., Cheng, X., Connolly, B. A., Dickman, M. J., Hurd, P. J., and Hornby, D. P. (2002). Zebularine: A Novel DNA Methylation Inhibitor that Forms a Covalent Complex with DNA Methyltransferases. *J. Mol. Biol.* 321 (4), 591–599. doi:10.1016/S0022-2836(02)00676-9

Zhou, Z., Li, H.-Q., and Liu, F. (2019). DNA Methyltransferase Inhibitors and Their Therapeutic Potential. *Ctmc* 18 (28), 2448–2457. doi:10.2174/1568026619666181120150122

Zhu, Q., Yu, L., Qin, Z., Chen, L., Hu, H., Zheng, X., et al. (2019). Regulation of OCT2 Transcriptional Repression by Histone Acetylation in Renal Cell Carcinoma. *Epigenetics* 14 (8), 791–803. doi:10.1080/15592294.2019.1615354

Conflict of Interest: The authors declare that the research was conducted in the absence of any commercial or financial relationships that could be construed as a potential conflict of interest.

frontiers in Cell and Developmental Biology

BRIEF RESEARCH REPORT
published: 11 January 2022
doi: 10.3389/fcell.2021.709618

Pharmacological Targeting of STING-Dependent IL-6 Production in Cancer Cells

Sumaiah S. Al-Asmari[1,2], Aleksandra Rajapakse[3], Tomalika R. Ullah[1,2], Geneviève Pépin[1,2], Laura V. Croft[3†] and Michael P. Gantier[1,2*†]*

[1]Centre for Innate Immunity and Infectious Diseases, Hudson Institute of Medical Research, Clayton, VIC, Australia, [2]Department of Molecular and Translational Science, Monash University, Clayton, VIC, Australia, [3]School of Biomedical Sciences, Centre for Genomics and Personalised Health, Cancer and Ageing Research Program at the Translational Research Institute, Queensland University of Technology (QUT), Brisbane, QLD, Australia

Activation of the STING pathway upon genotoxic treatment of cancer cells has been shown to lead to anti-tumoral effects, mediated through the acute production of interferon (IFN)-β. Conversely, the pathway also correlates with the expression of NF-κB-driven pro-tumorigenic genes, but these associations are only poorly defined in the context of genotoxic treatment, and are thought to correlate with a chronic engagement of the pathway. We demonstrate here that half of the STING-expressing cancer cells from the NCI60 panel rapidly increased expression of pro-tumorigenic IL-6 upon genotoxic DNA damage, often independent of type-I IFN responses. While preferentially dependent on canonical STING, we demonstrate that genotoxic DNA damage induced by camptothecin (CPT) also drove IL-6 production through non-canonical STING signaling in selected cancer cells. Consequently, pharmacological inhibition of canonical STING failed to broadly inhibit IL-6 production induced by CPT, although this could be achieved through downstream ERK1/2 inhibition. Finally, prolonged inhibition of canonical STING signaling was associated with increased colony formation of MG-63 cells, highlighting the duality of STING signaling in also restraining the growth of selected cancer cells. Collectively, our findings demonstrate that genotoxic-induced DNA damage frequently leads to the rapid production of pro-tumorigenic IL-6 in cancer cells, independent of an IFN signature, through canonical and non-canonical STING activation; this underlines the complexity of STING engagement in human cancer cells, with frequent acute pro-tumorigenic activities induced by DNA damage. We propose that inhibition of ERK1/2 may help curb such pro-tumorigenic responses to DNA-damage, while preserving the anti-proliferative effects of the STING-interferon axis.

Keywords: STING, IL-6, cancer, DNA damage, STING inhibitor, ERK1/2, Non-canonical STING

OPEN ACCESS

Edited by:
James A. L. Brown,
University of Limerick, Ireland

Reviewed by:
Niamh Buckley,
Queen's University Belfast, United Kingdom
Lei Huang,
Newcastle University, United Kingdom

***Correspondence:**
Laura V. Croft
laura.croft@qut.edu.au
Michael P. Gantier
michael.gantier@hudson.org.au

†These authors share senior authorship

Specialty section:
This article was submitted to Cellular Biochemistry, a section of the journal Frontiers in Cell and Developmental Biology

Received: *14 May 2021*
Accepted: *20 December 2021*
Published: *11 January 2022*

Citation:
Al-Asmari SS, Rajapakse A, Ullah TR, Pépin G, Croft LV and Gantier MP (2022) Pharmacological Targeting of STING-Dependent IL-6 Production in Cancer Cells. Front. Cell Dev. Biol. 9:709618. doi: 10.3389/fcell.2021.709618

INTRODUCTION

Upon activation by cytoplasmic DNA, cyclic guanosine monophosphate–adenosine monophosphate (cGAMP) synthase (cGAS) synthesizes cGAMP, which binds to the adaptor protein STING (stimulator of interferon [IFN] genes) (Zhang et al., 2013). This results in STING translocation from the ER to the Golgi, where it is palmitoylated to recruit TANK-binding kinase 1 (TBK1) and the inhibitor of nuclear factor kappa-B kinase subunit epsilon (IKKε) (Mukai et al., 2016; Balka et al.,

2020). This in turn activates IRF3 and NF-κB transcriptional programs, culminating in the production of IFN-β and pro-inflammatory cytokines such as IL-6 and TNFα, respectively.

In addition to its immune function in the sensing of cytosolic pathogenic DNA, cGAS can initiate immune responses to endogenous nuclear and mitochondrial DNA (Dou et al., 2017; Wu et al., 2019). Such cGAS sensing of cytosolic DNA arising from genome instability promotes senescence and replicative crisis, aimed at eliminating pre-cancerous cells (Dou et al., 2017; Glück et al., 2017; Nassour et al., 2019). Accordingly, since cancer cells have deregulated cell cycle checkpoints they frequently harbor cytoplasmic DNA, which is increased further upon genotoxic damage and radiotherapy exposure, and can lead to cGAS-STING activation (Chen et al., 2017; Dou et al., 2017; Harding et al., 2017; Mackenzie et al., 2017; Bakhoum et al., 2018; Nassour et al., 2019; Carozza et al., 2020); (Marcus et al., 2018; Schadt et al., 2019; Carozza et al., 2020).

While DNA damage-driven GAS-STING cell-intrinsic engagement in cancer cells has been shown to be involved in the recruitment of immune cells to promote anti-cancer activities, through the engagement of the IRF3/IFN-β arm (Ho et al., 2016; Takashima et al., 2016; Harding et al., 2017; Vanpouille-Box et al., 2017; Yamazaki et al., 2020; Suter et al., 2021; Tian et al., 2021), there is also evidence that chronic activation of the pathway can drive tumorigenesis and metastasis (Ahn et al., 2014; Lemos et al., 2016; Bakhoum et al., 2018). The latter is aligned with a correlation between cGAS-STING expression in human cancers and pro-inflammatory NF-κB signatures, including the expression of IL-6 (Dou et al., 2017; Bakhoum et al., 2018). Such NF-κB signals can fuel the resistance to the DNA damage (Didonato et al., 2012), and directly contribute to the growth of cancer cells (Chen et al., 2016; Bakhoum et al., 2018). As such, IL-6 production results in autocrine and paracrine activation of STAT3 signaling that promotes survival of cancer cells in response to DNA damage and pro-apoptotic mediators such as TNFα (Li et al., 2012; Yun et al., 2012). Further, IL-6 directly inhibits the IRF3/IFN-β arm of STING signaling in selected cancer cells, alleviating the tumor suppressive effects of the pathway *in vivo* (Wu et al., 2017; Suter et al., 2021).

Albeit currently proposed to be associated with chronic STING activation (Decout et al., 2021), little is known of the mechanisms regulating the engagement of STING-dependent pro-inflammatory NF-κB factors in the context of acute genotoxic treatment of cancer cells. A recent study reported the existence of a non-canonical STING pathway, rapidly driving IL-6 production with minimal IFN-β production upon DNA damage resulting from topoisomerase-2 inhibition in HaCaT keratinocytes (Dunphy et al., 2018). This non-canonical STING pathway was independent of cGAS/cGAMP/TBK1 and did not require translocation from the ER to the Golgi (Dunphy et al., 2018). However, whether this non-canonical STING pathway is involved in the response to acute genotoxic treatment of cancer cells is currently unknown.

Following on the observation that pharmacological inhibition of STING reduced IL-6 production upon topoisomerase 1 inhibition in mouse TC-1 cancer cells, we decided to broadly interrogate the role of STING signaling in the IL-6 response to acute DNA damage in human cancer cells. Our results collectively support a direct role for STING signaling in the frequent IL-6 production in response to genotoxic treatment of cancer cells, most often independent of a marked IRF3 signature. As such, we demonstrate that both canonical and non-canonical STING signaling can participate in the rapid IL-6 production seen upon DNA damage in different cancer cells, indicating that the pro-tumorigenic activities of the pathway are not limited to its chronic engagement. We also provide evidence that ERK1/2 pharmacological inhibition may provide therapeutic opportunities to limit production of IL-6 upon genotoxic treatment, while preserving the anti-proliferative effects of the STING-interferon axis.

MATERIALS AND METHODS

Cell Culture and Treatments

Human osteosarcoma MG-63 and HOS cells were purchased from ATCC (#CRL-1427 and #CRL-1543, respectively) and grown in ATCC-formulated Eagle's Minimum Essential Medium, supplemented with 10% heat-inactivated fetal bovine serum (Thermo Fisher Scientific) and 1 × antibiotic/antimycotic (Thermo Fisher Scientific). PC-3 cells purchased from ATCC (#CRL-1435) and BT-549 breast ductal carcinoma cells (a kind gift from Prof S. Lakhani) were grown in Roswell Park Memorial Institute (RPMI) 1,640 plus L-glutamine medium (Life Technologies) complemented with 1x antibiotic/antimycotic and 10% heat inactivated fetal bovine serum (referred to as complete RPMI). TC-1 cells (kind gift from Prof. N. McMillan) and HaCaT cells (wild type–kind gift from Prof. S.M. Jane) were cultured in Dulbecco's modified Eagle's medium plus L-glutamine supplemented with 1 × antibiotic/antimycotic (Thermo Fisher Scientific) and 10% heat-inactivated fetal bovine serum (referred to as complete DMEM). SK-OV-3 ovarian carcinoma cells (a kind gift from Prof J. Hooper) were cultured in McCoy's medium (Thermo Fisher Scientific) plus L-glutamine and 10% heat inactivated fetal bovine serum. MDA-MD-231 and HS-578T breast carcinoma cells (a kind gift from Prof S. Lakhani) were cultured in complete DMEM. HaCaT, MDA-MD-231, SK-OV-3 and BT-549 were authenticated using the *GenePrint®* 10 System kit from Promega. All the cells were cultured at 37°C with 5% CO_2. Cell lines were passaged 2–3 times a week and tested for *mycoplasma* contamination on a routine basis by PCR. For clonogenic assays, ~1,500 cells were added per well of a 6-well plate, and the drugs/medium changed every 2–3 days. After the indicated times, cells were fixed with 10% formalin and stained with 0.1% crystal violet (w/v) in 20% ethanol, before several thorough H_2O washes.

Further methods are available in **Supplementary Materials** and Methods.

RESULTS

Pharmacological Inhibition of Canonical STING Signaling Decreases CPT-Induced IL-6 in Mouse TC-1 Cells

We have recently reported that expression of the simian virus 40 (SV40) large T antigen could lead to potentiation of cGAS-STING engagement in cells treated with low-dose

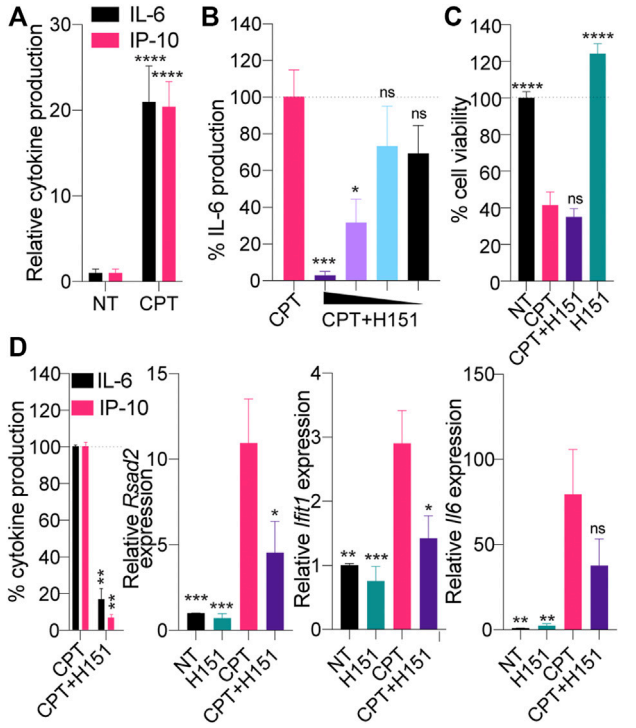

FIGURE 1 | (A) TC-1 cells were treated with 0.5 μM CPT for 48 h, and IL-6 and IP-10 levels in supernatants were determined by ELISA. Cytokine levels were normalized to the non-treated ("NT") condition after background correction with the NT condition. Data shown are averaged from three independent experiments in biological replicate (±s.e.m. and ordinary two-way ANOVA with Sidak's multiple comparison tests). **(B, C)** TC-1 cells were treated with 0.5 μM CPT in the presence of decreasing amount of H151 [7.2, 3.6, 1.8 or 0.9 μM for **(B)**, 3.6 μM for **(C)**] for 48 h and IL-6 levels in supernatants were determined by ELISA **(B)** or cell viability assessed with resazurin assay **(C)**. B) IL-6 levels were normalized to the "CPT only" and are shown as percentages. Data shown are averaged from two independent experiments in biological triplicate (±s.e.m. and ordinary one-way ANOVA with Dunnett's multiple comparison tests to the "CPT only" condition). **(C)** Data were normalized to the NT condition, after background correction with blank condition. Data shown are averaged from three independent experiments in biological replicate (±s.e.m. and ordinary one-way ANOVA with Dunnett's multiple comparison tests to the "CPT only" condition). **(D)** TC-1 cells were treated with 0.5 μM CPT with or without 3.6 μM H151 for 48 h, and IL-6 and IP-10 levels in supernatants were determined by ELISA, while cell lysates were processed for RNA purification. Left: cytokine levels were normalized to the "CPT only" condition and are shown as percentages. Right: Expression of the panel of 3 mouse IFN-driven genes was analyzed by RT-qPCR. Expression of the indicated genes was reported relative to 18 s expression and divided further by the mean of the NT condition. Data shown are averaged from three independent experiments in biological replicate. Left: ± s.e.m. and Mann-Whitney U tests are shown; right: ± s.e.m. and ordinary one-way ANOVA with Dunnett's multiple comparison tests to the "CPT only" condition. *$p \leq 0.05$, **$p \leq 0.01$, ***$p \leq 0.001$, ****$p \leq 0.0001$ and "ns" is non-significant.

topoisomerase 1 inhibition with camptothecin (CPT) treatment (Pépin et al., 2017a). To broaden our observations to other viral oncogenes, we initially investigated whether CPT could induce STING-dependent signaling in mouse epithelial TC-1 cancer cells, which were co-transformed with HPV-16 E6 and E7 and c-Ha-ras oncogenes (Lin et al., 1996). Focusing on IL-6 and IP-10 production as surrogate markers of the NF-κB and IRF3 branches of STING activation, respectively (Pépin et al., 2017b; Dunphy et al., 2018), we first showed that low-dose CPT significantly induced the production of both cytokines in TC-1 cells (**Figure 1A**).

To implicate STING directly in this response to CPT, we repeated the experiments above using a recently reported pharmacological inhibitor of canonical STING, by preventing its palmitoylation, referred to as H151 (Haag et al., 2018). CPT-driven IL-6 production by TC-1 cells was significantly inhibited by H151 in a dose-dependent manner, without increasing further the cell death induced by CPT (**Figures 1B,C**). Accordingly, while H151 decreased production of IP-10 and IL-6 protein by ELISA, we also observed a decrease in expression of interferon-stimulated genes (ISGs) *Rsad2* and *Ifit1,* along with *Il-6* at the mRNA level by RT-qPCR (**Figure 1D**).

Divergent Induction of IL-6 and ISGs in Response to DNA Damage in Human Cancer Cells

This concurrent induction of *Il-6*, *Rsad2* and *Ifit1* by CPT in TC-1 cells prompted us to broadly assess whether such convergent induction of the NF-κB and IRF3 branches was a frequent response to DNA damage in cancer cells. For this purpose, we relied on a published dataset comparing the time-dependent transcriptional responses of cancer cells from the NCI60 panel, treated with several genotoxic agents (Monks et al., 2018). Forty-two cell lines in this panel significantly expressed *STING* based on the Cancer Cell Line Encyclopedia (Barretina et al., 2012), and were used for our *in silico* studies (**Supplementary Table S1**). Transcriptional analyses of *IL-6*, *RSAD2, IFIT1* and *IFNB1* following treatment with the CPT analogue topotecan (Top) suggested that 15 and 21 out of 42 human cancer cell lines expressing *STING* showed increased *IL-6* expression >2 fold after 6 and 24 h Top treatment, respectively (**Figure 2A** and **Supplementary Table S1**).

Critically, the induction of *IFIT1/RSAD2* and *IFNB1* was mostly divergent from that of *IL-6*, while being more restricted. As an example, 14/42 cell lines showed >2-fold increase in *IFIT1* expression at 24 h, but only five also displayed increased *IL-6* levels (**Figure 2A**). A similar observation was made with Doxorubicin (Dox)-driven topoisomerase 2 inhibition; albeit some of the cells that induced *IL-6* > 2 fold differed from those treated with Topotecan. Nonetheless, Dox treatment induced *IL-6* in 23/35 cells lines at 24 h with a 2-fold threshold, versus 16/35 for *IFIT1*—with only five cell lines showing increases in both genes (**Figure 2A**). Collectively, these analyses revealed that while *IL-6* was rapidly induced in 50% of cancer cells by DNA damage, this induction was often independent of that of ISGs.

Inhibition of STING Palmitoylation Does Not Reduce IL-6 in MG-63 and SK-OV-3 Cells

To confirm the potential involvement of STING signaling in this rapid *IL-6* production upon DNA damage, we selected a

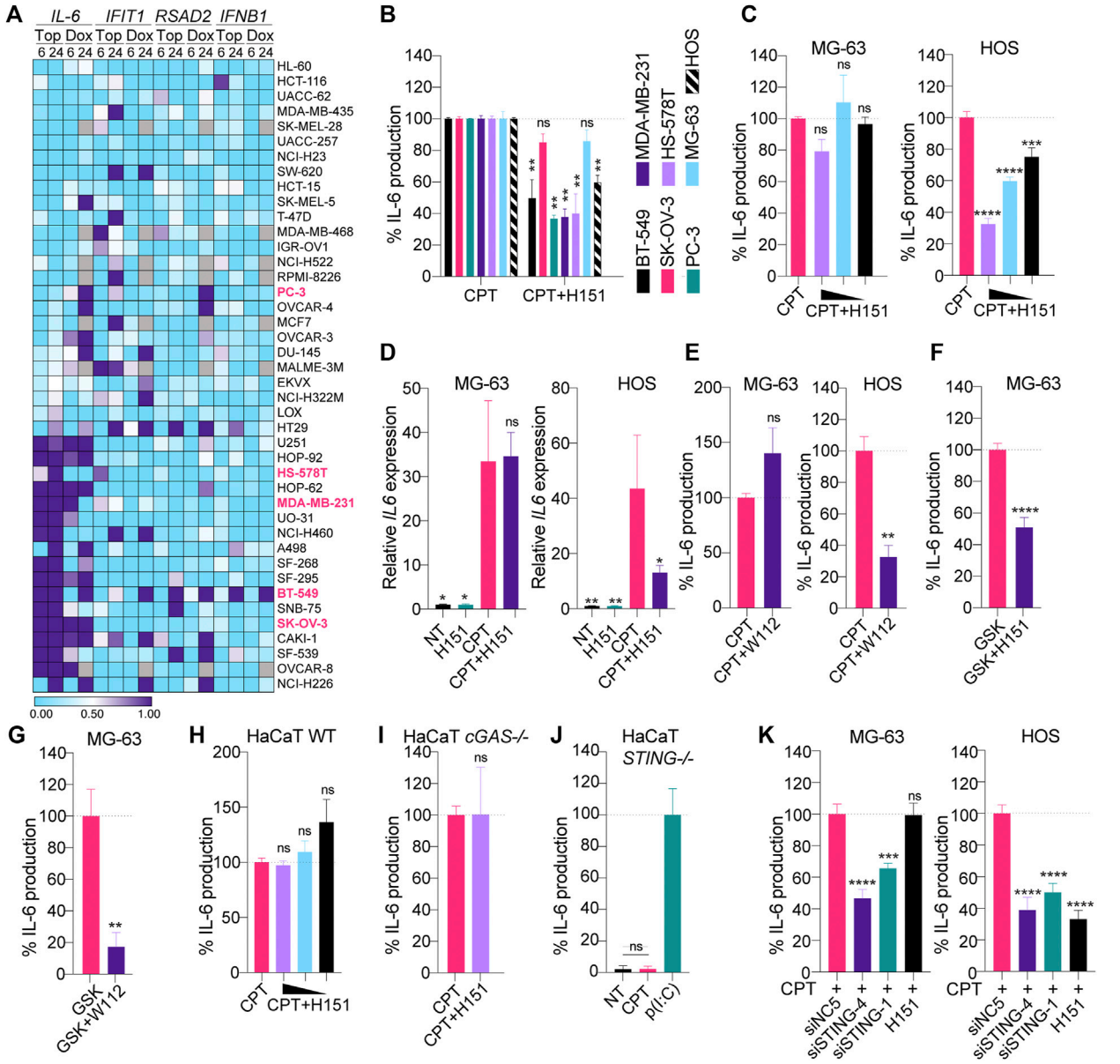

FIGURE 2 | (A) Selected NCI-60 cell lines expressing STING (see **Supplementary Table S1**) were treated for 6 or 24 h with 1 μM topotecan (Top) or doxorubicin (Dox) and analyzed by microarray as reported in the NCI Transcriptional Pharmacodynamics Workbench (Monks et al., 2018). The heatmap shows the $\log_2$ fold change to NT condition (the values below 0.5 are blue and the values above are purple). Missing values are shown in grey. **(B)** Indicated cell lines were treated with CPT (see Materials and Methods for dosage used) with or without 3.6 μM H151 for 24 (BT-549, HS-578T, MDA-MB-231, PC-3 and SK-OV-3 cells) or 48 h (MG-63 and HOS cells), and IL-6 levels in supernatants were determined by ELISA. IL-6 levels were normalized to the "CPT only" condition and are shown as percentages. Data shown are averaged from three independent experiments in biological replicate (±s.e.m. and Mann-Whitney U tests are shown). **(C)** MG-63 and HOS were treated with CPT with or without decreasing concentrations of H151 (3.6, 1.8 and 0.9 μM) for 48 h, and IL-6 levels in supernatants were determined by ELISA. IL-6 levels were normalized to the "CPT only" condition and are shown as percentages. Data shown are averaged from three independent experiments in biological replicate (±s.e.m. and ordinary one-way ANOVA with Dunnett's multiple comparison tests to the "CPT only" condition). **(D)** MG-63 and HOS were treated with CPT with or without 3.6 μM H151 for 48 h, and cell lysates were processed for RNA purification and RT-qPCR analyses. *IL-6* levels were reported relative to *18S* expression and divided further by the mean of the NT condition. Data shown are averaged from three independent experiments (±s.e.m. and ordinary one-way ANOVA with Dunnett's multiple comparison tests to the "CPT only" condition). **(E)** MG-63 and HOS were treated with CPT with or without 200 nM WEHI-122 for 48 h and IL-6 levels in supernatants were determined by ELISA. IL-6 levels were normalized to the "CPT only" condition and are shown as percentages. Data shown are averaged from three (MG-63) or two (HOS) independent experiments in biological replicate (±s.e.m. and Mann-Whitney U tests are shown). **(F, G)** MG-63 were treated overnight with 100 nM GSK#3, with or without 3.6 μM H151 **(F)** or 200 nM WEHI-112 **(G)**, and IL-6 levels in supernatants were determined by ELISA. IL-6 levels were normalized to the "GSK only" condition and are shown as percentages. Data shown are averaged from three **(F)** or two **(G)** independent experiments in biological replicate (±s.e.m. and Mann-Whitney U tests are shown). **(H, I, J)** Wild-type (WT) **(H)**, *cGAS*-deficient **(I)** and *STING*-deficient **(J)** HaCaT cells were treated with 0.2 μM CPT in the presence of decreasing amounts of H151 (3.6, 1.8 or 0.9 μM) **(H)** or 3.6 μM **(I)** for 24 h, and IL-6 levels in supernatants were determined by ELISA. **(J)** Cells were treated with poly(I:C) [p(I:C)] at 1 μg/ ml, where indicated. IL-6

(*Continued*)

FIGURE 2 | levels were normalized to the "CPT only" **(H, I)** or "p(I:C)" **(J)** condition and are shown as percentages. Data shown are averaged from two **(I)** or three **(H, J)** independent experiments in biological replicate [±s.e.m. and ordinary one-way ANOVA with Dunnett's multiple comparison tests to the "CPT only" condition **(H)**, and Mann-Whitney U tests are shown **(I, J)**]. **(K)** MG-63 and HOS were transfected with 10 nM of the indicated siRNAs for 24 or 48 h, respectively, prior to CPT treatment for 48 or 24 h, respectively, and IL-6 levels in supernatants were determined by ELISA. IL-6 levels were normalized to the "CPT + siNC5" condition and are shown as percentages (±s.e.m. and ordinary one-way ANOVA with Dunnett's multiple comparison tests to the "CPT + siNC5" condition). *$p \leq 0.05$, **$p \leq 0.01$, ***$p \leq 0.001$, ****$p \leq 0.0001$ and "ns" is non-significant.

subset of five cancer cell lines from this panel to which we had access (BT-549, HS-578T, MDA-MB-231, PC-3 and SK-OV-3 cells), that exhibited various profiles of *IL-6*/ISGs responses. For example, SK-OV-3 cells induced high amounts of *IL-6* but not ISG, while BT-549 cells robustly induced both *IL-6*/ISG responses (**Figure 2A**). MDA-MB-231 and HS-578T cells had more variable responses to Dox and Top but did induce *IL-6* and *IFIT1* >2 fold with Top, while PC3 displayed a stronger *IFIT1* induction than IL-6 with Top. We also tested two *STING*-expressing osteosarcoma lines we had previously found to produce IL-6 upon CPT treatment (HOS and MG-63 cells).

Low-dose CPT increased IL-6 production that was significantly inhibited by H151 in five cell lines (BT-549, HS-578T, MDA-MB-231, PC-3 and HOS cells), independent of increased cell death, supporting a direct contribution of canonical STING signaling in the pro-inflammatory response to CPT in these cells (**Figure 2B**; **Supplementary Figures S1A,B**). This aligned with the detection of *IFIT1*/ISG induction upon genotoxic treatment in our transcriptional analyses for BT-549, HS-578T, MDA-MB-231 and PC-3 cells (**Figure 2A**). Conversely, H151 failed to significantly reduce IL-6 production in MG-63 and SK-OV-3 cells (**Figure 2B**). Consistently with this, pharmacological inhibition of canonical STING or TBK1 failed to reduce the CPT-driven IL-6 induction at the mRNA and protein levels in MG-63, while it did in HOS cells (**Figures 2C–E**). MG-63, however, did produce IL-6 in response to a human synthetic STING agonist (referred to as GSK#3 herein - (Ramanjulu et al., 2018)), and this was significantly reduced by H151 or TBK1 inhibition (**Figures 2F,G**), confirming the capacity of MG-63 cells to also produce IL-6 through canonical STING signaling.

Pharmacological Inhibition of STING Palmitoylation Does Not Impact Non-Canonical STING Signaling

Non-canonical STING signaling does not require translocation from the ER to the Golgi and as such is not impacted by TBK1 inhibition (Dunphy et al., 2018). Since STING palmitoylation occurs at the Golgi, we speculated that the lack of inhibitory activity of H151 in MG-63 cells could relate to non-canonical STING signaling being at play in these cells upon CPT treatment. We first confirmed that H151 could not inhibit CPT-driven IL-6 production stemming from non-canonical STING signaling in wild-type and *cGAS*-deficient HaCaT cells (**Figures 2H,I**, Material and Methods, and **Supplementary Figures S1A,S2**). Importantly, *STING* deficiency entirely abolished CPT-driven IL-6 production in HaCaT cells, confirming the reliance on STING for this non-canonical response (**Figure 2J**) (Dunphy et al., 2018). In agreement with this, RNA interference mediated down-regulation of STING significantly decreased CPT-driven IL-6 production in both MG-63 and HOS cells, demonstrating the dependence on STING in both cell lines (**Figure 2K**; **Supplementary Figures S1C,D**). Collectively, these results demonstrated that the inhibitory activity of H151 was limited to canonical STING signaling and supported the engagement of non-canonical STING signaling upon genotoxic DNA damage in select cancer cell lines.

Inhibition of Downstream MAP Kinases Broadly Suppresses CPT-Driven IL-6

The lack of activity of H151 on non-canonical STING signaling led us to investigate whether targeting of downstream mediators of NF-κB signaling could help broadly dampen CPT-driven IL-6 production, independent of the type of STING signaling engaged. Non-canonical STING has been shown to rely on TRAF6 activity (Dunphy et al., 2018). While the signaling components operating downstream of TRAF6 to control STING-driven IL-6 have not been characterized to date, we posited a role for mitogen-activated protein kinases (p38 and ERK1/2) based on their known involvement in DNA-damage responses and control of IL-6 expression (Craig et al., 2000; Phong et al., 2010; Wei et al., 2011; Dainichi et al., 2019). Inhibition of ERK1/2 with SCH772984 (Morris et al., 2013) and p38 with SB202190 were initially assessed with dose responses on canonical STING signaling induced with the GSK#3 STING agonist in MG-63 cells (**Figures 3A,B**). p38 and ERK1/2 inhibition both significantly reduced STING-driven IL-6 production in these cells (**Figures 3A,B**), although the effect was more potent with ERK1/2 inhibition. In agreement with a selective effect on NF-κB signaling downstream of canonical STING signaling, ERK1/2 inhibition did not reduce but rather increased IP-10 production upon GSK#3 stimulation - consistent with the prior findings that ERK1/2 inhibit type-I IFN production (**Figure 3B**) (Janovec et al., 2018).

We next studied the effect of p38 and ERK1/2 inhibition in MG-63/HaCaT cells (non-canonical STING) and HOS cells (canonical STING) treated with low-dose CPT. Both inhibitors lead to a significant reduction of CPT-driven IL-6 in the three cell models, without impacting further cell viability (**Figures 3C,D**, **Supplementary Figure S1A**), suggesting that they may be suitable to control the production of pro-tumorigenic factors upon DNA damage.

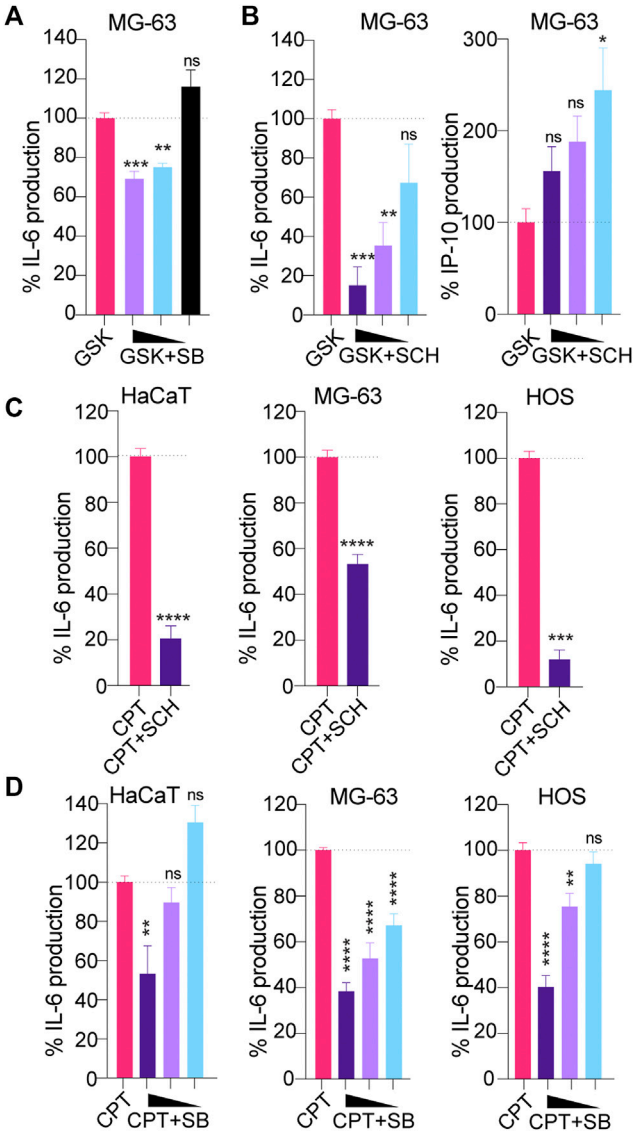

FIGURE 3 | (A, B) MG-63 were treated overnight with 100 nM of the STING agonist GSK#3 with or without decreasing concentrations of the p38 inhibitor SB202190 [SB] (at 3, 1.5 and 0.75 μM) **(A)** or decreasing concentrations of the ERK1/2 inhibitor SCH772984 [SCH] (at 1.25, 0.63 and 0.313 μM) **(B)**, and IL-6/IP-10 levels in supernatants were determined by ELISA. IL-6 and IP-10 levels were normalized to the "GSK only" condition and are shown as percentages. **(A, B)** Data shown are averaged from two independent experiments in biological replicate (±s.e.m. and ordinary one-way ANOVA with Dunnett's multiple comparison tests to the "GSK only" condition). **(C)** HaCaT WT, MG-63 and HOS were treated with CPT for 24 (HaCaT) or 48 h (MG-63 and HOS), with or without 1 μM SCH, and IL-6 levels in supernatants were determined by ELISA. IL-6 levels were normalized to the "CPT only" condition and are shown as percentages. Data shown are averaged from a minimum of three independent experiments in biological replicate (±s.e.m. and Mann-Whitney U tests are shown). **(D)** HaCaT WT, MG-63 and HOS were treated with CPT for 24 (HaCaT) or 48 h (MG-63 and HOS), with or without decreasing concentrations of SB (at 3, 1.5 and 0.75 μM) and IL-6 levels in supernatants were determined by ELISA. IL-6 levels were normalized to the "CPT only" condition and are shown as percentages. Data shown are averaged from a minimum of three independent experiments in

(*Continued*)

FIGURE 3 | biological replicate (±s.e.m. and ordinary one-way ANOVA with Dunnett's multiple comparison tests to the "CPT only" condition). *$p \leq 0.05$, **$p \leq 0.01$, ***$p \leq 0.001$, ****$p \leq 0.0001$ and "ns" is non-significant.

Pharmacological Inhibition of STING Palmitoylation can Lead to Increased Cancer Cell Growth

Having demonstrated the capacity of H151 to block CPT-induced canonical STING signaling in selected cell lines, we next assessed its impact on cancer cell proliferation, independent of DNA damage, compared to p38 and ERK1/2 inhibition. MG-63, HOS, and TC-1 cells were grown in the continuous presence of H151, SB202190 or SCH772984 for 7–12 days in clonogenic assays. Surprisingly, H151 and SB202190 robustly increased clone formation in MG-63 cells (**Figures 4A,B**). This positive effect of H151 on clone formation was limited to MG-63 cells and reflected by increased growth curves (**Figure 4C**). However, SB202190 also potentiated the growth of HOS cells and, to a lesser extent, TC-1 cells (**Figures 4A,B**). Conversely, ERK1/2 inhibition with SCH772984 strongly limited the expansion of MG-63 and TC-1 cells, and modestly impacted that of HOS cells (**Figures 4A,B**). Having previously shown that MG-63 had a functional cGAS-STING response (Valentin et al., 2021), we reasoned that H151 may block canonical STING signaling basally engaged in these cells, normally restraining their growth. Accordingly, the basal expression of several ISGs (*RSAD2*, *IFIT1*, *IFIT2*, *IFIT3*) was significantly decreased by H151 treatment in MG-63 cells (**Figure 4D**). In addition, treatment of MG-63 cells with increasing amounts of type-I IFN significantly decreased the growth of the cells (**Figure 4E**), supporting the concept that H151 increased cell proliferation through the inhibition of constitutive anti-proliferative interferon signaling.

Finally, since it appeared to limit CPT-driven inflammation from both canonical and non-canonical STING signaling, without promoting cancer cell proliferation, we also tested the effect of ERK1/2 inhibition with SCH772984 on CPT-treated PC-3, SK-OV-3 and BT-549 cells (**Figure 4F**). Although less potent than in the other cells, SCH772984 significantly reduced CPT-driven IL-6 in PC-3 and SK-OV-3 cells, supporting its broad anti-inflammatory effect independent of how STING is activated (noting that there was no significant effect of SCH772984 on cell viability–**Supplementary Figure S1E**). Nonetheless, SCH772984 did not significantly reduce IL-6 production in BT-549.

DISCUSSION

Well before its description as a selective agonist of murine Sting (Gao et al., 2013), the small molecule 5,6-dimethylxanthenone-4-acetic acid (DMXAA, or vadimezan) had been characterized as a strong anti-cancer drug that potentiated anti-cancer

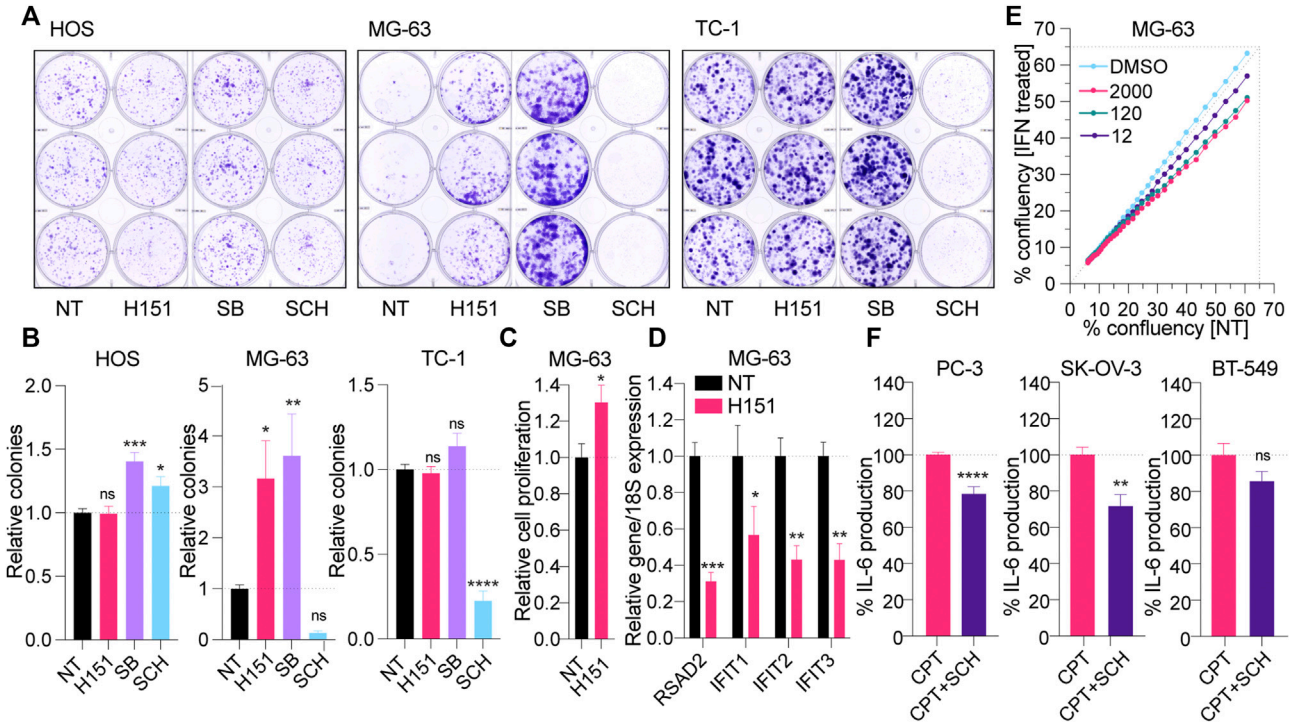

FIGURE 4 | (A, B) HOS, MG-63 and TC-1 cells were plated at low density and treated with 3.6 μM H151, 3 μM of the p38 inhibitor SB202190 [SB] or 1 μM of the ERK1/2 inhibitor SCH772984 [SCH] for 10, 12, and 7 days, respectively (see Materials and Methods). The clones formed were stained with crystal violet after fixing **(A)** and counted manually **(B)**. **(B)** The number of colonies were reported to the NT condition. The data shown are representative **(A)** or averaged **(B)** from three independent experiments (in biological triplicate) (±s.e.m. and ordinary one-way ANOVA with Dunnett's multiple comparison tests to the "NT" condition). **(C)** Proliferation of MG-63 cells treated with 3.6 μM H151 was measured by xCELLigence real-time monitoring over 48 h of treatment. Cell proliferation slopes were calculated and normalized to the NT condition. Data shown are averaged from three independent experiments in biological triplicate (±s.e.m. and Mann-Whitney U tests are shown). **(D)** MG-63 cells were treated or not with 3.6 μM H151 for 48 h, and cell lysates were processed for RNA purification and RT-qPCR analyses. Expression of the indicated genes was reported relative to 18S expression. Data shown are averaged from three independent experiments in biological duplicate and normalized to the NT condition (±s.e.m. and ordinary two-way ANOVA with Sidak's multiple comparison tests). **(E)** Relative confluency of MG-63 cells with or without (NT) increasing concentrations of recombinant IFN (12, 120, 2000 IU/ ml) was assessed over 48 h with Incucyte. Data shown are averaged from 6 wells per condition, and trends are representative of three independent experiments. **(F)** PC-3, SK-OV-3 and BT-549 cells were treated with CPT for 24 h with or without 1 μM SCH, and IL-6 levels in supernatants were determined by ELISA. IL-6 levels were normalized to the "CPT only" condition and are shown as percentages. Data shown are averaged from a minimum of three independent experiments in biological replicate (±s.e.m. and Mann-Whitney U tests are shown). *$p \leq 0.05$, **$p \leq 0.01$, ***$p \leq 0.001$, ****$p \leq 0.0001$ and "ns" is non-significant.

activities promoted by radio and chemotherapies in syngeneic murine cancer models (recently reviewed in (Le Naour et al., 2020)). Accordingly, several human STING agonists have been developed in recent years by academic and pharmaceutical industry laboratories (Ramanjulu et al., 2018; Chin et al., 2020; Pan et al., 2020), and clinical trials are underway to assess their efficacy against cancers in combination with immune checkpoint inhibitors (Le Naour et al., 2020). While it is clear that STING activation of the immune-cell compartment of the tumor microenvironment can have strong anti-tumoral activities, owing to production of anti-proliferative IFN-β (Parker et al., 2016) and the ensuing recruitment of CD8+T cells (Diamond et al., 2011), the cell-intrinsic role of STING signaling on the growth of cancer cells remains poorly defined.

In the current work, we investigated the cell-intrinsic effects of genotoxic DNA damage on STING signaling in human cancer cells. Our analyses of a dataset of 42 STING-expressing cancer cell lines demonstrated the frequent induction of IL-6 upon topoisomerase 1 and 2 inhibition in ≥ 50% of the cells, often independent of a marked ISG response. As such, 8/21 cells lines displaying *IL-6* increased with CPT ≥ two fold failed to show a significant induction of *IFIT1/RSAD2* or *IFNB1* at this threshold, indicating a preferential engagement of the NF-κB branch over that of IRF3 in a third of the cell lines. Although noticeable variations of *IL-6* induction existed for select cell lines between topoisomerase 1 and 2 inhibition, 16/21 cell lines responsive to Top also induced *IL-6* with Dox, often independently of ISG signatures. Nonetheless, 29/42 cell lines displayed increased induction of one of the 3 ISGs considered with either Dox or Top treatment, against 27/42 for *IL-6* induction. This confirms that both NF-κB and IRF3 branches are frequently engaged in cancer cells upon genotoxic treatment.

Critically, we showed that IL-6 induced by DNA damage was partially dependent on STING signaling in all the cell lines we tested–as revealed by a significant decrease in IL-6 production with pharmacological inhibition or down-regulation of *STING* expression. Given that up to 85% (819/934) of the cancer cell lines

in the Cancer Cell Line Encyclopedia expressed STING, we speculate that STING-dependent IL-6 induction in response to DNA damage is very frequent in cancer cells. This aligns with the literature supporting that IL-6 and its activation of STAT3 counteracts the effects of radio- and chemotherapy in many cancers (Yang et al., 2020). It remains possible, however, that CPT-driven IL-6 production in select cancer cells is independent of STING, and reliant on alternative pathways involving other innate immune sensors detecting DNA damage from the nucleus or the mitochondria (Burleigh et al., 2020; Tigano et al., 2021). While warranting further studies in larger datasets of cancer cells, this constitutes, to our knowledge, the first direct evidence that cell-intrinsic canonical STING signaling frequently contributes to the production of pro-tumorigenic IL-6 upon DNA damage in cancer cells.

The recent study by Dunphy *et al.* suggested the existence of a cGAS-independent, non-canonical STING signaling, activated upon DNA damage with the topoisomerase 2 inhibitor Dox in human immortalized and primary keratinocytes (Dunphy et al., 2018). Although the study did not define whether this pathway was frequently invoked upon DNA damage in cancer cells (beyond the case of PMA-differentiated THP-1 cells), it is noteworthy that this alternative STING pathway favored the activation of NF-κB driven pro-inflammatory factors such IL-6, with limited IRF3 signaling (Dunphy et al., 2018).

Here we confirmed the observation from Dunphy *et al.* that HaCaT cells lacking *cGAS* can produce IL-6 upon DNA damage, in a *STING*-dependent manner (Dunphy et al., 2018). In support of the concept of a non-canonical STING signaling pathway, we demonstrated that pharmacological inhibition of STING palmitoylation did not impact CPT-driven IL-6 in these cells. Critically, we provide evidence that the occurrence of non-canonical STING signaling is not limited to keratinocytes, and that it can also be activated by DNA damage in cancer cells such as MG-63 cells. While IL-6 production was dependent on *STING* expression in MG-63 cells, pharmacological inhibition of canonical STING/TBK1 signaling did not reduce CPT-driven IL-6 in these cells. Although additional experiments would be required to confirm that the *STING*-dependent responses to DNA damage seen in HaCaT operate the same way in MG-63 cells, the hallmarks of the responses in both cell lines support the concept that they share key similarities. How frequently this non-canonical STING signaling is engaged in human cancers remains to be determined, but the fact that it can be engaged independently of cGAS suggests that it could be relatively common. For example, analyses of TCGA datasets indicate that >30% of high expressing STING lung adenocarcinoma or testicular cancer tumors have low cGAS expression (**Supplementary Table S2**).

Importantly, albeit failing to respond to H151 inhibition, MG-63 and HaCaT cells both responded to transfected DNA through canonical cGAS-STING signaling (**Supplementary Figure S2**) (Valentin et al., 2021). Perhaps most surprisingly, we demonstrated that prolonged exposure to H151 increased the growth of MG-63 cells, concurrently with a significant decrease of a basal ISG signature (noting that MG-63 cells are known to produce high levels of type-I IFN) (Billiau et al., 1977). These observations support a basal anti-proliferative activity of STING in MG-63 cells, through the IRF3/IFN arm of the pathway, supported by the reduced growth of the cells cultured in the presence of type-I IFN. This points to the capacity of MG-63 cells to rapidly switch between steady-state canonical STING signaling, most likely resulting from low levels of cytoplasmic DNA, to non-canonical STING signaling activated by acute DNA damage.

The results collectively obtained in MG-63 cells crystalize the duality of the pathway in cancer cells, which can rapidly shift from anti-proliferative to pro-tumorigenic in the context of DNA damage. Given how frequently rapid induction of *IL-6* was observed in cancer cells, the current concept that pro-tumorigenic activities of the pathway would be limited to its chronic engagement clearly needs revision (Decout et al., 2021). These findings are also important to our understanding of how to best apply STING agonists in cancer immunotherapy involving DNA damage, since IL-6 was found to inhibit the anti-tumoral effects of STING activation *in vivo* (Suter et al., 2021).

With the aim of inhibiting the pro-tumorigenic NF-κB branch of STING signaling, but retaining that of IRF3/IFN-β, we discovered that inhibition of ERK1/2 was able to reduce IL-6 production upon canonical and non-canonical STING activation. Critically, ERK1/2 inhibition did not compromise the IRF3 branch of STING signaling, as seen with preserved IP-10 levels in MG-63 cells treated with a human STING agonist. Accordingly, in addition to its own anti-cancer activities (Kidger et al., 2018), pharmacological ERK1/2 inhibition may be a viable strategy to broadly decrease IL-6 production upon DNA damage, while retaining the anti-proliferative effects of the pathway, seen in MG-63 cells. Although further studies are warranted, this is the first description, to our knowledge, that ERK1/2 participate in the production of pro-inflammatory factors downstream of STING. Note that ERK1/2 phosphorylation has been reported in mouse embryonic fibroblasts stimulated with DMXAA (Abe and Barber, 2014). Nevertheless, ERK1/2 inhibition may not universally limit IL-6 production driven by DNA damage in cells where the IRF3 branch of STING signaling dominates the response to DNA damage, as suggested by our results in BT-549 cells.

In conclusion, we demonstrate here that STING is an important contributor to the rapid IL-6 production frequently seen upon DNA damage in cancer cells. Our results collectively indicate that targeting of signaling components operating downstream of STING to modulate NF-κB activity may be more useful than direct STING inhibitors to help prevent production of pro-tumorigenic factors such as IL-6. We propose that pharmacological targeting of ERK1/2, which is already investigated in cancer patients with oncogenic RAS-dependent tumors (Lu et al., 2020), may also help attenuate the resistance to radio- and chemotherapy treatments mediated in part by STING-dependent pro-inflammatory factors, while retaining the anti-tumor activity of the IRF3/IFN-β branch of the pathway.

DATA AVAILABILITY STATEMENT

The original contributions presented in the study are included in the article/**Supplementary Material**, further inquiries can be directed to the corresponding authors.

AUTHOR CONTRIBUTIONS

SA-A designed, performed and analyzed experiments. AR and TU performed and analyzed experiments. GP performed CRISPR/Cas9 experiments to generate HaCaT mutant cell lines. MG conceived the study and drafted the manuscript. LC and MG coordinated the study, and assisted in design and analysis of experiments. All authors reviewed the results and approved the final version of the manuscript.

FUNDING

This work was supported by the funding from the Australian National Health and Medical Research Council (1081167 and 1124485 to MG); the Australian Research Council (140100594 Future Fellowship to MG); the Quebec Fonds de Recherche du Québec (FRSQ)—Santé (35071 to GP); Noxopharm Ltd and the Victorian Government's Operational Infrastructure Support Program. Queensland Government (Advance Queensland Industry Research Fellowship to LVC).

ACKNOWLEDGMENTS

We thank N. McMillan for TC-1 cells, S.M. Jane for HaCaT cells, S. Lakhani for BT-549, MDA-MD-231 and HS-578T cells, J. Hooper for SK-OV-3 cells; S. Chu and F. Sharafath for help with the xCELLigence experiments; The Cancer Therapeutics CRC for the GSK human STING agonist; D. De Nardo for the WEHI-112 TBK1 inhibitor; and Frances Cribbin for editorial assistance; we also acknowledge the Monash Health Translational Precinct Research Platforms for access to the RT-qPCR instruments and cell line sequencing.

SUPPLEMENTARY MATERIAL

The Supplementary Material for this article can be found online at: https://www.frontiersin.org/articles/10.3389/fcell.2021.709618/full#supplementary-material

REFERENCES

Abe, T., and Barber, G. N. (2014). Cytosolic-DNA-Mediated, STING-dependent Proinflammatory Gene Induction Necessitates Canonical NF- B Activation through TBK1. *J. Virol.* 88, 5328–5341. doi:10.1128/jvi.00037-14

Ahn, J., Xia, T., Konno, H., Konno, K., Ruiz, P., and Barber, G. N. (2014). Inflammation-driven Carcinogenesis Is Mediated through STING. *Nat. Commun.* 5, 5166. doi:10.1038/ncomms6166

Bakhoum, S. F., Ngo, B., Laughney, A. M., Cavallo, J.-A., Murphy, C. J., Ly, P., et al. (2018). Chromosomal Instability Drives Metastasis through a Cytosolic DNA Response. *Nature* 553, 467–472. doi:10.1038/nature25432

Balka, K. R., Louis, C., Saunders, T. L., Smith, A. M., Calleja, D. J., D'Silva, D. B., et al. (2020). TBK1 and IKKε Act Redundantly to Mediate STING-Induced NF-Kb Responses in Myeloid Cells. *Cel Rep.* 31, 107492. doi:10.1016/j.celrep.2020.03.056

Barretina, J., Caponigro, G., Stransky, N., Venkatesan, K., Margolin, A. A., Kim, S., et al. (2012). The Cancer Cell Line Encyclopedia Enables Predictive Modelling of Anticancer Drug Sensitivity. *Nature* 483, 603–607. doi:10.1038/nature11003

Billiau, A., Edy, V. G., Heremans, H., Van Damme, J., Desmyter, J., Georgiades, J. A., et al. (1977). Human Interferon: Mass Production in a Newly Established Cell Line, MG-63. *Antimicrob. Agents Chemother.* 12, 11–15. doi:10.1128/aac.12.1.11

Burleigh, K., Maltbaek, J. H., Cambier, S., Green, R., Gale, M., James, R. C., et al. (2020). Human DNA-PK Activates a STING-independent DNA Sensing Pathway. *Sci. Immunol.* 5, eaba4219. doi:10.1126/sciimmunol.aba4219

Carozza, J. A., Böhnert, V., Nguyen, K. C., Skariah, G., Shaw, K. E., Brown, J. A., et al. (2020). Extracellular cGAMP Is a Cancer-Cell-Produced Immunotransmitter Involved in Radiation-Induced Anticancer Immunity. *Nat. Cancer* 1, 184–196. doi:10.1038/s43018-020-0028-4

Chen, Q., Boire, A., Jin, X., Valiente, M., Er, E. E., Lopez-Soto, A., et al. (2016). Carcinoma-astrocyte gap Junctions Promote Brain Metastasis by cGAMP Transfer. *Nature* 533, 493–498. doi:10.1038/nature18268

Chen, Y.-A., Shen, Y.-L., Hsia, H.-Y., Tiang, Y.-P., Sung, T.-L., and Chen, L.-Y. (2017). Extrachromosomal Telomere Repeat DNA Is Linked to ALT Development via cGAS-STING DNA Sensing Pathway. *Nat. Struct. Mol. Biol.* 24, 1124–1131. doi:10.1038/nsmb.3498

Chin, E. N., Yu, C., Vartabedian, V. F., Jia, Y., Kumar, M., Gamo, A. M., et al. (2020). Antitumor Activity of a Systemic STING-Activating Non-nucleotide cGAMP Mimetic. *Science* 369, 993–999. doi:10.1126/science.abb4255

Craig, R., Larkin, A., Mingo, A. M., Thuerauf, D. J., Andrews, C., Mcdonough, P. M., et al. (2000). p38 MAPK and NF-Kb Collaborate to Induce Interleukin-6 Gene Expression and Release. *J. Biol. Chem.* 275, 23814–23824. doi:10.1074/jbc.m909695199

Dainichi, T., Matsumoto, R., Mostafa, A., and Kabashima, K. (2019). Immune Control by TRAF6-Mediated Pathways of Epithelial Cells in the EIME (Epithelial Immune Microenvironment). *Front. Immunol.* 10, 1107. doi:10.3389/fimmu.2019.01107

Decout, A., Katz, J. D., Venkatraman, S., and Ablasser, A. (2021). The cGAS-STING Pathway as a Therapeutic Target in Inflammatory Diseases. *Nat. Rev. Immunol.* 21, 548–569. doi:10.1038/s41577-021-00524-z

Diamond, M. S., Kinder, M., Matsushita, H., Mashayekhi, M., Dunn, G. P., Archambault, J. M., et al. (2011). Type I Interferon Is Selectively Required by Dendritic Cells for Immune Rejection of Tumors. *J. Exp. Med.* 208, 1989–2003. doi:10.1084/jem.20101158

Didonato, J. A., Mercurio, F., and Karin, M. (2012). NF-κB and the Link between Inflammation and Cancer. *Immunological Rev.* 246, 379–400. doi:10.1111/j.1600-065x.2012.01099.x

Dou, Z., Ghosh, K., Vizioli, M. G., Zhu, J., Sen, P., Wangensteen, K. J., et al. (2017). Cytoplasmic Chromatin Triggers Inflammation in Senescence and Cancer. *Nature* 550, 402–406. doi:10.1038/nature24050

Dunphy, G., Flannery, S. M., Almine, J. F., Connolly, D. J., Paulus, C., Jønsson, K. L., et al. (2018). Non-canonical Activation of the DNA Sensing Adaptor STING by ATM and IFI16 Mediates NF-Kb Signaling after Nuclear DNA Damage. *Mol. Cel* 71, 745–760. e745. doi:10.1016/j.molcel.2018.07.034

Gao, P., Ascano, M., Zillinger, T., Wang, W., Dai, P., Serganov, A. A., et al. (2013). Structure-Function Analysis of STING Activation by c[G(2′,5′)pA(3′,5′)p] and Targeting by Antiviral DMXAA. *Cell* 154, 748–762. doi:10.1016/j.cell.2013.07.023

Glück, S., Guey, B., Gulen, M. F., Wolter, K., Kang, T.-W., Schmacke, N. A., et al. (2017). Innate Immune Sensing of Cytosolic Chromatin Fragments through cGAS Promotes Senescence. *Nat. Cel Biol* 19, 1061–1070. doi:10.1038/ncb3586

Haag, S. M., Gulen, M. F., Reymond, L., Gibelin, A., Abrami, L., Decout, A., et al. (2018). Targeting STING with Covalent Small-Molecule Inhibitors. *Nature* 559, 269–273. doi:10.1038/s41586-018-0287-8

Harding, S. M., Benci, J. L., Irianto, J., Discher, D. E., Minn, A. J., and Greenberg, R. A. (2017). Mitotic Progression Following DNA Damage Enables Pattern Recognition within Micronuclei. *Nature* 548, 466–470. doi:10.1038/nature23470

Ho, S. S. W., Zhang, W. Y. L., Tan, N. Y. J., Khatoo, M., Suter, M. A., Tripathi, S., et al. (2016). The DNA Structure-specific Endonuclease MUS81 Mediates DNA Sensor STING-dependent Host Rejection of Prostate Cancer Cells. *Immunity* 44, 1177–1189. doi:10.1016/j.immuni.2016.04.010

Janovec, V., Aouar, B., Font-Haro, A., Hofman, T., Trejbalova, K., Weber, J., et al. (2018). The MEK1/2-ERK Pathway Inhibits Type I IFN Production in Plasmacytoid Dendritic Cells. *Front. Immunol.* 9, 364. doi:10.3389/fimmu.2018.00364

Kidger, A. M., Sipthorp, J., and Cook, S. J. (2018). ERK1/2 Inhibitors: New Weapons to Inhibit the RAS-Regulated RAF-Mek1/2-Erk1/2 Pathway. *Pharmacol. Ther.* 187, 45–60. doi:10.1016/j.pharmthera.2018.02.007

Le Naour, J., Zitvogel, L., Galluzzi, L., Vacchelli, E., and Kroemer, G. (2020). Trial Watch: STING Agonists in Cancer Therapy. *OncoImmunology* 9, 1777624. doi:10.1080/2162402x.2020.1777624

Lemos, H., Mohamed, E., Huang, L., Ou, R., Pacholczyk, G., Arbab, A. S., et al. (2016). STING Promotes the Growth of Tumors Characterized by Low Antigenicity via Ido Activation. *Cancer Res.* 76, 2076–2081. doi:10.1158/0008-5472.can-15-1456

Li, S., Wang, N., and Brodt, P. (2012). Metastatic Cells Can Escape the Proapoptotic Effects of TNF-α through Increased Autocrine IL-6/STAT3 Signaling. *Cancer Res.* 72, 865–875. doi:10.1158/0008-5472.can-11-1357

Lin, K. Y., Guarnieri, F. G., Staveley-O'carroll, K. F., Levitsky, H. I., August, J. T., Pardoll, D. M., et al. (1996). Treatment of Established Tumors with a Novel Vaccine that Enhances Major Histocompatibility Class II Presentation of Tumor Antigen. *Cancer Res.* 56, 21–26.

Lu, Y., Liu, B., Liu, Y., Yu, X., and Cheng, G. (2020). Dual Effects of Active ERK in Cancer: A Potential Target for Enhancing Radiosensitivity (Review). *Oncol. Lett.* 20, 993–1000. doi:10.3892/ol.2020.11684

Mackenzie, K. J., Carroll, P., Martin, C.-A., Murina, O., Fluteau, A., Simpson, D. J., et al. (2017). cGAS Surveillance of Micronuclei Links Genome Instability to Innate Immunity. *Nature* 548, 461–465. doi:10.1038/nature23449

Marcus, A., Mao, A. J., Lensink-Vasan, M., Wang, L., Vance, R. E., and Raulet, D. H. (2018). Tumor-Derived cGAMP Triggers a STING-Mediated Interferon Response in Non-tumor Cells to Activate the NK Cell Response. *Immunity* 49, 754–763. e754. doi:10.1016/j.immuni.2018.09.016

Monks, A., Zhao, Y., Hose, C., Hamed, H., Krushkal, J., Fang, J., et al. (2018). The NCI Transcriptional Pharmacodynamics Workbench: A Tool to Examine Dynamic Expression Profiling of Therapeutic Response in the NCI-60 Cell Line Panel. *Cancer Res.* 78, 6807–6817. doi:10.1158/0008-5472.can-18-0989

Morris, E. J., Jha, S., Restaino, C. R., Dayananth, P., Zhu, H., Cooper, A., et al. (2013). Discovery of a Novel ERK Inhibitor with Activity in Models of Acquired Resistance to BRAF and MEK Inhibitors. *Cancer Discov.* 3, 742–750. doi:10.1158/2159-8290.cd-13-0070

Mukai, K., Konno, H., Akiba, T., Uemura, T., Waguri, S., Kobayashi, T., et al. (2016). Activation of STING Requires Palmitoylation at the Golgi. *Nat. Commun.* 7, 11932. doi:10.1038/ncomms11932

Nassour, J., Radford, R., Correia, A., Fusté, J. M., Schoell, B., Jauch, A., et al. (2019). Autophagic Cell Death Restricts Chromosomal Instability during Replicative Crisis. *Nature* 565, 659–663. doi:10.1038/s41586-019-0885-0

Pan, B. S., Perera, S. A., Piesvaux, J. A., Presland, J. P., Schroeder, G. K., Cumming, J. N., et al. (2020). An Orally Available Non-nucleotide STING Agonist with Antitumor Activity. *Science* 369, eaba6098. doi:10.1126/science.aba6098

Parker, B. S., Rautela, J., and Hertzog, P. J. (2016). Antitumour Actions of Interferons: Implications for Cancer Therapy. *Nat. Rev. Cancer* 16, 131–144. doi:10.1038/nrc.2016.14

Pépin, G., Nejad, C., Ferrand, J., Thomas, B. J., Stunden, H. J., Sanij, E., et al. (2017a). Topoisomerase 1 Inhibition Promotes Cyclic GMP-AMP Synthase-dependent Antiviral Responses. *mBio* 8, e01611–01617. doi:10.1128/mBio.01611-17

Pépin, G., Nejad, C., Thomas, B. J., Ferrand, J., Mcarthur, K., Bardin, P. G., et al. (2017b). Activation of cGAS-dependent Antiviral Responses by DNA Intercalating Agents. *Nucleic Acids Res.* 45, 198–205. doi:10.1093/nar/gkw878

Phong, M. S., Van Horn, R. D., Li, S., Tucker-Kellogg, G., Surana, U., and Ye, X. S. (2010). p38 Mitogen-Activated Protein Kinase Promotes Cell Survival in Response to DNA Damage but Is Not Required for the G 2 DNA Damage Checkpoint in Human Cancer Cells. *Mol. Cel Biol* 30, 3816–3826. doi:10.1128/mcb.00949-09

Ramanjulu, J. M., Pesiridis, G. S., Yang, J., Concha, N., Singhaus, R., Zhang, S.-Y., et al. (2018). Design of Amidobenzimidazole STING Receptor Agonists with Systemic Activity. *Nature* 564, 439–443. doi:10.1038/s41586-018-0705-y

Schadt, L., Sparano, C., Schweiger, N. A., Silina, K., Cecconi, V., Lucchiari, G., et al. (2019). Cancer-Cell-Intrinsic cGAS Expression Mediates Tumor Immunogenicity. *Cel Rep.* 29, 1236–1248. e1237. doi:10.1016/j.celrep.2019.09.065

Suter, M. A., Tan, N. Y., Thiam, C. H., Khatoo, M., Macary, P. A., Angeli, V., et al. (2021). cGAS-STING Cytosolic DNA Sensing Pathway Is Suppressed by JAK2-STAT3 in Tumor Cells. *Sci. Rep.* 11, 7243. doi:10.1038/s41598-021-86644-x

Takashima, K., Takeda, Y., Oshiumi, H., Shime, H., Okabe, M., Ikawa, M., et al. (2016). STING in Tumor and Host Cells Cooperatively Work for NK Cell-Mediated Tumor Growth Retardation. *Biochem. Biophysical Res. Commun.* 478, 1764–1771. doi:10.1016/j.bbrc.2016.09.021

Tian, J., Zhang, D., Kurbatov, V., Wang, Q., Wang, Y., Fang, D., et al. (2021). 5-Fluorouracil Efficacy Requires Anti-tumor Immunity Triggered by Cancer-cell-intrinsic STING. *EMBO J.* 40, e106065. doi:10.15252/embj.2020106065

Tigano, M., Vargas, D. C., Tremblay-Belzile, S., Fu, Y., and Sfeir, A. (2021). Nuclear Sensing of Breaks in Mitochondrial DNA Enhances Immune Surveillance. *Nature* 591, 477–481. doi:10.1038/s41586-021-03269-w

Valentin, R., Wong, C., Alharbi, A. S., Pradeloux, S., Morros, M. P., Lennox, K. A., et al. (2021). Sequence-dependent Inhibition of cGAS and TLR9 DNA Sensing by 2′-O-Methyl Gapmer Oligonucleotides. *Nucleic Acids Res.* 49, 6082–6099. doi:10.1093/nar/gkab451

Vanpouille-Box, C., Alard, A., Aryankalayil, M. J., Sarfraz, Y., Diamond, J. M., Schneider, R. J., et al. (2017). DNA Exonuclease Trex1 Regulates Radiotherapy-Induced Tumour Immunogenicity. *Nat. Commun.* 8, 15618. doi:10.1038/ncomms15618

Wei, F., Yan, J., and Tang, D. (2011). Extracellular Signal-Regulated Kinases Modulate DNA Damage Response - A Contributing Factor to Using MEK Inhibitors in Cancer Therapy. *Cmc* 18, 5476–5482. doi:10.2174/092986711798194388

Wu, X., Yang, J., Na, T., Zhang, K., Davidoff, A. M., Yuan, B.-Z., et al. (2017). RIG-I and IL-6 Are Negative-Feedback Regulators of STING Induced by Double-Stranded DNA. *PLoS One* 12, e0182961. doi:10.1371/journal.pone.0182961

Wu, Z., Oeck, S., West, A. P., Mangalhara, K. C., Sainz, A. G., Newman, L. E., et al. (2019). Mitochondrial DNA Stress Signalling Protects the Nuclear Genome. *Nat. Metab.* 1, 1209–1218. doi:10.1038/s42255-019-0150-8

Yamazaki, T., Kirchmair, A., Sato, A., Buqué, A., Rybstein, M., Petroni, G., et al. (2020). Mitochondrial DNA Drives Abscopal Responses to Radiation that Are Inhibited by Autophagy. *Nat. Immunol.* 21, 1160–1171. doi:10.1038/s41590-020-0751-0

Yang, P.-L., Liu, L.-X., Li, E.-M., and Xu, L.-Y. (2020). STAT3, the Challenge for Chemotherapeutic and Radiotherapeutic Efficacy. *Cancers* 12, 2459. doi:10.3390/cancers12092459

Yun, U. J., Park, S. E., Jo, Y. S., Kim, J., and Shin, D. Y. (2012). DNA Damage Induces the IL-6/STAT3 Signaling Pathway, Which Has Anti-senescence and

Growth-Promoting Functions in Human Tumors. *Cancer Lett.* 323, 155–160. doi:10.1016/j.canlet.2012.04.003

Zhang, X., Shi, H., Wu, J., Zhang, X., Sun, L., Chen, C., et al. (2013). Cyclic GMP-AMP Containing Mixed Phosphodiester Linkages Is an Endogenous High-Affinity Ligand for STING. *Mol. Cel* 51, 226–235. doi:10.1016/j.molcel.2013.05.022

Conflict of Interest: MG receives funding from Noxopharm Ltd. to study the activity of STING inhibitors in cancer. MG does not personally own any shares/equity in Noxopharm Ltd.

The remaining authors declare that the research was conducted in the absence of any commercial or financial relationships that could be construed as a potential conflict of interest.

Publisher's Note: All claims expressed in this article are solely those of the authors and do not necessarily represent those of their affiliated organizations, or those of the publisher, the editors and the reviewers. Any product that may be evaluated in this article, or claim that may be made by its manufacturer, is not guaranteed or endorsed by the publisher.

Advantages of publishing in Frontiers

OPEN ACCESS
Articles are free to read for greatest visibility and readership

FAST PUBLICATION
Around 90 days from submission to decision

HIGH QUALITY PEER-REVIEW
Rigorous, collaborative, and constructive peer-review

TRANSPARENT PEER-REVIEW
Editors and reviewers acknowledged by name on published articles

Frontiers
Avenue du Tribunal-Fédéral 34
1005 Lausanne | Switzerland

Visit us: www.frontiersin.org
Contact us: frontiersin.org/about/contact

REPRODUCIBILITY OF RESEARCH
Support open data and methods to enhance research reproducibility

DIGITAL PUBLISHING
Articles designed for optimal readership across devices

FOLLOW US
@frontiersin

IMPACT METRICS
Advanced article metrics track visibility across digital media

EXTENSIVE PROMOTION
Marketing and promotion of impactful research

LOOP RESEARCH NETWORK
Our network increases your article's readership